UNIVERSIDAD NACIONAL AUTONOMA DE MEXICO

INSTITUTO DE BIOTECNOLOGIA

Análisis del transcriptoma en cepas de *Escherichia coli* que carecen del sistema de fosfotransferasa (PTS) y su comparación con la progenitora silvestre.

TESIS
Que para obtener el titulo de:
DOCTORA EN CIENCIAS BIOQUÍMICAS
Presenta:
M. en C. Noemí Flores Mejía

Cuernavaca, Morelos 2005

UNIVERSIDAD NACIONAL AUTONOMA DE MEXICO
INSTITUTO DE BIOTECNOLOGIA

Análisis del transcriptoma en cepas de *Escherichia coli* que carecen del sistema de fosfotransferasa (PTS) y su comparación con la progenitora silvestre.

TESIS
Que para obtener el titulo de:
DOCTORA EN CIENCIAS BIOQUÍMICAS
Presenta:
M. en C. Noemí Flores Mejía

Cuernavaca, Morelos 2005

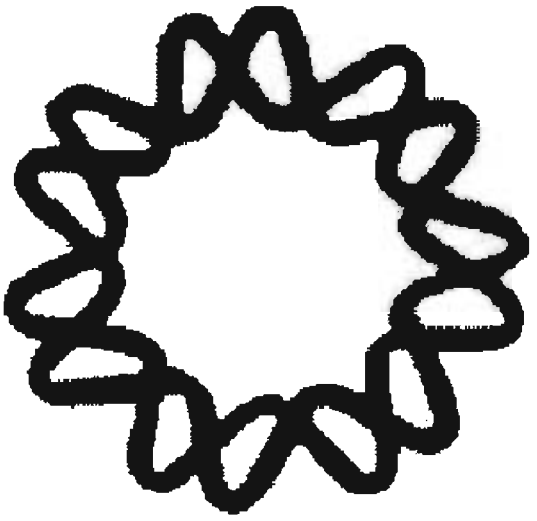

Esta tesis se realizó en el Instituto de Biotecnología/UNAM, en el Departamento de Ingeniería Celular y Biocatálisis bajo la dirección del Dr. Francisco Gonzalo Bolívar Zapata.

Agradecimientos

Al Dr. Francisco Bolivar por brindarme su apoyo y valioso conocimiento.

Al Dr. Fernando Valle por haberme introducido al interesante mundo del Metabolismo en Escherichia coli.

Al Dr. Adelfo Escalante por su colaboración en este proyecto y su apoyo académico

A Lidia Leal quien participó con mucho entusiasmo en este proyecto

A mis cotutores quienes participaron con gran entusiasmo en este proyecto:
Dra. Alicia González
Dra. Paulina Balbás
Dr. Enrique Merino
Dr. Mario Soberón

Al Dr. Salvador Flores por su asesoría académica.

A Mercedes Enzaldo por su apoyo técnico.

A Ana Lilia Viñas por su apoyo secretarial.

A mis compañeros.

A mis padres

Y muy especialmente a mi esposo Raúl.

Indice

1. Sumary

Phosphoenolpyruvate (PEP) is a key intermediate of cellular metabolism and a precursor of commercially relevant products. In *Escherichia coli* 50% of the glucose-derived PEP is consumed by the PEP:carbohydrate phosphotransferase system (PTS) for glucose transport. PTS, encoded by the *ptsHIcrr* operon, was deleted from JM101 to generate strain PB11 (PTS^-Glc^-). PB12, a mutant derived from PB11, grows faster than the parental strain on glucose (PTS^-Glc^+ phenotype). This strain can redirect some of the PEP not utilized by PTS into the high yield synthesis of aromatic compounds from glucose. In this thesis, we report a comparative transcription analysis among these strains of more than 100 genes involved in central carbon metabolism during growth on glucose. It was found that in the PTS^- strains that have reduced glucose transport capacities, several genes encoding proteins with functions related to carbon transport and metabolism were upregulated. Therefore, it could be inferred that these strains synthesize autoinducers of these genes when sensing very low internal glucose or glucose-6P concentrations, probably for scavenging purposes. This condition that is permanently present in the PTS^- strains even when growing in high glucose concentrations allowed the simultaneous utilization of glucose and acetate as carbon sources. It was found that the gal operon is upregulated in these strains, as well as the *aceBAK*, *poxB* and *acs* genes among others. In PB12, *glk*, *pgi*, the TCA cycle and certain respiratory genes are also upregulated. A mutation in *arcB* in PB12 is apparently responsible for the upregulation of the TCA cycle and certain respiratory genes.

2. Resúmen

El fosfoenolpiruvato (PEP) es un intermediario clave del metabolismo cellular y es precursor de productos de valor comercialmente. En *Escherichia coli* el 50% del PEP derivado de la glicólisis, se consume por el sistema de fosfotransferasa PEP:carbohidrato dependiente (PTS) para el transporte de glucosa. Este sistema, codificado por el operón *ptsHIcrr*, se deletó en la cepa JM101 para generar la cepa PB11 (PTS^-Glc^-). PB12, es una cepa mutante derivada de PB11, que crece más rápido que la cepa parental en glucosa (fenotipo PTS^-Glc^+). Esta cepa puede redirigir parte del PEP no utilizado por PTS hacia la síntesis de compuestos aromáticos a partir de glucosa con alto rendimiento. En la tesis se reporta un análisis transcripcional comparativo entre estas cepas de mas de 100 genes involucrados en el metabolismo central de carbono, durante crecimiento en medio mínimo con glucosa. Se encontró que en las cepas PTS^- que tienen capacidades de transporte reducidas, varios genes que codifican para proteínas con funciones relacionadas con el transporte y el metabolismo se sobreexpresaron. Por lo tanto, se pudo inferir que estas cepas producen autoinductores de estos genes cuando la célula sensa muy bajas concentraciones de glucosa o glucosa-6P interna, probablemente con propósitos de "scavenging". Esta condición que es permanente en las cepas PTS^- aún cuando crecen en altas concentraciones de glucosa

permite la utilización simultánea de glucosa y acetato como fuentes de carbono. Se encontró que el operón *gal* está sobreexpresado en estas cepas, así como los genes *aceBAK*, *poxB* y *acs* entre otros. En PB12, *glk*, *pgi*, los genes del ciclo TCA y ciertos genes respiratorios también están sobreregulados. Una mutación en *arcB* en la cepa PB12 aparentemente es responsable de la sobreexpresión de los genes que codifican para proteínas del ciclo TCA y de ciertos genes cuyos productos están involucrados en la respiración.

3. Introducción y antecedentes.

La disponibilidad de fuente de carbono, así como la presencia/ausencia de nitrógeno, oxígeno y otros nutrientes, son las principales señales medioambientales que determinan los ajustes metabólicos necesarios para la adaptación de las redes metabólicas a una condición fisiológica en bacterias. Así, el estudio de la regulación del metabolismo de carbono en procariotes se ha enfocado a una búsqueda intensiva en las últimas décadas a este respecto. Ya que la red metabólica central de carbono incluye reacciones y rutas generales compartidas por muchos organismos, los estudios que se han llevado a cabo en *Escherichia coli* han constituido una plataforma para el estudio del metabolismo de carbono en otros microorganismos. El hecho de que para muchos microorganismos la glucosa es la fuente de carbono preferida ha dado como resultado el desarrollo de una red reguladora compleja denominada "represión catabólica por carbono" que permite la utilización de glucosa sobre algunos otros carbohidratos o fuentes de carbono cuando una mezcla de ellos está presente en el medio (Fraenkel, 1996). Para esto, la bacteria, al igual que otros organismos, tiene sistemas sensores que monitorean su alrededor y gracias a ello pueden inducir o reprimir sistemas genéticos para la utilización de un gran número de fuentes de carbono, detectar gradientes de concentración de nutrientes, adaptarse a cambios de fuerza osmótica, a condiciones de estrés, a cambios de ambiente aeróbico o anaeróbico, y a limitación de nutrientes. Muchas señales del exterior celular captadas por sistemas sensores, son convertidas en una respuesta que puede involucrar un cambio en la síntesis de proteínas, la regulación de una actividad enzimática, cambios en movilidad, u otros procesos. Varios de estos sistemas sensores tienen en común la fosforilación de proteínas en un residuo de histidina, serina o ácido aspártico. A este tipo de sistemas sensores se les denomina sistemas de dos componentes en los que uno de los componentes es el sensor y el otro es el regulador de la respuesta celular. Uno de estos sistemas sensores de dos componentes (Nam et al., 2001) y el principal regulador de la represión catabólica es el de la fosfotransferasa de carbohidratos dependiente de fosfoenolpiruvato (PTS).

3.1. Sistema PTS

El sistema de fosfotransferasa fosfoenolpiruvato:carbohidrato (PTS) (figura 1) es un sistema protéico que pertenece a la clase de transportadores del grupo de los translocadores, que están ampliamente distribuidos en bacterias (Saier, 2002). Una de las principales funciones de este sistema es el transporte

permite la utilización simultánea de glucosa y acetato como fuentes de carbono. Se encontró que el operón *gal* está sobreexpresado en estas cepas, así como los genes *aceBAK*, *poxB* y *acs* entre otros. En PB12, *glk*, *pgi*, los genes del ciclo TCA y ciertos genes respiratorios también están sobreregulados. Una mutación en *arcB* en la cepa PB12 aparentemente es responsable de la sobreexpresión de los genes que codifican para proteínas del ciclo TCA y de ciertos genes cuyos productos están involucrados en la respiración.

3. Introducción y antecedentes.

La disponibilidad de fuente de carbono, así como la presencia/ausencia de nitrógeno, oxígeno y otros nutrientes, son las principales señales medioambientales que determinan los ajustes metabólicos necesarios para la adaptación de las redes metabólicas a una condición fisiológica en bacterias. Así, el estudio de la regulación del metabolismo de carbono en procariotes se ha enfocado a una búsqueda intensiva en las últimas décadas a este respecto. Ya que la red metabólica central de carbono incluye reacciones y rutas generales compartidas por muchos organismos, los estudios que se han llevado a cabo en *Escherichia coli* han constituido una plataforma para el estudio del metabolismo de carbono en otros microorganismos. El hecho de que para muchos microorganismos la glucosa es la fuente de carbono preferida ha dado como resultado el desarrollo de una red reguladora compleja denominada "represión catabólica por carbono" que permite la utilización de glucosa sobre algunos otros carbohidratos o fuentes de carbono cuando una mezcla de ellos está presente en el medio (Fraenkel, 1996). Para esto, la bacteria, al igual que otros organismos, tiene sistemas sensores que monitorean su alrededor y gracias a ello pueden inducir o reprimir sistemas genéticos para la utilización de un gran número de fuentes de carbono, detectar gradientes de concentración de nutrientes, adaptarse a cambios de fuerza osmótica, a condiciones de estrés, a cambios de ambiente aeróbico o anaeróbico, y a limitación de nutrientes. Muchas señales del exterior celular captadas por sistemas sensores, son convertidas en una respuesta que puede involucrar un cambio en la síntesis de proteínas, la regulación de una actividad enzimática, cambios en movilidad, u otros procesos. Varios de estos sistemas sensores tienen en común la fosforilación de proteínas en un residuo de histidina, serina o ácido aspártico. A este tipo de sistemas sensores se les denomina sistemas de dos componentes en los que uno de los componentes es el sensor y el otro es el regulador de la respuesta celular. Uno de estos sistemas sensores de dos componentes (Nam et al., 2001) y el principal regulador de la represión catabólica es el de la fosfotransferasa de carbohidratos dependiente de fosfoenolpiruvato (PTS).

3.1. Sistema PTS

El sistema de fosfotransferasa fosfoenolpiruvato:carbohidrato (PTS) (figura 1) es un sistema protéico que pertenece a la clase de transportadores del grupo de los translocadores, que están ampliamente distribuidos en bacterias (Saier, 2002). Una de las principales funciones de este sistema es el transporte

y fosforilación dependiente de PEP de varios azúcares denominados azúcares PTS. Este sistema está compuesto por dos componentes generales denominados EI y Hpr cuya función es transferir el grupo fosfato del PEP a un componente azúcar específico IIA y posteriormente al componente de membrana IIB quien transporta y forforila al azúcar PTS. Los componentes generales del sistema EI (codificado por el gene *ptsI*), Hpr (codificado por *ptsH*), y el componente azúcar-específico $EIIA^{Glc}$ (codificado por *crr*), el transportador de glucosa $EIICB^{Glc}$ (codificado por *ptsG*), así como el complejo AMPc-CRP, son miembros del modulón de represión catabólica que regula la actividad de muchos operones catabólicos y el transporte de carbohidratos. Los primeros tres genes están organizados en el operón *ptsHIcrr*, mientras *ptsG* se encuentra en otro locus. Una mutación en cualquiera de estos genes tiene efectos pleiotrópicos debido a alteraciones en los niveles de cAMP, y una capacidad de crecimiento limitada en azúcares PTS y no-PTS (Kirkpatrick et al, 2001; Arnold et al, 2001; Schellhorn and Stones, 1992).

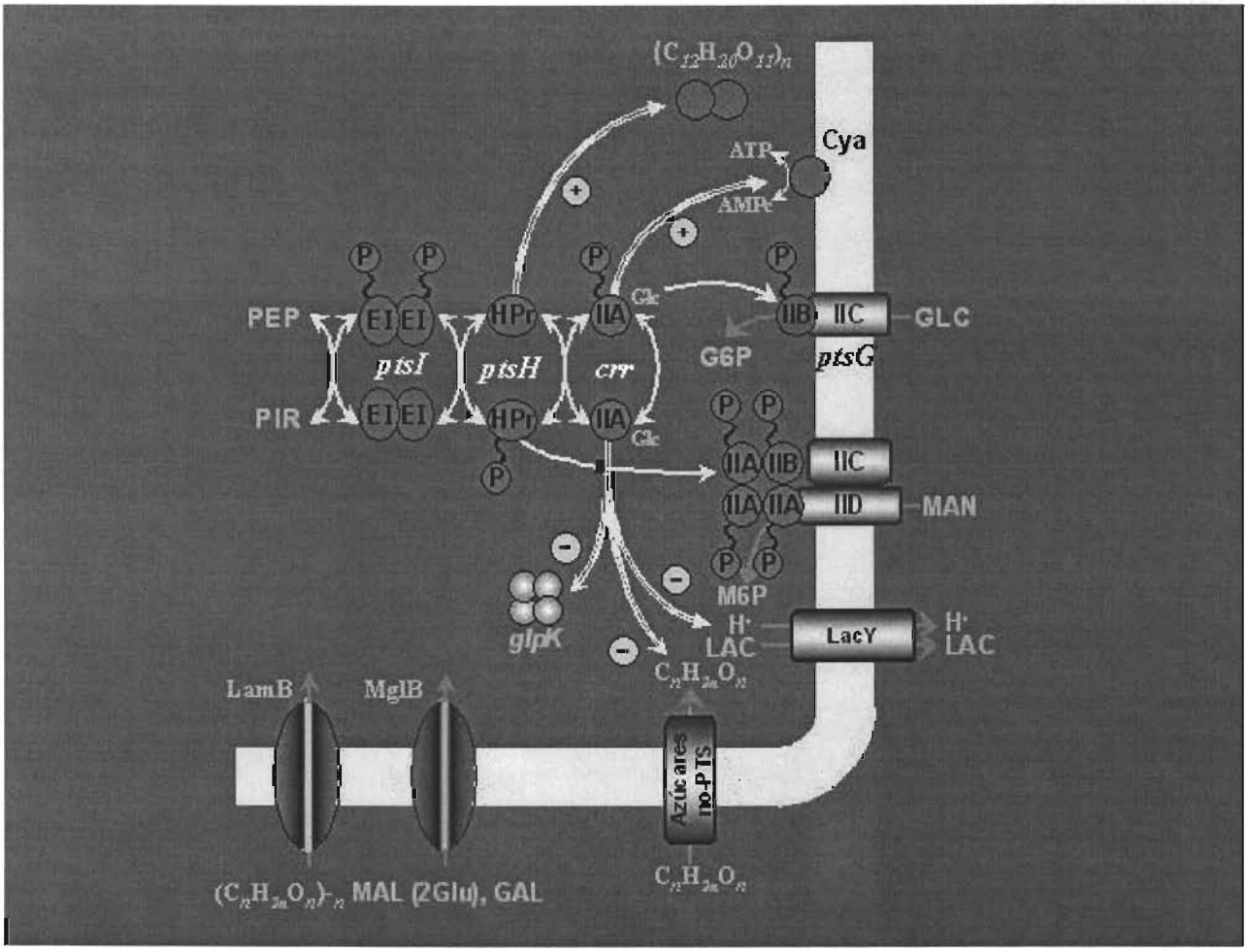

Figura 1. Sistema PTS

Algunos de los componentes PTS de glucosa tienen efectos indirectos de regulación a nivel de la transcripción. Por ejemplo, se ha demostrado que $EIICB^{Glc}$ tiene propiedades regulatorias, primordialmente mediadas a través de la interacción directa con el regulador global Mlc (codificado por *mlc*). Este efecto regulador se ejerce sobre el gene *ptsG*, el operon *ptsHIcrr* y otros genes *pts* (Notley-McRobb and Ferenci, 2000; Seitz *et al,* 2003; Zeppenfeld *et al,* 2000), así como sobre el gene *gapA* y el operón *gapB-pgk* (Charpentier *et al,* 1998). De Reuse y Danchin (1991) proponen que el componente $EIICB^{Glc}$ es el sensor de un sistema de dos componentes que controla al operón *pts*, así como a otros genes (De Reuse and Danchin, 1991; De Reuse *et al,* 1992; Nam *et al,* 2001).

Además, el componente $EIIA^{Glc}$ del sistema PTS para glucosa tiene un papel regulador en la represión catabólica y en la exclusión del inductor mediada por PTS. Esto ocurre a través del componente $EIIA^{Glc}$ desfosforilado, el cual se une reversiblemente a transportadores no-PTS, como el de lactosa, melibiosa, maltosa, rafinosa o glicerol impidiendo su función. En su forma fosforilada, $EIIA^{Glc}$ activa a la adenilato ciclasa para sintetizar AMPc. Además, se ha demostrado que el componente $EIIA^{Glc}$ fosforilado ($EIIA^{Glc}$-P) tiene un efecto regulador sobre la subunidad σ^S de la RNA polimerasa codificada por *rpoS*. Este regulador central en condiciones de ayuno de nutrientes está sujeto a regulación compleja a nivel de la transcripción, la traducción y estabilidad del producto. El efecto de AMPc sobre *rpoS* parece estar mediado transcripcionalmente, mientras que $EIIA^{Glc}$-P controla negativamente la traducción del RNAm de *rpoS* (Ueguchi *et al,* 2001). Así, el estado de fosforilación de $EIIA^{Glc}$ constituye el enlace principal entre catabolismo de carbono y ayuno controlando la traducción del RNAm de *rpoS* (Hengge-Aronis, 2002). Por lo tanto, PTS forma parte de una red reguladora global que controla la capacidad de la célula para encontrar, seleccionar, transportar y metabolizar varios tipos de fuentes de carbono (Postma *et al,* 1996).

3.2. Ingeniería de vías metabólicas y relevancia del PEP

El objetivo central de la ingeniería de vías metabólicas es el de optimizar la formación del o los productos deseados e incrementar la eficiencia en la utilización de los nutrientes durante un proceso de fermentación a través de la alteración de alguna(s) ruta(s) metabólica(s) (Bailey, 1999).

Uno de los principales retos en el desarrollo de un proceso comercial basado en la fermentación utilizando microorganismos, es la reducción de los costos de producción. Las metas más comunes a alcanzar para lograr este objetivo comprenden: incrementar la productividad, el rendimiento y la concentración final del producto con lo que se disminuyen los costos de fermentación, del sustrato y su purificación.

A nivel de fermentación industrial, la glucosa es una de las fuentes de carbono más baratas y comunes que se utiliza para crecer microorganismos. Este compuesto se transporta al interior de la célula y se convierte, a través de varios intermediarios, en compuestos base que sirven a su vez para construir las biomoléculas que conforman a la célula. De la glucosa, así mismo, tarnbién

se obtiene la energía que se utiliza en todos los procesos fisiológicos. Los aproximadamente 75-100 compuestos primarios que sirven para construir todas las moléculas que conforman a la célula, se sintetizan a partir de doce metabolitos precursores que se presentan en la tabla 1.

Glucosa 6-fosfato	Fosfoenolpiruvato
Fructosa 6-fosfato	Piruvato
Ribosa 5-fosfato	Acetil-coenzima A
Eritrosa 4-fosfato	α-cetoglutarato
Triosa-fosfato	Succinil-coenzima A
3-fosfoglicerato	Oxaloacetato

Tabla 1. Metabolitos precursores para la biosíntesis de compuestos celulares.

Todos estos compuestos derivan de glucosa a través de la glicólisis, la vía de las pentosas y el ciclo de los ácidos tricarboxílicos (TCA) (figura 2).

Las bacterias que crecen en un medio mínimo que contiene solo sales minerales y glucosa, necesitan sintetizar estos doce metabolitos precursores. Pero no todos se necesitan en las mismas concentraciones. Por ejemplo, los aminoácidos aromáticos que se sintetizan a partir de algunos de estos compuestos, son relativamente poco abundantes en la célula. Por esta razón, la célula mantiene un cierto flujo de carbono en cada vía metabólica, el cual depende en general, de la demanda de los productos que se formen a partir de ella (Neidhardt et al., 1990a).

El costo efectivo y la producción eficiente de compuestos o derivados de la ruta común de aromáticos requiere que las fuentes de carbono tales como glucosa, lactosa y galactosa se conviertan al producto deseado con un alto porcentaje de rendimiento. Así, desde el punto de vista de producción industrial, los compuestos aromáticos y otros derivados biosintéticos de esta ruta, pueden ser valiosos para aumentar el flujo de fuentes de carbono en y a través de la ruta común de compuestos aromáticos, para incrementar la producción del compuesto deseado.

El fosfoenolpiruvato (PEP) es uno de los compuestos precursores mas importantes en las rutas biosintéticas (Holms, 1986) (Fig. 3), particularmente en la de biosíntesis de aminoácidos aromáticos. La principal fuente de este compuesto proviene de la vía de glicólisis. El mayor porcentaje de este compuesto se transforma en piruvato por dos rutas; por el sistema PTS (66%) y por la acción de las piruvato cinasas PykA y PykF(14%). La otra vía que utiliza PEP en una proporción importante, es la que lo transforma a oxaloacetato (16%), uno de los intermediarios mas importantes del ciclo de Krebs. De lo anterior se deduce que una mínima parte del PEP se dirige a la formación de aminoácidos aromáticos (alrededor del 3 a 4%) (Fig. 3).

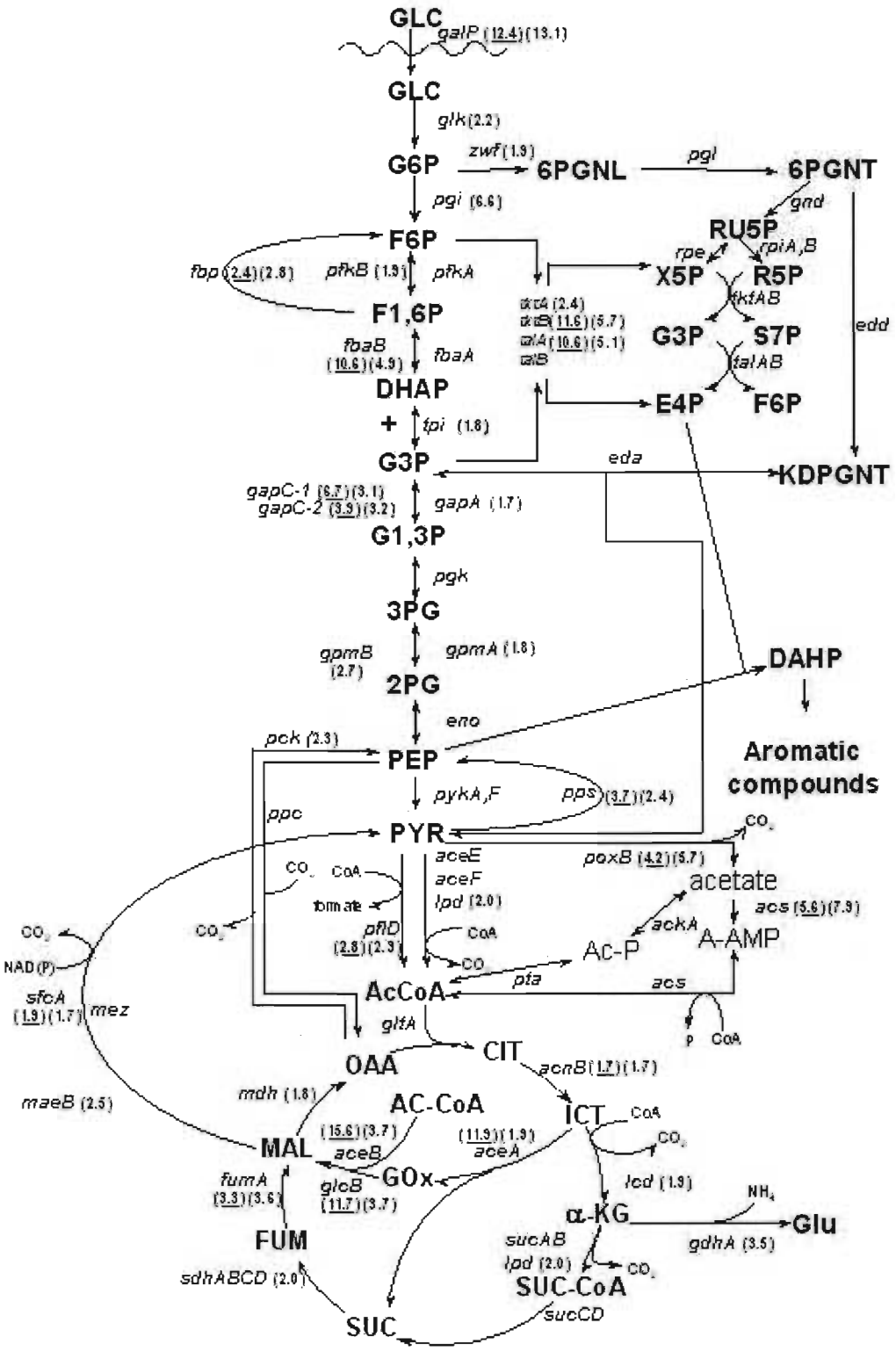

Figura 2. Vías del metabolismo central de carbono.

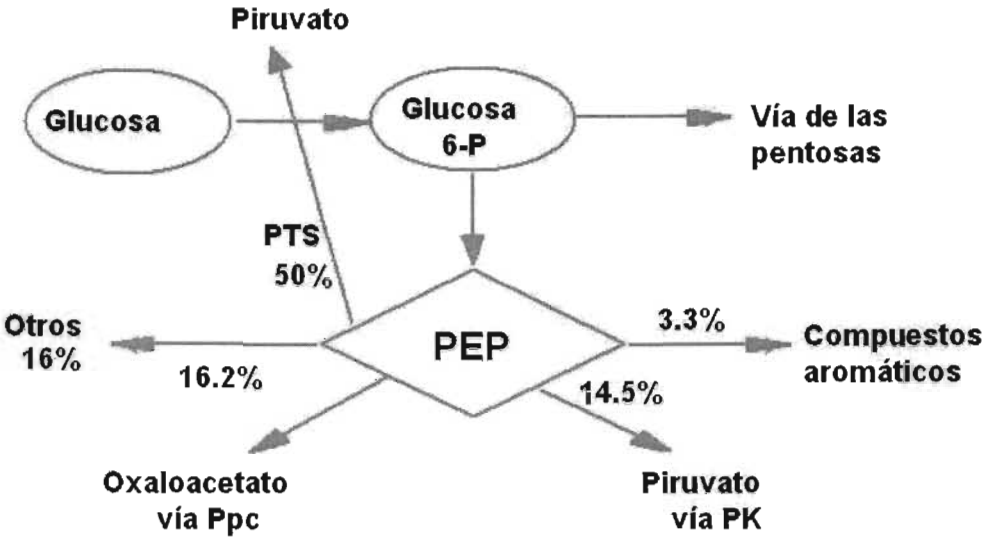

Figura 3. Utilización de PEP en *Escherichia coli*

3.3. Importancia de contar con cepas PTS⁻Glc⁺.

La mitad del PEP producido durante la glicólisis es consumido por PTS durante la internalización de glucosa. Esta restricción metabólica limita la cantidad de PEP disponible para la síntesis de varios metabolitos derivados de este precursor cuando *E. coli* utiliza glucosa como única fuente de carbono. Por esta razón, se ha hecho un esfuerzo importante enfocado al desarrollo de cepas de *E. coli* para Ingeniería de vías metabólicas y propósitos de producción que puedan transportar eficientemente glucosa por un mecanismo independiente de PEP (Saier, 2002). Sin embargo, la inactivación de PTS provoca un amplio rango de efectos debido a su importante papel en la fisiología celular. Por ejemplo, una deleción del operón *ptsHIcrr* en *E. coli* disminuye el transporte de glucosa y la tasa de crecimiento (fenotipo PTS^-) (Flores, 1995; Flores *et al,* 2002). Por lo cual las cepas PTS^- no son apropiadas para propósitos de producción. Por lo tanto, se requieren otras modificaciones genéticas para incrementar la capacidad de transporte de glucosa en una mutante PTS^-. Se han reportado diferentes enfoques que permiten alcanzar, con diferentes grados de éxito, esté objetivo con el fin de mejorar una cepa de producción de metabolitos específicos (Flores *et al,* 1996; Chen *et al,* 1997; Chandran *et al,* 2003; Báez-Viveros *et al,* 2004).

En nuestro laboratorio hemos aislado mutantes de *Escherichia coli* carentes del sistema PTS con el objetivo de utilizarlas para incrementar el rendimiento de ciertos metabolitos precursores de compuestos aromáticos a partir de glucosa como fuente de carbono. La hipótesis es que el PEP que normalmente se utiliza para transportar glucosa mediante el sistema PTS, al no ser utilizado en las bacterias PTS^-, pueda canalizarse hacia la síntesis de 3-deoxi-D-arabino-heptulosonato-7-fosfato (DAHP) que es el primer precursor de la síntesis de compuestos aromáticos (figura 2).

Se ha señalado que las bacterias de *Escherichia coli* carentes del sistema PTS crecen lentamente en medio mínimo con glucosa (fenotipo PTS^-), por ello no son adecuadas para el propósito de incrementar la producción de compuestos aromáticos. Por tal razón, hemos aislado cepas mutantes a partir de una cepa PTS^- (PB11) que crecen mas rápidamente en medio mínimo con glucosa como fuente de carbono utilizando un cultivo en lote hasta que las células alcanzaron la fase estacionaria, seguido de un sistema de cultivo continuo con diferentes tasas de dilución ($D = 0.4\text{-}0.8\ h^{-1}$) con tres tiempos de retención (t_R)cada una. A partir de este experimento se aislaron cepas PTS^-Glc^+, entre ellas las cepas PB12 y PB13 (Flores, 1995; Flores et al., 1996). Cabe señalar que aunque la cepa PB13 se aisló en una $D = 0.8\ h^{-1}$ y que inicialmente esta cepa tenía una μ de 0.69, con el paso del tiempo esta cepa perdió dicha característica aún en los gliceroles congelados y su μ final ha sido de 0.49.

Hemos demostrado que cepas PTS^-Glc^+ y entre ellas la PB12, una vez que son modificadas genéticamente (a través de incrementar los genes *tktA* y $aroG^{fbr}$ en multicopia), son capaces de canalizar parte del PEP no utilizado en el transporte de glucosa hacia la síntesis de compuestos aromáticos. Por la importancia biotecnológica de las cepas PTS^-Glc^+, a continuación se presentan los procedimientos que permitieron obtener estas cepas.

3.4. Construcción de cepas PTS^- y PTS^-Glc^+.

Para obtener una cepa capaz de transportar glucosa utilizando una ruta metabólica diferente a la del sistema PTS, se deletó el operón *pts* de una cepa con genotipo conocido. Para ello se transdujo a la cepa JM101 la deleción *Δ(ptsH-I, crr)kan* contenida en la cepa TP2811, mediante el bacteriofago P1. Se seleccionaron colonias resistentes a kanamicina y se contraseleccionaron colonias blancas en medio Mac Conkey suplementado con glucosa y Km (Mck-glc-Km). De este modo se obtuvo la cepa mutante PB11 *Δ (ptsH, ptsI, crr)* Km^R a la que se le determinó el fenotipo PTS. Esta cepa es resistente a kanamicina y fosfomicina, no puede utilizar azúcares PTS y crece en carbohidratos no-PTS. Los resultados se muestran en la tabla 2.

Tabla 2. fenotipos de las cepas PTS^+, PTS^-, PTS^-Glc^+.

Cepa	Km	Fm	Glc	Fru	Man	Gli	Mal	lac	Gal
JM101	S	S	+	+	+	+	+	-	+
PB11	R	R	-	-	-	+	+	-	+
PB12	R	R	+	-	-	+	+	-	+
PB13	R	R	+	-	-	+	+	-	+

(-) No crece, (+) si crece, (R) resistente, (S) sensible.

En la literatura se reporta que las mutantes *pts*$^-$ tienen un tiempo de duplicación de entre 10 y 20 horas y que en medio mínimo con glucosa como única fuente de carbono se generan mutantes espontáneas que pueden usar este azúcar por una vía diferente a PTS (Biville et al., 1991). Estas mutantes tienen velocidades de crecimiento (μ) similares a las de la cepa silvestre. Estos datos sugirieron que posiblemente pudiera haber diferencias en las velocidades de crecimiento entre revertantes PTS^-Glc^+ dependiendo de la facilidad con que puedan transportar la glucosa.

Por tal razón, se decidió hacer un cultivo continuo en el que se varió la tasa de dilución del medio de cultivo para permitir la selección de diferentes mutantes de acuerdo a su velocidad de crecimiento.

Para fines biotecnológicos, sólo son aceptables en principio velocidades de crecimiento de por lo menos el 50% con respecto a la cepa progenitora, por lo cual se partió de una tasa de dilución correspondiente a una $\mu = 0.4$ que era la mínima requerida y se fue aumentando hasta llegar a la velocidad correspondiente a la de la cepa silvestre, en este caso JM101 ($\mu = 0.83$). La curva del cultivo continuo de la PB11 se muestra en la figura 4.

La fermentación duró más de 200 hrs y se platearon muestras en cajas de Mck-glc-Km en cada cambio de la tasa de dilución. Aparecieron colonias rojas desde que se inició el cultivo continuo. Se tomaron dos colonias de cada una de las diluciones 0.4, 0.6, Y 0.8 (Cols. 4, 10, 32, 40, 99 Y 103 respectivamente) para determinar si había diferencias en las velocidades de crecimiento dependiendo del flujo con que fueron seleccionadas. Las curvas de crecimiento se muestran en la figura 5.

Efectivamente, existen diferentes velocidades de crecimiento entre las diferentes colonias aisladas. De todas estas, se escogieron una de menor y una de similar velocidad de crecimiento con respecto a la JM101. Estas dos cepas se denominaron PB12 (menor μ) y PB13 (Flores et al., 1996). Una caracterización preliminar de éstas cepas se presenta a continuación.

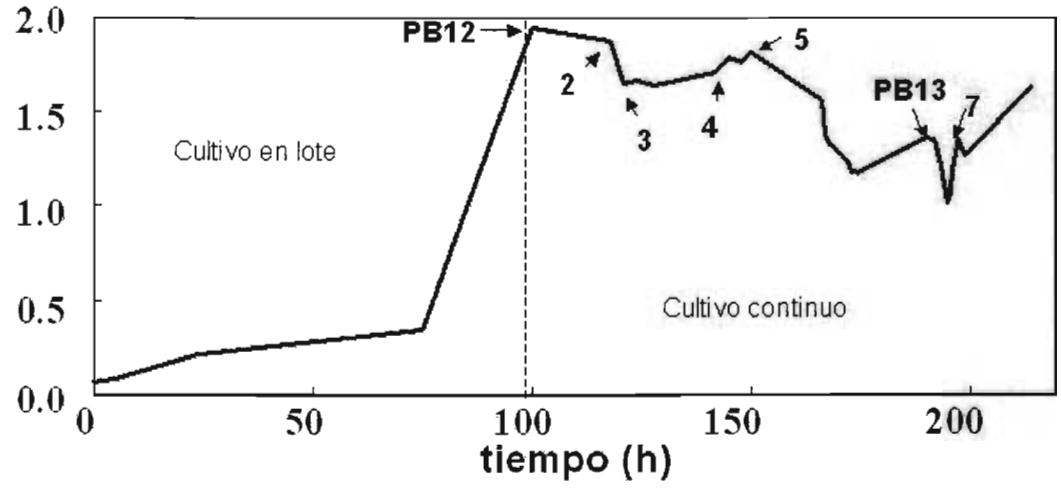

Figura 4. Aislamiento de mutantes PTS$^-$Glc$^+$ a partir del cultivo continuo de la cepa PB11.

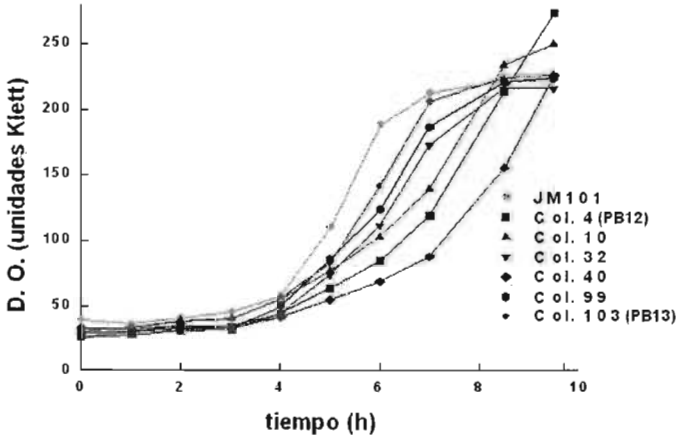

Figura 5. Caracterización cinética de las mutantes PTS$^-$Glc$^+$ obtenidas a partir de la PB11.

3.5. Caracterización genética y bioquímica preliminar de las cepas PTS⁻Glc⁺.

Se han caracterizado algunas de estas cepas PTS⁻Glc⁺ y se sabe que al menos dos mutaciones no cotransducibles son responsables de este nuevo fenotipo. Se ha determinado también que las cepas PB12 y PB13 utilizan la permeasa de galactosa (GalP) y la glucocinasa (Glk) para transportar y fosforilar glucosa en ausencia de PTS (Flores et al., 1996; Flores et al., 2002).

Como parte de la caracterización preliminar de éstas cepas, se determinaron sus velocidades de crecimiento y sus capacidades de transporte de glucosa. También se determinaron estos parámetros en las cepas JM101 y PB11. (Flores et al., 2002). Además, se midieron las actividades específicas de Glk, Pgi y Zwf en estas cepas. Los resultados se muestran en la tabla 3.

Tabla 3. Velocidades de crecimiento (μ), y transporte de (^{14}C)-glucosa (τ) en diferentes cepas de *Escherichia coli*. Se presentan también las actividades específicas de Glk, Pgi y Zwf.

Cepa	Fenotipo	μ^a	τ^b	Glk^c	Pgi^c	Zwf^c
JM101	silvestre	0.71	20.0	57	1448	180
PB11	PTS⁻	0.10	1.7	ND	134	136
PB12	PTS⁻Glc⁺	0.42	10.3	127	5699	267
PB13	PTS⁻Glc⁺	0.49	11.7	136	4737	314

[a] en h^{-1}, en medio M9 con 2 g/l de glucosa.

[b] en nmol ^{14}C-glc min^{-1} mg $prot^{-1}$.

[c] en mmol de sustrato producido glc min^{-1} mg $prot^{-1}$.

ND – no determinado.

3.6. Caracterización de los flujos de carbono por RMN en las cepas PTS⁻ y PTS⁻Glc⁺.

La distribución de flujos de carbono en las cepas isogénicas PTS⁺, PTS⁻ y PTS⁻Glc⁺ se ha estudiado por espectroscopia de resonancia magnética nuclear (RMN). Se demostró que los flujos de carbono se modificaron en varios nodos y porciones del metabolismo central de carbono en las cepas PTS⁻ y PTS⁻Glc⁺ comparados con la cepa silvestre JM101 (figura 6). Los resultados demostraron claramente que estas cepas PTS⁻ ajustaron sus capacidades metabólicas debido a la ausencia de PTS. Por ejemplo, en la vía Embden-Meyerhof (EMP), el flujo de carbono del primer nodo aumentó a un 95% en la PB12 PTS⁻Glc⁺ (GalP/Glk) comparado con las cepas parentales silvestre JM101 (77%) y la PB11 PTS⁻ (42%) (Flores et al., 2002). En concordancia con esto, está el dato de que las actividades específicas de Glk y Pgi en la PB12 aumentaron 2 y 4 veces respectivamente comparadas con la cepa JM101 (Tabla 3). Como resultado de estas modificaciones, PB12 crece mas rápido que la PB11 (μ= 0.42 vs 0.1 h^{-1}) pero menos que la JM101 (μ= 0.71 h^{-1}) (Flores et al., 2002).

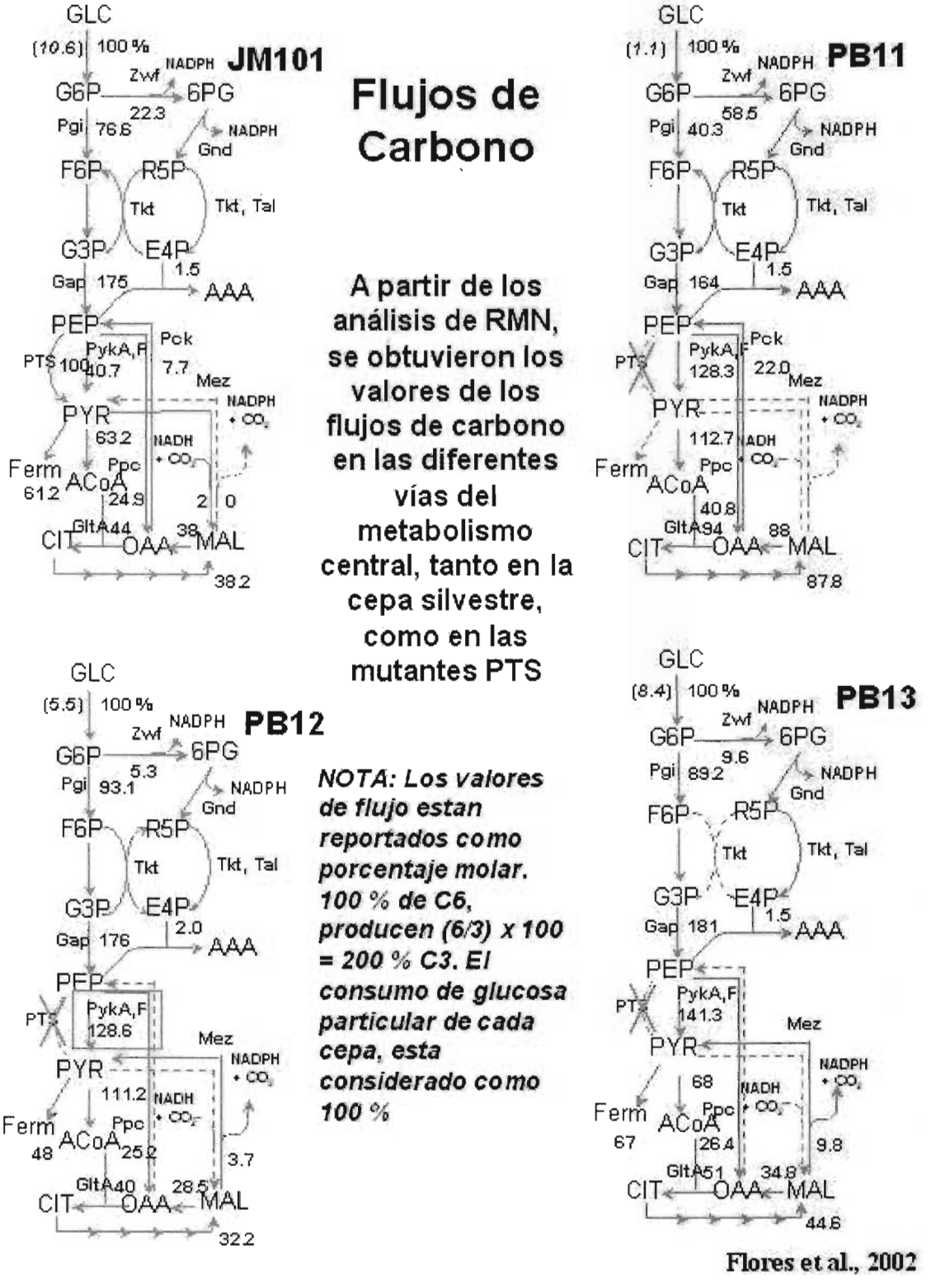

Figura 6. Flujos de carbono determinados por RMN

4. Objetivo

Con base en estos antecedentes, se consideró relevante avanzar en la caracterización de éstas cepas a través de analizar los niveles de transcripción del genoma de estas diferentes cepas que pensamos pueden tener valor industrial. En particular se hizo el análisis de la cepa PB12, creciendo en medio mínimo con glucosa como fuente de carbono, con el propósito de conocer qué genes, en particular los relacionados con el metabolismo central de carbono, habían cambiado su expresión con relación a las cepas parentales PB11 y JM101.

Conforme con lo anterior se realizaron experimentos de medición del transcriptoma con microarreglos de laminilla y se demostró que en las cepas PB11 y en menor medida en PB12, existe un incremento en la expresión de varios genes con relación a la cepa silvestre JM101 (Flores et al., 2005b). Sin embargo, los resultados con microarreglos no eran 100% repetitivos en los múltiples microarreglos que se realizaron y por ello se decidió determinar de manera mas fina y repetitiva la expresión de algunos de estos genes a través de montar el sistema de PCR de tiempo real (RT-PCR).

Mediante este método se determinaron los valores de expresión relativa de alrededor de 200 genes relacionados con el metabolismo central de *Escherichia coli* en las cepas JM101, PB11 y PB12. Los resultados de este trabajo se publicaron en el artículo intitulado: "Adaptation for fast growth on glucosa by differential expresión of central carbon metabolism and *gal* regulon genes in an *Escherichia coli* strain lacking the phosphoenolpyruvate:carbohydrate phosphotransferase system" *(Flores et al., 2005a).*

5. Materiales y métodos

5.1. Cepas bacterianas, plásmidos, medios de cultivo y condiciones de crecimiento.

Las cepas de *Escherichia coli* utilizadas en este trabajo se enlistan en la tabla 4. PB12 se obtuvo a partir de PB11, una cepa PTS^- derivada de JM101 (Flores, 1995; Flores, 1996). La cepa PB121 se obtuvo por transformación de la PB12 con el plásmido pBB31 que porta el gene *arcB* silvestre.

Cepas	Genotipo	Referencia
E. coli JM101	F′ *tra*D36 *proA*$^+$ *proB*$^+$ *lac*I^q *lac*ZΔM15/*supE thi* Δ(*lac-proAB*)	Bolívar et al, 1977
E. coli PB11	JM101 Δ(*ptsH, ptsI, crr*)::*kan*	Flores et al, 1996
E. coli PB12	PB11, PTS^-Glc^+	Flores et al, 1996
E. coli PB121	PB12, pBB31 (*arcB*$^+$)	Este trabajo

Tabla 4. Cepas bacterianas utilizadas en este estudio.

4. Objetivo

Con base en estos antecedentes, se consideró relevante avanzar en la caracterización de éstas cepas a través de analizar los niveles de transcripción del genoma de estas diferentes cepas que pensamos pueden tener valor industrial. En particular se hizo el análisis de la cepa PB12, creciendo en medio mínimo con glucosa como fuente de carbono, con el propósito de conocer qué genes, en particular los relacionados con el metabolismo central de carbono, habían cambiado su expresión con relación a las cepas parentales PB11 y JM101.

Conforme con lo anterior se realizaron experimentos de medición del transcriptoma con microarreglos de laminilla y se demostró que en las cepas PB11 y en menor medida en PB12, existe un incremento en la expresión de varios genes con relación a la cepa silvestre JM101 (Flores et al., 2005b). Sin embargo, los resultados con microarreglos no eran 100% repetitivos en los múltiples microarreglos que se realizaron y por ello se decidió determinar de manera mas fina y repetitiva la expresión de algunos de estos genes a través de montar el sistema de PCR de tiempo real (RT-PCR).

Mediante este método se determinaron los valores de expresión relativa de alrededor de 200 genes relacionados con el metabolismo central de *Escherichia coli* en las cepas JM101, PB11 y PB12. Los resultados de este trabajo se publicaron en el artículo intitulado: "Adaptation for fast growth on glucosa by differential expresión of central carbon metabolism and *gal* regulon genes in an *Escherichia coli* strain lacking the phosphoenolpyruvate:carbohydrate phosphotransferase system" *(Flores et al., 2005a).*

5. Materiales y métodos

5.1. Cepas bacterianas, plásmidos, medios de cultivo y condiciones de crecimiento.

Las cepas de *Escherichia coli* utilizadas en este trabajo se enlistan en la tabla 4. PB12 se obtuvo a partir de PB11, una cepa PTS^- derivada de JM101 (Flores, 1995; Flores, 1996). La cepa PB121 se obtuvo por transformación de la PB12 con el plásmido pBB31 que porta el gene *arcB* silvestre.

Cepas	Genotipo	Referencia
E. coli JM101	F′ *tra*D36 *proA*$^+$ *proB*$^+$ *lac*I^q *lac*ZΔM15/*supE thi* Δ(*lac-proAB*)	Bolívar et al, 1977
E. coli PB11	JM101 Δ(*ptsH, ptsI, crr*)::*kan*	Flores et al, 1996
E. coli PB12	PB11, PTS^-Glc^+	Flores et al, 1996
E. coli PB121	PB12, pBB31 (*arcB*$^+$)	Este trabajo

Tabla 4. Cepas bacterianas utilizadas en este estudio.

Los cultivos para aislamiento de RNA y ensayos enzimáticos se hicieron por duplicado y se crecieron en fermentadores de 1 L en medio M9 suplementado con 2 g/L de glucosa, a 37°C, 600 rpm y una tasa de flujo de aire de 1vvm, iniciando con una OD600 de 0.05 y las muestras se colectaron en la fase logarítmica a una OD600 de 1.

Para los ensayos de sensibilidad de crecimiento a azul de toluidina, las células se crecieron en placas de agar-peptona con 0.2mg/ml de azul de toluidina. Para los análisis de complementación se utilizó el plásmido pBB31 que lleva el gene *arcB* silvestre (Iuchi and Lin, 1988; 1992).

5.2 Selección de mutantes PTS⁻ Glc+ por cultivo continuo (quimiostato).

Se usó el fermentador Multigen (New Brunswick Scientific Co.) con una jarra para flujo continuo de 2 L. Se manejó con 1.3 L de M9 suplementado con glucosa (2 g/L) y Km (30 μg/ml). El inóculo se preparó con la cepa PB11 crecida en dos cajas de medio Luria-Km con tapíz confluente. Este tapete de células se resuspendió en 10 ml de medio M9 y se agregó al fermentador. Las condiciones de crecimiento fueron: 1 vvm (volúmen de aire por volúmen de medio por minuto), 37°C, 600 rpm, el pH se mantuvo en 7.0 con hidróxido de amonio 50 %. El cultivo se dejó crecer hasta que las células alcanzaron la fase estacionaria y entonces se empezó a lavar a diferentes tasas de dilución (0.08, 0.4, 0.5, 0.6, 0.7, 0.75 Y 0.8). El flujo correspondiente a cada tasa de dilución se mantuvo por al menos tres tiempos de retención o hasta comprobar que la densidad óptica del cultivo no disminuía. En cada cambio de flujo, se tomó una muestra y se plateó en cajas de Mck-glc-Km para aislar colonias rojas. De estas, se seleccionaron dos colonias rojas de cada punto y se determinó su fenotipo.

5.3. Extracción de RNA y síntesis de cDNA.

La extracción de RNA total se llevó a cabo mediante el método de fenol caliente equilibrado en agua. El RNA total se trató con DNasa y se cuantificó cuidadosamente por absorbancia a 260/280 nm y su integridad se verificó en geles de agarosa al 1.2%. El cDNA se sintetizó por el método de síntesis de primera cadena de DNA utilizando primers específicos (b) (tabla 5). Este cDNA se usó como templado para los ensayos de RT-PCR. La reproducibilidad del método se determinó a través de dos experimentos separados de síntesis de cDNA a partir de dos fermentaciones diferentes de cada cepa.

5.4. Determinación y análisis de secuencias nucleotídicas de los genes mglB, galP, galE, galS, galR, glk, pgi, crp, fruR, arcA, y arcB

Con el fin de determinar si alguno de estos genes contenía alguna mutación responsable del fenotipo Glc^+ en las cepas mutantes PTS^-Glc^+, se amplificaron y secuenciaron los productos de PCR de cada uno de estos genes. Cada fragmento contiene al menos 200 pb de la región regulatoria del extremo 5', el gene estructural y al menos 100 pb de la región 3'. Los oligos para obtener estos

productos de PCR se diseñaron con el programa Clone Manager y se enlistan en la tabla 5. Los productos de PCR se obtuvieron a partir de DNA cromosomal de las cepas JM101, PB11 y PB12 y se amplificó con la polimerasa Elongasa. Los productos se analizaron de acuerdo al tamaño esperado y se purificaron con el kit para purificación de productos de PCR (Marligen, BioScience Inc.). Se utilizaron 100 ng de DNA cromosomal de las cepas JM101, PB11 y PB12 como templados para la amplificación por PCR con Elongase enzyme mix de acuerdo a las recomendaciones del proveedor (Invitrogen, Inc.). Los productos de PCR se analizaron de acuerdo al tamaño esperado y se purificaron por el kit PCR purification kit (Marligen, BioScience Inc.).

Las secuencias nucleotídicas se determinaron a partir de productos de PCR por el método Taq FS Dye Terminator Cycle Fluorescence-Based Sequencing, con el equipo Perkin Elmer/Applied Biosystems Model 377-18 sequencer.

5.5. PCR de tiempo real (RT-PCR).

El PCR de tiempo real se realizó con el ABI Prism 7000 Sequence Detection System (Perkin-Elmer/Applied Biosystems) utilizando el kit SYBR Green PCR Master Mix (Perkin-Elmer/Applied Biosystems). Las condiciones de amplificación fueron 10 min a 95°C, un ciclo de dos pasos a 95°C por 15 s y 60°C por 60 s en un total de 40 ciclos. Los prímeros para la amplificación específica (Tabla 5) se diseñaron con el programa Primer Express software (PE Applied Biosystems). El tamaño de todos los amplímeros fue de 101 pb. La concentración final de los prímeros, en un total de 15 μl, fue 0.2 μM. Se agregaron 5 ng de cDNA a cada reacción. Todos los experimentos se realizaron por triplicado para cada gene de cada cepa obteniendo resultados similares (con diferencias menores a 0.3 SD). Se incluyó siempre un control sin templado y con la mezcla de reacción para cada gene. La técnica de cuantificación utilizada para analizar los datos fue el método $2^{-\Delta\Delta C_T}$ descrito por Livak and Shmittgen (2001), y los resultados fueron graficados y se presentan en la tabla 6.

Todos los datos se normalizaron utilizando el gene *ihfB* como control interno ("housekeeping gene") con el fin de ajustar la concentración de cDNA de las muestras. Esto debido a que se detectó el mismo nivel de expresión de este gene en todas las cepas en las condiciones de crecimiento de éste estudio. Para cada gene analizado en todas las cepas, el nivel de transcripción del gene de la cepa silvestre JM101 se consideró con un valor de 1.0 y fue usado como el control para normalizar los datos. Por lo tanto, los datos están reportados como valores de expresión relativa, comparados al nivel de expresión de la JM101. Los resultados presentados en la tabla 6 y las figuras 7 y 8 son los promedios de cuatro mediciones de RT-PCR independientes de los valores de expresión para cada gene. La mitad de esos 4 valores se obtuvieron de dos diferentes cDNAs generados a partir de una fermentación y los otros dos de otra fermentación idéntica. Los valores de expresión obtenidos por RT-PCR para cada gene difieren en menos del 30% que representa una desviación Standard muy buena si se tiene en cuenta que los resultados reportados hasta ahora en la literatura varían de 1 a 19 veces (Bustin, 2000).

mdh	mdha	5'- CGGGTCTGCAACCCTGTCTA -3'
	mdhb	5'- CGTAGGCACATTCGACAACG -3'
e. Genes anapleróticos		
maeB	maeBa	5'- TGGTTTGCGATTCAAAAGGC -3'
	maeBb	5'- GAGGGTACGTTTGCCGTCAT -3'
sfcA	sfcAa	5'- ATAAAGGCAGTGCCTTCAGCA -3'
	sfcAb	5'- TGCTCGTTCCGCTTGTTCTT -3'
mdh	mdha	5'- CGGGTCTGCAACCCTGTCTA -3'
	mdhb	5'- CGTAGGCACATTCGACAACG -3'
pps	ppsa	5'- TCAGCAGGAAACCTTCCTCAA -3'
	ppsb	5'- GATAAGAGATGGCGCGATCG -3'
pckA	pckAa	5'- ACATGTTTATTCGCCCGAGC -3'
	pckAb	5'- CTGTTCTTTCCACTGCGGGT -3'
ppc	ppca	5'- CAGAAATCACCGTCAGCAGC -3'
	ppcb	5'- CATAATGCGACGCCAGCTCT -3'
f. Gluconeogénesis		
gpmB	gpmBa	5'- GGTATTGCACTGGGATGCCT -3'
	gpmBb	5'- TAATCCACGCGCGAAATAGA -3'
gapC-1	gapC-1a	5'- CAACGACACCATTGTTTCCG -3'
	gapC-1b	5'- TCATCGTGCCGACTTCTATCC -3'
gapC-2	gapCa	5'- ATCATTGGCAGCCATTTCG -3'
	gapCb	5'- TTATCGTACCAGGCGACCGT -3'
fbaB	fbaBa	5'- GTACAACACCGGGCGTCTG -3'
	fbaBb	5'- GCGGGTTAGCAGCAAATGAA -3'
glpX	glpXa	5'- CTAAACCACGCCACGATGC -3'
	glpXb	5'- ACAGGTGAGAATTGAGGCCG -3'
fbp	fbpa	5'- AAACAGGTTGCGGCAGGTTA -3'
	fbpb	5'- CCGAGCGAAGGATCGTAAGT -3'
pfkB	pfkBa	5'- GTTGGCGGATGAAAATGTCC -3'
	pfkBb	5'- AACGATACTGCTCACCGCTTG -3'
g. Respiración		
nuoA	nuoAa	5'- CTGGTGGCCATGTTCTTCGT -3'
	nuoAb	5'- GCTTCCACAAAGCCTACCCA -3'
nuoF	nuoFa	5'- TATCCGTACTCCCGAAACGC -3'
	nuoFb	5'- CGCCTTCGTAACCGTTTTTG -3'
nuoN	nuoNa	5'- TGTCGCGTTGGGTAAAAACC -3'
	nuoNb	5'- GAGAGAGTTTGAAGCCGAGGC -3'
ndh	ndha	5'- GTCGATCGTAACCACAGCCA -3'
	ndhb	5'- GCATGGGCCAGATAGCTCAA -3'
sdhA	sdhAa	5'- GACACCGTGAAAGGGTCGG -3'
	sdhAb	5'- AGGCCCATGTGTTCGAGTTC -3'
sdhB	sdhBa	5'- TGAACGGCAAGAATGGTCTG -3'
	sdhBb	5'- GATCACCGGTAAACCTGGCA -3'
sdhC	sdhCa	5'- TGGCGTATCACGTCGTCGTA -3'
	sdhCb	5'- AAAGGAGATTTTGGCGGAGC -3'
sdhD	sdhDa	5'- GATCGGTTTCTTCGCCTCTG -3'
	sdhDb	5'- CGGTCAACACCTGCCACAT -3'
ubiE	ubiEa	5'- GGCAGAATCCATCCGTATGC -3'
	ubiEb	5'- CCCCTGCCGTCAGATTGTAG -3'
frdA	frdAa	5'- TCTCTCAGGCCTTCTGGCAC -3'
	frdAb	5'- TTTTTTCTCGCCGAGGTGAC -3'
frdB	frdBa	5'- TTGAGGTGGTGCGCTATAACC -3'
	frdBb	5'- GCCCAGCGCATCCAGTAAT -3'
frdC	frdCa	5'- ACCGAAAGCGGCCAATATC -3'
	frdCb	5'- GGATTACGATGGTGGCAACC -3'
frdD	frdDa	5'- TGGTCGCGTATTCCTGTTCC -3'
	frdDb	5'- CCGCAGGTACGTGGATTTTC -3'
napA	napAa	5'- GATGGGCTGCTATGACGACA -3'
	napAb	5'- GGTTAGTGATGCGCGACCA -3'
narG	narGa	5'- CGATTATCCGGCGACTTACG -3'
	narGb	5'- TCTCGCTCTGGGTGTTCCAG -3'
cyoA	cyoAa	5'- GGCATTGCTACCGTGAATGA -3'
	cyoAb	5'- AGACGCGGAATGAAGAAGGA -3'
cyoB	cyoBa	5'- CTGACCTCCGTCGACCATAAA -3'
	cyoBb	5'- TGGCTACGCATCATAATGGC -3'
cyoC	cyoCa	5'- CACGGTCTGCACGTCACTTC -3'
	cyoCb	5'- CACATGATGCGGGTACGGT -3'
cyoD	cyoDa	5'- CCTGGCAATGGCAGTGGTAC -3'
	cyoDb	5'- TGAAGACAAACGCCGTCATG -3'
h. Genes de fermentación, producción y utlización de acetato		
ldhA	ldhAa	5'- GGCGTGATGATCGTCAATACC -3'
	ldhAb	5'- ACGTCCATACCCAACGAACC -3'
pta	ptaa	5'- ACAATGTTGATCCGGCGAAG -3'
	ptab	5'- CATATCGATCGCACGAGTCG -3'
ackA	ackAa	5'- CTGGTTCTGAACTGCGGTAGTTC -3'
	ackAb	5'- GGCAGGTGGAAACATTCGG -3'
adhE	adhEa	5'- AAGTCCCTGTGTGCTTTCGG -3'
	adhEb	5'- TGCAGAGCCTGACCATCAGA -3'
poxB	poxBa	5'- AAAAGCCGATCGCAAGTTTC -3'
	poxBb	5'- GGTGAATGGCTTTCTCGCTC -3'
i. Reguladores		
cyaA	cyaAa	5'- AGCGCCAATTGCTACAACGT -3'
	cyaAb	5'- ACGGAAGCGGTTTTCATCAA -3'
crp	crpa	5'- ACCCGTCAGGAAATTGGTCA -3'
	crpb	5'- TTACCGTGTGCGGAGATCAG -3'
fruR	fruRa	5'- TCTTGTGATCCCCGATCTGG -3'
	fruRb	5'- AGCAGGCAATCAGCAGTTGA -3'
arcA	arcAa	5'- ATCACCAAACCGTTCAACCC -3'
	arcAb	5'- ACGCTACGACGTTCTTCGCT -3'
arcB	arcBa	5'- AATCTGACGGCGCAGGATAA -3'
	arcBb	5'- TGACCCAGCTGTTGCAGATG -3'
mlc	mlca	5'- GGTCCAGTCTCGCGTATCGA -3'
	mlcb	5'- TCTTGCACCAGGTGTGCTTC -3'
ihfA	ihfAa	5'- GGCGAACAGGTGAAACTCTCTG -3'
	ihfAb	5'- GTAATGGGAATATCCTCGCCC -3'
ihfB	ihfBa	5'- GCCAAGACGGTTGAAGATGC -3'
	ihfBb	5'- GAGAAACTGCCGAAACCGC -3'
iclR	iclRa	5'- CTTTATGGTCGGCAGCAGCT -3'
	iclRb	5'- ATTGACCGTTTCGCCAGACT -3'
fadR	fadRa	5'- CGCTGGGCTTCTACCACAAA -3'
	fadRb	5'- AATCTCGCCACTCTCATGCC -3'
rpoS	rpoSa	5'- GGACGCGACTCAGCTTTACC -3'
	rpoSb	5'- CGACATCTCCACGCAGTGC -3'

6. Resultados y discusión

Para entender el fenotipo mutante PTS$^-$Glc$^+$ es importante diferenciar los fenotipos causados por la deleción del operón *ptsIHcrr* en la cepa PB11 (PTS$^-$) de los seleccionados en la cepa PB12 (PTS$^-$Glc$^+$). Por lo tanto, los resultados se presentan y discuten de manera comparativa, donde los valores de transcripción relativa por RT-PCR de 104 genes de la cepa silvestre JM101 se comparan contra los de las cepas PTS$^-$ y PTS-Glc$^+$ (PB11 y PB12 respectivamente). Los genes analizados incluyen el regulón *gal* que es responsable del transporte de glucosa

mdh	mdha	5'- CGGGTCTGCAACCCTGTCTA -3'
	mdhb	5'- CGTAGGCACATTCGACAACG -3'
e. Genes anapleróticos		
maeB	maeBa	5'- TGGTTTGCGATTCAAAAGGC -3'
	maeBb	5'- GAGGGTACGTTTGCCGTCAT -3'
sfcA	sfcAa	5'- ATAAAGGCAGTGCCTTCAGCA -3'
	sfcAb	5'- TGCTCGTTCCGCTTGTTCTT -3'
mdh	mdha	5'- CGGGTCTGCAACCCTGTCTA -3'
	mdhb	5'- CGTAGGCACATTCGACAACG -3'
pps	ppsa	5'- TCAGCAGGAAACCTTCCTCAA -3'
	ppsb	5'- GATAAGAGATGGCGCGATCG -3'
pckA	pckAa	5'- ACATGTTTATTCGCCCGAGC -3'
	pckAb	5'- CTGTTCTTTCCACTGCGGGT -3'
ppc	ppca	5'- CAGAAATCACCGTCAGCAGC -3'
	ppcb	5'- CATAATGCGACGCCAGCTCT -3'
f. Gluconeogénesis		
gpmB	gpmBa	5'- GGTATTGCACTGGGATGCCT -3'
	gpmBb	5'- TAATCCACGCGCGAAATAGA -3'
gapC-1	gapC-1a	5'- CAACGACACCATTGTTTCCG -3'
	gapC-1b	5'- TCATCGTGCCGACTTCTATCC -3'
gapC-2	gapCa	5'- ATCATTGGCAGCCATTTCG -3'
	gapCb	5'- TTATCGTACCAGGCGACCGT -3'
fbaB	fbaBa	5'- GTACAACACCGGGCGTCTG -3'
	fbaBb	5'- GCGGGTTAGCAGCAAATGAA -3'
glpX	glpXa	5'- CTAAACCACGCCACGATGC -3'
	glpXb	5'- ACAGGTGAGAATTGAGGCCG -3'
fbp	fbpa	5'- AAACAGGTTGCGGCAGGTTA -3'
	fbpb	5'- CCGAGCGAAGGATCGTAAGT -3'
pfkB	pfkBa	5'- GTTGGCGGATGAAAATGTCC -3'
	pfkBb	5'- AACGATACTGCTCACCGCTTG -3'
g. Respiración		
nuoA	nuoAa	5'- CTGGTGGCCATGTTCTTCGT -3'
	nuoAb	5'- GCTTCCACAAAGCCTACCCA -3'
nuoF	nuoFa	5'- TATCCGTACTCCCGAAACGC -3'
	nuoFb	5'- CGCCTTCGTAACCGTTTTTG -3'
nuoN	nuoNa	5'- TGTCGCGTTGGGTAAAAACC -3'
	nuoNb	5'- GAGAGAGTTTGAAGCCGAGGC -3'
ndh	ndha	5'- GTCGATCGTAACCACAGCCA -3'
	ndhb	5'- GCATGGGCCAGATAGCTCAA -3'
sdhA	sdhAa	5'- GACACCGTGAAAGGGTCGG -3'
	sdhAb	5'- AGGCCCATGTGTTCGAGTTC -3'
sdhB	sdhBa	5'- TGAACGGCAAGAATGGTCTG -3'
	sdhBb	5'- GATCACCGGTAAACCTGGCA -3'
sdhC	sdhCa	5'- TGGCGTATCACGTCGTCGTA -3'
	sdhCb	5'- AAAGGAGATTTTGGCGGAGC -3'
sdhD	sdhDa	5'- GATCGGTTTCTTCGCCTCTG -3'
	sdhDb	5'- CGGTCAACACCTGCCACAT -3'
ubiE	ubiEa	5'- GGCAGAATCCATCCGTATGC -3'
	ubiEb	5'- CCCCTGCCGTCAGATTGTAG -3'
frdA	frdAa	5'- TCTCTCAGGCCTTCTGGCAC -3'
	frdAb	5'- TTTTTTCTCGCCGAGGTGAC -3'
frdB	frdBa	5'- TTGAGGTGGTGCGCTATAACC -3'
	frdBb	5'- GCCCAGCGCATCCAGTAAT -3'
frdC	frdCa	5'- ACCGAAAGCGGCCAATATC -3'
	frdCb	5'- GGATTACGATGGTGGCAACC -3'
frdD	frdDa	5'- TGGTCGCGTATTCCTGTTCC -3'
	frdDb	5'- CCGCAGGTACGTGGATTTTC -3'
napA	napAa	5'- GATGGGCTGCTATGACGACA -3'
	napAb	5'- GGTTAGTGATGCGCGACCA -3'
narG	narGa	5'- CGATTATCCGGCGACTTACG -3'
	narGb	5'- TCTCGCTCTGGGTGTTCCAG -3'
cyoA	cyoAa	5'- GGCATTGCTACCGTGAATGA -3'
	cyoAb	5'- AGACGCGGAATGAAGAAGGA -3'
cyoB	cyoBa	5'- CTGACCTCCGTCGACCATAAA -3'
	cyoBb	5'- TGGCTACGCATCATAATGGC -3'
cyoC	cyoCa	5'- CACGGTCTGCACGTCACTTC -3'
	cyoCb	5'- CACATGATGCGGGTACGGT -3'
cyoD	cyoDa	5'- CCTGGCAATGGCAGTGGTAC -3'
	cyoDb	5'- TGAAGACAAACGCCGTCATG -3'
h. Genes de fermentación, producción y utlización de acetato		
ldhA	ldhAa	5'- GGCGTGATGATCGTCAATACC -3'
	ldhAb	5'- ACGTCCATACCCAACGAACC -3'
pta	ptaa	5'- ACAATGTTGATCCGGCGAAG -3'
	ptab	5'- CATATCGATCGCACGAGTCG -3'
ackA	ackAa	5'- CTGGTTCTGAACTGCGGTAGTTC -3'
	ackAb	5'- GGCAGGTGGAAACATTCGG -3'
adhE	adhEa	5'- AAGTCCCTGTGTGCTTTCGG -3'
	adhEb	5'- TGCAGAGCCTGACCATCAGA -3'
poxB	poxBa	5'- AAAAGCCGATCGCAAGTTTC -3'
	poxBb	5'- GGTGAATGGCTTTCTCGCTC -3'
i. Reguladores		
cyaA	cyaAa	5'- AGCGCCAATTGCTACAACGT -3'
	cyaAb	5'- ACGGAAGCGGTTTTCATCAA -3'
crp	crpa	5'- ACCCGTCAGGAAATTGGTCA -3'
	crpb	5'- TTACCGTGTGCGGAGATCAG -3'
fruR	fruRa	5'- TCTTGTGATCCCCGATCTGG -3'
	fruRb	5'- AGCAGGCAATCAGCAGTTGA -3'
arcA	arcAa	5'- ATCACCAAACCGTTCAACCC -3'
	arcAb	5'- ACGCTACGACGTTCTTCGCT -3'
arcB	arcBa	5'- AATCTGACGGCGCAGGATAA -3'
	arcBb	5'- TGACCCAGCTGTTGCAGATG -3'
mlc	mlca	5'- GGTCCAGTCTCGCGTATCGA -3'
	mlcb	5'- TCTTGCACCAGGTGTGCTTC -3'
ihfA	ihfAa	5'- GGCGAACAGGTGAAACTCTCTG -3'
	ihfAb	5'- GTAATGGGAATATCCTCGCCC -3'
ihfB	ihfBa	5'- GCCAAGACGGTTGAAGATGC -3'
	ihfBb	5'- GAGAAACTGCCGAAACCGC -3'
iclR	iclRa	5'- CTTTATGGTCGGCAGCAGCT -3'
	iclRb	5'- ATTGACCGTTTCGCCAGACT -3'
fadR	fadRa	5'- CGCTGGGCTTCTACCACAAA -3'
	fadRb	5'- AATCTCGCCACTCTCATGCC -3'
rpoS	rpoSa	5'- GGACGCGACTCAGCTTTACC -3'
	rpoSb	5'- CGACATCTCCACGCAGTGC -3'

6. Resultados y discusión

Para entender el fenotipo mutante PTS$^-$Glc$^+$ es importante diferenciar los fenotipos causados por la deleción del operón *ptsIHcrr* en la cepa PB11 (PTS$^-$) de los seleccionados en la cepa PB12 (PTS$^-$Glc$^+$). Por lo tanto, los resultados se presentan y discuten de manera comparativa, donde los valores de transcripción relativa por RT-PCR de 104 genes de la cepa silvestre JM101 se comparan contra los de las cepas PTS$^-$ y PTS-Glc$^+$ (PB11 y PB12 respectivamente). Los genes analizados incluyen el regulón *gal* que es responsable del transporte de glucosa

en las cepas PTS$^-$ y genes involucrados en varias funciones de diferentes secciones del metabolismo central de carbono.

6.1. Transporte y fosforilación de glucosa en cepas PTS$^-$.

Escherichia coli silvestre creciendo en condiciones micromolares de glucosa sintetiza galactosa y maltodextrinas como autoinductores que dereprimen la síntesis de los sistemas de transporte de alta afinidad por glucosa: MglB y la maltoporina LamB, responsables del transporte de glucosa bajo estas condiciones. Otros genes que se inducen en estas condiciones incluyen el operón *galETK* (Death y Ferenci, 1994; Ferenci, 2001). Recientemente, el análisis de la expresión génica en cepas de *E. coli* silvestre en respuesta a un cambio de condiciones de glucosa no limitante a glucosa limitante ($(\mu=0.1h^{-1})$ en cultivos en quimiostato, demuestra que en estas condiciones, varios genes incluyendo *mglB* (10 veces) y *lamB* (20 veces), así como *aceA*, el operón *acs* (*acs, yjcG*), y *fumA* están sobreexpresados (Hua *et al.*, 2004).

La cepa PB11 PTS$^-$ crece muy lentamente en medio mínimo con relativamente alta concentración de glucosa (2g/L) como única fuente de carbono. Por lo tanto, es de esperarse que esta cepa sense bajas concentraciones de glucosa o glucosa-6P interna (condiciones similares a las reportadas por Hua, 2004). Para determinar si esta condición fisiológica permite la inducción de sistemas de transporte de alta afinidad similares o alternativos a los reportados, se determinaron los niveles de expresión relativos de genes relacionados a esta respuesta en las cepas PTS$^-$ y en la cepa silvestre JM101. Como se muestra en la tabla 6, La cepa PB11 desregula la transcripción de *mglB* (13 veces) y *lamB* (17.6 veces) comparada con la cepa JM101. Esta cepa también induce la expresión de otros genes del regulón *gal* como *galP* (12.4 veces), *galS* (4.9 veces), *galE* (38.8 veces), *galT* (35.6 veces), *galK* (39 veces). De estos datos se puede inferir que en esta condición de crecimiento, PB11 induce la síntesis de galactosa como autoinductor del regulón *gal* (Death y Ferenci, 1994). Esto a su vez, debe inactivar GalS y GalR, los represores del regulón (Geanacopoulos y Adhya, 1997), dando como resultado la inducción de los genes del regulón *gal*, permitiendo así la internalización de glucosa a través de los transportadores de galactosa (Ferenci, 2001) ya que GalP y Mgl tienen mayor afinidad por glucosa que por su propio azúcar (Vyas et al., 1991).

Los resultados indican que la PB11 probablemente utilice MglB y/o GalP para transportar glucosa a través de la membrana citoplasmática hacia el citosol en estas condiciones de crecimiento. Sin embargo, el bajo crecimiento en glucosa indica que esta cepa es incapaz de fosforilar toda la glucosa que entra con la cantidad de Glk disponible en esta cepa PTS$^-$ (Curtis y Epstein, 1975; Flores *et al.*, 2002).

La cepa PB12 es una mutante derivada de PB11 que ha recuperado la capacidad de crecer rápido en glucosa. Esto se puede explicar por el hecho de que el gene *glk* se transcribe a un mayor nivel (2 veces) comparada con la cepa PB11 y la silvestre. Por lo tanto, el producto proteico (Glk) de este gene desregulado cuya actividad específica también se incrementa 2 veces en la PB12 (Flores *et al.*, 2002), permite un mayor grado de fosforilación de la glucosa transportada en la PB12 que en la PB11. La PB12 que no tiene ninguna mutación

en los genes del regulón *gal*, también utiliza GalP para transportar glucosa (Flores *et al.*, 1996; Flores *et al.*, 2002). En éste sentido y de acuerdo con lo anterior, en esta cepa el nivel de transcrito de *galP* es 12.4 veces mayor que en la cepa silvestre. Así, la glucosa puede ser transportada por GalP y fosforilada a una mayor velocidad por Glk en la PB12 comparada con la PB11 permitiendo una mayor tasa de crecimiento.

Diferencias en las capacidades de crecimiento entre estas cepas pueden también estar relacionadas a la disponibilidad de moléculas reguladoras como AMPc. El complejo CRP-AMPc juega un papel importante en la activación de la transcripción de muchos genes incluyendo aquellos del regulón *gal*, y se sabe que una deleción del gene *crp* inactiva completamente la expresión del operón *galETK* y del gene *galS* (Weickert y Adhya, 1993; Geanacopoulos y Adhya, 1997). También se ha reportado que algunas cepas de *E. coli* que llevan una deleción del operón PTS producen menos AMPc que las cepas silvestres (Levy *et al.*, 1990). No obstante, los resultados obtenidos indican que estas cepas PTS$^-$ deben tener suficiente complejo CRP-AMPc para activar aquellos genes que lo requieren como *galETK, galS* y otros como genes de TCA. Esto está apoyado por el hecho de que en PB11 y PB12, el nivel de transcripción de *cyaA*, que codifica para la adenilato ciclasa, está ligeramente sobreexpresado. Los resultados indican que en ausencia del componente IIA^{Glc} de PTS, que está involucrado en la activación de la adenilato cilcasa (Postma *et al.*, 1996), podría haber otras enzimas que pudieran llevar a cabo esta activación en estas cepas, si esto fuera necesario.

6.2. Catabolismo de glucosa-6P a piruvato.

El análisis de los flujos de carbono y los valores de RT-PCR indican que PB11 y PB12 tienen diferentes capacidades que les permiten metabolizar glucosa (y otras moléculas) como fuente de carbono. Como ya se mencionó, las cepas PTS$^-$ requieren Glk para fosforilar glucosa. La PB11 que tiene un bajo flujo glicolítico (42%) en el primer paso de la vía EMP comparado con la silvestre (77%) y la PB12 (95%), transporta glucosa a una tasa muy baja y está usando tanto la vía de las pentosas como la vía glicolítica para catabolizar glucosa-6P en proporciones similares. Sin embargo, la PB12 recuperó un crecimiento relativo mas rápido (μ = 0.42 h^{-1}) probablemente debido a una sobreexpresión de *glk* y también de *pgi* que permite una tasa mayor de fosforilación y una transformación inicial de glucosa en fructosa-6P. Esta cepa ha modificado su flujo en los pasos iniciales incrementando su flujo glicolítico en el primer paso de la vía a 95% (Flores *et al.*, 2002).

Originalmente pensamos que el alto flujo glicolítico en los pasos iniciales del catabolismo de glucosa en la PB12 podría ser responsable de la síntesis de una alta poza de fructosa-6P, fructosa-1,6diP o ambos que aquella usualmente presente en una cepa silvestre. Esta situación, de ser cierta, podría resultar en la inactivación *in vivo* de Cra (o FruR), el represor codificado por *fruR*. Ya que *glk* se reprime por Cra, bajo este escenario la transcripción de *glk* podría sobreexpresarse en esta cepa (Meyer *et al.*, 1967; Saier y Ramseier, 1996). Sin embargo, éste no parece ser el caso ya que el nivel de transcripción de varios genes como *pykF, pckA* y *edd* que también se reprimen por Cra, no incrementa en la PB12. Para establecer si el cambio en la expresión de *glk* y *pgi* pudieran ser el

resultado de una mutación en sus regiones reguladoras, se determinó la secuencia nucleotídica de aproximadamente 250 pb hacia arriba del sitio de inicio de la traducción y las regiones estructurales completas de estos dos genes en todas las cepas. Sin embargo, no se detectó ninguna mutación. También se determinaron las secuencias nucleotídicas de la región reguladora y estructural de *fruR*, sin encontrar tampoco ninguna mutación.

Es importante tener en cuenta que no hay diferencias significativas en los flujos de carbono de la cepa silvestre y la PB12 en los pasos restantes de la vía EMP desde fructosa-6P hasta la síntesis de PEP, mientras que hay una disminución en el flujo de la PB11 comparado al de las otras cepas en esta parte de la vía (Flores *et al.*, 2002). Estos resultados concuerdan con los valores de RT-PCR que muestran que los niveles de expresión de los genes involucrados en la transformación de fructosa-6P en PEP de la JM101 y la PB12 se expresan básicamente al mismo nivel, mientras que este grupo de genes en general, están ligeramente disminuidos en la cepa PB11. Sin embargo, este último grupo de valores debe tomarse con cautela debido a que algunos de ellos se encuentran dentro de los límites del error experimental.

Las cepas PTS$^-$ no pueden sintetizar piruvato (PYR) a partir de PEP usando PTS. Por tanto, deben usar las dos piruvato cinasas codificadas por *pykA* y *pykF* para este propósito. En estas cepas PTS$^-$ los valores de flujo de carbono de PEP a PYR vía las piruvato cinasas son significativamente mayores que el de la cepa silvestre para compensar la ausencia de PTS. Sin embargo, la expresión de los genes *pyk* disminuye ligeramente en la PB11 y no cambian significativamente en la PB12. Estos resultados indican que la actividad de piruvato cinasa total presente en las cepas PTS$^-$ es suficiente para convertir PEP en PYR a tasas similares a las de la JM101. El PEP también puede convertirse en oxaloacetato (OAA) por la enzima fosfoenolpiruvato carboxilasa (Ppc) codificada por *ppc*, cuya transcripción está ligeramente disminuida en las cepas PB11 y PB12 comparadas con la JM101.

6.3. Transformación de piruvato en acetato y acetil coenzima A.

Una vez que el piruvato se ha sintetizado a partir de PEP, puede ser transformado en acetil coenzima A (AcCoA), para poder ser incorporado en el ciclo TCA y/o al "shunt" de glioxalato. En *E. coli* silvestre creciendo en condiciones aeróbicas y altas concentraciones de glucosa, esta reacción es catalizada principalmente por el complejo de la piruvato deshidrogenasa (Pdh) codificada por los genes *aceE, aceF* y *lpd* que conforman el operón *pdh* (Quail *et al.*, 1994). La expresión de los dos primeros genes está disminuida en la cepa PB11, mientras que el valor de *lpd* es similar comparado con la JM101.

En el caso de la PB12, los primeros dos genes están ligeramente sobreexpresados y *lpd* está sobreexpresado dos veces. Estos valores de transcripción en las dos cepas PTS$^-$, especialmente en la PB11, no concuerdan con el aumento de dos veces en los flujos de carbono detectados de PYR a AcCoA comparados con la cepa silvestre. Sin embargo, en este contexto es importante hacer notar que el gene *poxB* que codifica para la piruvato oxidasa (PoxB), una enzima que convierte piruvato en acetato y simultáneamente reduce quinonas en la membrana, está altamente sobreexpresado (4 a 5 veces) en

ambas cepas PTS$^-$. Estos resultados soportan nuestra propuesta de que en las cepas PTS$^-$ esta enzima puede estar produciendo acetato, que a su vez puede ser transformado en AcCoA, lo cual explica el incremento en el flujo de carbono entre PYR y AcCoA. Esto concuerda con la sobreexpresión (6 y 8 veces en PB11 y PB12 respectivamente) del gene *acs* cuyo producto, la acetil-CoA sintasa (Acs) convierte acetato en AcCoA (Phue and Shiloach, 2004). Además, el gene *yjcG* (*actP*) que es parte del operón *acs* y codifica para una acetato permeasa (Gimenez *et al.*, 2003), también está sobreexpresado. Como se discutirá posteriormente, el acetato (o un metabolito relacionado) producido probablemente por PoxB puede ser el autoinductor del operón *acs* y de los genes del "shunt" de glioxalato que están sobreexpresados en las cepas PTS$^-$.

6.4. Los genes que codifican para las enzimas del TCA y el "shunt" de glioxalato.

AcCoA y OAA son sustratos de la citrato sintasa (GltA). Los flujos de carbono a través de GltA y Ppc representan las principales rutas para alimentar de carbono al ciclo TCA. Por otro lado, la extracción de carbono a partir de este ciclo es catalizada principalmente por la enzima fosfoenolpiruvato carboxicinasa (Pck) para sintetizar PEP y las enzimas málicas (MEZ) para producir PYR así como otras enzimas que lo utilizan para procesos biosintéticos (Neidhart *et al.*, 1990). El flujo de carbono a través de GltA está incrementado en la PB11 mientras la transcripción del gene *gltA* es básicamente la misma comparada con JM101 y PB12. Estos resultados indican que la cantidad de la enzima GltA presente en las cepas PTS$^-$ debe tener la capacidad de llevar a cabo la síntesis de citrato sin un incremento adicional en la transcripción de su gene.

En la cepa PB11 el flujo de carbono entre citrato y malato tiene casi triplicado su valor con respecto a la JM101 y la PB12. Este resultado concuerda con la sobreexpresión de varios genes involucrados directamente en la biosíntesis de malato en esta cepa. Entre estos genes están *aceB* (15.6 veces), *aceA* (11.9 veces) y *aceK* (5.5 veces) que integran el operón *aceBAK* y codifican para las enzimas del "shunt" de glioxalato. Los productos de estos genes convierten isocitrato en malato y succinato con la utilización de una molécula extra de AcCoA en el proceso (Cronan y Laporte, 1996). Es de particular interés que la expresión de *glcB* que codifica para otra malato sintasa también está altamente elevada (11.7 veces) en esta cepa. La expresión de *fumA* (3.3 veces) y *fumC* (4.3 veces), dos enzimas que convierten fumarato en malato, están también altamente expresadas. Sin embargo, *fumC* que se induce en condiciones de estrés, no se considera una enzima de TCA (Cunninham y Guest, 1998). Los genes restantes del TCA (con excepción de *acnA* que también es un gene de estrés) se expresan básicamente al mismo nivel de la cepa silvestre. Estos resultados indican que la cepa PB11 está usando principalmente el "shunt" de glioxalato para sintetizar malato y succinato. Esta estrategia debería permitir a la cepa PTS$^-$, que se encuentra bajo estrés nutricional debido a la baja concentración interna de glucosa o glucosa-6P, la posibilidad de retener más átomos de carbono en la célula. Esta hipótesis está sustentada por el hecho de que el AcCoA no se oxida completamente cuando se utiliza el "shunt" de glioxalato. Por lo tanto, no se producen dos moléculas de CO_2 y se incorpora una molécula extra de AcCoA en cada vuelta del "shunt". Esta propuesta concuerda con los resultados reportados

por Hua et al., (2004) quien demuestra que en una cepa silvestre de *E. coli* creciendo en condiciones de limitación de glucosa (μ = 0.1 h^{-1}), se sobreexpresan los genes *aceA* y *fumA* y produce menos CO_2 que cuando crece en condiciones no limitantes de glucosa.

Las cepas PB12 y JM101 tienen flujos de carbono similares entre citrato y malato. Es claro que los genes que codifican para las enzimas del "shunt" de glioxalato están aún sobreexpresadas en la PB12 pero no tanto como en la PB11: *aceB* (15.6 *vs.* 3.7, veces) *aceA*, (11.9 *vs.* 1.9 veces), *aceK* (5.5 *vs.* 1.9 veces). Los genes restantes de TCA están también ligeramente sobreexpresados en la PB12, entre 1.3 y 2 veces con respecto a la PB11 y JM101. Algunos de los valores de los genes del TCA están dentro de los límites del error experimental, pero si son reales, esto puede sugerir que la PB12, en contraste con la PB11, usa tanto el "shunt" de glioxalato como el TCA.

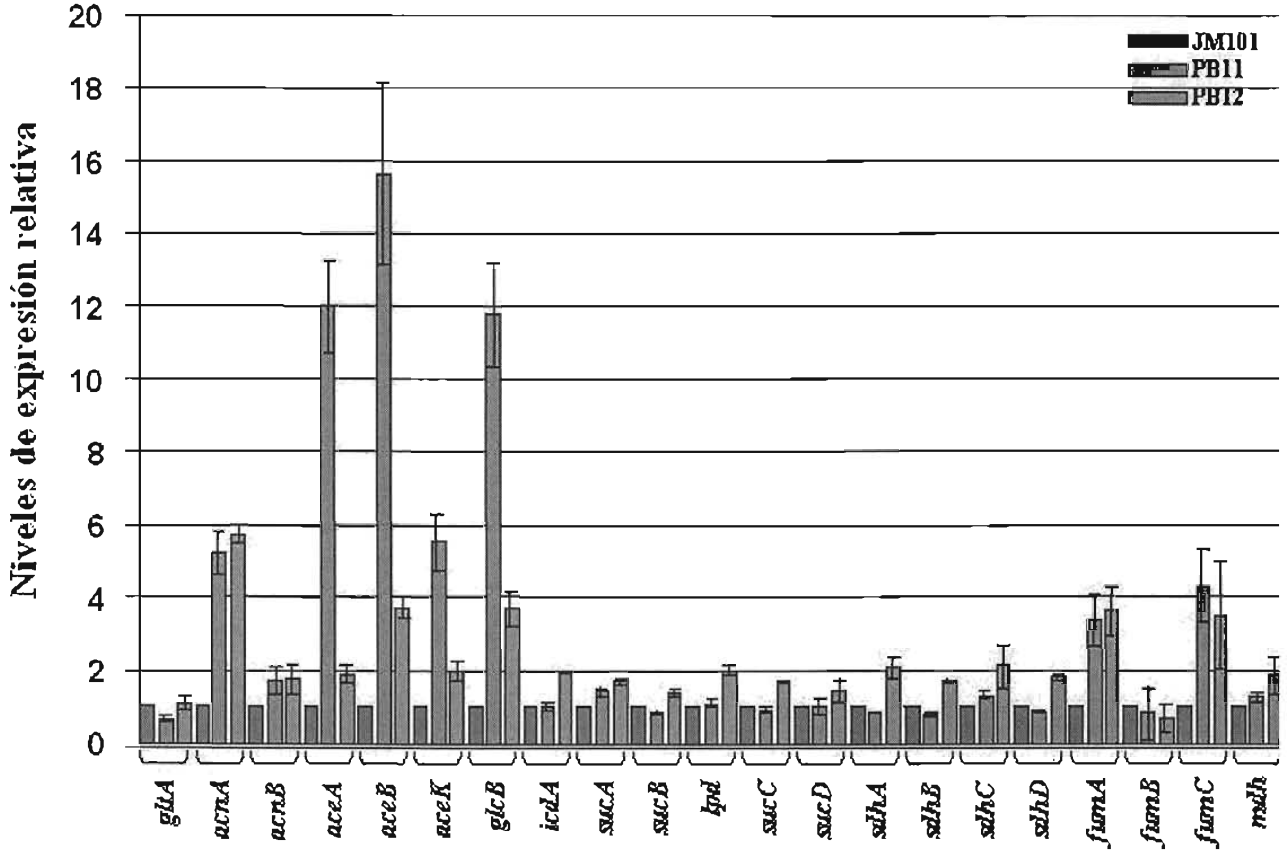

Figura 7. Valores de expresió relativa de genes que codifican para las enzimas del ciclo TCA.

6.5. Genes anapleróticos y capacidades gluconeogénicas de las cepas PTS⁻.

El malato puede ser transformado en OAA usando la malato deshidrogenasa codificada por *mdh* y el OAA puede ser transformado en PEP por la PEP-carboxicinasa (Pck) codificada por el gene *pckA*. En la PB12 ambos genes están sobreexpresados y se transcriben casi al mismo nivel en la JM101 y en la PB11.

El malato también puede convertirse en PYR por las enzimas MEZ (MaeB y SfcA) codificadas por los genes *maeB* y *sfcA*. Ambos genes se sobreexpresan alrededor de 2 veces en la PB12 mientras sólo *sfcA* se sobreexpresa en la PB11 (1.9 veces). Finalmente, el gene *pps* que codifica para PEP sintasa, que convierte PYR en PEP, se sobreexpresa 3.7 y 2.4 veces respectivamente en PB11 y PB12. Los flujos de carbono previamente determinados indican que la PB11 aparentemente utiliza la enzima Pck para la transformación de OAA en PEP. Sin embargo, *pckA* se transcribe básicamente al mismo nivel en la PB11 y la JM101 mientras *sfcA*, *pps* y *maeB* se sobreexpresan en la PB11 indicando que esta cepa está usando los productos de estos genes en vez de Pck para drenar carbono del TCA. Por otro lado, en la PB12 los flujos de carbono indican que esta cepa está usando las enzimas MEZ para la biosíntesis de PYR a partir de malato para depleción de carbono del ciclo. Esto concuerda con la sobreexpresión de estos dos genes en esta cepa y con el incremento de las actividades específicas de MaeB y SfcA que están incrementadas en la cepa PB12 (J. Sigala, comunicación personal). Estos resultados indican que ambas cepas PTS⁻ pueden tener la posibilidad de utilizar simultáneamente sus capacidades glicolíticas y gluconeogénicas. Por esta razón determinamos y comparamos los valores de RT-PCR de varios genes involucrados en la transformación de PEP en glucosa así como otros genes que también pueden participar en la respuesta gluconeogénica en estas cepas.

Se sabe que algunas enzimas codificadas por los genes glicolíticos también participan en la respuesta gluconeogénica. De hecho, hay ciertos isoesquizómeros que se han involucrado específicamente en ésta vía, incluyendo las enzimas codificadas por *fbaB, fbp,* y *pfkB* (Frankel, 1996). Como se puede ver (Tabla 6), estos genes y también *gpmB, gapC*$_1$ y *gapC*$_2$, que pueden participar en la gluconeogénesis, están sobreexpresados tanto en la PB12 como en la PB11.

Considerando juntos estos resultados, aunados a la sobreexpresión de los operones *aceBAK* y *acs*, responsables de la utilización de acetato en las cepas PTS⁻, proponemos que estas cepas pueden utilizar simultáneamente ambas capacidades: glicolíticas y gluconeogénicas en presencia de altas concentraciones de glucosa en el medio. Para demostrar esta propuesta, se determinó la capacidad de estas cepas para crecer en medio mínimo conteniendo dos fuentes de carbono: glucosa y acetato. Las tres cepas se crecieron hasta la fase exponencial en medio mínimo con glucosa (2g/L). Las células se colectaron, se lavaron y se usaron como inóculo para un nuevo cultivo en medio con glucosa (2 g/L) y acetato (1 g/L). Como se muestra en la figura 9, la cepa silvestre creció a la misma μ de 0.71h^{-1} pero después de dos horas en la fase estacionaria, se detectó una segunda fase de crecimiento a una μ mas baja. Las mediciones de acetato y

glucosa en el medio claramente demuestran que la cepa silvestre utiliza glucosa

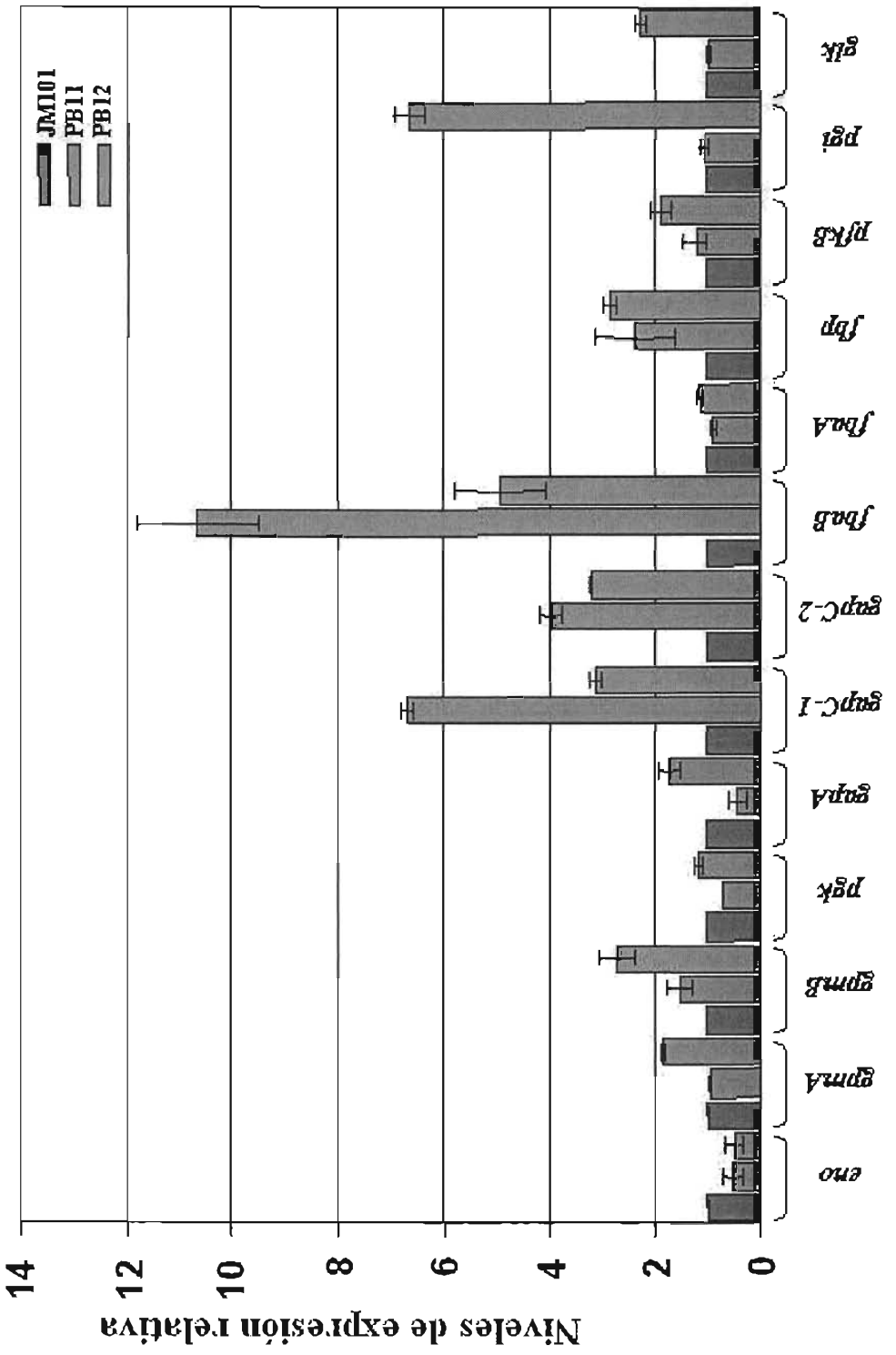

Figura 8. Valores de expresión relativa de genes involucrados en gluconeogénesis.

como única fuente de carbono durante la primera etapa de crecimiento y acetato en la segunda etapa, como se esperaba.

Por el contrario, PB11 y PB12 no presentan un patrón de crecimiento diáuxico y ambas cepas crecieron mas rápido [PB11 (μ= 0.3 *vs.* μ= 0.1h^{-1}), y PB12 (μ= 0.48 h^{-1} *vs.* μ= 0.4h^{-1})] que las cepas creciendo en glucosa como única fuente de carbono. Las mediciones de concentración de glucosa y acetato demuestran que estas cepas PTS$^-$ usan ambas fuentes de carbono simultáneamente (N. Flores, manuscrito en preparación). Estos resultados apoyan la hipótesis de que estas cepas pueden utilizar simultáneamente sus capacidades glicolíticas y gluconeogénicas en ausencia del sistema PTS.

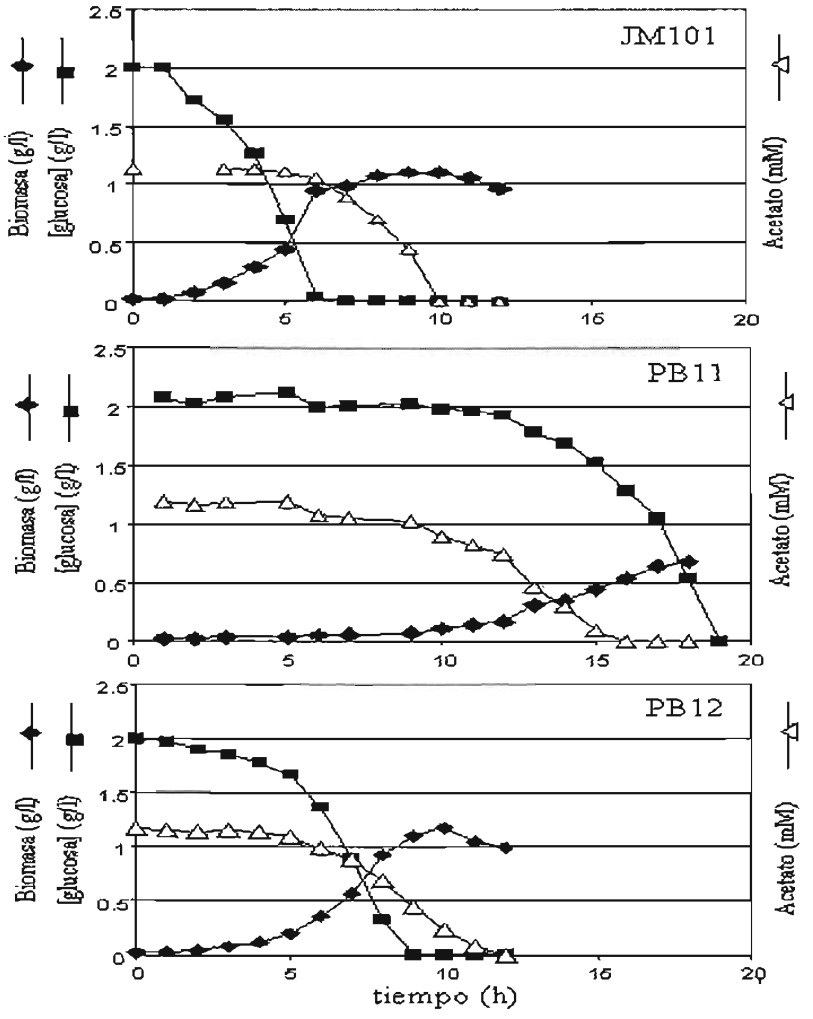

Figura 9. Cinéticas de crecimiento y utilización de fuentes de carbono de la cepa silvestre JM101 y las derivadas PTS$^-$ en medio mínimo con glucosa y acetato.

6.6. Regulación de los genes del "shunt" de glioxalato y del TCA en cepas PTS⁻.

Cuando la PB12 recuperó la capacidad de utilizar glucosa mas eficientemente que la PB11, también recuperó parcialmente la capacidad de modular la expresión de los genes del "shunt" de glioxalato. Sin embargo, el patrón de expresión de los genes del "shunt" de glioxalato y del TCA es diferente en PB12 del de PB11 y JM101, indicando que los reguladores de estas vías metabólicas deben estar funcionando aún, aunque no exactamente de la misma manera. Por tal razón, se secuenciaron algunos de genes reguladores cuyos productos proteicos participan en la regulación de los genes del "shunt" de glioxalato y del TCA y sólo se detectó una mutación en el gene *arcB* de la cepa PB12.

Las enzimas del TCA están reguladas principalmente a nivel transcripcional por dos moduladores específicos: CRP y el sistema de dos componentes ArcA/B, aunque hay otros reguladores específicos para ciertos genes. La represión catabólica de los genes del TCA se ha demostrado en cepas mutantes *crp*⁻ en donde la expresión de estos genes disminuye (Cronan y Laporte, 1996; Gosset *et al.*, 2004). Sin embargo, PB11 y PB12 tienen suficiente AMPc y CRP para permitir la activación de *galETK* y *galS* que están controlados por este regulador, lo cual está apoyado por la sobreexpresión de estos genes (tabla 6). Por otro lado, todos los genes que codifican para las enzimas de TCA y el "shunt" de glioxalato así como otros genes, están reprimidos por el sistema de dos componentes ArcA/B (Iuchi y Lin, 1988; Iuchi *et al.*, 1990; Liu y DeWulf, 2004). Durante condiciones anaeróbicas, ArcB se autofosforila y cataliza la transfosforilación de ArcA. En estas condiciones, ArcA está a su máximo nivel de fosforilación y ocurre la represión total de los genes regulados por ArcA-P. En condiciones aeróbicas, las formas oxidadas de las quinonas inhiben la autofosforilación de ArcB (Georgellis *et al.*, 2001). En esta condición sólo una pequeña fracción de ArcA se puede fosforilar y por tanto la represión de muchos de los genes regulados por ArcA-P disminuye (Shen and Gunsalus, 1997). Esto explica por qué la expresión de todos los genes del TCA y el "shunt" de glioxalato se incrementa de 1.3 a 2 veces en cepas *arcA*⁻ aún en aerobiosis (Iuchi y Lin, 1988; Cunningham *et al.*, 1997; Shen y Gunsalus 1997; Chao *et al* 1997; Park *et al* 1997; Cunningham y Guest 1998). Como ya se mencionó, en la cepa PB11 la mayoría de los genes del TCA se transcriben aproximadamente al mismo nivel de la JM101 con excepción de *fumA,* y el operón *aceBAK* que están sobreexpresados. Este operón está regulado por varios moduladores: CRP, ArcA, IclR, Ihf, FadR y posiblemente FruR (Cra) (Cronan and Laporte, 1996). La alta sobreexpresión de este operón en la PB11 probablemente es el resultado de la inactivación de algunos de estos represores pero principalmente IclR. Este represor se libera de la región –35 del promotor y se induce la transcripción en cepas silvestres adaptadas a crecimiento en acetato. Sin embargo, el acetato no está directamente involucrado en la regulación del operón *aceBAK*. Se ha propuesto que algún metabolito relacionado podría unirse a IclR para desreprimir al operón *aceBAK* (Cortay *et al.*, 1991; Cronan and Laporte, 1996). También se ha demostrado que FadR activa la expresión de *iclR* y por tanto regula indirectamente al operón *aceBAK* (Gui *et al.*, 1996). ArcA también reprime al operón *aceBAK* bajo condiciones anaeróbicas; aunque la inactivación de *arcA* permite un incremento de dos veces en la expresión de *aceBAK* aún en

condiciones aeróbicas (Iuchi and Lin, 1988). Para explicar como se induce el operón *aceBAK* en la PB11 es importante notar que esta cepa no produce acetato como producto de fermentación ya que no ha sido detectado en el medio (Flores *et al.*, 2002). Sin embargo, *poxB* está altamente sobreexpresado (4 a 5 veces) en las cepas PTS$^-$. Si PoxB está realmente activo en estas condiciones, el acetato (o un metabolito relacionado) producido de este modo, puede actuar como autoinductor de *aceBAK* inactivando IclR. Es interesante que la transcripción de *fadR* e *iclR* está claramente disminuida en PB11 comparada con JM101 y PB12. Esta situación podría también jugar un papel importante en la sobreexpresión de *aceBAK* en la PB11, ya que podría indicar que hay menos cantidad de represor IclR en la PB11 que en las otras dos cepas.

Cuando se analizan los perfiles de transcripción de los genes de TCA y del "shunt" de glioxalato en la cepa PB12, es importante notar como ya se ha mencionado, que todos los genes de TCA están ligeramente sobreregulados (entre 1.3 y 2 veces) así como los genes del operón *aceBAK* que están sobreexpresados entre 2 y 3.7 veces con respecto a la JM101. Algunas de estas diferencias se pueden explicar por la presencia de una mutación en el gene *arcB* de la cepa PB12 que cambió un residuo de Tyr en la posición 71 a un residuo de Cys. Esto podría inactivar o disminuir la función de Arc en esta cepa. Como una caracterización inicial de ésta mutante, se demostró su sensibilidad a azul de toluidina, un fenotipo característico de las mutantes *arcA*$^-$ y *arcB*$^-$ (Iuchi *et al.*, 1988). La cepa PB12 no puede crecer en placas de agar con azul de toluidina y la introducción de un plásmido que lleva el gene silvestre del gene *arcB* restablece su capacidad de crecer en este compuesto (Figura 10). Cuando la cepa PB12 recupera la capacidad de crecer rápidamente en glucosa, también recupera la capacidad, al menos parcialmente, de reprimir el operón *aceBAK*. En concordancia, los genes *iclR* y *fadR* se transcriben básicamente a los mismos niveles en PB12 y JM101. Sin embargo, es importante reconocer que el operón aceBAK está sobreexpresado en la PB12 (3.7 a 2 veces) en menor extensión que la PB11 (15.6 – 5.5 veces), pero aún mayor que la transcripción de los genes de TCA en la misma cepa PB12 (1.3 y 2 fold). Por lo tanto, para explicar las diferencias en los niveles de expresión entre los genes de TCA y del "shunt" de glioxalato, parece razonable proponer que el represor IclR en la PB12 está parcialmente inactivado. Si este fuese el caso, el acetato producido por PoxB, cuyo gene está sobreexpresado 5 veces en esta cepa, podría jugar un papel en la inactivación parcial de IclR. Por lo tanto, la mutación en *arcB* ($ArcB_{Tyr71Cys}$) puede ser responsable de la sobreexpresión de los genes de TCA (1.3 a 2 veces) pero solo parcialmente responsable de la sobreexpresión del operón *aceBAK* en la PB12.

6.7. Regulación de otros genes por ArcA/B: lpd, el locus glc y ciertos genes que codifican para enzimas respiratorias.

Hay otros genes regulados por ArcA/B y entre ellos *lpd*, que codifica para el componente deshidrogenasa E3 de Pdh y Sdh. La expresión de este gene está también incrementada 2 veces en la PB12. En *E. coli*, el locus *glc* asociado con la utilización de glicolato, incluye el gene *glcB* que codifica para una malato sintasa y

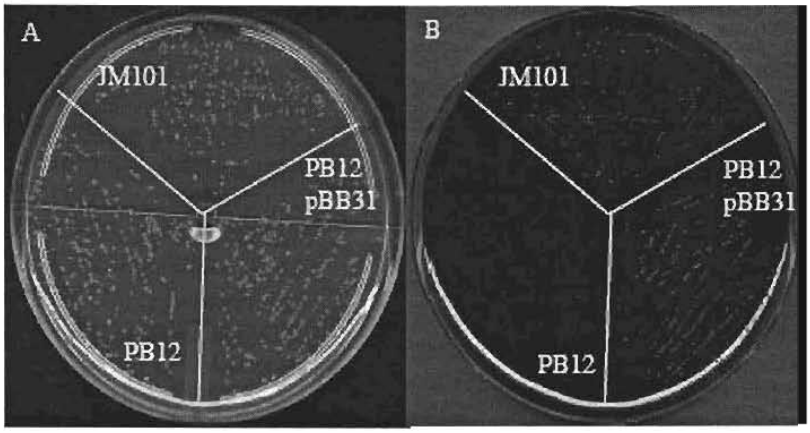

Figura 10. Crecimiento de la cepa PB12 con la mutación en ArcB (PB121). Esta cepa es sensible a azul de toluidina. Panel A crecimiento en medio sin azul de toluidina. Panel B crecimiento con azul de toluidina.

otros genes necesarios para la actividad oxidasa de glicolato, así como *glcC* que codifica para una proteína activadora. Las rutas metabólicas especificadas por los operones *glc* y *aceBAK* producen glioxalato como intermediario común, el cual se utiliza por las dos malato sintasas codificadas por *glcB* y *aceA*. Pellicer *et al.,* (1999) demostraron que mutantes nulas en cualquiera de estos genes no exhiben fenotipo alguno debido a la inducción cruzada del operón *aceBAK* por glicolato y el operón *glc* por acetato . En el mismo estudio, también se demostró que la regulación del operón *glc* incluyendo *glcB*, está bajo control positivo de GlcC codificado por un gene divergente. Además, se demostró que la expresión del operón *glc* al igual que la del operón *aceBAK*, está controlada negativamente por ArcA. De manera interesante, el patrón de transcripción de *glcB* es similar al del operón *aceBAK* en las cepas PB11 y PB12: está altamente expresado en la PB11 (mas de 10 veces) y menos, pero aún relativamente sobreexpresado en la PB12. Nosotros pensamos que el acetato producido vía PoxB, podría también jugar un papel importante en la sobreexpresión del operón *glc* y del gene regulador *glcC* en las cepas PB11 y PB12. La inactivación de ArcB o el incremento de su actividad desfosforilante en ArcA-P (Georgellis, *et al.*, 1998; Malpica *et al.*, 2004) en PB12 podría contribuir a la sobreexpresión de *glcC* y *glcB* como ocurre con el operón *aceBAK*.

En la PB11 la transcripción de los genes que codifican para cuatro de las reductasas del sistema respiratorio (CyoABCD, CydAB, FrdABCD, NarG) está disminuida al igual que *ubiE* que está involucrado en la biosíntesis de ubiquinona. La transcripción de los genes que codifican para las deshidrogenasas involucradas en la transferencia de electrones desde sustratos a quinonas durante el primer paso de la cadena respiratoria (*NuoAN, Ndh, SdhABCD*), están también disminuidos comparados con los de las cepas JM101 y PB12. El único gene respiratorio que está altamente expresado en la PB11 (4 veces) y en la PB12 (5 veces) es *poxB*, cuya enzima utiliza PYR como donador de electrones y produce acetato en estas cepas PTS^-. Este gene podría jugar un papel dual al menos en la PB11: en la respiración por reducir las quinonas en la membrana y en la inducción de los operones *aceBAK* y *acs* produciendo acetato. No obstante, parece que las

capacidades respiratorias de la PB11 están disminuidas comparadas con las de las otras dos cepas. ArcA regula la expresión de varios de estos genes y la expresión de *sdhABCD*, y *cyoABCD*, que son ejemplos de esta situación, están aparentemente ligeramente sobreexpresados en la PB12 comparada con JM101 y PB11. Sin embargo, este último grupo de valores se debe tomar con cautela debido a que algunos de ellos se encuentran dentro de los límites de error experimental.

6.8. Genes relacionados con los procesos de fermentación y producción y utilización de acetato en cepas PTS⁻.

Los niveles de transcripción de genes involucrados en la producción de productos de fermentación (*ldhA, adhE, pta,* y *ackA*) están ligeramente disminuidos en la PB11 comparados con la JM101. De hecho, se ha reportado que la PB11 no produce ningún producto de fermentación detectable (Flores *et al.,* 2002). Los valores de transcripción de estos genes son básicamente los mismos entre la cepa PB12 y la JM101 con excepción de *pta* que está sobreexpresado (1.8 veces) en esta cepa PTS⁻.

La PB12 produce pequeñas cantidades de lactato y menos acetato (que se produce en la fase log) que la JM101 (Flores *et al.,* 2002; Flores S., comunicación personal).

Se ha propuesto que en *E. coli* la ruta de acetato fosfotransacetilasa-cinasa codificada por *pta* y *ackA*, funciona primariamente con un papel catabólico generando ATP durante crecimiento aeróbico en exceso de glucosa. Estas enzimas también catalizan la ruta reversa de alta afinidad que se activa cuando el acetato está presente extracelularmente en grandes cantidades. Sin embargo, la ruta de Acs que incluye la AcCoA sintasa (Acs) y una permeasa de acetato, codificadas por los genes *acs* y *yjcG* (*actP*), se inducen por acetato para propósitos de "scavenging" de ésta molécula (Gimenez *et al.,* 2003; Phue y Shiloach, 2004). Como se mencionó anteriormente, pensamos que estas dos cepas PTS⁻ pudieran usar PoxB para producir acetato como el autoinductor responsable de la sobreexpresión de los operones *aceBAK* y *acs*. El acetato producido internamente debería ser transformado en AcCoA por Acs, codificada por *acs* que está altamente sobreexpresado al igual que los genes *yjcG* (*actP*) y *poxB* en ambas cepas PTS⁻, y finalmente se incorpora en TCA y/o en el "shunt" de glioxalato.

Es relevante enfatizar que *poxB* y *acs* así como muchos otros genes, tienen promotores dependientes de RpoS (Chang *et al*, 1994; Shin *et al.*, 1997; Hengge-Aronis, 2002). La transcripción de *rpoS* está elevada en las cepas PB11 y PB12 (2.9 y 2.2 veces respectivamente). Esto podría explicar la sobreexpresión de los genes *poxB* y *acs* en estas cepas PTS⁻.

Todos estos resultados indican que las cepas PTS⁻ han modificado sus capacidades de convertir PYR en AcCoA no solo con el uso de la Pdh sino también con la participación de la piruvato oxidasa y la AcCoA sintasa.

6.9. La vía de las pentosas fosfato y la capacidad de sintetizar compuesto aromáticos en la cepa PB12.

En la cepa JM101 22% de la glucosa-6P se dirige a través de la glucosa deshidrogenasa (Zwf) cuando crece aeróbicamente en glucosa como única fuente de carbono. La transcripción del gene *zwf* en PB11 está ligeramente disminuida mientras que en PB12 está ligeramente sobreexpresado. Estos resultados concuerdan con las actividades específicas de Zwf (Flores *et al.*, 2002). Se ha demostrado previamente que la PB12 utiliza intermediarios de la ruta EMP para sintetizar ribosa-5P (R5P) y eritrosa-4P (E4P) por la acción secuencial de transcetolasas y transaldolasas (Frankel, 1996; Flores *et al.*, 2002). Como se puede ver en la tabla 6c, los genes *tktB* y *talA* que forman parte de un operón que codifica para la transcetolasa B y la transaldolasa A, están altamente sobreexpresadas en las cepas PB11 (11 veces) y PB12 (5 veces). La expresión de los genes *tktA, talB, rpiB, rpiA, rpe* y *eda* también está sobreexpresada en la cepa PB12.

6.10. La expresión de genes que codifican para proteínas reguladoras.

Determinamos los valores de transcripción de varios genes cuyos productos son proteínas reguladoras de la expresión genética. La transcripción de algunos de estos genes (tabla 6i), como *crp* no cambia significativamente en la PB11. Sin embargo, hay algunos otros genes cuyo nivel de transcripción está ligeramente elevado como *cyaA, arcB,* y *rpoS* en esta cepa PTS^-. Por otro lado, la transcripción de *iclR* y *fadR* está disminuida en la PB11. En PB12, la transcripción de algunos de estos genes como *crp, arcA* y *arcB* no cambia significativamente; pero la expresión de la mayoría de los genes restantes está ligeramente elevada.

La disminución en la expresión de los genes *iclR* y *fadR* puede jugar un papel importante en la desrepresión (15-5.5 veces) del operón *aceBAK* en PB11. Por otro lado, la sobreexpresión de estos dos genes en la PB12 puede dar como resultado una activación parcial de IclR y FadR así como del operón *aceBAK* (3.7 - 2 veces). De manera similar, el incremento en la transcripción de *rpoS* en ambas cepas puede explicar la sobreexpresión de varios genes (*poxB*, *acs*, *fumA*, *acnA*, *tktB, talA* y otros) que tienen promotores dependientes de RpoS.

Table 6. Niveles de transcripción relativa determinados por RT-PCR de varios grupos de genes de las cepas JM101, PB11 and PB12.

Ruta, proceso o grupo de genes	Proteína para la que codifica	Niveles de expresión como $2^{-\Delta\Delta Ct}$ con JM101 como valor de normalización 1.	
		PB11	PB12
a. regulón *gal*			
galE	UDP-glucosa 4-epimerasa	38.8 ± 6.864	46.6 ± 6.506
galT	Gal-1P uridiltransferasa	35.6 ± 2.376	42.5 ± 3.995
galK	galactocinasa	39.0 ± 2.376	48.21± 3.995
galM	Aldosa-1-epimerasa	8.1 ± 3.946	3.3 ± 0.692
galP	Permeasa de galactosa	12.4 ± 1.086	13.1 ± 1.867
galS	Repressor transcripcional del regulón *gal*	4.9 ± 0.477	3.2 ± 0.526
galR	Repressor transcripcional del regulón *gal*	3.2 ± 0.199	1.2 ± 0.472
galU	UTP-glucosa-1P uridiltransferasa	1.7 ± 0.309	2.1± 0.366
mglB	Transportador ABC de galactosa	13.4 ± 0.098	9.0 ± 1.606
*lamB**	Receptor de maltosa de alta afinidad	17.6 ± 0.374	0.9 ± 0.019
*pgm**	fosfoglucomutasa	1.7 ± 0.310	2.3 ± 0.458
b. Glicólisis			
glk	glucocinasa	1.0 ± 0.032	2.2 ± 0.103
pgi	Fosfoglucosa isomerasa	1.0 ± 0.080	6.6 ± 0.282
pfkA	fosfofructocinasa	0.3 ± 0.040	0.5 ± 0.012
fbaA	Fructosa bifosfato aldolasa	0.9 ± 0.046	1.1 ± 0.052
tpiA	Triosa fosfato isomerasa	0.5 ± 0.034	1.8 ± 0.029
gapA	Gliceraldehído-3P deshidrogenasa	0.4 ± 0.151	1.7 ± 0.214
pgk	Fosfoglicerato cinasa	0.7 ± 0.001	1.2 ± 0.060
gpmA	Fosfoglicerato mutasa	0.9 ± 0.007	1.8 ± 0.039
eno	enolasa	0.5 ± 0.169	0.5 ± 0.146
pykA	Piruvato cinasa A	0.4 ± 0.002	1.0 ± 0.045
pykF	Piruvato cinasa F	0.8 ± 0.010	0.9 ± 0.001
aceE	Piruvato deshidrogenasa (E1)	0.4 ± 0.025	1.4 ± 0.023
aceF	Piruvato deshidrogenasa (E2)	0.6 ± 0.022	1.2 ± 0.004
lpd	Piruvato deshidrogenasa (E3) (ver TCA)	1.1 ± 0.107	2.0 ± 0.128
c. Vía de las pentosas fosfato			
zwf	Glucose-6P-1-deshidrogenasa	0.7 ± 0.063	1.9 ± 0.175
gnd	6-fosfogluconato deshidrogenasa	0.8 ± 0.110	1.2 ± 0.069
rpe	Ribulosa fosfato epimerasa	0.7 ± 0.092	0.9 ± 0.046
rpiA	Ribosa-5-fosfato isomerasa A	0.6 ± 0.000	1.6 ± 0.150
rpiB	Ribosa-5-fosfato isomerasa B	1.4 ± 0.307	1.9 ± 0.291
tktA	Transcetolasa A	0.5 ± 0.050	2.4 ± 0.114
tktB	Transcetolasa B	11.6 ± 0.228	5.7 ± 0.122
talA	Transaldolasa A	10.6 ± 1.924	5.1 ± 0.732
talB	Transaldolasa V	1.1 ± 0.061	1.6 ± 0.002
eda	2-K-3-deoxi-fosfogluconato aldolasa	0.5 ± 0.038	1.2 ± 0.047
edd	Fosfogluconato dehidratasa	0.3 ± 0.024	0.5 ± 0.088
d. Ciclo de los ácidos tricarboxílicos y el "shunt" de glioxalato			
gltA	Citrato sintasa	0.8 ± 0.083	1.3 ± 0.171
*acnA**	Aconitasa A	5.2 ± 0.594	5.7 ± 0.232
acnB	Aconitasa B	1.7 ± 0.364	1.7 ± 0.422
aceB	Malato sintasa A	15.6 ± 2.519	3.7 ± 0.308
aceA	Isocitrato liasa	11.9 ± 1.248	1.9 ± 0.225
aceK	Isocitrato deshidrogenasa fosfatasa/cinasa	5.5 ± 0.774	1.9 ± 0.255
glcB	Malato sintasa G	11.7 ± 1.417	3.7 ± 0.477
*glcC**	Regulador transcripcional dual	3.6 ± 0.299	6.9 ± 0.134
icdA	Isocitrato deshidrogenasa	1.0 ± 0.103	1.9 ± 0.003
sucA	2-oxoglutarato deshidrogenasa (E10)	1.4 ± 0.099	1.7 ± 0.068
sucB	Dihidrolipoamida succinato transferasa	0.8 ± 0.035	1.4 ± 0.086
ldp	Dihidrolipoato deshidrogenasa	1.1 ± 0.107	2.0 ± 0.128
sucC	SuccinilCoA sintetasa subunidad β	0.9 ± 0 072	1.6 ± 0.026
sucD	SuccinilCoA sintetasa subunidad α	1.0 ± 0.213	1.4 ± 0.302
sdhA	Succinato deshidrogenasa	0.9 ± 0.004	2.0 ± 0.278

sdhB	Succinato deshidrogenasa	0.8 ± 0.043	1.7 ± 0.027
sdhC	Succinato deshidrogenasa	1.3 ± 0.112	2.1 ± 0.593
sdhD	Succinato deshidrogenasa	0.9 ± 0.017	1.8 ± 0.052
fumA	Fumarasa A	3.3 ± 0.675	3.6 ± 0.673
fumB	Fumarasa B	0.8 ± 0.705	0.7 ± 0.365
*fumC**	Fumarasa C	4.3 ± 0.989	3.5 ± 1.482
mdh	Malato deshidrogenasa	1.2 ± 0.141	1.8 ± 0.520
e. Genes anapleróticos			
maeB	Enzima málica	1.2 ± 0.201	2.5 ± 0.032
sfcA	Enzima málica	1.9 ± 0.332	1.7 ± 0.100
mdh	Malato deshidrogenasa	1.2 ± 0.141	1.8 ± 0.520
ppsA	PEP sintasa	3.7 ± 0.216	2.4 ± 0.092
pckA	Piruvato carboxicinasa	0.8 ± 0.068	2.3 ± 0.026
ppc	PEPcarboxilasa	0.6 ± 0.059	0.8 ± 0.009
f. Gluconeogénesis			
maeB	Enzima málica	1.2 ± 0.201	2.5 ± 0.032
sfcA	Enzima málica	1.9 ± 0.332	1.7 ± 0.100
mdh	Malato deshidrogenasa	1.2 ± 0.141	1.8 ± 0.520
ppsA	PEP sintasa	3.7 ± 0.216	2.4 ± 0.092
pckA	Piruvato carboxicinasa	0.8 ± 0.068	2.3 ± 0.026
ppc	PEPcarboxilasa	0.6 ± 0.059	0.8 ± 0.009
eno	enolasa	0.5 ± 0.169	0.5 ± 0.146
gpmA	Fosfoglicerato mutasa 1	0.9 ± 0.007	1.8 ± 0.039
gpmB	Fosfoglicerato mutasa 2	1.5 ± 0.227	2.7 ± 0.357
pgk	Fosfoglicerato kinasa	0.7 ± 0.001	1.2 ± 0.060
gapA	Gliceraldehído-3P deshidrogenasa	0.4 ± 0.151	1.7 ± 0.214
gapC-1	Gliceraldehído-3P deshidrogenasa	6.7 ± 0.108	3.1 ± 0.091
gapC-2	Gliceraldehído-3P deshidrogenasa	3.9 ± 0.193	3.2 ± 0.015
fbaB	Fructosa bifosfato aldolasa	10.6 ± 1.137	4.9 ± 0.858
fbaA	Fructosa bifosfato aldolasa	0.9 ± 0.046	1.1 ± 0.052
fbp	Fructosa 1,6-bifosfatasa	2.4 ± 0.751	2.8 ± 0.138
pfkB	fosfofructocinasa	1.2 ± 0.224	1.9 ± 0.205
pgi	Fosfoglucosa isomerasa	1.0 ± 0.080	6.6 ± 0.282
g. Respiración			
nuoA	NADH deshidrogenasa 1	0.4 ± 0.007	2.4 ± 0.112
nuoF	NADH deshidrogenasa 1	0.3 ± 0.117	1.4 ± 0.109
nuoN	NADH deshidrogenasa 1	0.4 ± 0.021	1.0 ± 0.084
ndh	NADH deshidrogenasa II	0.6 ± 0.036	1.1 ± 0.076
sdhA	Succinato deshidrogenasa	0.8 ± 0.004	2.0 ± 0.278
sdhB	Succinato deshidrogenasa	0.8 ± 0.043	1.7 ± 0.027
sdhC	Succinato deshidrogenasa	1.3 ± 0.112	2.1 ± 0.593
sdhD	Succinato deshidrogenasa	0.9 ± 0.017	1.8 ± 0.052
ubiE	Metil transferasa	0.4 ± 0.013	1.6 ± 0.015
frdA	Fumarato reductasa	0.2 ± 0.009	0.6 ± 0.035
frdB	Fumarato reductasa	0.1 ± 0.009	0.7 ± 0.045
frdC	Fumarato reductasa	0.2 ± 0.030	0.7 ± 0.010
frdD	Fumarato reductasa	0.2 ± 0.049	0.8 ± 0.063
napA	Nitrato reductasa	0.1 ± 0.010	0.9 ± 0.132
narG	Nitrato reductasa A	0.2 ± 0.043	1.2 ± 0.113
cydB	Citocromo d ubiquinol oxidasa	0.4 ± 0.030	0.9 ± 0.039
cyoA	Citocromo o ubiquinol oxidasa	0.6 ± 0.015	1.5 ± 0.071
cyoB	Citocromo o ubiquinol oxidasa	0.3 ± 0.035	1.4 ± 0.140
cyoC	Citocromo o ubiquinol oxidasa	0.3 ± 0.011	1.2 ± 0.160
cyoD	Citocromo o ubiquinol oxidasa	0.3 ± 0.029	1.1 ± 0.092
h. Genes de fermentación, producción y utlización de acetato			
ldhA	Lactato deshidrogenasa	0.6 ± 0.019	1.1 ± 0.244
pta	Fosfato acetil transferasa	0.7 ± 0.129	1.5 ± 0.329
ackA	Acetato cinasa	0.4 ± 0.121	0.8 ± 0.013
adhE	Alcohol deshidrogenasa	0.6 ± 0.079	0.9 ± 0.041
poxB	Piruvato oxidasa	4.2 ± 0.353	5.7 ± 0.485
acs	Acetil CoA-sintetasa	5.6 ± 0.745	8.0 ± 0.136
yjcG (*actP*)	Transportador de acetato	5.1 ±0.455	7.2 ± 0.219
i. Reguladores			
cyaA	Adenilato ciclasa	1.4 ± 0.063	1.8 ± 0.098

crp	Regulador transcripcional dual	0.8 ± 0.020	1.0 ± 0.053
fruR	Regulador transcripcional dual	1.3 ± 0.002	1.5 ± 0.074
arcA	Regulador transcripcional dual	1.2 ± 0.020	1.3 ± 0.094
arcB	Regulador transcripcional dual	2.3 ± 0.707	1.3 ± 0.722
mlc	Repressor transcripcional	1.1 ± 0.003	1.7 ± 0.061
ihfA	Regulador transcripcional dual	1.8 ± 0.045	1.7 ± 0.060
ihfB	Regulador transcripcional dual	1.0 ± 0.000	1.0 ± 0.000
iclR	Repressor transcripcional	0.4 ± 0.035	1.4 ± 0.075
fadR	Regulador transcripcional dual	0.6 ± 0.031	1.6 ± 0.082
rpoS	Factor sigma 38 de la RNA polimerasa	2.9 ± 0.086	2.2 ± 0.156

Esta tabla muestra los niveles de transcripción relativos de diferentes grupos de genes involucrados en diferentes vías y procesos metabólicos. Para cada gene en todas las cepas, el nivel de transcripción del gene de la cepa silvestre se usó como el valor para normalizar los datos usando el valor de RT-PCR de esta cepa como valor de 1. Por lo tanto, los datos de esta tabla están reportados como valores de expresión relativa, comparados al nivel de expresión de JM101. Los genes marcados con asterisco no son parte de la ruta o regulón, pero se incluyen ya que sus productos están relacionados a las enzimas codificas por ese grupo específico de genes, o por porpósitos comparativos.

7. Conclusiones relevantes

Como resultado del análisis por RT-PCR, se detectaron diferencias significativas a nivel transcripcional de varios genes (Tabla 6). Estos resultados han contribuido a entender las diferentes capacidades metabólicas en las cepas PB11 PTS^- y PB12 PTS^-Glc^+. Algunos de los cambios importantes y comentarios son los siguientes:

a) La cepa PB11 crece muy lentamente en glucosa porque no puede transportar y fosforilar la glucosa eficientemente. Por tanto, la célula podría estar sensando internamente concentraciones muy bajas de glucosa o glucosa-6-P. Como respuesta a esta condición de ayuno-estrés, se puede inferir que la célula debe sintetizar varios autoinductores, para propósitos de "scavenging" (Ferenci, 2001; Hua *et al.*, 2004). Uno de estos autoinductores debe ser la galactosa que permite la sobreexpresión del regulón *gal*, y esto permite a la PB11 transportar glucosa a través de GalP y/o MglB. Proponemos también que el acetato que probablemente se produce por PoxB, podría ser otro autoinductor sintetizado en esta condición en PB11. Acetato (o un metabolito relacionado) podría funcionar como el autoinductor de los operones involucrados en su utilización como *aceBAK, acs* y *glc* que están altamente sobreexpresados en PB11. Es de gran relevancia que RpoS, cuyo gene codificante está también sobreexpresado en las cepas PTS^-, debiera estar involucrado en la transcripción de los genes *poxB* y *acs*, aún en medio con altas concentraciones de glucosa. La cepa PB12 PTS^-Glc^+ es capáz de crecer mas rápido que la PB11, principalmente porque los genes *glk* y *pgi* están sobreexpresados en PB12, permitiendo una mejor fosforilación y isomerización en fructosa-6-P. El regulón *gal* así como los operones *aceBAK*, *acs* y *glc* están sobreexpresados en esta cepa; por tanto PB12 debería también producir galactosa y acetato (o un metabolito relacionado) como autoinductores. La sobreexpresión de estos operones podría explicar por qué ambas cepas PTS^- pueden utilizar simultáneamente glucosa y acetato como fuentes de carbono.

crp	Regulador transcripcional dual	0.8 ± 0.020	1.0 ± 0.053
fruR	Regulador transcripcional dual	1.3 ± 0.002	1.5 ± 0.074
arcA	Regulador transcripcional dual	1.2 ± 0.020	1.3 ± 0.094
arcB	Regulador transcripcional dual	2.3 ± 0.707	1.3 ± 0.722
mlc	Repressor transcripcional	1.1 ± 0.003	1.7 ± 0.061
ihfA	Regulador transcripcional dual	1.8 ± 0.045	1.7 ± 0.060
ihfB	Regulador transcripcional dual	1.0 ± 0.000	1.0 ± 0.000
iclR	Repressor transcripcional	0.4 ± 0.035	1.4 ± 0.075
fadR	Regulador transcripcional dual	0.6 ± 0.031	1.6 ± 0.082
rpoS	Factor sigma 38 de la RNA polimerasa	2.9 ± 0.086	2.2 ± 0.156

Esta tabla muestra los niveles de transcripción relativos de diferentes grupos de genes involucrados en diferentes vías y procesos metabólicos. Para cada gene en todas las cepas, el nivel de transcripción del gene de la cepa silvestre se usó como el valor para normalizar los datos usando el valor de RT-PCR de esta cepa como valor de 1. Por lo tanto, los datos de esta tabla están reportados como valores de expresión relativa, comparados al nivel de expresión de JM101. Los genes marcados con asterisco no son parte de la ruta o regulón, pero se incluyen ya que sus productos están relacionados a las enzimas codificas por ese grupo específico de genes, o por porpósitos comparativos.

7. Conclusiones relevantes

Como resultado del análisis por RT-PCR, se detectaron diferencias significativas a nivel transcripcional de varios genes (Tabla 6). Estos resultados han contribuido a entender las diferentes capacidades metabólicas en las cepas PB11 PTS^- y PB12 PTS^-Glc^+. Algunos de los cambios importantes y comentarios son los siguientes:

a) La cepa PB11 crece muy lentamente en glucosa porque no puede transportar y fosforilar la glucosa eficientemente. Por tanto, la célula podría estar sensando internamente concentraciones muy bajas de glucosa o glucosa-6-P. Como respuesta a esta condición de ayuno-estrés, se puede inferir que la célula debe sintetizar varios autoinductores, para propósitos de "scavenging" (Ferenci, 2001; Hua *et al.*, 2004). Uno de estos autoinductores debe ser la galactosa que permite la sobreexpresión del regulón *gal*, y esto permite a la PB11 transportar glucosa a través de GalP y/o MglB. Proponemos también que el acetato que probablemente se produce por PoxB, podría ser otro autoinductor sintetizado en esta condición en PB11. Acetato (o un metabolito relacionado) podría funcionar como el autoinductor de los operones involucrados en su utilización como *aceBAK, acs* y *glc* que están altamente sobreexpresados en PB11. Es de gran relevancia que RpoS, cuyo gene codificante está también sobreexpresado en las cepas PTS^-, debiera estar involucrado en la transcripción de los genes *poxB* y *acs*, aún en medio con altas concentraciones de glucosa. La cepa PB12 PTS^-Glc^+ es capáz de crecer mas rápido que la PB11, principalmente porque los genes *glk* y *pgi* están sobreexpresados en PB12, permitiendo una mejor fosforilación y isomerización en fructosa-6-P. El regulón *gal* así como los operones *aceBAK*, *acs* y *glc* están sobreexpresados en esta cepa; por tanto PB12 debería también producir galactosa y acetato (o un metabolito relacionado) como autoinductores. La sobreexpresión de estos operones podría explicar por qué ambas cepas PTS^- pueden utilizar simultáneamente glucosa y acetato como fuentes de carbono.

Además, las tasas de crecimiento de las cepas PTS$^-$ aumentaron cuando se creció en ambas fuentes de carbono sin ninguna fase lag detectable. Este resultado es un claro indicio de que las enzimas que se requieren para la incorporación rápida de acetato (codificadas en los operones *aceBAK* y *acs*) están ya presentes en las células. Estos resultados están de acuerdo con el alto incremento (2 veces) en los flujos de carbono entre piruvato y AcCoA presente en las cepas PTS$^-$, y también con el aumento (2.5 veces) en el flujo de carbono entre citrato y malato en PB11, comparado con la JM101 (Flores *et al.,* 2002).

Cuando *E. coli* silvestre se crece en condiciones limitantes de glucosa (starvation-stress), o en cultivos en quimiostato con glucosa limitada a una tasa de crecimiento específica de 0.1 h^{-1}, se induce la producción de galactosa como autoinductor del operón *gal*, esto en cambio permite la síntesis de MglB, el transportador de alta afinidad por glucosa, para la internalización de glucosa (Death y Ferenci, 1994; Hua *et al.,* 2004). Debido a que la célula también sobreexpresa los operones *aceBAK* y *acs*, es razonable inferir que al igual que en las cepas PTS$^-$, la cepa silvestre en estas condiciones de crecimiento limitadas por glucosa también pudieran producir acetato como autoinductor con propósitos de "scavenging".

Estos resultados indican que una cepa silvestre creciendo en condiciones de limitación de glucosa utilizan principalmente la permeasa de alta afinidad MglB y Glk para transportar y fosforilar glucosa, en lugar de PTS. Cuando la célula encuentra glucosa en altas concentraciones, PTS funciona otra vez y utiliza este carbohidrato como la fuente de carbono preferencial (Ferenci, 2001). Esto resulta en el apagado de las señales de "scavenging" reprimiendo los operones *gal*, *aceBAK* y *acs*. Por lo tanto, la capacidad adaptativa a estrés de una cepa de *E. coli* silvestre para sintetizar autoinductores cuando sensa bajas concentraciones de glucosa, se encuentra congelada genéticamente de manera permanente en las cepas PTS$^-$ debida a la ausencia del sistema PTS. También, la obligación de usar Glk en estas cepas no permite a la célula acoplar eficientemente el transporte de glucosa a su fosforilación y catabolismo. Esta situación, de hecho una condición de ayuno-estrés, puede ser responsable de que la célula sense concentraciones de glucosa o glucosa-6P a muy bajas concentraciones, aún en presencia de altas concentraciones de glucosa en el medio, pero ciertamente a diferentes niveles entre las cepas PB11 y PB12;

b) PB12 tiene la capacidad de sintetizar compuestos aromáticos con un alto rendimiento a partir de glucosa (qs de 63 vs. 33 y 6.6 mmolC/g_{DCW}h en JM101, PB12 y PB11 respectivamente). Estos resultados se han explicado en términos de la alta disponibilidad metabólica de PEP, que resulta del transporte dependiente de ATP en esta cepa (Flores *et al.*, 1996; Báez *et al.*, 2001; Báez-Víveros *et al.*, 2004). Los datos obtenidos en este trabajo proporcionan nueva información que permite entender la relación entre las características fenotípicas de la cepa PB12 y su alta capacidad para sintetizar compuestos aromáticos. En esta cepa, se detectó la sobreexpresión de los genes *tktA, tktB, talA* y *talB* cuyos productos están relacionados a la síntesis de eritrosa-4P, el precursor de compuestos aromáticos a partir de intermediarios de la vía EMP. Adicionalmente, los genes gluconeogénicos *maeB, sfcA, pckA, pps, fbaB, fbp y pfkB* están sobreexpresados. Este resultado es

significativo en el contexto de la biosíntesis de compuestos aromáticos ya que el producto proteico del gene *pps* convierte PYR en PEP y de este modo contribuye al incremento de la disponibilidad metabólica de este segundo precursor aromático. Además, la capacidad gluconeogénica que coexiste con la capacidad glicolítica detectadas en ésta cepa, permitiendo la utilización simultánea de glucosa y acetato, es un rasgo fisiológico que puede permitir a la PB12 utilizar simultáneamente glucosa y otras fuentes de carbono, sin efecto de represión catabólica y esto puede potencialmente aumentar el rendimiento en la síntesis de compuestos aromáticos;

c) Se encontró una mutación puntual en el gene *arcB* en la cepa PB12. Esta mutación cambió un residuo de tirosina en uno de cisteína en la posición 71 de la región transmembranal 2 de ArcB. Hay dos residuos de cisteína en ArcB en la región denominada "linker" de la proteína ArcB y datos recientes indican que estos dos residuos son responsables en ArcB de sensar el estado redox de la célula al ser reducidos u oxidados por la poza de quinonas (Malpica *et al.*, 2004). Es interesante señalar que durante condiciones oxidantes la desfosforilación de ArcA-P, una actividad necesaria para reducir su actividad regulatoria, procede al menos "*in vitro*", vía $ArcA_{Asp54}$-P → $ArcB_{His717}$-P → $ArcB_{Asp576}$-P →Pi ruta reversa (Georgellis *et al*, 1998). Así, una possible explicación es que el nuevo residuo de cisteína podría participar en la formación de un puente disulfuro entre dos subunidades de ArcB. Esto podría dar como resultado una conformación de ArcB con una actividad de desfosforilasa incrementada. Esta mutación pudiera explicar la ligera sobreexpresión de los genes de TCA y algunos respiratorios en esta cepa durante crecimiento aeróbico. Es importante enfatizar que la PB12 exhibe el mismo fenotipo de sensibilidad a crecimiento en azul de toluidina que las cepas mutantes Δ*arcA* y Δ*arcB* (Iuchi *et al*, 1988), y que la introducción de un plásmido que lleva el gene *arcB* restablece su capacidad de crecimiento (figura 10). No obstante, el significado de esta mutación se está estudiando en mayor detalle. Recientemente, se demostró que el modulón ArcA probablemente abarca mas de 100 operones para mediar un papel en la adaptación celular (Liu y DeWulf, 2004). Por lo tanto, la selección de una mutación en *arcB* en la cepa PB11 puede ser una alternativa interesante para estabilizar genéticamente y/o permitir la sobreexpresión de varios genes que pudieran permitir una mayor flexibilidad metabólica. En PB12, el fenotipo $PTS^{-}Glc^{+}$ es el resultado de al menos dos mutaciones no ligadas genéticamente (en adición a la deleción de los genes PTS) (Flores, 1995), responsables de la sobreexpresión de los genes *glk* y *pgi* que permite un rápido crecimiento en glucosa, y la mutación *arcB*. Es difícil sugerir cual de éstas mutaciones ocurrió primero. Sin embargo, nos inclinamos por la posibilidad de que la mutación en *arcB* ocurrió en un fondo genético donde *glk* y *pgi* estaban sobreexpresadas ya que en estas condiciones la célula cataboliza glucosa mas eficientemente y crece mas rápido. Este fondo genético podría permitir la selección de una mutación para una utilización mejor de las enzimas del ciclo de TCA y de ciertas enzimas respiratorias que en la PB11;

d) Se determinaron las secuencias nucleotídicas de varios genes. Como se mencionó, solo se ha identificado una mutación puntual en *arcB* en PB12. No

obstante, se desconoce si el sistema regulador ArcAB regula la expresión de *glk* y *pgi* o la expresión de otros genes en diferentes vías que también se sobreexpresan en PB12 comparada con PB11 y JM101. Por lo tanto, en PB12 podría haber una o más mutaciones en diferentes genes aún no identificados o relacionados a esta respuesta. Estamos trabajando en la aislamiento de genes responsables de este fenotipo.

8. Perspectivas

Finalmente, hay mucho por hacer con el objeto de caracterizar y mejorar la utilización de éstas cepas con propósitos de producción. Inicialmente, uno de los sistemas reguladores que estudiaremos en mas detalle es el del regulador transcripcional RpoS. RpoS es la subunidad sigma de la RNA polimerasa que puede reemplazar parcialmente al factor sigma vegetativo (sigma 70) bajo condiciones de estrés. Como consecuencia, la transcripción de numerosos genes dependientes de sigma S se activa. La regulación del gene rpoS es un fenómeno complejo en el que participan varios efectores como cAMP-CRP. Este modulador aparentemente juega un papel tanto de activador como de represor dependiendo de las condiciones de crecimiento (Hengge-Aronis, 2002). Parece que la ausencia de PTS induce una respuesta de estrés o "scavenging" por carbono, lo cual causa la sobreexpresión de rpoS la cual en cambio puede ser responsable de la sobreexpresión de varios genes de respuesta a estrés como *poxB, acs, acnA, fumC, pps, tktB* y otros.

Trabajaremos también en la caracterización fina de la mutante *arcB* en PB12, en la búsqueda de las mutaciones responsables del incremento de la transcripción de *glk, pgi* y de otros genes que se expresan altamente en la PB12 con relación a la PB11 (el sistema *relA-spoT*).

Finalmente se construirán cepas que porten el gene *poxB* inactivado y se analizará la capacidad para producir acetato como inductor en estas cepas.

9. Referencias

Báez, J.L., Bolívar, F. y Gosset, G., 2001. Determination of 3-Deoxy-D-*Arabino*heptulosonate 7-phosphate productivity and yield from glucose in *Escherichia coli* devoid of the glucose phosphotransferase transport system. Biotechnol. Bioeng. 73, 530-35.

Báez-Viveros, J.L., Osuna, J., Hernández-Chávez, G., Soberón, X., Bolívar, F. y Gosset, G., 2004. Metabolic engineering and protein directed evolution increase the yield of Lphenylalanine synthesized from glucose in *E. coli*. Biotechnol. Bioeng. 87:516-524.

Bailey, JE., 1991.Toward a science of metabolic engineering. Science 252, 1668–75.

Biville, F., Turlin, E. y Gasser, F. 1991. Mutants of Escherichia coli producing pyrroloquinoline quinone. J. General Microbiol. 137,1775-1782.

Bustin, S. A. 2000. Absolute quantification of mRNA using real-time reverse transcription polymerase chain reaction assays. J. Mol. Endocrin. 25, 169-193.

Chang, Y. Y., Wang, A. Y., and Cronan, J. E., 1994. Expression of *Escherichia coli* pyruvate oxidase (PoxB) depends on the sigma factor encoded by *rpoS* (*katF*) gene. Mol. Microbiol. 11, 1019-1028.

Chao, G., Shen, J., Tseng, C.P., Park, S.,J., and Gunsalus, R.P., 1997. Aerobic regulation of isocitrate dehydrogenase gene (*icd*) expression in *Escherichia coli* by the *arcA* and *fnr* gene products. J. Bacteriol. 179(13), 4299-4304.

Cortay, J.S., Negre, D., Galinier, A., Duclos, B., Perriere, G., and Cozzonne, A.J., 1991. Regulation of the acetate operon in *Escherichia coli*; purification and functional characterization of the IclR repressor. EMBO J. 10(3), 675-79.

Cronan, J.E., and Laporte, D.C., 1996. Tricarboxilic acid cycle and glyoxylate bypass. In: "*Escherichia coli* and *Salmonella*: Cellular and Molecular Biology. F.C. Neidhart Ed., 2nd. Ed. pp. 206-215, ASM Washington, D.C. USA.

Cunningham, L., and Guest, J.R., 1998. Transcription and transcript processing in the *sdhCDAB* and *sucABCD* operon of *Escherichia coli*. Microbiology 144, 2113-23.

Cunningham, L., Gruer, M.J., and Guest, J.R., 1997. Transcriptional regulation of the aconitase genes (*acnA* and *acnB*) of *Escherichia coli*. Microbiology 143, 3795-3805.

Curtis, S. J. and Epstein, W., 1975. Phosphorylation of D-glucose in mutants defective in glucose phosphotransferase, mannose phosphotransferase and glucokinase. J. Bacteriol. 122, 1189-99.

Death, A. y Ferenci, T., 1994. Between feast and famine: endogenous inducer synthesis in the adaptation of *Escherichia coli* to growth with limiting carbohydrates. J. Bacteriol. 176, 5101-07.

Ferenci, T., 2001. Hungry bacteria-definition and properties of a nutritional state. Environ. Microbiol. 3, 605-09.

Flores, N., 1995. Construcción y caracterización de cepas de *Escherichia coli* mutantes en el sistema de transporte de carbohidratos PTS. Tésis de maestría, Instituto de Biotecnología, UNAM, México.

Flores, N., Xiao, J., Berry, A., Bolívar, F. y Valle, F., 1996. Pathway engineering for the production of aromatic compounds in *Escherichia coli*. Nat. Biotechnol. 14, 620-23.

Flores, S., Gosset, G., Flores, N., de Graaf, A.A. y Bolívar, F., 2002. Analysis of carbon metabolism in *Escherichia coli* strains with an inactive phosphotransferase system by ^{13}C labeling and NMR spectroscopy. Metab. Eng. 4, 124-37.

Flores, N., Flores, S., Escalante, A., deAnda, R., Leal, L., Malpica, R., Georgellis, D., Gosset, G. Y Bolivar, F. (2005a). "Adaptation for fast growth on glucose by differential expression of central carbon metabolism and *gal* regulon genes in an *Escherichia coli* strain lacking the phosphoenolpyruvate:carbohydrate phosphotransferase system". Metab. Engineering. En prensa.

Flores,S., Flores,N., de Anda, R., González,A., Escalante,A., Gosset,G. y Bolívar, F. (2005b) "Nutrient Scavenging Response in an *Escherichia coli* Strain Lacking the Phosphoenolpyruvate: Carbohydrate Phosphotransferase System, as Explored by Gene Expression Profile". En revision.

Frankel, D.G., 1996. Glycolisis. In: *Escherichia coli* and *Salmonella*: Cellular and Molecular Biology. Neidhart F.C. Ed. 2nd ed. pp. 189-196 ASM Washington, D.C. USA.

Geanacopoulos, M. and Adhya, S., 1997. Functional characterization of roles of GalR and GalS as regulators of the *gal* regulon. J. Bacteriol. 179, 228-34.

Georgellis, D. Kwon O., and Lin, E.C., 2001. Quinones as the redox signal for the Arc two component system of bacteria. Science 292, 2314-16.

Georgellis, D., O. Kwon, P. De Wulf, y E. C. Lin. 1998. Signal decay through a reverse phosphorelay in the Arc two-component signal transduction system. J. Biol. Chem. 273:32864–32869.

Gimenez, R., Nuñez, M.F., Badia, J., Aguilar, J., and Baldosa, L., 2003. The gene *yjcG,* cotranscribed with gene *acs,* encodes an acetate permease in *Escherichia coli*. J. Bacteriol. 185, 6448-55.

Gosset, Zhang, Z., Nayyar, S., Cuevas, W.A., and Saier, M.H., 2004.Transcriptome analysis of Crp-dependant catabolite control of gene expression in *Escherichia coli*. J. Bacteriol. 186, 3516-24.

Gui, L., Sunnarbory, A., and LaPorte, D.C., 1996. Regulated expression of a repressor protein: FadR activates *IclR*. J. Bacteriol. 178, 4704-09.

Hengge-Aronis, R., 2002. Signal transduction and regulatory mechanisms involved in control of the sigma S (RpoS) subunit of RNA polymerase. Microbiol. Mol. Biol. Revs. 66, 373-95.

Holms, W. H. 1986. The central metabolic pathways of Escherichia coli: relationship between flux and control at a branch point, efficiency of conversion to biomass, and excretion of acetate. Current topics in cellular regulation. (B. L. Horecker, E. R. Stadtman eds.)

Hua, Q., Yand, C., Oshima, T., Mori, H., y Shimizu, K., 2004. Analysis of gene expression in *Escherichia coli* in response to changes of growth-limiting nutrient in chemostat cultures. Appl. Environ. Microbiol. 70, 2354-66.

Iuchi, S., and Lin, E.C.C., 1988. *arcA* (*dye*), a global regulatory gene in *Escherichia coli* mediating repression of enzymes in aerobic pathways. Proc. Natl. Acad. Sci. USA. 85, 1988-1992.

Iuchi, S., Matsuda, Z., Fijiwara, T., and Lin, E.C.C., 1990. The *arcB* gene of *Escherichia coli* encoded a sensor regulator protein for anaerobic repression of the *arc* modulon. Mol. Microbiol. 4(5), 715-27.

Iuchi, S., y Lin, E.C.C., 1988. *arcA* (*dye*), a global regulatory gene in *Escherichia coli* mediating repression of enzymes in aerobic pathways. Proc. Natl. Acad. Sci. USA. 85, 1988-1992.

Levy, S., Zeng, G. and Danctiing, A., 1990. Cycle cAMP synthesis in *Escherichia coli* strains bearing known deletions in the *pts* phosphotransferase operon. Gene 86, 27-33.

Liu, X., and DeWulf, P. 2004. Probing the ArcP modulon of *Escherichia coli* by whole genome transcriptional analysis and sequence recognition profiling. J. Biol. Chem. 279, 12588-97.

Malpica, R., Franco, B., Rodríguez, C., Kwon O., y Georgellis, D., 2004. Identification of a quinone sensitive redox switch in the ArcB sensor kinase. Proc. Natl. Acad. Sci. USA 101, 13318-23.

Meyer, D., Schneider, C., Halacker, R., Peist, R. and Boos, W., 1997. Molecular characterization of glucokinase from *E. coli* K-12. J. Bacteriol. 179, 1298-1306.

Nam, T., Cho, S., Shin, D., Kim, J.,Jeong, J., Lee, J., Roe, J., Peterkofsky, A., Kang, S., Ryu, S. y Seok, Y. 2001. The Escherichia coli glucose transporter enzyme $IICB^{Glc}$ recruits the global repressor Mlc. EMBO J. 20:491-498.

Niedhart, F.C., Ingraham, J.L., and Scheachter, R., 1990a. Physiology of the bacterial cell. A molecular approach. Sinauer Associates Inc. Massachusetts, USA.

Niedhart, F.C., Ingraham, J.L., and Scheachter, R., 1990. Biosynthesis and fueling. In: Physiology of the bacterial cell. A molecular approach. pp. 133-73, Sianuer, USA.

Park, S.J., Chao, G., and Gunsalus, R.P., 1997. Aerobic regulation of the *sucABCD* genes of *E. coli*, which encode α-ketoglutarate dehydrogenase and succinyl coenzyme A synthase: role of ArcA, Fnr and the upstream *sdhCDAB* promoter. J. Bacteriol. 179, 4138-42.

Pellicer, M.A., Fernández, C., Badia, J., Aguilar, J., Linn, E., and Baldosa, L., 1999. Crossinduction of *glc* and *ace* operons of *E. coli* attributable to pathway intersection. J. Biol. Chem. 274, 1745-52.

Phue, J.N., and Shiloach, J., 2004. Transcription levels of key metabolic genes are the cause for different glucose utilization pathways in *E. coli* B (BL21) and *E. coli* K (JM109). J. Biotechnol. 109, 21-30.

Postma, PW, Lengeler, JW, Jacobson, GR., 1996. Phosphoenolpyruvate: carbohydrate phosphotransferase systems. In Neidhardt FC. Ed. 2nd. Ed. In *Escherichia coli* and *Salmonella*: cellular and molecular biology. Pp. 1:1149-1174, ASM Press. USA.

Quail, M. A., Haydon, D. J. and Guest, J. R., 1994. The *pdhR-aceEF-lpd* operon of *E. coli* expresses the pyruvate dehydrogenase complex. Mol. Microbiol. 12, 95-104.

Saier, M.H. and Ramseier, T.M., 1996. The catabolite repressor/activator (Cra) protein of enteric bacteria. J. Bacteriol. 178, 3411-17.

Saier, M. H., 2002. Vectorial metabolism and the evolution of the transport systems. J. Bacteriol. 182, 5029-5035.

Shen, J., and Gunsalus, R.P., 1997. Role of multiple ArcA recognition sites in anaerobic regulation of succinate dehydrogenase (*sdhCDAB*) gene expression in *Escherichia coli*. Mol. Microbiol. 26, 223-26.

Shin, S., Song, S. G., Lee, D. S., Pan, J. G., and Park, C., 1997. Involment of *iclR* and *rpoS* in the induction of *acs*, the gene for acetyl coenzyme A synthetase of *Escherichia coli* K-12. FEMS Microbiol. Lett.146, 103-108

Weickert M. and Adhya S., 1993. The galactose regulon of *Escherichia coli*. Mol. Microbiol. 10, 245-51.

10. Artículos relacionados publicados por Noemí Flores como autor.

Ponce, E., **Flores, N.**, Martínez, A., Valle, F. and Bolivar, F. (1995). "Cloning of the two pyruvate kinase isoenzyme structural genes from *Escherichia coli*: the relative roles of these enzymes in pyruvate biosynthesis". J. Bacteriol. **177**: 5719-5722.

Flores, N., Xiao, J., Berry, A., Bolivar, F. y Valle, F. (1996). "Pathway engineering for the production of aromatic compounds in *Escherichia coli*". Nature Biotechnology **14**:620-623.

Valle, F., Muñoz, E. Ponce, E. **Flores, N.** and Bolivar, F. (1996). "Basic and applied aspects of metabolic diversity: the phosphoenolpyruvate node". J. Industrial Microbiology. **17**:458-462.

R. Sigüenza, **N. Flores**, G. Hernández, A. Martínez, F. Bolivar and F. Valle. "Kinetic characterization in batch and continuous culture of *Escherichia coli* mutants affected in phosphoenolpyruvate metabolism; differences in acetic acid production.. World Journal of Microbiology & Biotechnology. (1999). **15** :587-592.

S., Flores ,G.Gosset , **N.Flores** ,de Graaf, "Analysis of carbon metabolism in Escherichia coli strains with an inactive phosphotransferase system by 13C labeling and NMR spectroscopy". *Metabolic Engineering* , (2002), **4**:124-137.

11. Artículos en prensa o sometidos.

Flores, N., Flores, S., Escalante, A., deAnda, R., Leal, L., Malpica, R., Georgellis, D., Gosset, G. Y Bolivar, F. (2005). "Adaptation for fast growth on glucosa by differential expresión of central carbon metabolism and *gal* regulon genes in an *Escherichia coli* strain lacking the phosphoenolpyruvate:carbohydrate phosphotransferase system". Metab. Engineering. En prensa.

Flores,S., **Flores,N.**, de Anda, R., González,A., Escalante,A., Gosset,G. y Bolívar, F. (2005) "Nutrient Scavenging Response in an *Escherichia coli* Strain Lacking the Phosphoenolpyruvate: Carbohydrate Phosphotransferase System, as Explored by Gene Expression Profile". Sometido en la revista Appl. Environ. Microbiol.

12. Otros artículos donde Noemí Flores es autor.

Balbás, P., de Anda, R., Flores, N., Alvarado, X., Cruz, N., Valle, F. and Bolivar, F.(1988). "Overproduction of proteins by recombinant DNA: human insulin". Cell function and disease (Cañedo, L., Todd, L., Jaz, J. and Parker, L., eds.) Plenum Press, New York, N. Y. 59-74.

N. Flores, F. Valle, F. Bolivar and E. Merino.(1992). "Recovery of DNA from agarose gels stained with methylene blue". Biotechniques **13**:203-205.

I. Castaño, N. Flores, F. Valle, A. Covarrubias and F. Bolivar.(1992). "*glt*F, a member of the *glt*BDF operon of *Escherichia coli*, is involved in nitrogen-regulated gene expression". Molecular Microbiology **6**:2733-2741.

Oliver, G., Gosset, G., Sánchez-Pescador, R., Lozoya, E., Lailig M. Ku., Flores, N., Becerril, B., Valle, F. and Bolivar, F.(1987). "Determination of the nucleotide sequence for the glutamate synthase structural genes of *Escherichia coli* K-12". Gene **60**:1-11.

Balbás, P., Soberón, X., Merino, E., Zurita, M., Lomelí, H., Valle, F., Flores, N. and Bolivar, F.(1986)."Plasmid vector pBR322 and its special-purpose derivatives-a review". Gene **50**:3-40.

Flores, N., de Anda, R., Güereca, L., Cruz, N., Antonio, S., Balbás, P., Bolivar, F. and Valle, F.(1986)."A new expression vector for the production of fused proteins in *Escherichia coli*". Appl. Microbiol. Biotechnol. **25**:267-271.

Valle, F. Y Flores, N. 2004. Overexpression of chromosomal genes in Escherichia coli. Methods in Molecular Biology. Recombinant Gene expression:Reviews and protocols, Second edition. (eds. P. Balbás y A. Lorence) Umana Press Inc., Totowa, NJ. **267**:113-122.

ARTICLE IN PRESS

Available online at www.sciencedirect.com

SCIENCE DIRECT®

ELSEVIER

Metabolic Engineering ▮ (▮▮▮▮) ▮▮▮–▮▮▮

METABOLIC ENGINEERING

www.elsevier.com/locate/ymben

Adaptation for fast growth on glucose by differential expression of central carbon metabolism and *gal* regulon genes in an *Escherichia coli* strain lacking the phosphoenolpyruvate: carbohydrate phosphotransferase system

Noemí Flores[a], Salvador Flores[a], Adelfo Escalante[a], Ramón de Anda[a], Lidia Leal[a], Roxana Malpica[b], Dimitris Georgellis[b], Guillermo Gosset[a], Francisco Bolívar[a,*]

[a]*Departamento de Ingeniería Celular y Biocatálisis, Instituto de Biotecnología, Universidad Nacional Autónoma de México, Apdo. Postal 510-3, Cuernavaca, Morelos 62271, México*

[b]*Departamento de Genética Molecular, Instituto de Fisiología Celular, Universidad Nacional Autónoma de México. Av. Universidad 3000 D.F., México*

Received 9 July 2004; accepted 5 October 2004

Abstract

Phosphoenolpyruvate (PEP) is a key intermediate of cellular metabolism and a precursor of commercially relevant products. In *Escherichia coli* 50% of the glucose-derived PEP is consumed by the PEP:carbohydrate phosphotransferase system (PTS) for glucose transport. PTS, encoded by the *ptsHIcrr* operon, was deleted from JM101 to generate strain PB11 (PTS^-Glc^-). PB12, a mutant derived from PB11, grows faster than the parental strain on glucose (PTS^-Glc^+ phenotype). This strain can redirect some of the PEP not utilized by PTS into the high yield synthesis of aromatic compounds from glucose. Here, we report a comparative transcription analysis among these strains of more than 100 genes involved in central carbon metabolism during growth on glucose. It was found that in the PTS^- strains that have reduced glucose transport capacities, several genes encoding proteins with functions related to carbon transport and metabolism were upregulated. Therefore, it could be inferred that these strains synthesize autoinducers of these genes when sensing very low internal glucose concentrations, probably for scavenging purposes. This condition that is permanently present in the PTS^- strains even when growing in high glucose concentrations allowed the simultaneous utilization of glucose and acetate as carbon sources. It was found that the *gal* operon is upregulated in these strains, as well as the *aceBAK*, *poxB* and *acs* genes among others. In PB12, *glk*, *pgi*, the TCA cycle and certain respiratory genes are also upregulated. A mutation in *arcB* in PB12 is apparently responsible for the upregulation of the TCA cycle and certain respiratory genes.

Keywords: *Escherichia coli*; PTS^-; *arcA*; *arcB*; *galP*; *glk*; *pgi*; *rpoS*; RT–PCR; Starvation-stress response; TCA; Glyoxylate shunt; Autoinducers; Acetate; Phosphoenolpyruvate; Pyruvate

1. Introduction

Metabolic engineering can be defined as the modification of cellular enzymatic, transport and regulatory activities with the aim of strain improvement (Bailey, 1991). This discipline has been applied in *Escherichia coli* to improve productivity and yield in the synthesis of specific metabolites. Some of the strategies followed to achieve these goals include modification or elimination of the phosphoenolpyruvate (PEP):carbohydrate phosphotransferase system (PTS). This protein system belongs to the group translocator class of transporters, which are widespread in bacteria (Saier, 2002). One of

*Corresponding author. Fax: +52 777 317 2388.
E-mail address: noemi@ibt.unam.mx (N. Flores).

1096-7176/$ - see front matter © 2004 Elsevier Inc. All rights reserved.
doi:10.1016/j.ymben.2004.10.002

the main functions of PTS is the transport and PEP-dependent phosphorylation of several sugars. This system is composed by the non-sugar-specific protein components Enzyme I and HPr whose function is to relay a phosphate group from PEP to sugar-specific IIA and IIB PTS proteins. PTS is also involved in the regulation of several cellular processes such as catabolite repression and chemotaxis (Postma et al., 1996). Therefore, PTS forms part of a global regulatory network that controls the capacity of cells to find, select, transport and metabolize several types of carbon sources.

Half of the PEP produced during glycolysis is consumed by PTS for glucose internalization. This metabolic constraint limits the amount of PEP available for the synthesis of several metabolites derived from this precursor when *E. coli* uses glucose as the carbon source. For this reason, considerable effort has been focused on developing *E. coli* strains that can transport glucose efficiently by a PEP-consumption independent mechanism. However, inactivation of PTS causes a wide range of effects due to its important role in the physiology of the cell. For example, a deletion of the *ptsHIcrr* operon in *E. coli* decreases glucose transport and growth rates (PTS^- phenotype) (Flores, 1995; Flores et al., 2002). As such, PTS^- strains are not suitable for production purposes. Therefore, further genetic modifications are required to increase glucose transport capacity in a PTS^- mutant. Different approaches have been reported to achieve this purpose with varying degrees of success (Flores et al., 1996; Chen et al., 1997; Chandran et al., 2003; Hernández-Montalvo et al., 2003).

We have obtained spontaneous mutants from PB11 (PTS^-) that lack the *ptsHIcrr* operon but grow faster on glucose than the PTS^- parental strain. These strains were isolated by an adaptive evolution process, in which PB11 was grown in a chemostat, with glucose fed at progressively higher rates (Flores, 1995; Flores et al., 1996). Initial characterization of these strains revealed that rapid glucose consumption and high growth rates depend on functional *galP* and *glk* genes that code for galactose permease (GalP) and glucokinase (Glk), respectively (Flores et al., 1996; Flores et al., 2002; Hernández et al., 2003). Using one of these mutants, PB12, we have shown that some of the PEP, which is not consumed for glucose transport due to the lack of PTS, could be redirected into the aromatic pathway, increasing the yield from glucose into the synthesis of 3-deoxy-D-*arabino*-heptulosonate-7-P (DAHP) (Gosset et al., 1996; Báez et al., 2001) and L-phenylalanine (Báez-Viveros et al., 2004). The carbon flux distribution in these isogenic PTS^+, PTS^- and PTS^-Glc^+ strains has been studied by biochemical analysis and nuclear magnetic resonance (NMR) spectroscopy. It was demonstrated that carbon flux distribution was modified at various nodes and portions of the central carbon metabolism in the PTS^- and PTS^-Glc^+ strains as compared to the wild-type JM101. This result clearly indicates that these PTS^- strains adjusted their metabolic capacities due to the absence of the PTS. For example, at the Embden–Meyerhof pathway (EMP), the carbon flux of the first node increased to 95% in the PB12 PTS^-Glc^+ (GalP/Glk) strain as compared to the wild-type JM101 (77%) and PB11 PTS^- (42%) parental strains (Flores et al., 2002). In agreement, it was also found that in PB12 the specific activities of Glk and Pgi increased approximately two- and four-fold, respectively, as compared with the wild-type strain JM101. As a result of these modifications, PB12 grows faster than PB11 (μ of 0.42 vs 0.1 h^{-1}) but slower than the wild-type strain (μ of 0.71 h^{-1}) (Flores et al., 2002).

It seems that during the process utilized for the isolation of PB12, at least two non-cotransducible mutations were selected to allow this strain to consume glucose in the absence of PTS at a much higher rate than PB11 (Flores, 1995; Flores et al., 1996). It has been reported that *E. coli* strains can adapt their metabolism for higher growth rates on specific carbon sources as a result of specific mutations (Raghunathan and Palsson, 2003). We are interested in identifying the mutations that were selected in PB12 and the genes involved in the differential utilization of glucose, carbon catabolism and other metabolic capacities present in these modified strains. In this contribution, we report a transcriptome analysis using RT–PCR measurements of more than 100 genes coding for enzymes that participate in the following pathways and processes: EMP, pentose pathway, TCA cycle, glyoxylate shunt, anaplerotic enzymes, gluconeogenesis, fermentation and respiration processes, and the *gal* operon. We have also determined the nucleotide sequences of 11 genes (regulatory and coding regions) from the three strains, looking for the mutations responsible for the observed changes.

2. Materials and methods

2.1. Bacterial strains, plasmids, media and growth conditions

E. coli strains used in this work are listed in Table 1. Strain PB12 was obtained from PB11, a PTS^- mutant derivative of *E. coli* JM101 (Flores, 1995; Flores et al., 1996). Duplicate cultures for RNA isolation and enzymatic assays were grown on 1 L fermentors on M9 medium with 2 g/l of glucose, at 37 °C, 600 r.p.m. and air flow rate of 1 v.v.m., starting at an OD_{600} of 0.05 and collected when growing in the log phase at an OD_{600} of 1.

For toluidine blue growth-sensitivity assays, cells were grown on peptone-agar plates containing 0.2 mg/ml of toluidine blue. Plasmid pBB31 that carries the wild-type

Table 1
Bacterial strains used in this study

Strains	Relevant characteristics	Source or reference
E. coli JM101	F′ *tra*D36 *proA*$^+$ *proB*$^+$ *lacI*^{q} *lacZ*ΔM15/*supE thi* Δ(*lac-proAB*)	Bolivar et al. (1977)
E. coli PB11	JM101 Δ(*ptsH, ptsI, crr*)::*kan*	Flores et al. (1996)
E. coli PB12	PB11, PTS$^-$Glc$^+$	Flores et al. (1996)
E. coli PB121	PB12, pBB31 (*arcB*$^+$)	This work

arcB gene (Table 1) was utilized for complementation analysis (Iuchi and Lin, 1988, 1992).

2.2. RNA extraction and cDNA synthesis

Total RNA extraction was performed using hot-phenol equilibrated with water. After extractions, RNA was precipitated with 3 M sodium acetate/ethanol and centrifuged 20,000*g* at 4 °C. Supernatant was discarded and the RNA resuspended in water. RNA was treated with DNase kit (DNA-free™, Ambion) and its concentration carefully measured by densitometry in agarose gels and by 260/280 nm ratio absorbance. cDNA was synthesized using RevertAid™ H First Strand cDNA Synthesis kit (Fermentas Inc.) and a mixture of specific DNA primers (Table 2). cDNA was used as template for RT–PCR assays. Reproducibility of this procedure was determined by performing two separate cDNA synthesis experiments from the RNA extracted for each strain. Similar results were obtained for the transcription of all the genes that were measured.

2.3. Nucleotide sequence determination and analysis of *mglB, galP, galE, galS, galR, glk, pgi, crp, fruR, arcA and arcB* genes

Regulatory (at least 200 base pairs (bp) located at the 5′ end and at least 100 bp at the 3′ end of the structural gene) and coding regions of these genes were amplified by PCR using a set of primers designed with the Clone Manager Program. Chromosomal DNA (100 ng) from JM101, PB11 and PB12 strains was used as template for amplification with the Elongase enzyme mix, according to the supplier's recommendations (Invitrogen Inc.). PCR products were analyzed for expected size and purified using a PCR purification kit (Marligen, BioScience Inc.). Nucleotide sequences (data not shown) were determined from PCR templates by the method of Taq FS Dye Terminator Cycle Fluorescence-Based Sequencing, with a Perkin-Elmer/Applied Biosystems Model 377-18 sequencer.

2.4. Real-time PCR

Real-time PCR (RT–PCR) was performed with the ABI Prism 7000 Sequence Detection System (Perkin-

Table 2
Primer sets used for RT–PCR assays, PCR amplification and sequencing

Pathway, process or group of genes	Primer name	Primer sequence
a. gal regulon		
galE	galEa	5′-AGCGCCAATTGCTACAACGT-3′
	galEb	5′-ACGGAAGCGGTTTTCATCAA-3′
galT	galTa	5′-TGCCGAACAGAAATCACCAA-3′
	galTb	5′-GCACGACGGCTAACCAGTGT-3′
galK	galKa	5′-GGCTGTAACTGCGGGATCAT-3′
	galKb	5′-GAAACTGCTTTGGTCCCCAG-3′
galM	galMa	5′-CCATTACTTATCGCGCCACA-3′
	galMb	5′-GTGATTGCGCACGTCAGACT-3′
galP	galPa	5′-CATGTATTACGCGCCGAAAA-3′
	galPb	5′-TGGCAAGTACGTTGGTCAGG-3′
galS	galSa	5′-AGGTTAGCGACACCATTGGC-3′
	galSb	5′-TTTCTGATGCTGCTGAGCGA-3′
galR	galRa	5′-CAGCAAGGTCATACCCGCAT-3′
	galRb	5′-CCACTTTCAGCAAGGGCATC-3′
galU	galUa	5′-AAAGGGAAGAGCCATGACTGC-3′
	galUb	5′-CAGGCTTTAAATTCCGTGCC-3′
mglB	mglBa	5′-CCAGCATGTTATTCGGTGCC-3′
	mglBb	5′-AGCCTTGCGCACTACAGACA-3′
lamB	lamBa	5′-AACTTCCTCTGGCGGTTGC-3′
	lamBb	5′-ACCTGTCCAACCAATACCGG-3′
pgm	pgma	5′-GTATCTCCCTCGACGAAGCG-3′
	pgmb	5′-CGCGGCCATATCAACGATAT-3′
b. Glycolysis		
glk	glka	5′-GAAGCGGTCATTCGCGTTTA-3′
	glkb	5′-GTCATCGCCACCCAGTCAC-3′
pgi	pgia	5′-ACTAACGGTCAGCACGCGTT-3′
	pgib	5′-TCAGAGAGCGGGTTATGGGT-3′
pfkA	pfka	5′-CCATGTAGGAACCGTCACCG-3′
	pfkb	5′-GTTGGCGGATGAAAATGTCC-3′
fbaA	fbaAa	5′-GGAAATCGAACTGGGTTGCA-3′
	fbaAb	5′-CGTAATCAACGTCTTCCGGC-3′
tpiA	tpiAa	5′-AACTCCGGCTCAGGCACAG-3′
	tpiAb	5′-AGCCGCCGTACTGAATGATC-3′
gapA	gapAa	5′-GGCTCCGCTGGCTAAAGTTA-3′
	gapAb	5′-GGCCATCAACGGTTTTCTGA-3′
pgk	pgka	5′-AGATTACCTCGACGGCGTTG-3′
	pgkb	5′-TGGACAGGGTTTCGTCGTCT-3′
gpmA	gpmAa	5′-AGGCGTAAGCGAAGCAAAAG-3′
	gpmAb	5′-GGGTATGGATAGCGCGTTTC-3′
eno	enoa	5′-GTTTCGTCGGTATGGCAGCT-3′
	enoB	5′-GCCTTTACCCAGGAAACGG-3′
pykA	pykAa	5′-CGTTACCACGTTAGGCCCAG-3′
	pykAb	5′-GCGAGCCGTGAGAAAAGTTC-3′
pykF	pykFa	5′-TGTCTGGTGAATCCGCAAAA-3′
	pykFb	5′-CTCGAGACGGCTGTTCATCA-3′

Table 2 (*continued*)

Pathway, process or group of genes	Primer name	Primer sequence
aceE	aceEa	5′-CGTGAAGAAGGTGTTGAGCG-3′
	aceEb	5′-TTGCTGATACCTGTGCCTGC-3′
aceF	aceFa	5′-GTCGTATCCTGCGCGAAGAC-3′
	aceFb	5′-CAGCATGCCAGGGATACCAC-3′
lpd	lpda	5′-GGTGGTGCGATTGTCGGTAC-3′
	lpdb	5′-TGGATGGTCAGTGCGATGTC-3′
c. Pentose pathway		
zwf	zwfa	5′-GCACGCGTAGTCATGGAGAA-3′
	zwfb	5′-CGGTAAACCTGGCACTCCTC-3′
gnd	gnda	5′-GATCGGCGTAGTCGGTATGG-3′
	gndb	5′-TCTTCTCACGGGAACGGTTG-3′
rpe	rpea	5′-GCCAATGGTGCTGAAATCCT-3′
	rpeb	5′-CAGCGAAATCAGGCACAATG-3′
rpiA	rpiAa	5′-GATGGGCGGCACTTCAGTAT-3′
	rpiAb	5′-GCCTTTCATTGTACCGAGCG-3′
rpiB	rpiBa	5′-GAGAGGTTGATGGCGGGATT-3′
	rpiBb	5′-AGGTTCGCTACAGACGACCG-3′
tktA	tktAa	5′-AGTCCTGTGGCGTGATTTCC-3′
	tktAb	5′-AGATCAGCATGGAGCCGTG-3′
tktB	tktBa	5′-CCCGAAAAGACCTTGCCAAT-3′
	tktBb	5′-AATATCAGCCATGCCCATCG-3′
talA	talAa	5′-CTCAAAATCGTACCCGGTCG-3′
	talAb	5′-TACAAGTCCACCAGATGGCG-3′
talB	talBa	5′-ACCGTAGTGGCCGACACTG-3′
	talBb	5′-GGAATCTGCGCTGCGTTAAG-3′
eda	edaa	5′-ATCCGTGCTATCGCCAAAGA-3′
	edab	5′-AACTGTGCACCCGCTTCAGT-3′
edd	edda	5′-GTACCGCTGATGGCACGTCT-3′
	eddb	5′-GCTTTGAGCAGTTCACGCAC-3′
d. TCA cycle and glyoxylate shunt		
gltA	gltAa	5′-AGGCACGCTGGGTCAAGAT-3′
	gltAb	5′-TAGATTCGCAGGATGCGGTT-3′
acnA	acnAa	5′-TGGCTTCTTCCCAATCGATG-3′
	acnAb	5′-CCTGCGCTTTGGCATATTTT-3′
acnB	acnBa	5′-CCTGGTGTTGTTGGTCCGAT-3′
	acnBb	5′-TTACGCGAAGAACCCGTACC-3′
aceA	aceAa	5′-ACATGGGCGGCAAAGTTTTA-3′
	aceAb	5′-AACCAGCAGGGTTGGAACG-3′
aceB	aceBa	5′-GAACTGGCTTTCACAAGGCC-3′
	aceBb	5′-TGTGGCGTAAAATGCGTCAC-3′
aceK	aceKa	5′-GCGTTATCAGCGACCTACCG-3′
	aceKb	5′-GTTGTCTGTCCCCAGCGTTT-3′
glcB	glcBa	5′-CTCCAGCACAGTTTGTCGGTT-3′
	glcBb	5′-ATTGGCATCGATTTGCAGCT-3′
glcC	glcCa	5′-TCGCCCTATTTGCGAAGTG-3′
	glcCb	5′-CACACAGTCGACGTTCCGAG-3′
icdA	icdAa	5′-GACCGAAGCGGCTGACTTAA-3′
	icdAb	5′-GCAGTTTAGCGCCATCCATC-3′
sucA	sucAa	5′-GCGGCAAAGAAACCATGAAA-3′
	sucAb	5′-TTCGGTGCTGGTAATGTGCA-3′
sucB	sucBa	5′-GCAGTACGGTGAAGCGTTTG-3′
	sucBb	5′-CTTCCGGGTAACGTTTCAGG-3′
ldp	ldpa	5′-GGTGGTGCGATTGTCGGTAC-3′
	ldpb	5′-TGGATGGTCAGTGCGATGTC-3′
sucC	sucCa	5′-CCAAAATCTTCATGGGCCTG-3′
	sucCb	5′-GCAAATCAGATCGCCCTGTT-3′
sucD	sucDa	5′-TGGGTTACATCGCTGGTGTG-3′
	sucDb	5′-AGCGAATTTCTCATCCGCAG-3′

Table 2 (*continued*)

Pathway, process or group of genes	Primer name	Primer sequence
sdhA	sdhAa	5′-GACACCGTGAAAGGGTCGG-3′
	sdhAb	5′-AGGCCCATGTGTTCGAGTTC-3′
sdhB	sdhBa	5′-TGAACGGCAAGAATGGTCTG-3′
	sdhBb	5′-GATCACCGGTAAACCTGGCA-3′
sdhC	sdhCa	5′-TGGCGTATCACGTCGTCGTA-3′
	sdhCb	5′-AAAGGAGATTTTGGCGGAGC-3′
sdhD	sdhDa	5′-GATCGGTTTCTTCGCCTCTG-3′
	sdhDb	5′-CGGTCAACACCTGCCACAT-3′
fumA	fumAa	5′-ATGTCGATCAACTGCAAGCG-3′
	fumAb	5′-GAAGCCGCCGTGTTTTTTAC-3′
fumB	fumBa	5′-GTACCCTCGGTACTGCAGCC-3′
	fumBb	5′-AGCGCTTGCTAACTTGACGG-3′
*fumC**	fumCa	5′-CCCTAACGACGACGTGAACA-3′
	fumCb	5′-GAGGAATGAGTTGCTTGCGC-3′
mdh	mdha	5′-CGGGTCTGCAACCCTGTCTA-3′
	mdhb	5′-CGTAGGCACATTCGACAACG-3′
e. Anaplerotic genes		
maeB	maeBa	5′-TGGTTTGCGATTCAAAAGGC-3′
	maeBb	5′-GAGGGTACGTTTGCCGTCAT-3′
sfcA	sfcAa	5′-ATAAAGGCAGTGCCTTCAGCA-3′
	sfcAb	5′-TGCTCGTTCCGCTTGTTCTT-3′
mdh	mdha	5′-CGGGTCTGCAACCCTGTCTA-3′
	mdhb	5′-CGTAGGCACATTCGACAACG-3′
pps	ppsa	5′-TCAGCAGGAAACCTTCCTCAA-3′
	ppsb	5′-GATAAGAGATGGCGCGATCG-3′
pckA	pckAa	5′-ACATGTTTATTCGCCCGAGC-3′
	pckAb	5′-CTGTTCTTTCCACTGCGGGT-3′
ppc	ppca	5′-CAGAAATCACCGTCAGCAGC-3′
	ppcb	5′-CATAATGCGACGCCAGCTCT-3′
f. Gluconeogenesis		
gpmB	gpmBa	5′-GGTATTGCACTGGGATGCCT-3′
	gpmBb	5′-TAATCCACGCGCGAAATAGA-3′
gapC-1	gapC-1a	5′-CAACGACACCATTGTTTCCG-3′
	gapC-1b	5′-TCATCGTGCCGACTTCTATCC-3′
gapC-2	gapCa-2a	5′-ATCATTGGCAGCCATTTCG-3′
	gapCb-2b	5′-TTATCGTACCAGGCGACCGT-3′
fbaB	fbaBa	5′-GTACAACACCGGGCGTCTG-3′
	fbaBb	5′-GCGGGTTAGCAGCAAATGAA-3′
glpX	glpXa	5′-CTAAACCACGCCACGATGC-3′
	glpXb	5′-ACAGGTGAGAATTGAGGCCG-3′
fbp	fbpa	5′-AAACAGGTTGCGGCAGGTTA-3′
	fbpb	5′-CCGAGCGAAGGATCGTAAGT-3′
pfkB	pfkBa	5′-GTTGGCGGATGAAAATGTCC-3′
	pfkBb	5′-AACGATACTGCTCACCGCTTG-3′
g. Respiration		
nuoA	nuoAa	5′-CTGGTGGCCATGTTCTTCGT-3′
	nuoAb	5′-GCTTCCACAAAGCCTACCCA-3′
nuoF	nuoFa	5′-TATCCGTACTCCCGAAACGC-3′
	nuoFb	5′-CGCCTTCGTAACCGTTTTTG-3′
nuoN	nuoNa	5′-TGTCGCGTTGGGTAAAAACC-3′
	nuoNb	5′-GAGAGAGTTTGAAGCCGAGGC-3′
ndh	ndha	5′-GTCGATCGTAACCACAGCCA-3′
	ndhb	5′-GCATGGGCCAGATAGCTCAA-3′
sdhA	sdhAa	5′-GACACCGTGAAAGGGTCGG-3′
	sdhAb	5′-AGGCCCATGTGTTCGAGTTC-3′
sdhB	sdhBa	5′-TGAACGGCAAGAATGGTCTG-3′
	sdhBb	5′-GATCACCGGTAAACCTGGCA-3′

Table 2 (*continued*)

Pathway, process or group of genes	Primer name	Primer sequence
sdhC	sdhCa	5′-TGGCGTATCACGTCGTCGTA-3′
	sdhCb	5′-AAAGGAGATTTTGGCGGAGC-3′
sdhD	sdhDa	5′-GATCGGTTTCTTCGCCTCTG-3′
	sdhDb	5′-CGGTCAACACCTGCCACAT-3′
ubiE	ubiEa	5′-GGCAGAATCCATCCGTATGC-3′
	ubiEb	5′-CCCCTGCCGTCAGATTGTAG-3′
frdA	frdAa	5′-TCTCTCAGGCCTTCTGGCAC-3′
	frdAb	5′-TTTTTTCTCGCCGAGGTGAC-3′
frdB	frdBa	5′-TTGAGGTGGTGCGCTATAACC-3′
	frdBb	5′-GCCCAGCGCATCCAGTAAT-3′
frdC	frdCa	5′-ACCGAAAGCGGCCAATATC-3′
	frdCb	5′-GGATTACGATGGTGGCAACC-3′
frdD	frdDa	5′-TGGTCGCGTATTCCTGTTCC-3′
	frdDb	5′-CCGCAGGTACGTGGATTTTC-3′
napA	napAa	5′-GATGGGCTGCTATGACGACA-3′
	napAb	5′-GGTTAGTGATGCGCGACCA-3′
narG	narGa	5′-CGATTATCCGGCGACTTACG-3′
	narGb	5′-TCTCGCTCTGGGTGTTCCAG-3′
cyoA	cyoAa	5′-GGCATTGCTACCGTGAATGA-3′
	cyoAb	5′-AGACGCGGAATGAAGAAGGA-3′
cyoB	cyoBa	5′-CTGACCTCCGTCGACCATAAA-3′
	cyoBb	5′-TGGCTACGCATCATAATGGC-3′
cyoC	cyoCa	5′-CACGGTCTGCACGTCACTTC-3′
	cyoCb	5′-CACATGATGCGGGTACGGT-3′
cyoD	cyoDa	5′-CCTGGCAATGGCAGTGGTAC-3′
	cyoDb	5′-TGAAGACAAACGCCGTCATG-3′
h. Fermentation and acetate production and utilization genes		
ldhA	ldhAa	5′-GGCGTGATGATCGTCAATACC-3′
	ldhAb	5′-ACGTCCATACCCAACGAACC-3′
pta	ptaa	5′-ACAATGTTGATCCGGCGAAG-3′
	ptab	5′-CATATCGATCGCACGAGTCG-3′
ackA	ackAa	5′-CTGGTTCTGAACTGCGGTAGTTC-3′
	ackAb	5′-GGCAGGTGGAAACATTCGG-3′
adhE	adhEa	5′-AAGTCCCTGTGTGCTTTCGG-3′
	adhEb	5′-TGCAGAGCCTGACCATCAGA-3′
poxB	poxBa	5′-AAAAGCCGATCGCAAGTTTC-3′
	poxBb	5′-GGTGAATGGCTTTCTCGCTC-3′
i. Regulators		
cyaA	cyaAa	5′-AGCGCCAATTGCTACAACGT-3′
	cyaAb	5′-ACGGAAGCGGTTTTCATCAA-3′
crp	crpa	5′-ACCCGTCAGGAAATTGGTCA-3′
	crpb	5′-TTACCGTGTGCGGAGATCAG-3′
fruR	fruRa	5′-TCTTGTGATCCCCGATCTGG-3′
	fruRb	5′-AGCAGGCAATCAGCAGTTGA-3′
arcA	arcAa	5′-ATCACCAAACCGTTCAACCC-3′
	arcAb	5′-ACGCTACGACGTTCTTCGCT-3′
arcB	arcBa	5′-AATCTGACGGCGCAGGATAA-3′
	arcBb	5′-TGACCCAGCTGTTGCAGATG-3′
mlc	mlca	5′-GGTCCAGTCTCGCGTATCGA-3′
	mlcb	5′-TCTTGCACCAGGTGTGCTTC-3′
ihfA	ihfAa	5′-GGCGAACAGGTGAAACTCTCTG-3′
	ihfAb	5′-GTAATGGGAATATCCTCGCCC-3′
ihfB	ihfBa	5′-GCCAAGACGGTTGAAGATGC-3′
	ihfBb	5′-GAGAAACTGCCGAAACCGC-3′
iclR	iclRa	5′-CTTTATGGTCGGCAGCAGCT-3′
	iclRb	5′-ATTGACCGTTTCGCCAGACT-3′
fadR	fadRa	5′-CGCTGGGCTTCTACCACAAA-3′
	fadRb	5′-AATCTCGCCACTCTCATGCC-3′
rpoS	rpoSa	5′-GGACGCGACTCAGCTTTACC-3′
	rpoSb	5′-CGACATCTCCACGCAGTGC-3′

Elmer/Applied Biosystems) using the SYBR Green PCR Master Mix (Perkin-Elmer/Applied Biosystems). Amplification conditions were 10 min at 95 °C, and a two-step cycle at 95 °C for 15 s and 60 °C for 60 s for a total of 40 cycles. The primers for specific amplification (Table 2) were designed using the Primer Express software (PE Applied Biosystems). The size of all amplimers was 101 bp. The final primer concentration, in a total volume of 15 μl, was 0.2 μM. Five nanograms of target cDNA for each gene was added to the reaction mixture. All experiments were performed in triplicate for each gene of each strain, obtaining very similar values (differences of less than 0.3 SD). A non-template control reaction mixture was included for each gene. The quantification technique used to analyze data was the $2^{-\Delta\Delta C_T}$ method described by Livak and Shmittgen (2001), and the results were plotted.

The data were normalized using the *ihfB* gene as an internal control (housekeeping gene). We detected the same expression level of this gene in all the strains in the conditions in which the bacteria were grown. For each analyzed gene in all strains the transcription level of the wild-type gene, considered as one, was used as the control to normalize the data. Therefore, data are reported as relative expression levels, compared to the expression level of JM101. Results presented in Table 3 and in Figs. 1–3 are the averages of four independent measurements of the RT–PCR expression values for each gene. Half of the values were obtained from two different cDNAs generated from one fermentation and the other two from another identical fermentation. The RT–PCR expression values obtained for each gene differ less than 30%.

3. Results and discussion

The key to understanding the PTS$^-$ Glc$^+$ mutant phenotype is to differentiate the phenotypes caused by the deletion of the *ptsIHcrr* operon in the PTS$^-$ PB11 strain from the ones selected in the PTS$^-$Glc$^+$ PB12 strain. Therefore, the results are presented and discussed in a comparative approach, where the relative RT–PCR transcription values of 104 genes from the JM101

Table 3
Relative transcription levels determined by RT–PCR of several groups of genes from strains JM101, PB11 and PB12

Pathway, process or group of genes	Expression levels as $2^{-\Delta\Delta C_t}$ with JM101 as normalizing value	
	PB11	PB12
a. gal regulon		
galE	38.8±6.864	46.6±6.506
galT	35.6±2.376	42.5±3.995
galK	39.0±2.376	48.2±3.995
galM	8.1±3.946	3.3±0.692
galP	12.4±1.086	13.1±1.867
galS	4.9±0.477	3.2±0.526
galR	3.2±0.199	1.2±0.472
galU	1.7±0.309	2.1± 0.366
mglB	13.4±0.098	9.0±1.606
*lamB**	17.6±0.374	0.9±0.019
*pgm**	1.7±0.310	2.3±0.458
b. Glycolysis		
glk	1.0±0.032	2.2±0.103
pgi	1.0±0.080	6.6±0.282
pfkA	0.3±0.040	0.5±0.012
fbaA	0.9±0.046	1.1±0.052
tpiA	0.5±0.034	1.8±0.029
gapA	0.4±0.151	1.7±0.214
pgk	0.7±0.001	1.2±0.060
gpmA	0.9±0.007	1.8±0.039
eno	0.5±0.169	0.5±0.146
pykA	0.4±0.002	1.0±0.045
pykF	0.8±0.010	0.9±0.001
aceE	0.4±0.025	1.4±0.023
aceF	0.6±0.022	1.2±0.004
lpd	1.1±0.107	2.0±0.128
c. Pentose pathway		
zwf	0.7±0.063	1.9±0.175
gnd	0.8±0.110	1.2±0.069
rpe	0.7±0.092	0.9±0.046
rpiA	0.6±0.000	1.6±0.150
rpiB	1.4±0.307	1.9±0.291
tktA	0.5±0.050	2.4±0.114
tktB	11.6±0.228	5.7±0.122
talA	10.6±1.924	5.1±0.732
talB	1.1±0.061	1.6±0.002
eda	0.5±0.038	1.2±0.047
edd	0.3±0.024	0.5±0.088
d. TCA cycle and glyoxylate shunt		
gltA	0.8±0.083	1.3±0.171
*acnA**	5.2±0.594	5.7±0.232
acnB	1.7±0.364	1.7±0.422
aceB	15.6±2.519	3.7±0.308
aceA	11.9±1.248	1.9±0.225
aceK	5.5±0.774	1.9±0.255
glcB	11.7±1.417	3.7±0.477
*glcC**	3.6±0.299	6.9±0.134
icdA	1.0±0.103	1.9±0.003
sucA	1.4±0.099	1.7±0.068
sucB	0.8±0.035	1.4±0.086
ldp	1.1±0.107	2.0±0.128
sucC	0.9±0.072	1.6±0.026
sucD	1.0±0.213	1.4±0.302
sdhA	0.9±0.004	2.0±0.278
sdhB	0.8±0.043	1.7±0.027
sdhC	1.3±0.112	2.1±0.593
sdhD	0.9±0.017	1.8±0.052
fumA	3.3±0.675	3.6±0.673
fumB	0.8±0.705	0.7±0.365
*fumC**	4.3±0.989	3.5±1.482
mdh	1.2±0.141	1.8±0.520
e. Anaplerotic genes		
maeB	1.2±0.201	2.5±0.032
sfcA	1.9±0.332	1.7±0.100
mdh	1.2±0.141	1.8±0.520
ppsA	3.7±0.216	2.4±0.092
pckA	0.8±0.068	2.3±0.026
ppc	0.6±0.059	0.8±0.009
f. Gluconeogenesis		
maeB	1.2±0.201	2.5±0.032
sfcA	1.9±0.332	1.7±0.100
mdh	1.2±0.141	1.8±0.520
ppsA	3.7±0.216	2.4±0.092
pckA	0.8±0.068	2.3±0.026
ppc	0.6±0.059	0.8±0.009
eno	0.5±0.169	0.5±0.146
gpmA	0.9±0.007	1.8±0.039
gpmB	1.5±0.227	2.7±0.357
pgk	0.7±0.001	1.2±0.060
gapA	0.4±0.151	1.7±0.214
gapC-1	6.7±0.108	3.1±0.091
gapC-2	3.9±0.193	3.2±0.015
fbaB	10.6±1.137	4.9±0.858
fbaA	0.9±0.046	1.1±0.052
fbp	2.4±0.751	2.8±0.138
pfkB	1.2±0.224	1.9±0.205
pgi	1.0±0.080	6.6±0.282
g. Respiration		
nuoA	0.4±0.007	2.4±0.112
nuoF	0.3±0.117	1.4±0.109
nuoN	0.4±0.021	1.0±0.084
ndh	0.6±0.036	1.1±0.076
sdhA	0.8±0.004	2.0±0.278
sdhB	0.8±0.043	1.7±0.027
sdhC	1.3±0.112	2.1±0.593
sdhD	0.9±0.017	1.8±0.052
ubiE	0.4±0.013	1.6±0.015
frdA	0.2±0.009	0.6±0.035
frdB	0.1±0.009	0.7±0.045
frdC	0.2±0.030	0.7±0.010
frdD	0.2±0.049	0.8±0.063
napA	0.1±0.010	0.9±0.132
narG	0.2±0.043	1.2±0.113
cydB	0.4±0.030	0.9±0.039
cyoA	0.6±0.015	1.5±0.071
cyoB	0.3±0.035	1.4±0.140
cyoC	0.3±0.011	1.2±0.160
cyoD	0.3±0.029	1.1±0.092
h. Fermentation and acetate production and utilization genes		
ldhA	0.6±0.019	1.1±0.244

Table 3 (*continued*)

Pathway, process or group of genes	Expression levels as $2^{-\Delta\Delta C_t}$ with JM101 as normalizing value	
	PB11	PB12
pta	0.7±0.129	1.5±0.329
ackA	0.4±0.121	0.8±0.013
adhE	0.6±0.079	0.9±0.041
poxB	4.2±0.353	5.7±0.485
acs	5.6±0.745	8.0±0.136
yjcG (*actP*)	5.1±0.455	7.2±0.219
i. Regulators		
cyaA	1.4±0.063	1.8±0.098
crp	0.8±0.020	1.0±0.053
fruR	1.3±0.002	1.5±0.074
arcA	1.2±0.020	1.3±0.094
arcB	2.3±0.707	1.3±0.722
mlc	1.1±0.003	1.7±0.061
ihfA	1.8±0.045	1.7±0.060
ihfB	1.0±0.000	1.0±0.000
iclR	0.4±0.035	1.4±0.075
fadR	0.6±0.031	1.6±0.082
rpoS	2.9±0.086	2.2±0.156

This table shows the relative transcription levels of the different groups of genes involved in different pathways and processes. For each gene in all strains, the transcription level of the gene for the wild-type strain was used as the control to normalize the data using the wild-type RT–PCR value for that gene as one. Therefore, data in this table and in Figs. 2 and 3 are reported as relative expression levels, compared to the expression level of JM101. The results are the averages of four independent measurements of the RT–PCR expression values for each gene. Two of the values were obtained from one fermentation and the two others from an independent fermentation grown on identical conditions for each strain. The RT–PCR expression values obtained for each gene differ between them in most of the genes by less than 30% (see Materials and methods for a more detailed explanation). Genes marked with an asterisk are not part of the specific pathway or regulon, but are included because their products are related to the enzymes coded by the specific group of genes, or for comparative purposes; see text and figure legends for detailed explanations.

wild-type strain are compared with PTS$^-$ and PTS$^-$Glc$^+$ strains. These analyzed genes include the *gal* regulon that is responsible for glucose transport in PTS$^-$ strains and genes involved in various functions in different sections of the central carbon metabolism.

3.1. Glucose transport and phosphorylation in PTS$^-$ strains

Wild-type *E. coli* strains growing on micromolar concentrations of glucose synthesize galactose and maltodextrines as autoinducers that derepress the synthesis of the high-affinity glucose transport systems MglB and the LamB maltoporin, which are responsible for glucose transport under these conditions. Other genes induced in these conditions include the *galETK* operon (Death and Ferenci, 1994; Ferenci, 2001). Recently, the analysis of gene expression in wild-type *E. coli* in response to a shift from glucose non-limiting to glucose-limiting growth conditions ($\mu = 0.1\ h^{-1}$) in chemostat cultures demonstrated that in these conditions, several genes including *mglB* (10-fold) and *lamB* (20-fold), as well as *aceA*, the *acs* operon (*acs*, *yjcG*), and *fumA* are upregulated (Hua et al., 2004).

A culture of PB11 PTS$^-$ strain grows very slowly in minimal medium containing a relatively high concentration of glucose (2 g/l) as the sole carbon source. Therefore, it can be expected that this strain senses very low concentration of internal glucose or glucose-6-P. In order to determine if this physiological condition leads to the induction of high-affinity and/or alternative glucose transport systems, the relative transcription levels of genes related to this response were determined in PTS$^-$ strains and in JM101. As shown in Table 3a, PB11 upregulates the transcription of *mglB* (13-fold) and *lamB* (17.6-fold) as compared to the wild-type JM101 strain. This strain also induces other genes of the *gal* regulon like *galP* (12.4-fold), *galS* (4.9-fold), *galE* (38.8-fold), *galT* (35.6-fold) and *galK* (39-fold). From these results it can be inferred that in this growing condition, PB11 induces the synthesis of galactose as an autoinducer of the *gal* regulon. This in turn should inactivate GalS and GalR, the repressors of the *gal* regulon (Geanacopoulos and Adhya, 1997), resulting in the induction of all the *gal* regulon genes, and thus permitting the internalization of glucose through the galactose transporters (Ferenci, 2001).

These results indicate that PB11 may utilize either MglB and/or GalP for glucose transport through the cytoplasmic membrane into the cytosol, in these growing conditions. However, the slow growth on glucose indicates that this strain is incapable of phosphorylating all the incoming glucose with the amount of Glk activity present in this PTS$^-$ strain (Fig. 1) (Curtis and Epstein, 1975; Flores et al., 2002).

Strain PB12 is a PB11-derived mutant that has recovered the capacity to grow fast in glucose. This can be explained by the fact that *glk* is transcribed at a higher level (two-fold) in PB12 than in the wild-type and PB11 strains (Table 3b). Therefore, the product of this upregulated gene, whose specific activity is also increased (two-fold) in PB12 (Flores et al., 2002), allows a higher degree of glucose phosphorylation of the transported glucose in PB12 than in PB11. PB12 that does not carry any mutation in the *gal* regulon genes (data not shown) uses GalP for transporting glucose (Flores et al., 1996; Flores et al., 2002). Concurrently, in this strain the *galP* transcript level is 12.4-fold higher than the wild-type. Hence, glucose can be transported by GalP and phosphorylated at a higher rate by Glk in PB12 than in PB11, thus allowing a high growth rate.

Differences in growth capacities between these strains could also be related to the availability of regulatory molecules like cAMP. CRP-cAMP plays an important

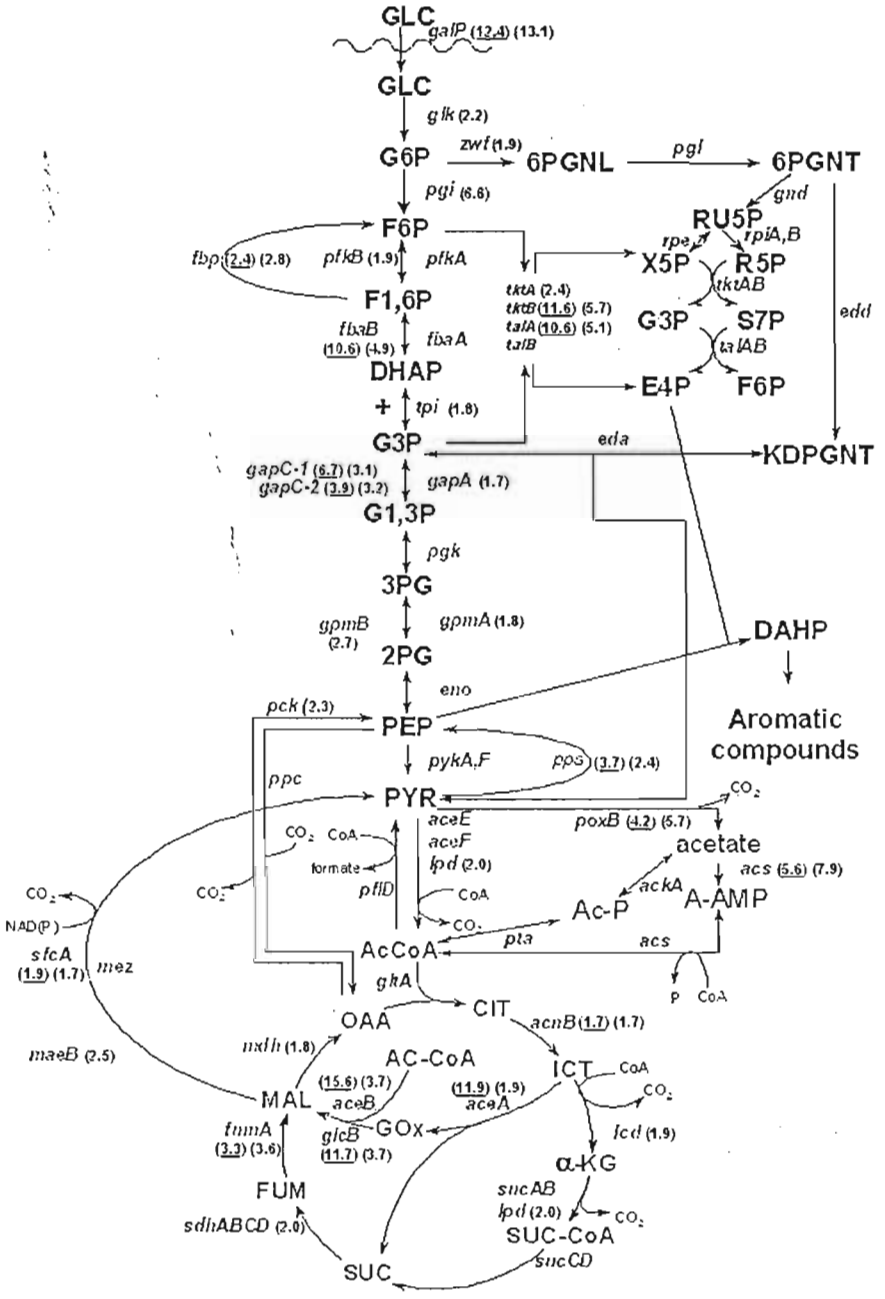

Fig. 1. Central metabolic routes. Central metabolic routes showing key metabolites and the genes involved in their transformation. RT–PCR values of those upregulated genes (1.7-fold or higher) are shown close to the gene in parenthesis for PB12 and underlined in parenthesis for PB11; see Table 3 for the complete set of RT–PCR values. The abbreviations are as follows: glucose (GLC), glucose-6-phosphate (G6P), fructose-6-phosphate (F6P), fructose-1,6-phosphate (F1,6P), dihydroxy-acetone phosphate (DHAP), glyceraldehyde-3-phosphate (G3P), glyceraldehyde-1,3-phosphate (G1,3P), 3-phosphoglycerate (3PG), 2-phosphoglycerate (2PG), phosphoenolpyruvate (PEP), pyruvate (PYR), acetyl-CoA (AcCoA), acetyl phosphate (Ac-P), acetyl-AMP (A-AMP), citrate (CIT), isocitrate (ICT), glyoxylate (Gox), α-ketoglutarate (α-KG), succinyl-coenzyme A (SUC-CoA), succinate (SUC), fumarate (FUM), malate (MAL), oxaloacetate (OAA), 6-phosphogluconolactone (6PGNL), 6-phosphogluconate (6PGNT), ribulose-5-phosphate (RU5P), ribose-5-phosphate (R5P), xylulose-5-phosphate (X5P), seudoheptulose-7-phosphate (S7P), erythrose-4-phosphate (E4P), 2-keto-3-deoxy-6-phosphogluconate (KDPGNT), 3-deoxy-D-arabino-heptulosonate-7-phosphate (DAHP).

role in transcription activation of most of the *gal* regulon genes among others, and it is known that a deletion of the *crp* gene completely inactivates the expression of the *galETK* operon and the *galS* gene (Weickert and Adhya, 1993; Geanacopoulos and Adhya, 1997). It has also been reported that some *E. coli* strains carrying a deletion of the PTS$^-$ operon produce less cAMP than the wild-type strains (Levy

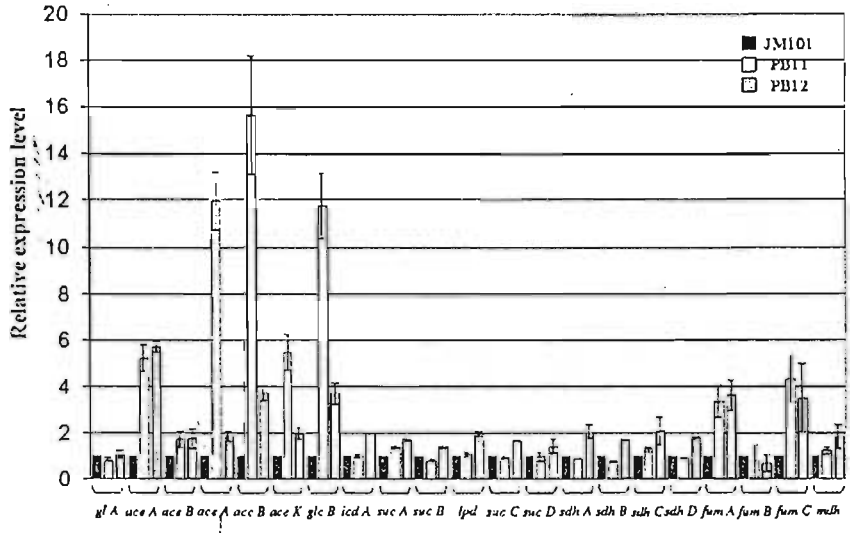

Fig. 2. Relative transcription expression values of genes that code for the enzymes of the TCA cycle and the glyoxylate shunt. This figure and Table 3d present the relative transcription values of 20 genes coding for enzymes involved in the TCA cycle and in the glyoxylate pathway in these strains, as well as the genes coding for *acnA*, *fumC* and *glcB*. It is important to remember that for aconitase as well as fumarase, there are two major aerobic enzymes AcnB and FumA, whose transcriptional regulation is typical of TCA enzymes, whereas the enzymes AcnA and FumC are adapted for stress-related responses and are regulated by RpoS; nevertheless, all these four genes as well as all the TCA cycle and the glyoxylate genes are regulated by ArcA (Cunningham et al., 1997). See Sections 3.4 and 3.6 for detailed explanation.

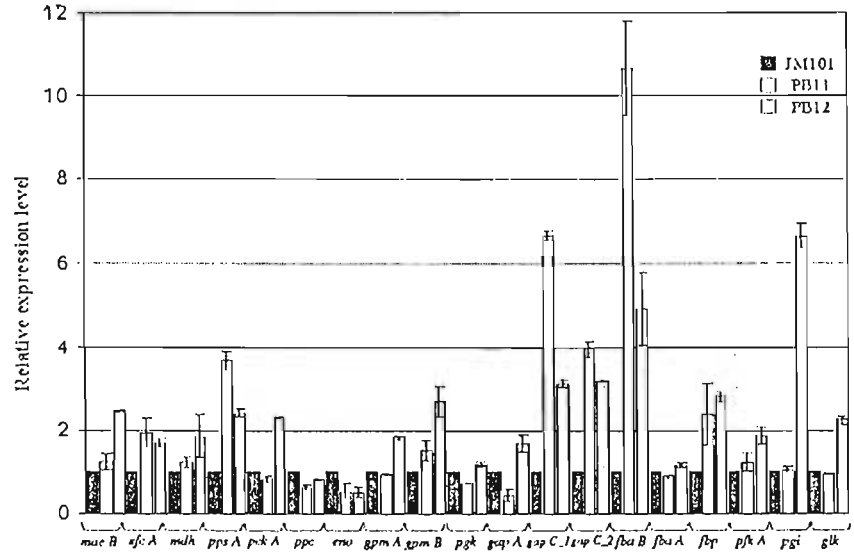

Fig. 3. Relative transcription expression values of genes involved in gluconeogenesis. This figure and Table 3f present the comparative expression of genes whose products have been involved in gluconeogenesis. The transcription values of *mdh*, *maeB*, *sfcA*, *pckA*, *ppc* and *ppsA* have been presented in Table 3e, while the expression of all these genes and also *eno*, *gpmA*, *pgkA*, *fba* and *pgi* are shown in Table 3b. Table 3f and this figure include the expression of *gpmB*, $gapC_1$, $gapC_2$, *fbaB*, *fbp* and *pfkB*. It is known that certain genes like *pfkB*, *fbp*, *fbaB*, and *ppsA* are involved in gluconeogenesis, because their inactivation inhibits the growth of the cell in gluconeogenic substrates carrying the mutation (Frankel, 1996). No function has been assigned for *gpmB*, $gapC_1$ and $gapC_2$, whose expression is also upregulated. These last genes have been included in the figure because they could participate in gluconeogenesis in these strains. See Sections 3.4, 3.5 and 3.7 for explanation.

et al., 1990). Nevertheless, the results obtained here indicate that these PTS$^-$ strains should have enough CRP-cAMP to activate those genes that require it, like *galETK*, *galS* (Table 3a) and others, like the TCA genes (see Section 3.6). This is supported by the facts that in PB11 and PB12, the transcription level of the *crp* gene is similar to the one present in the wild-type strain JM101 and the transcription of *cyaA*, encoding for the adenylate cyclase, is slightly upregulated in PTS$^-$ strains (Table 3i). These results indicate that in the absence of the IIA^{Glc} component of PTS that is involved in the activation of adenylate cyclase (Postma et al., 1996),

there might be other enzymes that could perform this activation in these strains, if it is indeed required.

3.2. Glucose-6-P catabolism into pyruvate (PYR)

Analysis of carbon fluxes and RT–PCR values indicate that PB11 and PB12 have different metabolic capacities that enable them to metabolize glucose (and other molecules, Section 3.6) as carbon source. As mentioned, PTS$^-$ strains require Glk to phosphorylate glucose (Curtis and Epstein, 1975; Flores et al., 2002). PB11 that has a relatively low glycolytic flux (42%) in the first step of the EM pathway as compared to the wild-type (77%) and PB12 (95%) transports glucose at a very slow rate and uses both the pentose and the glycolytic pathways to catabolize glucose-6-P in similar proportions. However, PB12 regained a relative rapid growth on glucose ($\mu = 0.42\,h^{-1}$), probably due to an upregulation of *glk* and also *pgi* that permits a higher rate of phosphorylation and initial transformation of glucose into fructose-6-P (Table 3b). This strain has modified its flux by increasing its glycolytic carbon flux in the first step of the pathway to 95% (Flores et al., 2002).

We originally thought that the relatively higher glycolytic flux in the initial steps of the glucose catabolism in PB12 could be responsible for the synthesis of a larger pool of fructose-6-P, fructose-1,6-*bis*-P or both than those usually present in a wild-type strain. This situation, in turn, could result in the in vivo inactivation of the Cra (or FruR) repressor coded by *fruR*. Since *glk* is repressed by Cra, under this scenario *glk* transcription would be upregulated in this strain (Meyer et al., 1997; Saier and Ramseier, 1996). However, this does not seem to be the case, because the transcription level of several other genes, such as *pykF*, *pckA* and *edd* that are repressed by Cra, does not increase in PB12 as compared to JM101 (Table 3b) (Saier and Ramseir, 1996). To ascertain whether the change in the expression of *glk* and *pgi* could be the result of a mutation at their regulatory regions, we determined the nucleotide sequence of approximately 250 bp upstream of the translation initiation codon and the complete coding regions of these two genes in all strains. However, no mutation was detected. The nucleotide sequences of the regulatory and structural regions of *fruR* were also determined without detecting any mutation.

It is important to point out that there are no significant carbon flux differences between the wild-type and the PB12 strain in the remaining steps of the EM pathway from fructose-6-P down to the synthesis of PEP, whereas there is a decreased flux in PB11 as compared to the other strains in this part of the pathway (Fig. 1) (Flores et al., 2002). These results are in agreement with RT–PCR values, showing that the expression levels of the genes involved in the transformation of fructose-6-P into PEP of JM101 and PB12 are expressed basically at the same level, while this group of genes, in general, are apparently slightly downregulated in PB11 (Table 3b). However, this last set of values should be taken with caution because some of them are within the limits of experimental error.

PTS$^-$ strains cannot synthesize PYR from PEP using PTS. Therefore, they should use the two PYR kinases encoded by *pykA* and *pykF* for this purpose (Fig. 1). In these PTS$^-$ strains the carbon flux values from PEP to PYR via PYR kinases are significantly higher than in the wild-type (Flores et al., 2002). Therefore, we were expecting higher transcript levels for the *pykA* or *pykF* genes in the PTS$^-$ mutants as compared to the wild-type, to compensate for the absence of PTS. However, the expression of the *pyk* genes did not increase but even slightly decreased in PB11 and did not change significantly in PB12 as compared to JM101 (Table 3b). These results indicate that the total PYR kinase activity present in these PTS$^-$ *E. coli* strains (Ponce et al., 1998) is sufficient to convert PEP into PYR at a similar rate as in the JM101 strain. PEP can also be converted into oxaloacetate by the PEP carboxylase (Ppc) enzyme coded by *ppc*, whose transcription is slightly downregulated in PB11 and PB12 as compared to JM101 (Table 3e).

3.3. PYR transformation into acetate and acetyl CoA

Once PYR has been synthesized from PEP, it can be transformed into acetyl CoA (AcCoA) in order to be incorporated into the TCA cycle and/or the glyoxylate shunt. In wild-type *E. coli* growing on high glucose concentrations and aerobic conditions, this reaction is catalyzed mainly by the PYR dehydrogenase complex (Pdh) coded by *aceE*, *aceF* and *lpd* that conform to the *pdh* operon (Quail et al., 1994). The first two genes are downregulated in PB11 as compared to JM101, while the value for *lpd* is similar in both strains. In the case of PB12, the first two genes are slightly upregulated and *lpd* is two-fold upregulated (Fig. 1, Table 3b). These transcription values in the two PTS$^-$ strains, especially in PB11, are not in agreement with the two-fold increase in carbon fluxes detected from PYR to AcCoA as compared to the wild-type strain (Flores et al., 2002).

However, in this context it is important to point out that the *poxB* gene that codes for PYR oxidase (PoxB), an enzyme that converts PYR into acetate and simultaneously reduces quinones in the membrane, is highly upregulated (four- to five-fold) in both PTS$^-$ strains (Fig. 1, Table 3h). We propose that in the PTS$^-$ strains this enzyme could be producing acetate, which can be transformed into AcCoA, explaining the increase in carbon flux between PYR and AcCoA in PTS$^-$ strains (Fig. 1). This is in agreement with the upregula-

In *E. coli*, the *glc* locus associated with glycolate utilization includes *glcB* encoding malate synthase and other genes needed for glycolate oxidase activity like *glcC* that codes for a Glc activator protein. The metabolic pathways specified by *glc* and *aceBAK* operons yield glyoxylate as a common intermediate, which is utilized by the two malate synthases coded by *glcB* and *aceA*. Pellicer et al. (1999) demonstrated that null mutations in either gene exhibit no phenotype because of cross induction of the *aceBAK* operon by glycolate and the *glc* operon by acetate. In the same study, it was also demonstrated that the regulation of the *glc* operon including *glcB* is under the positive control of GlcC encoded by a divergent gene. Furthermore, it was shown that the expression of the *glc* operon like the *aceBAK* operon is negatively controlled by ArcA.

Interestingly, the transcription pattern of *glcB* is similar to the *aceBAK* operon in PB11 and PB12. It is highly upregulated in PB11 (more than 10-fold) and less but still relatively highly (3.7-fold) upregulated in PB12. We propose that acetate, produced via PoxB, should also play a role in the upregulation of the *glc* operon and the *glcC* regulator gene in PB11 and PB12 (Table 3d). The inactivation of ArcB or enhancement of its ArcA-P dephosphorylating activity (Georgellis et al., 1998; Malpica et al., 2004) in PB12 could contribute to the upregulation of *glcC* and *glcB* genes as it occurs with the *aceBAK* operon.

In PB11, the genes that code for four of the respiratory reductase systems (CyoABCD, CydAB, FrdABCD, NarG) as well as *ubiE* that is involved in the biosynthesis of ubiquinone are downregulated. The genes coding for the dehydrogenases involved in electron transfer from substrates to quinones during the first step of the respiratory chains (*NuoAN*, *Ndh*, *SdhABCD*) are also downregulated as compared with JM101 and PB12. The only respiratory gene that is highly upregulated in PB11 (four-fold) and in PB12 (five-fold) is *poxB*, whose encoded enzyme utilizes PYR as an electron donor and produces acetate in these PTS^- strains (Table 3g). This gene could be playing a dual role, at least in PB11: in respiration by reducing quinones in the membrane and in the induction of the *aceBAK* and *acs* operons by producing acetate. Nevertheless, it appears that the respiratory capabilities of PB11 are diminished as compared to the two other strains. ArcA regulates the expression of several of these genes (Lynch and Lin, 1996; Iuchi et al., 1990), and as can be seen in Table 3g, the expression of *sdhABCD*, and *cyoABCD*, which are examples of this situation, are apparently slightly upregulated in PB12 as compared to PB11 and JM101. However, this last set of values should be taken with caution because some of them are within the limits of experimental error.

3.8. Fermentation processes and acetate production and utilization genes in the PTS strains

The transcription levels of genes involved in the production of fermentation products (*ldhA*, *adhE*, *pta*, *ackA*) are slightly downregulated in PB11 as compared to JM101 (Table 3h). In fact, it has been reported that PB11 does not produce any detectable fermentation products (Flores et al., 2002). The transcription values of these genes are basically the same between PB12 and JM101 with the exception of *pta* that is upregulated (1.8-fold) in this PTS^- strain. PB12 produces small amounts of lactate and also less acetate (produced at the late log phase) than JM101 (Flores et al., 2002; S. Flores, pers. comm.).

It has been proposed that in *E. coli* the phosphotransacetylase-acetate kinase pathway, coded by *pta* and *ackA*, functions primarily in a catabolic role, generating ATP during aerobic growth on excess glucose. These enzymes also catalyze the low-affinity reverse pathway that is activated when acetate is present extracellularly in large quantities. However, the Acs pathway that includes the AcCoA synthetase (Acs) and an acetate permease, coded by the *acs* and *yjcG* (*actP*) genes, is induced by acetate for the purpose of scavenging this molecule (Gimenez et al., 2003; Phue and Shiloach, 2004). As previously mentioned, we propose that the two PTS^- strains could be using PoxB to produce acetate as an autoinducer responsible of *aceBAK* and *acs* operon upregulation. This internally produced acetate should be transformed into AcCoA by Acs, coded by *acs* that is also highly upregulated as are the *yjcG* (*act*P) and *poxB* genes, in both PTS^- strains, and finally incorporated into the TCA cycle and/or glyoxylate shunt (Table 3h).

It is relevant to emphasize that *poxB* and *acs* as well as many other genes have RpoS-dependent promoters (Chang et al., 1994; Shin et al., 1997; Hengge-Aronis, 2002). The transcription of *rpoS* is upregulated in PB11 and PB12, 2.9- and 2.2-fold, respectively (Table 3i). This should explain the upregulation of the *poxB* and *acs* genes in these strains. All these results indicate that the PTS^- strains have modified their capabilities of converting PYR into AcCoA not only with the use of Pdh but also with the participation of the PYR oxidase and the AcCoA synthetase.

3.9. The pentose pathway and the capacity to synthesize aromatic compounds in PB12

JM101 directs 22% of total glucose-6-P through the glucose dehydrogenase (Zwf) enzyme when growing aerobically on glucose as the carbon source. The *zwf* gene in PB11 is slightly downregulated while in PB12 it is slightly upregulated when compared with JM101. These results are in agreement with the specific activities

monitored for Zwf in these strains (Flores et al., 2002). It has been previously demonstrated that PB12 uses intermediates of the EM pathway to synthesize ribose-5-P and eritrose-4-P (E-4P) by the sequential action of transaldolases and transketolases (Frankel, 1996; Flores et al., 2002). As can be seen in Table 3c, *tktB* and *talA* genes that code for transketolase B and transaldolase A are both highly upregulated in PB11 (11-fold) and in PB12 (five-fold) as compared with JM101. The expression of *tktA*, *talB*, *rpiB*, *rpiA*, *rpe* and *eda* is also upregulated in PB12.

3.10. The expression of genes coding for regulatory proteins

We determined the transcription values for several genes whose products are known to be regulatory proteins. As can be seen in Table 3i, the transcription of some of these genes like *crp* did not change significantly in PB11 when compared to JM101. However, there are some other genes whose transcription is moderately upregulated, like *cyaA*, *arcB* and *rpoS* in this PTS$^-$ strain. On the other hand, the transcription of *iclR* and *fadR* is downregulated in PB11 as compared to JM101. In PB12, the transcription of some of these genes like *crp*, *arcA* and *arcB* did not change significantly as compared to JM101; however, most of the remaining genes seem to be slightly upregulated.

The downregulation of *iclR* and *fadR* could play an important role in the derepression (15- to 5.5-fold) of *aceBAK* operon in PB11. On the other hand, the upregulation of these two genes in PB12 may result in partial activation of IclR and FadR and thus a partial repression of the *aceBAK* operon (3.7- to two-fold). Similarly, the increase of transcription of *rpoS* in both PTS$^-$ strains could explain the upregulation of several genes (*poxB*, *acs*, *fumA*, *acnA* and others) that have RpoS-dependent promoters.

3.11. Concluding remarks

As a result of this analysis, significant transcriptional differences were detected for several genes. These results have contributed to the understanding of the different metabolic capacities in the PB11 PTS$^-$ and PB12 PTS$^-$Glc$^+$ strains. Some of the important changes and commentaries are the following:

(a) PB11 grows very slowly in glucose because it cannot transport and phosphorylate the carbohydrate efficiently. Therefore, the cell should sense internally very low glucose or glucose-6-P concentrations. As a response of this starvation-stress condition, it can be inferred that the cell should synthesize several autoinducers, for scavenging purposes (Ferenci, 2001; Hua et al., 2004). Among these autoinducers, should be galactose that permits the upregulation of the *gal* operon, and this allows PB11 to transport glucose through GalP and/or MglB. We also propose that acetate, which is probably produced by PoxB, might be another autoinducer synthesized in this condition in PB11. Acetate (or a related metabolite) could function as the autoinducer of the operons involved in its utilization like *aceBAK*, *acs* and *glc* that are highly upregulated in PB11. Interestingly, RpoS, whose coding gene is also upregulated in the PTS$^-$ strains, should be involved in the transcription of *poxB* and *acs* genes, even in media with high glucose concentration.

PB12 PTS$^-$Glc$^+$ is capable of growing faster than PB11, mainly because the *glk* and *pgi* genes are upregulated in PB12, allowing better glucose phosphorylation and isomerization into fructose-6-P. The *gal* regulon as well as the *aceBAK*, *acs* and *glc* operons are upregulated in this strain; therefore, PB12 should also be producing galactose and acetate (or a related metabolite) as autoinducers. The upregulation of these operons would explain why both PTS$^-$ strains can utilize simultaneously glucose and acetate as carbon sources. Furthermore, the growth rates of PTS$^-$ strains increased when growing in both carbon sources without any detectable lag phase. This result is a clear indication that the enzymes required for rapid incorporation of acetate (coded by the *aceBAK* and *acs* operons) are already present in the cells. These results are in agreement with the high increase (two-fold) in carbon fluxes between PYR and AcCoA present in PTS$^-$ strains, and also with the high increase (2.5-fold) in carbon flux between citrate and malate in PB11, as compared to JM101 (Flores et al., 2002).

When wild-type *E. coli* is grown on glucose-limiting starvation-stress conditions or in chemostat cultures with limited glucose with a specific growth rate of $0.1\,h^{-1}$, it induces the production of galactose as an autoinducer of the *gal* operon that in turn allows the synthesis of the high-affinity glucose transport MglB for the internalization of glucose (Death and Ferenci, 1994; Hua et al., 2004). As the cell also upregulates *aceA* and the *acs* operon (Hua et al., 2004), it is reasonable to infer that like in the PTS$^-$ strains, wild-type strains in this limited glucose growing conditions also produce acetate as an autoinducer for scavenging purposes. These results indicate that a wild-type strain growing in glucose-limiting conditions utilizes mainly the MglB high-affinity permease and Glk to transport and phosphorylate glucose, instead of PTS. When the cell finds glucose in high concentration, PTS works again and utilizes this carbohydrate as the preferential carbon source (Ferenci, 2001). This results in the shutting down of the scavenging signals, repressing the *gal*, *aceBAK* and *acs* operons. Therefore, the adaptative stress capability of a wild-type *E. coli* for synthesizing autoinducers when sensing very low glucose concentrations is genetically frozen and permanently present in

the PTS$^-$ strains because of the lack of the PTS. Also, the obligation of using Glk in these strains does not allow the cell to efficiently couple the transport of glucose to its phosphorylation and catabolism. This situation, in fact a stress-starvation condition, could be responsible for the cell sensing internal glucose or glucose-6-P at very low concentrations, even in the presence of high glucose in the growing medium, but certainly at different levels between PB11 and PB12.

(b) PB12 has the capacity to synthesize aromatic compounds with a high yield from glucose. These results have been explained in terms of the higher PEP metabolic availability, resulting from the ATP-dependent glucose transport in these strains (Flores et al., 1996; Báez et al., 2001; Báez-Viveros et al., 2004). The data obtained in this work provide new information that helps to understand the relationship between the phenotypic characteristics of strain PB12 and its high capacity to synthesize aromatic compounds. In this strain, the upregulation of *tktA*, *tktB*, *talA* and *talB* whose protein products are related to the synthesis of the aromatic precursor E4P from EMP intermediaries was detected. Additionally, the gluconeogenic genes *maeB*, *sfcA*, *pckA*, *pps*, *fbaB*, *fbp* and *pfkB* were upregulated. This result is significant in the context of the biosynthesis of aromatic compounds, since the protein product of the *pps* gene converts PYR into PEP and thus contributes to the increase in the metabolic availability of this second aromatic precursor. Furthermore, the gluconeogenic capacity coexisting with glycolytic capabilities detected in this strain, enabling the simultaneous utilization of glucose and acetate, is a physiological trait that could allow PB12 to utilize simultaneously glucose and other carbon sources and this could potentially increase the yield in the synthesis of aromatic compounds.

(c) A point mutation was found in the *arcB* gene of PB12. This mutation changed an original tyrosine into a cysteine residue at position 71 in the transmembrane region 2 of ArcB (Kwon et al., 2000). There are two Cys residues in the linker region of ArcB protein and recent data indicate that these two residues in ArcB are responsible for sensing the redox stage of the cell by being reduced or oxidized by the quinone pool (Malpica et al., 2004). It is of interest to note that during oxidizing conditions dephosphorylation of ArcA–P, a reaction needed to curtail its regulatory activity, was previously shown to proceed, at least in vitro, via an ArcA^{Asp54}–P→ArcB^{His717}–P→ArcB^{Asp576}–P→Pi reverse pathway (Georgellis et al., 1998). Thus, a possible explanation is that the new Cys residue might participate in disulfide bridge formation between two subunits of ArcB. This could result in a conformation of ArcB with enhanced ArcA–P dephosphorylating activity. This mutation could explain the slight upregulation of TCA cycle and certain respiratory genes in this strain during aerobiosis. It is important to emphasize that PB12 exhibits the same toluidine blue sensitive growth phenotype as the Δ*arcA* and Δ*arcB* strains (Iuchi and Lin, 1988), and that the introduction of a plasmid carrying the *arcB* gene restores its growth capacity. Nevertheless, the significance of this mutation remains to be studied in more detail. Recently, it was shown that the ArcA modulon probably recruits more than a 100 operons to mediate a role in cellular adaptation (Liu and DeWulf, 2004). Therefore, the selection of a mutation in *arcB* in PB11 could be an interesting alternative to genetically stabilize and/or permit the upregulation of several genes that in turn could allow certain metabolic flexibility. In PB12, the PTS$^-$Glc$^+$ phenotype is the result of at least two mutations not genetically linked (in addition to the deletion of the PTS genes) (Flores, 1995), one (or more) responsible for the upregulation of the *glk* and *pgi* genes that permits a faster growth in glucose, and the *arcB* mutation. It is hard to suggest which of these mutations occurred first. However, we favor the possibility that the *arcB* mutation occurred in the *glk–pgi* upregulated background because in these conditions the cell catabolizes glucose more efficiently and grows faster. This genetic background could allow the selection of a mutation for a better utilization of the TCA cycle and certain respiratory enzymes than in PB11.

(d) The nucleotide sequences of several genes were determined. As mentioned, only a single point mutation was found in *arcB* in PB12. Nevertheless, ArcAB regulatory system is neither known to regulate the expression of *glk* and *pgi* nor the expression of several other genes in different pathways that are also upregulated in PB12 as compared to PB11 and JM101. Therefore, in PB12 there might be one or more mutations in different genes not yet identified or related to this response. We are currently working on the isolation of the genes responsible for this phenotype.

Finally, there is still a lot to be done with the goal of characterizing and improving the utilization of these strains for production purposes. Initially, one of the regulatory systems that we will also study in more detail is the RpoS transcriptional regulator. RpoS is the sigma S subunit of the RNA polymerase that can partially replace the vegetative sigma factor (sigma 70) under stress conditions. As a consequence, transcription of numerous sigma S-dependent genes is activated. The regulation of its coding gene *rpoS* is a complex phenomenon in which several effectors participate like cAMP-CRP. This modulator apparently plays both activator and repressor roles depending on the cell growth condition (Hengge-Aronis, 2002). It seems likely that the absence of PTS induces a permanent stress-scavenging carbon response which causes the upregulation for *rpoS* that in turn could be responsible of the

upregulation of several stress responsive genes like *poxB*, *acs*, *acnA*, *fumC*, *pps*, *tktB* and others.

Acknowledgments

We thank Fernando Valle for the critical reading of the manuscript. We also thank Mercedes Enzaldo for technical support, Georgina Hernández for the detection of acetate and glucose by HPLC, as well as Paul Gaytán, Jorge Yáñez and Eugenio López for the synthesis of oligonucleotides and the sequencing of the genes (Instituto de Biotecnología-UNAM, México). S. Flores was supported by fellowships from CONACyT and UNAM. This work was partially supported by CONACyT Grants NC-230, 43243 and 37342-N, and DGAPA-PAPIIT, UNAM Grants IN220403-2, and IN218902.

References

Báez, J.L., Bolivar, F., Gosset, G., 2001. Determination of 3-deoxy-D-*arabino*-heptulosonate 7-phosphate productivity and yield from glucose in *Escherichia coli* devoid of the glucose phosphotransferase transport system. Biotechnol. Bioeng. 73, 530–535.

Báez-Viveros, J.L., Osuna, J., Hernández-Chávez, G., Soberón, X., Bolivar, F., Gosset, G., 2004. Metabolic engineering and protein directed evolution increase the yield of L-phenylalanine synthesized from glucose in *Escherichia coli*. Biotechnol. Bioeng. 87, 516–524.

Bailey, JE., 1991. Toward a science of metabolic engineering. Science 252, 1668–1675.

Bolivar, F., Rodriguez, R.L., Greene, P.J., Betlach, M.C., Heyneeker, H.L., Boyer, H.W., Crosa, J.H., Falkow, S., 1977. Construction and characterization of new cloning vehicles. II. A multipurpose cloning system. Gene 2, 95–113.

Chandran, S.S., Yi, J., Draths, K.M., Daeniken, R., Weber, W., Frost, J.W., 2003. Phosphoenolpyruvate availability and the biosynthesis of shikimic acid. Biotechnol. Prog. 19, 808–814.

Chang, Y.Y., Wang, A.Y., Cronan, J.E., 1994. Expression of *Escherichia coli* pyruvate oxidase (PoxB) depends on the sigma factor encoded by *rpoS* (*katF*) gene. Mol. Microbiol. 11, 1019–1028.

Chao, G., Shen, J., Tseng, C.P., Park, S.J., Gunsalus, R.P., 1997. Aerobic regulation of isocitrate dehydrogenase gene (*icd*) expression in *Escherichia coli* by the *arcA* and *fnr* gene products. J. Bacteriol. 179 (13), 4299–4304.

Chen, R., Hatzimanikatis, V., Yap, W.M.G.J., Postma, P.W., Bailey, J.E., 1997. Metabolic consequences of phosphotransferase (PTS) mutation in a phenylalanine-producing recombinant *Escherichia coli*. Biotechnol. Progr. 13, 768–775.

Cortay, J.S., Negre, D., Galinier, A., Duclos, B., Perriere, G., Cozzonne, A.J., 1991. Regulation of the acetate operon in *Escherichia coli*: purification and functional characterization of the IclR repressor. EMBO J. 10 (3), 675–679.

Cronan, J.E., Laporte, D.C., 1996. Tricarboxilic acid cycle and glyoxylate bypass. In: Neidhart, F.C. (Ed.), *Escherichia coli* and *Salmonella*: Cellular and Molecular Biology, 2nd ed. ASM, Washington, DC, USA, pp. 206–215.

Cunningham, L., Guest, J.R., 1998. Transcription and transcript processing in the *sdhCDAB* and *sucABCD* operon of *Escherichia coli*. Microbiology 144, 2113–2123.

Cunningham, L., Gruer, M.J., Guest, J.R., 1997. Transcriptional regulation of the aconitase genes (*acnA* and *acnB*) of *Escherichia coli*. Microbiology 143, 3795–3805.

Curtis, S.J., Epstein, W., 1975. Phosphorylation of D-glucose in mutants defective in glucose phosphotransferase, mannose phosphotransferase and glucokinase. J. Bacteriol. 122, 1189–1199.

Death, A., Ferenci, T., 1994. Between feast and famine: endogenous inducer synthesis in the adaptation of *Escherichia coli* to growth with limiting carbohydrates. J. Bacteriol. 176, 5101–5107.

Ferenci, T., 2001. Hungry bacteria—definition and properties of a nutritional state. Environ. Microbiol. 3, 605–609.

Flores, N., 1995. Master Degree Thesis. Construction and characterization of *Escherichia coli* strains lacking PTS. Institute of Biotechnology, UNAM, Mexico.

Flores, N., Xiao, J., Berry, A., Bolivar, F., Valle, F., 1996. Pathway engineering for the production of aromatic compounds in *Escherichia coli*. Nat. Biotechnol. 14, 620–623.

Flores, S., Gosset, G., Flores, N., de Graaf, A.A., Bolivar, F., 2002. Analysis of carbon metabolism in *Escherichia coli* strains with an inactive phosphotransferase system by ^{13}C labeling and NMR spectroscopy. Metab. Eng. 4, 124–137.

Frankel, D.G., 1996. Glycolysis. In: Neidhart, F.C. (Ed.), *Escherichia coli* and *Salmonella*: Cellular and Molecular Biology, 2nd ed. ASM, Washington, DC, USA, pp. 189–196.

Geanacopoulos, M., Adhya, S., 1997. Functional characterization of roles of GalR and GalS as regulators of the *gal* regulon. J. Bacteriol. 179, 228–234.

Georgellis, D., Kwon, O., De Wulf, P., Lin, E.C., 1998. Signal decay through a reverse phosphorelay in the Arc two-component signal transduction system. J. Biol. Chem. 273, 32864–32869.

Georgellis, D., Kwon, O., Lin, E.C., 2001. Quinones as the redox signal for the Arc two-component system of bacteria. Science 292, 2314–2316.

Gimenez, R., Nuñez, M.F., Badia, J., Aguilar, J., Baldosa, L., 2003. The gene *yjcG*, cotranscribed with gene *acs*, encodes an acetate permease in *Escherichia coli*. J. Bacteriol. 185, 6448–6455.

Gosset, G., Yong-Xiao, J., Berry, A., 1996. A direct comparison of approaches for increasing carbon flow to aromatic biosynthesis in *Escherichia coli*. J. Ind. Microbiol. 17, 47–52.

Gosset, G., Zhang, Z., Nayyar, S., Cuevas, W.A., Saier, M.H., 2004. Transcriptome analysis of Crp-dependant catabolite control of gene expression in *Escherichia coli*. J. Bacteriol. 186, 3516–3524.

Gui, L., Sunnarbory, A., LaPorte, D.C., 1996. Regulated expression of a repressor protein: FadR activates *IclR*. J. Bacteriol. 178, 4704–4709.

Hengge-Aronis, R., 2002. Signal transduction and regulatory mechanisms involved in control of the sigma S (RpoS) subunit of RNA polymerase. Microbiol. Mol. Biol. Rev. 66, 373–395.

Hernández-Montalvo, V., Martinez, A., Hernández-Chávez, G., Bolivar, F., Valle, F., Gosset, G., 2003. Expression of *galP* and *glk* in a *Escherichia coli* PTS mutant restores glucose transport and increases glycolytic flux to fermentation products. Biotechnol. Bioeng. 83, 687–694.

Hua, Q., Yand, C., Oshima, T., Mori, H., Shimizu, K., 2004. Analysis of gene expression in *Escherichia coli* in response to changes of growth-limiting nutrient in chemostat cultures. Appl. Environ. Microbiol. 70, 2354–2366.

Iuchi, S., Lin, E.C.C., 1988. *arcA* (*dye*), a global regulatory gene in *Escherichia coli* mediating repression of enzymes in aerobic pathways. Proc. Natl. Acad. Sci. USA 85, 1988–1992.

Iuchi, S., Lin, E.C.C., 1992. Mutational analysis of signal transduction by ArcB, a membrane sensor protein responsible for anaerobic repression of operons involved in the central aerobic pathways in *Escherichia coli*. J. Bacteriol. 174, 3972–3980.

Iuchi, S., Matsuda, Z., Fijiwara, T., Lin, E.C.C., 1990. The *arcB* gene of *Escherichia coli* encoded a sensor regulator protein for anaerobic repression of the *arc* modulon. Mol. Microbiol. 4 (5), 715–727.

Kwon, O., Georgellis, D., Lynch, A.S., Boyd, D., Lin, E.C.C., 2000. The ArcB sensor kinase of *Escherichia coli* genetic exploration of the transmembrane region. J. Bacteriol. 182, 2960–2966.

Levy, S., Zeng, G., Danctiing, A., 1990. Cycle cAMP synthesis in *Escherichia coli* strains bearing known deletions in the *pts* phosphotransferase operon. Gene 86, 27–33.

Liu, X., DeWulf, P., 2004. Probing the ArcP modulon of *Escherichia coli* by whole genome transcriptional analysis and sequence recognition profiling. J. Biol. Chem. 279, 12588–12597.

Livak, K., Shmittgen, T.D., 2001. Analysis of relative gene expression data using real-time quantitative PCR and the $2^{-\Delta\Delta C_T}$ method. Methods 25, 402–408.

Lynch, A.S., Lin, E.C.C., 1996. Responses to molecular oxygen. In: Neidhart, F.C. (Ed.), Cellular and Molecular Biology, 2nd ed. ASM, Washington, DC, USA, pp. 1526–1538.

Malpica, R., Franco, B., Rodríguez, C., Kwon, O., Georgellis, D., 2004. Identification of a quinone sensitive redox switch in the ArcB sensor kinase. Proc. Natl. Acad. Sci. USA 101, 13318–13323.

Meyer, D., Schneider, C., Halacker, R., Peist, R., Boos, W., 1997. Molecular characterization of glucokinase from *Escherichia coli* K-12. J. Bacteriol. 179, 1298–1306.

Neidhart, F.C., Ingraham, J.L., Scheachter, R., 1990. Biosynthesis and fueling. In: Physiology of the Bacterial Cell. A Molecular Approach. Sianuer, USA, pp. 133–173.

Park, S.J., Chao, G., Gunsalus, R.P., 1997. Aerobic regulation of the *sucABCD* genes of *Escherichia coli*, which encode α-ketoglutarate dehydrogenase and succinyl coenzyme A synthase: role of ArcA, Fnr and the upstream *sdhCDAB* promoter. J. Bacteriol. 179, 4138–4142.

Pellicer, M.A., Fernández, C., Badia, J., Aguilar, J., Linn, E., Baldosa, L., 1999. Cross-induction of *glc* and *ace* operons of *Escherichia coli* attributable to pathway intersection. J. Biol. Chem. 274, 1745–1752.

Phue, J.N., Shiloach, J., 2004. Transcription levels of key metabolic genes are the cause for different glucose utilization pathways in *Escherichia coli* B (BL21) and *Escherichia coli* K (JM109). J. Biotechnol. 109, 21–30.

Ponce, E., Martinez, A., Bolivar, F., Valle, F., 1998. Stimulation of glucose catabolism through the pentose pathway by the absence of the two pyruvate kinase isoenzymes in *Escherichia coli*. Biotechnol. Bioeng. 58, 292–295.

Postma, P.W., Lengeler, J.W., Jacobson, G.R., 1996. Phosphoenol-pyruvate: carbohydrate phosphotransferase systems. In: Neidhardt, F.C. (Ed.), *Escherichia coli* and *Salmonella*: Cellular and Molecular Biology, 2nd ed. ASM Press, USA, pp. 1149–1174.

Quail, M.A., Haydon, D.J., Guest, J.R., 1994. The *pdhR-aceEF-lpd* operon of *Escherichia coli* expresses the pyruvate dehydrogenase complex. Mol. Microbiol. 12, 95–104.

Raghunathan, A., Palsson, B., 2003. Scalable method to determine mutations that occur during adaptative evolution of *Escherichia coli*. Biotechnol. Lett. 25, 435–441.

Saier, M.H., 2002. Vectorial metabolism and the evolution of the transport systems. J. Bacteriol. 182, 5029–5035.

Saier, M.H., Ramseier, T.M., 1996. The catabolite repressor/activator (Cra) protein of enteric bacteria. J. Bacteriol. 178, 3411–3417.

Shen, J., Gunsalus, R.P., 1997. Role of multiple ArcA recognition sites in anaerobic regulation of succinate dehydrogenase (*sdhCDAB*) gene expression in *Escherichia coli*. Mol. Microbiol. 26, 223–226.

Shin, S., Song, S.G., Lee, D.S., Pan, J.G., Park, C., 1997. Involment of *iclR* and *rpoS* in the induction of *acs*, the gene for acetyl coenzyme A synthetase of *Escherichia coli* K-12. FEMS Microbiol. Lett. 146, 103–108.

Weickert, M., Adhya, S., 1993. The galactose regulon of *Escherichia coli*. Mol. Microbiol. 10, 245–251.

Pathway engineering for the production of aromatic compounds in *Escherichia coli*

Noemí Flores, Jimmy Xiao[1], Alan Berry[1], Francisco Bolivar, and Fernando Valle*

*Instituto de Biotecnología, Universidad Nacional Autónoma de México, Apdo. Postal 510-3, Cuernavaca, Morelos 62250, México. [1]Genencor International Inc., 180 Kimball Way, South San Francisco, CA 94080. *Corresponding author (e-mail: valle@ibt.unam.mx).*

Received 7 December 1995; accepted 4 March 1996.

Glucose is the preferred substrate for certain fermentation processes. During its internalization and concomitant formation of glucose-6-phosphate through the glucose phosphotransferase system (PTS), one molecule of phosphoenolpyruvate (PEP) is consumed. Together with erythrose 4-phosphate (E4P), PEP is condensed to form 3-deoxy-D-arabino-heptulosonate 7-phosphate (DAHP), the first intermediate of the common segment of the aromatic pathway. From this metabolic route, several commercially important aromatic compounds can be obtained. We have selected *Escherichia coli* mutants that can transport glucose efficiently by a non-PTS uptake system. In theory, this process should increase the availability of PEP for other biosynthetic reactions. Using these mutants, in a background where the DAHP synthase (the enzyme that catalyzes the condensation of PEP and E4P into DAHP) was amplified, we were able to show that at least some of the PEP saved during glucose transport, can be redirected into the aromatic pathway. This increased carbon commitment to the aromatic pathway was enhanced still further upon amplification of the *E. coli tktA* gene that encodes for a transketolase involved in the biosynthesis of E4P.

Keywords: amino acid overproduction, glucose transport, glycolysis, phosphoenolypyruvate

The metabolic route known as the shikimate pathway or common aromatic pathway leads to the production of many aromatic compounds, including the aromatic amino acids and other metabolites such as folate, *p*-aminobenzoate, and enterobactin. In addition, the introduction of specific genes into an organism having a suitably modified aromatic pathway expands the range of compounds that can be produced[1]. A good example of this is the production of indigo from glucose in *Escherichia coli*[2] (Fig. 1).

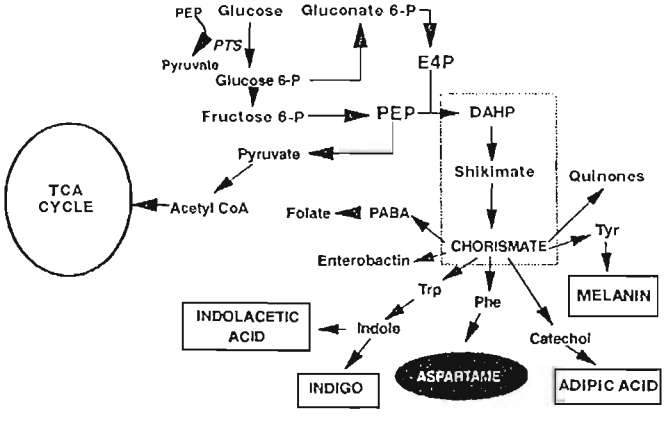

Figure 1. Pathways of central metabolism in *E. coli*. The derivation of carbon skeletons for the biosynthesis of aromatic compounds is shown. The shikimate or common aromatic pathway is indicated by the dotted square. Some metabolites derived from chorismate by normal biosynthesis in *E. coli* are displayed. Other compounds that have been produced in *E. coli* by the action of heterologous enzyme(s) are also shown (open squares). Aspartame has been made by a chemical coupling process, using Phe produced by fermentation.

To reduce the cost of industrial biosynthetic production of aromatic compounds and other derivatives, it is desirable to increase the flux of carbon skeletons into and through the common aromatic pathway. A theoretical analysis of the pathways involved in the production of aromatic compounds in *E. coli* indicates that the yield of these metabolites is limited by phosphoenolpyruvate (PEP) availability[3,4]. This compound is one of the major building blocks in several biosynthetic pathways, and it is the phosphate donor utilized by the phosphotransferase system (PTS) in the internalization of glucose[5]. Two moles of PEP are produced from 1 mol of glucose through the glycolytic pathway. One mol of PEP, however, is subsequently used by the PTS during glucose transport, leaving only 1 mol of PEP per mol of glucose consumed that is available for other metabolic reactions.

Some of the approaches utilized to solve the limitation of PEP have been the use of non-PTS carbon sources, pyruvate recycling to PEP by PEP synthase overproduction[3,4], and inactivation of pyruvate kinase[6]. Another approach is the selection of mutants capable of transporting glucose by a non-PTS mechanism, i.e., without PEP consumption. For example, *Salmonella typhimurium* mutants that can transport glucose by facilitated diffusion through the galactose permease (GalP) have been reported[7]. In these mutants, glucose is phosphorylated by glucokinase using ATP as the phosphate donor. However, these mutants grow very slowly and have not been used extensively[7].

In this report, we describe the selection of *E. coli* strains having an inactivated PTS, that uses GalP, glucokinase, and ATP to internalize and phosphorylate glucose. These mutants differ from other PTS$^-$ Glucose$^+$ strains in that they were selected for their ability to achieve fast (wildtype) growth rates. Using these

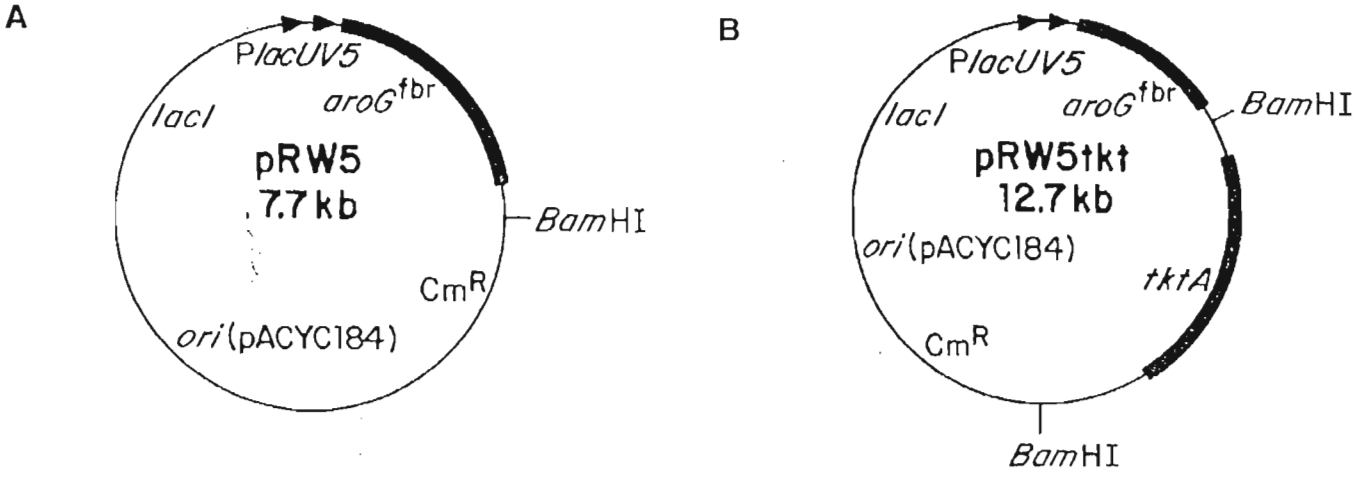

Figure 2. Relevant characteristics of plasmids containing the *tktA* and/or aroG^{fbr} genes. Only the relevant cloned gene(s) and restriction site(s) are shown. (A) Plasmid pRW5 contains the *E. coli aroG*^{fbr} gene cloned under the control of two lacUV5 promoters. (B) Plasmid pRW5tkt was derived from pRW5 and contains the *tktA* gene from *E. coli* under its own regulatory signals.

mutants, we were able to redirect more glucose-derived carbon into the aromatic pathway.

Results and discussion

Selection and characterization of PTS$^-$ Glucose$^+$ strains. The isolation of spontaneous Glucose$^+$ revertants that arose from *E. coli* strains lacking the *pts* genes, has been reported[4]. Using a similar approach, we have found that when *E. coli* strains devoid of the *ptsH*, *ptsI*, and *crr* genes are cultivated in a fermentor in minimal medium with glucose as the only carbon source, a heterogeneous population of PTS$^-$ Glucose$^+$ revertants can be detected after approximately two days (unpublished results). From this heterogeneous population, using continuous culture, we were able to select several PTS$^-$ Glucose$^+$ variants that can grow with different maximum growth rates in minimal medium with glucose as the only carbon source.

Two strains that showed a stable PTS$^-$ Glucose$^+$ phenotype were further characterized. It should be mentioned that the Δ*ptsHIcrr* mutation affects not only the transport of PTS carbohydrates, but also blocks the utilization of other carbon sources like Krebs cycle intermediates and certain amino acids[5]. In Table 1, we present the phenotypic characterization of two JM101 PTS$^-$ Glucose$^+$ derivatives (strains PB12 and PB13), as well as the PTS$^-$ Glucose$^-$ progenitor (strain PB11). The revertants retained several of the phenotypes associated with the *pts*$^-$ genotype[4], but regained the ability to oxidize glucose and other carbon sources. Importantly, in all of the PTS$^-$ Glucose$^+$ revertants tested, interruption of the *galP* gene with a *Tn*10 transposon eliminated the Glucose$^+$ phenotype (data not shown). The two PTS$^-$ Glucose$^+$ strains PB12 and PB13 differ in their doubling time in minimal medium with glucose as the only carbon source (1.64 h and 1.01 h respectively; data not shown).

Redirecting carbon flow into the aromatic pathway. Based on these data, it is probable that the PTS$^-$ Glucose$^+$ strains transport glucose through GalP, and once in the cytoplasm, this carbohydrate is phosphorylated by glucokinase (using ATP). This scheme should leave the two PEP molecules generated by the glycolytic pathway available for other metabolic routes. However, considering that in *E. coli*, PEP is an allosteric regulator of several enzymes, especially phosphofructokinase[9], PEP accumulation would be limited[10].

To test the hypothesis that PTS$^-$ Glucose$^+$ mutants can consume extra PEP available by directing it into the aromatic pathway, we repeated the isolation scheme described above to obtain PTS$^-$ Glucose$^+$ derivatives of *E. coli* strain PB103, which has been used to overproduce tryptophan (unpublished results). One stable PTS$^-$ Glucose$^+$ derivative of PB103 was selected for further experiments (strain NF9). In this strain, the phenotypes fosfomycin resistance (see Experimental protocol) and *galP* dependency for glucose transport were confirmed (data not shown). In minimal medium with glucose as the only carbon source, both PB103 and NF9 grew

Table 1. Phenotypic characterization of *E. coli* strains.

Carbon source	Strain JM101 PTS$^+$	Strain PB11 PTS$^-$Gluc$^-$	Strain PB12 PTS$^-$Gluc$^+$	Strain PB13 PTS$^-$Gluc$^+$
Glucose	+	–	+	+
L-Asn	+	–	–	–
L-Gln	+	–	–	+/–
L-Pro	+	–	–	–
L-Asp	+	–	–	–
L-Glu	+	–	–	–
L-Thr	+	–	–	–
D-Ala	+	–	–	+
Glycyl-L-Asp	+	+/–	+	+
Glycyl-L-Glu	+	+/–	+	+
N-Acetyl-D-glucosamine	+	–	–	–
D-Galactonic acid-ß lactone	–	–	+	+
Glycerol	+	+	+	+
Sacharic acid	+	–	–	–
D-Glucoronic	+	+	+	+
D-Malic acid	+	–	+/–	+
Fumaric acid	+	–	–	–
D-Sorbitol	+	–	–	–
Lactose	–	–	–	–
Fructose	+	–	–	–
D-Mannose	+	–	–	–
D-Galactose	+	+	+	+
L-Rhamnose	+	–	+	+
D-Gluconic acid	+	+	+	+
α-Methyl galactoside	+	–	+	+
L-Galactonic acid-ß lactone	+	–	+	+
Mucic acid	+	–	+	+

–, no color; +/– faint color; +, strong color. Color development indicates oxidation of the carbon source.

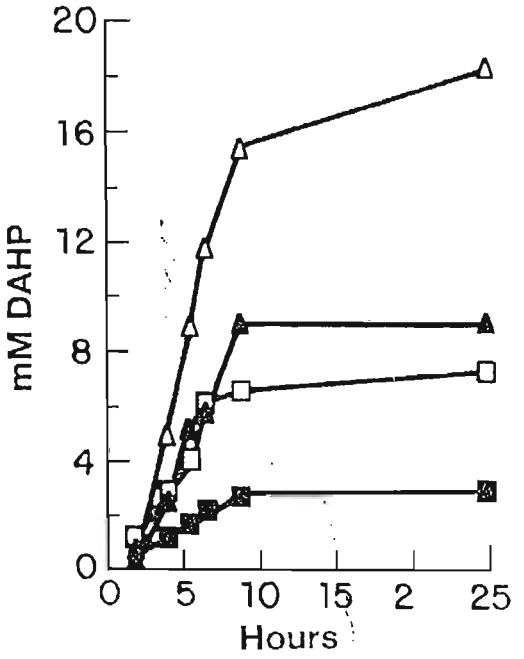

Figure 3. DAHP production in PB103 and NF9 strains carrying different plasmids. Strain NF9 is a Pts⁻ Glucose⁺ derivative of PB103 (see Experimental protocol). Both Glucose⁺ strains (PB103 and NF9) have the same generation time (1.25 h). ■, PB103/pRW5; □, PB103/pRW5tkt; ▲, NF9/pRW5; and △, NF9/pRW5tkt.

with a doubling time of 1.25 h.

Strains PB103 and NF9 were each transformed with plasmid pRW5 or pRW5tkt. Plasmid pRW5 (see Fig. 2A) contains the cloned *aroG*^{fbr} gene that encodes an allosterically insensitive 3-deoxy-D-arabino-heptulosonate 7-phosphate (DAHP) synthase enzyme, which catalyzes the condensation of PEP and E4P to produce DAHP. Plasmid pRW5tkt (Fig. 2B) is identical to pRW5, but also contains the cloned *E. coli tktA* encoding transketolase, which is a pentose phosphate pathway enzyme that catalyzes two separate reactions each of which produces E4P. Therefore, amplification of the *tktA* gene increases the intracellular concentration of E4P[11].

E. coli strains that overproduce DAHP synthase excrete DAHP into the extracellular medium (unpublished observation). This reflects the inability of 3-hydroquinate synthase (the second enzyme in the aromatic pathway that normally consumes DAHP), to keep up with the rate of DAHP production. In the present work we exploited this DAHP excretion as an indicator of carbon commitment to the aromatic pathway in the strain/plasmid combinations described above.

Figure 3 shows that the PTS⁻ Glucose⁺ strain NF9 carrying plasmid pRW5 produced 2.9-fold more DAHP than the parental PTS⁺ strain PB103 carrying the same plasmid. Furthermore, when the *aroG*^{fbr} and tktA genes were overexpressed simultaneously (pRW5tkt), strain NF9 produced 2.4-fold more DAHP than PB103 containing the same cloned genes, and 2.4-fold more DAHP than NF9 carrying only the amplified *aroG*^{fbr} (pRW5, see Fig. 3). Each data point in Figure 3 represents the average of duplicate flasks. Furthermore, several variations of the experiment have been carried out, and in all cases, the results were essentially identical (G. Gosset and J. Xiao, unpublished observations). The possibility that the differences in DAHP excretion between the pB103 and NF9 hosts reflects a difference in the level of 3-dehydroquinate synthase (encoded by *aroB*), is unlikely because further experiments showed that by amplifying (in a multicopy plasmid) the *aroACBLE* genes that code for five of the six steps of the common aromatic pathway, the increase in DAHP production (i.e., carbon flow), translated into an increased synthesis of tyrosine and phenylalanine (A. Berry unpublished results).

These data indicate that this PTS⁻ Glucose⁺ strain does in fact direct more PEP into DAHP formation. Further, the results obtained with the strains overexpressing *tktA* corroborate that the formation of DAHP can be limited by E4P availability[3].

In summary, these data indicate that PTS⁻ Glucose⁺ mutants, selected for their ability to achieve fast growth rates, can be used to increase PEP availability, and thus carbon commitment, to the aromatic pathway. We believe that this strategy has an advantage over the approach of overproducing the PEP synthase reported by others[3]. In the latter case, the amplification of PEP synthase forces the cells to "go backwards", against the PTS and the two pyruvate kinase isoenzymes present in *E. coli*[19]. In addition, the necessity of overexpressing another cloned gene (*ppsA*) represents an extra metabolic load to the cells. On the other hand, elimination of PTS removes the major pathway of PEP consumption in *E. coli*[12], and also reduces the metabolic pressure towards pyruvate formation caused by the simultaneous presence of PTS and pyruvate kinases[19].

Experimental protocol

Bacterial strains and plasmids. The *E. coli* strains used in this work were: JM101 (*supE, thi,* (Δ*lac-proAB*) F′, [*traD36,* lacI^{q}, *lacZ*ΔM15, *proAB*])[14]; PB103 (F⁻ Δ*lacU169 trpR, tnaA2*), a Trp⁺ derivative of strain C534[15], and TP2811 (F⁻, *xyl, argH1, lacX74, aroB, ilvA,* Δ(*ptsH, ptsI, crr*) ::Km^{R})[16]. Plasmid pRW5 is a pACYC184 derivative that contains the *E. coli aroG*^{fbr} gene cloned under tandem *lac* promoter control[3] (Fig. 2A). A BamHI DNA fragment carrying the *tktA* gene from *E. coli* was cloned into the unique BamH1 site of pRW5 to generate plasmid pRW5tkt[11] (Fig. 2B).

Mutant selection. Pts⁻ derivatives of JM101 and PB103 (strains PB11 and NF6, respectively), were obtained by P1 *vir* phage transduction using TPB2811 as donor as described by Silhavy et al.[17]. Several of the phenotypic characteristics of the Pts⁻ mutation were confirmed using MacConkey-agar-base plates supplemented with different carbohydrates. Also, the resistance to the antibiotic fosfomycin was used as another indicator of the PTS⁻ phenotype[18]. Strains PB11 or NF6 were used to inoculate a 1L chemostat containing M9 medium (without casamino acids)[14] supplemented with 0.2% glucose. The incubation temperature was 37°C. The dissolved oxygen was maintained above 20% by controlling the impeller speed, and the pH of the medium was maintained at 7.0 by base addition. After the culture reached an OD_{600} of approximately 2.5, the washing of the fermentor was initiated by feeding fresh M9 medium at a rate of 0.52 L/hr. This flow rate should wash out all the cells growing with a specific growth rate of less than 0.4 h^{-1} (under the same conditions the specific growth rate of the Pts⁺ parental strain was 0.8 h^{-1}). After at least 3 residence times, the feed flow rate was increased to wash out cells with a growth rate less than 0.5 h^{-1}. This procedure was repeated using incremental increases in flow rate (0.1 L/hr), until strains were selected that had a specific growth rate of at least 0.8 h^{-1}. Before each incremental increase in the feed flow rate, samples were taken from the chemostat, diluted and plated on MacConkey-glucose plates. The MacConkey media has a pH-dependant dye that changes color in response to the acidic byproducts of sugar metabolism. After incubating the plates 24 h at 37°C, they were examined for colonies having a normal *E. coli* morphology and a homogeneous red color. Only those mutants having these characteristics were studied further. Strains PB12 and PB13 were derived from strain PB11, while strain NF9 was derived from strain NF6.

Phenotypic characterization of PTS⁻ Glucose⁺ mutants. The ability of the *E. coli* strains to oxidize different carbon sources was examined using Biolog ES MicroPlates as described previously[20]. This type of plate assay is based on tetrazolium chloride (TTC) dye reduction as an indicator of sole-carbon-source utilization. Strains capable of catabolizing the test substrate reduce TTC and produce a deep red color, whereas colonies failing to catabolize the substrate remain uncolored. Furthermore, the degree of red color represent variations in the rate and/or degree of catabolism[21]. After 24 h of incubation, the ES plates were examined, and the relative rates of carbon

source oxidation were recorded. After performing several experiments with this system, we found that the quantitative values varied. However, the ability or inability to oxidize a particular carbon source was reproducible.

Measurement of DAHP production. Strains were grown with shaking in 30 ml flasks, at 35°C. The medium used was YE, which contains 15 g/L yeast extract, 14 g/L K_2HPO_4, 16 g/L KH_2PO_4, 5 g/L $(NH_4)_2SO_4$, 15 g/L glucose, 1 g/L $MgSO_4$ and 1 drop of P-2000 antifoam (Dow Chemical, MI). Cultures were inoculated with cells from overnight seed cultures. The initial OD_{600} of the cultures was 0.2. To induce the expression of the *aroG*^{fbr} gene present in plasmids pRW5 and pRW5tkt, IPTG (isopropyl-β-D-thiogalactopyranoside) was added to the cultures when they reached an OD_{600} of 2.0. The pH of the cultures was maintained at 6.5 through the experiment by periodic additions of 45% KOH. Samples were taken at specific time intervals, the cells were removed by centrifugation, and the supernatants assayed for DAHP using the standard thiobarbituric acid assay[22].

Acknowledgments

This work was supported by grants 2031-N9302 from Consejo Nacional de Ciencia y Tecnología, Mexico, and Genencor International Inc.

1. Frost, J. and Lievense, J. 1994. Prospects for biocatlytic synthesis of aromatics in the 21st century. *New J. Chem.* 18:341–348.
2. Murdock, D., Ensley, B.D., Serdar, C., and Thalen, M. 1993. Construction of metabolic operons catalyzing the de novo biosynthesis of indigo in *Escherichia coli*. *Bio/Technology* 11:381–385.
3. Patnaik, R. and Liao, J.C. 1994. Engineering of *Escherichia coli* central metabolism for aromatic metabolite production with near theoretical yield. *Appl. and Environ. Microbiol.* 60:3903–3098.
4. Patnaik, R., Spitzer, R.G., and Liao, J.C. 1995. Pathway engineering for production of aromatics in *Escherichia coli*: Confirmation of stoichiometric analysis by independent modulation of AroG, TktA and Pps activities. *Biotech. Bioeng.* 46:361–370.
5. Postma, P.W. 1987. Phosphotransferase system for glucose and other sugars, pp.127–141 in Escherichia coli *and* Salmonella typhimurium. *Cellular and Molecular Bology*. Neidhardt, F.C. (ed.). American Society for Microbiology, Washington, D.C.
6. Mori, M., Yokota, A., Sugitomo. S., and Kawamura, K. 1987. Process for the isolation of a strain with reduced pyruvate kinase activity or completly lacking it. Patent JP 62,205,782.
7. Saier, M.H., Jr., Bromberg, F.G., and Roseman, S. 1973. Characterization of constitutive galactose permease mutants in *Salmonella typhimurium*. *J. Bacteriol.* 113:512–514.
8. Biville, F., Turlin, E., and Gasser, F. 1991. Mutants of *Escherichia coli* producing pyrroloquinoline quinone. *J. Gen. Microbiol.* 137:1775–1782.
9. Fraenkel, D.G. 1987. Glycolisis, pentose phosphate pathway, and Entner-Doudoroff pathway, pp. 142–150 in Escherichia coli *and* Salmonella typhimurium. *Cellular and Molecular Biology*. Neidhardt, F.C. (ed.). American Society for Microbiology, Washington, D.C.
10. Ponce, E., Flores, N., Martinez, A., Valle, F., and Bolivar, F. 1995. Cloning of the two pyruvate kinase isoenzyme structural genes from *Escherichia coli*: the relative roles of these enzymes in pyruvate biosynthesis. *J. Bacteriol.* 177:5719–5722.
11. Frost, J.W. 1992. Enhanced production of common aromatic pathway compounds. Patent US 5,168,056.
12. Holms, W. 1986. The central metabolic pathways of *Escherichia coli*: relationships between flux and control at a branch point, efficiency of conversion to biomass, and excretion of acetate, pp. 69-105 in *Current Topics in Cellular Regulation*. Horecker, B.L. and Stadtman, E.R. (eds.). Academic Press, New York.
13. Yanisch-Perron, C., Vieira, J., and Messing, J. 1985. Improved M13 phage cloning vectors and host strains: nucleotide sequence of the M13mp18 and pUC19 vectors. *Gene* 33:103–119.
14. Mascarenhas, D. 1987. Tryptophan producing microorganisms. Patent WO 87/01130.
15. Levy, S., Zeng, G.Q., and Danchin. A. 1990. cAMP synthesis in strains bearing well characterized deletions in the central pts genes of *Escherichia coli*. *Gene* 86:27–33.
16. Draths, K.M., Pompliano, D.L., Conley, D.L., Frost, J.W., Berry, A., Disbrow, G.L., Staversky, R.J., and Lievense, J.C. 1992. Biocatalytic synthesis of aromatics from D-glucose: the role of transketolase. *J. Am. Chem. Soc.* 114:3956–3962.
17. Silhavy, T., Berman, M., and Enquist, L. 1984. pp. 110–112 in *Experiments with Gene Fusions*. Cold Spring Harbor Laboratory Press, New York.
18. Cordaro, J.C., Melton, T., Stratis, J.P., Atagun, M., Gladding, C., Hartman, P.E., and Roseman S. 1976. Fosfomycin resistance: selection method for Internal and extended deletions of the phosphoenolpyruvate:sugar phosphotransferase genes of *Salmonella typhimurium*. *J. Bacteriol.* 128:785–793.
19. Maniatis, T., Fritsch, E.F., and Sambrook, J. 1989. *Molecular Cloning. A Laboratory Manual*. Cold Spring Harbor Laboratory Press, New York.
20. Ramseier, T.M., Bledig, S., Michotey, V., Feghali, R., and Saier M.H., Jr. 1995. The global regulatory protein FruR modulates the direction of carbon flow in *Escherichia coli*. *Mol. Microbiol.* 16:1157–1169.
21. Bochner, B.R. and Savageau, M.A. 1977. Generalized Indicator plates for genetic, metabolic, and taxonomic studies with microorganisms. *Appl. Environ. Microbiol.* 33:434–444.
22. Srinivasan, P.R. and Sprinson, D.B. 1959. 2-keto-3-deoxy-D-arabo-heptonic acid 7 phosphate synthase. *J. Biol. Chem.* 234:716–722.

Metabolic Engineering 4, 124–137 (2002)
doi:10.1006/mben.2001.0209, available online at http://www.idealibrary.com on IDEAL®

Analysis of Carbon Metabolism in *Escherichia coli* Strains with an Inactive Phosphotransferase System by ^{13}C Labeling and NMR Spectroscopy

S. Flores,* G. Gosset,* N. Flores,* A. A. de Graaf,† and F. Bolívar*

*Departamento de Microbiología Molecular, Instituto de Biotecnología, Universidad Nacional Autónoma de México, Apdo. Postal 510, 62250 Cuernavaca, México; and †Forschungszentrum Jülich, Institut für Biotechnologie 1, D-52425 Jülich, Germany

Received May 24, 2001; accepted September 14, 2001; published online February 14, 2002

We have developed *Escherichia coli* strains that internalize glucose utilizing the GalP permease instead of the phosphoenolpyruvate:carbohydrate phosphotransferase system. It has been demonstrated that a strain with these modifications (PTS^-Glc^+) can direct more carbon flux into the aromatic pathway than the wild-type parental strain (N. Flores *et al.*, 1996, *Nat. Biotechnol.* 14, 620–623; G. Gosset *et al.*, 1996, *J. Ind. Microbiol.* 17, 47–52; J. L. Baéz *et al.*, 2001, *Biotechnol. Bioeng.* 73, 530–535). In this study, we have determined and compared the carbon fluxes of a wild-type strain (JM101), a PTS^-Glc^- strain, and two isogenic PTS^-Glc^+ derivatives named PB12 and PB13 by combining genetic, biochemical, and NMR approaches. It was determined that in these strains a functional *glk* gene in the chromosome is required for rapid glucose consumption; furthermore, glucokinase-specific activities were higher than in the wild-type strain. ^{13}C labeling and NMR analysis allowed the determination of differences *in vivo* which include higher glycolytic fluxes of 93.1 and 89.2% compared with the 76.6% obtained for the wild-type *E. coli*. In PB12 and PB13 we found a flux through the malic enzymes of 4 and 10%, respectively, compared to zero in the wild-type strain. While flux through the Pck enzyme was absent in PB12 and PB13, in the wild type it was 7.7%. Finally, it was found that in the JM101 and PB12 strains both the oxidative and the nonoxidative branches of the pentose phosphate pathway contributed to ribose 5-phosphate synthesis, whereas in PB13 this pentose was synthesized almost exclusively through the oxidative branch. The determined carbon fluxes correlate with biochemical and genetic characterizations.

Key Words: NMR; glucose transport; phosphoenolpyruvate; central carbon metabolism; metabolic engineering.

INTRODUCTION

Central metabolic pathways are the source of precursor compounds for all other pathways and also a significant source for energy and reducing power in the cell. This explains why this part of the cell metabolism has been the target of basic studies and metabolic engineering efforts for the improvement of industrial strains. In the case of *Escherichia coli*, metabolic engineering studies have been primarily focused on the main central metabolic sections that are active during growth on glucose as the sole carbon source: the Embden–Meyerhof (EM)[1] pathway, the pentose phosphate (PP) pathway, and the tricarboxylic acid cycle (TCA) (Varma *et al.*, 1993; Schuster *et al.*, 1999).

Among the metabolites of the central metabolism, phosphoenolpyruvate (PEP) plays a key role in cell physiology since it is a phosphate donor in the PEP:carbohydrate phosphotransferase system (PTS), a direct precursor of several amino acids, and because it participates in the ATP-yielding reaction catalyzed by pyruvate kinases (Postma *et al.*, 1996; Valle *et al.*, 1996). Thus, a number of studies have been focused on understanding and manipulating metabolic fluxes around the PEP and pyruvate nodes. Several approaches have been employed in order to increase the metabolic availability of PEP, like the overexpression of the gene coding for PEP synthase (*pps*), the inactivation of the genes coding for the two pyruvate kinase isoenzymes (Ponce *et al.*, 1995), and, more recently,

[1] Abbreviations used: Metabolic pathways—EM, Embden–Meyerhof; PP, pentose phosphate; TCA, tricarboxylic acid cycle. Enzymes—GalP, galactose permease; Gap, glyceraldehyde-3-phosphate dehydrogenase; Glk, glucokinase; GltA, citrate synthase; Gnd, 6-phosphogluconate dehydrogenase; Mdh, malate dehydrogenase; Mez, NAD- and NADP-dependent malic enzymes; Pck, phosphoenolpyruvate carboxykinase; Pgi, phosphoglucose isomerase; Ppc, phosphoenolpyruvate carboxylase; PTS, phosphoenolpyruvate:carbohydrate phosphotransferase system; PykAF, pyruvate kinases A and F; Rpe, ribulose-5-phosphate 3-epimerase; Rpi, ribose-5-phosphate isomerase; Tal, transaldolase; Tkt, transketolase; Zwf, glucose-6-phosphate dehydrogenase. Compounds and others—ACoA, acetyl-coenzyme A; CIT, citrate; E4P, erythrose 4-phosphate; F6P, fructose 6-phosphate; Ferm, fermentation products; G3P, glyceraldehyde 3-phosphate; G6P, glucose 6-phosphate; Glc, glucose; MAL, malate; NADPH, nicotinamide adenine dinucleotide phosphate (reduced form); NADH, nicotinamide adenine dinucleotide (reduced form); OAA, oxaloacetate; 6PG, 6-phosphogluconate; PEP, phosphoenolpyruvate; PYR, pyruvate; P5P, pentose 5-phosphate; R5P, ribose 5-phosphate; TSP, sodium trimethylsilylproprionate-2,2,3,3-d_4; DAHP, 3-deoxy-D-arabino-heptulosonate 7-phosphate.

1096-7176/02 $35.00

Metabolic Engineering 4, 124–137 (2002)
doi:10.1006/mben.2001.0209

the utilization of strains with an inactive PTS, but with the capacity to consume glucose rapidly (Patnaik *et al.*, 1995; Flores *et al.*, 1996; Gosset *et al.*, 1996). In the latter work, starting from a strain with an inactive PTS (PTS^-), which grows very slowly on glucose (Glc^-), a method based on continuous culture was employed to select for mutants that had growth rates similar to that of a PTS^+ strain. Initial characterization of these PTS^-Glc^+ strains revealed that a functional *galP* gene on the chromosome is required for rapid growth on glucose (Flores, 1995). This result strongly suggests that in these mutants, GalP has replaced the transport functions of the $IICB^{Glc}$ PTS protein; this result is not surprising, considering that it has been reported that GalP can transport, in addition to galactose, other sugars such as glucose (McDonald *et al.*, 1997). Further characterization of these PTS^-Glc^+ strains, in the context of aromatic amino acid biosynthesis, has revealed that they can direct more carbon flux into intermediates or final products of the aromatic pathway, compared to isogenic PTS^+ strains (Gosset *et al.*, 1996). Thus, the measured molar yield from glucose for the synthesis of the first intermediate in the aromatic pathway, 3-deoxy-D-arabinoheptulosonate 7-phosphate (DAHP), was 0.71 mol_{DAHP}/mol_{Glc}, in a PTS^-Glc^+ *aroB*$^-$ strain in which genes coding for a feedback inhibition-resistant DAHP synthase and transketolase were overexpressed. In contrast, in an isogenic PTS^+ strain, the yield reached only 0.43 mol_{DAHP}/mol_{Glc} (Baéz *et al.*, 2001). These results indicate that by avoiding PTS^--dependent PEP consumption for glucose transport in the PTS^-Glc^+ strains, a larger fraction of this precursor metabolite is now available to be redirected into specific biosynthetic pathways.

These results show that the PTS^-Glc^+ strains have the potential to become useful production strains for aromatic compounds and also for other metabolites derived from PEP; however, to fully understand and to be able to utilize these strains at their maximum potential, further physiological characterization is required. Therefore, the purpose of the present study was to obtain a detailed metabolic characterization of two PTS^-Glc^+ strains, PB12 and PB13, and their isogenic progenitor strains JM101 (PTS^+) and PB11 (PTS^-Glc^-). This study was based on determining the flux distributions[2] of central metabolic pathways using carbon-13 labeling and nuclear magnetic resonance (NMR) spectroscopy, complemented by generating and studying mutants in genes encoding for certain enzymes of the EM and PP pathways. Results obtained showed that in the PTS^-Glc^+ strains, glucose phosphorylation is dependent on the presence of a functional *glk* gene in the chromosome. NMR data also revealed important differences in carbon flux distribution between the PTS^-Glc^+ and the PTS^+ strains at the level of the glucose 6-phosphate, PEP, oxaloacetate, and malate nodes.

[2] All flux values are given as percentage of glucose utilization rate in that strain expressed in mmol Glc · h−1 · g biomass^{-1}.

MATERIALS AND METHODS

Bacterial Strains and Plasmids

Mutant strains PB12 and PB13 were obtained from PB11, a PTS^-Glc^- mutant derivative of *E. coli* JM101, using a continuous culture selection method previously described (Flores, 1995). Mutant strains SM1, NF29, and NF30 (Table 1) were obtained by P1 transduction from an *E. coli* strain, ATCC47002, that has integrated the *glk*::Cm construction. Inactivations of *pgi* and *gnd* genes were obtained by cloning the corresponding gene in a pBR322-derived plasmid and interrupting the corresponding genes with a chloramphenicol resistance gene present in the pLoxCat4 plasmid (Bolívar *et al.*, 1977; Palmeros, 2001); the corresponding plasmid with interrupted genes was modified by exchanging the replication origin for the permissive R6K origin. Permissive plasmids with interrupted *pgi* or *gnd* genes were used to generate the respective chromosomal gene inactivation by allelic exchange. Double recombinant strains were chosen by the Ap^s/Cm^r phenotype and verified by PCR and enzyme activity analysis.

Growth Conditions and Sample Preparations

Cultures for growth-rate determination, [^{14}C]glucose uptake, NMR, and enzymatic assays were grown on M9 medium supplemented with 2 g/L glucose starting at an OD_{600} between 0.04 and 0.05 and collected when growing in the logarithmic phase at an OD_{600} of 1. Samples for NMR analysis were taken from batch cultivation in a 2-L fermentor with a working volume of 1 L of M9 medium supplemented with 80% [1-^{13}C]glucose and 20% [U-$^{13}C_6$]glucose (both from Cambridge Isotope Laboratories, Andover, MA) to a final concentration of 3 g/L; cells were collected when they reached an OD_{600} of 1. The total working volume was harvested and dried at 105°C for at least 10 h. Two hundred fifty milligrams was used for acidic hydrolysis in 6 M HCl at 90°C for 18 h. The hydrolysates were lyophilized and redissolved in 700 μl D_2O with 2 mM sodium trimethylsilylproprionate-2,2,3,3-d_4 (TSP) (Aldrich) as chemical shift standard. In the resulting mixtures, cysteine and tryptophan were lost due to oxidation, and asparagine and glutamine were deaminated.

TABLE 1

Escherichia coli Strains and Plasmids Used

Strain or plarmid	Relevant genotype	Source or reference
Strain		
JM101	*Sup*E, *thi*, Δ(*lac-pro*AB), F′	Bolívar *et al.*, 1977
SM1	JM101 *glk*::Cm	This study
SM6	JM101 *gnd*::Cm	This study
SM14	JM101 *pgi*::Cm	This study
PB11	JM101 Δ(*pts*H, *pts*I, *crr*)::Kan^R	Flores, 1995
PB12	PTS$^-$Glc$^+$	Flores, 1995
NF29	PB12 *glk*::Cm	This study
SM8	PB12 *gnd*::Cm	This study
SM31	PB12 *pgi*::Cm	This study
PB13	PTS$^-$Glc$^+$	
NF30	PB13 *glk*::Cm	This study
SM9	PB13 *gnd*::Cm	This study
SM32	PB13 *pgi*::Cm	This study
Plasmid		
pGlk1	pBR322 carrying the *E. coli glk* gene	Flores, 1995
pGlk5	pGlk1 carrying *glk*::Cm^R	This study
pMN6	PBR322 carrying the *E. coli gnd* gene	Nasoff and Wolf, 1980
pGnd1	pMN6 carrying *gnd*::Cm^R	This study
pGnd5	pGnd1 carrying R6K replication origin	This study
pPgi1	pCR-Blunt carrying the *E.coli pgi* gene	Flores, 1995
pPgi5	pPgi carrying *pgi*::Cm^R	This study
pPgi8	pPgi carrying R6K replication origin	This study

[^{14}C]Glucose Uptake

Initial rates of [^{14}C]glucose uptake were measured by harvesting cells at an OD_{600} of 1, washing once with cold Tris buffer, resuspending in 540 μl of M9 medium, and maintaining on an ice bath. Cells were incubated for 10 min at 37° C and then the reaction was started by the addition of 30 μl of [^{14}C]glucose (1 mM, 5 mCi/mmol) while stirring. An aliquot of the cells with incorporated [^{14}C]glucose was added to a membrane plate and washed with cold M9 medium three times; the membrane was air-dried, and the incorporated [^{14}C]glucose was monitored in a scintillation counter.

Enzymatic Assays

Twenty-five milliliters of the corresponding culture with an OD_{600} of 1 was centrifuged and washed with phosphate buffer (pH 6.8; 10^{-2} M KH_2PO_4 and 10^{-2} M KH_2PO_4) containing 10^{-2} M 2-mercaptoethanol and 10^{-2} M sodium azide. Cells were resuspended in 1 ml of the same buffer and disrupted by sonic treatment of four pulses of 15 s in a cold bath. Pgi-specific activity was determined as described by Maitra and Lobo (1971). Glk-, Zwf-, and Gnd-specific activities were determined as reported by Lessie and Vander Wyk (1972); all activities are reported as nmol substrate produced · min^{-1} · mg protein^{-1}, using a molar extinction coefficient for NADPH of 6.22.

NMR Spectroscopy and Mathematical Modeling

Concentrations of glucose, acetate, lactate, and ethanol in the culture broth were determined by standard one-dimensional proton NMR at 400 MHz of samples containing 200 μl culture supernatant mixed with 500 μl D_2O. TSP (2 mM) was used as a chemical shift and concentration standard.

Carbon-13 labeling patterns of amino acids, glycerol, and nucleotides present in hydrolysates of 100–200 mg of labeled cell material were determined by NMR spectroscopy using a 400-MHz wide-bore NMR spectrometer (Bruker, Karlsruhe). ^{13}C multiplet fine structures reflecting isotopomer composition of metabolites were analyzed from two-dimensional [^{1}H, ^{13}C] HSQC NMR spectra (Szyperski, 1995). The acquisition parameters were t_{1max} = 520 ms, t_{2max} = 231 ms; data size before zero filling was 3072 points in t_1 and 2048 points in t_2. Sweep width was 4.42 kHz for ^{1}H and 2.95 kHz for ^{13}C; the carrier position was 4.78 ppm for ^{1}H and 63.1 ppm for ^{13}C. The States protocol for quadrature detection was used. Pulse widths were 10 μs for both ^{1}H and ^{13}C. A shifted squared sine bell window was employed in both dimensions prior to Fourier transformation. A single 2D HSQC was recorded over the weekend (53.5 h) for the aliphatic and aromatic resonances. By comparing the multiplets of tyrosine with multiplets resolved in a 1D ^{13}C spectrum from the same sample, it was verified that no distortions of relative multiplet intensities due to ^{13}C off-resonance effects in the 2D HSQC spectrum occurred. All NMR data processing was performed using the Bruker XWINNMR software. Multiplets were extracted as 1D traces from the 2D spectrum by interactively summing those traces along the ^{13}C axis that contained the multiplet signals at a good signal-to-noise ratio. After manual baseline correction, integration was performed interactively.

In the 2D NMR spectra, in addition to the usual signals of amino acids, signals from cytidine and uridine (Fig. 1) were found. These nucleosides (i.e., dephosphorylated nucleotides) probably resulted from hydrolysis of RNA and apparently survived the 6 N HCl treatment. No phosphorylated species were detected. The nucleoside multiplet data were input to the flux estimation as measurement values for ribose 5-phosphate and as such are complementary to, and in part redundant with, the information obtained from histidine.

The isotopomeric composition of alanine in this study, in which a mixture of uniformly labeled and [1-^{13}C]glucose

Metabolic Engineering 4, 124–137 (2002)
doi:10.1006/mben.2001.0209

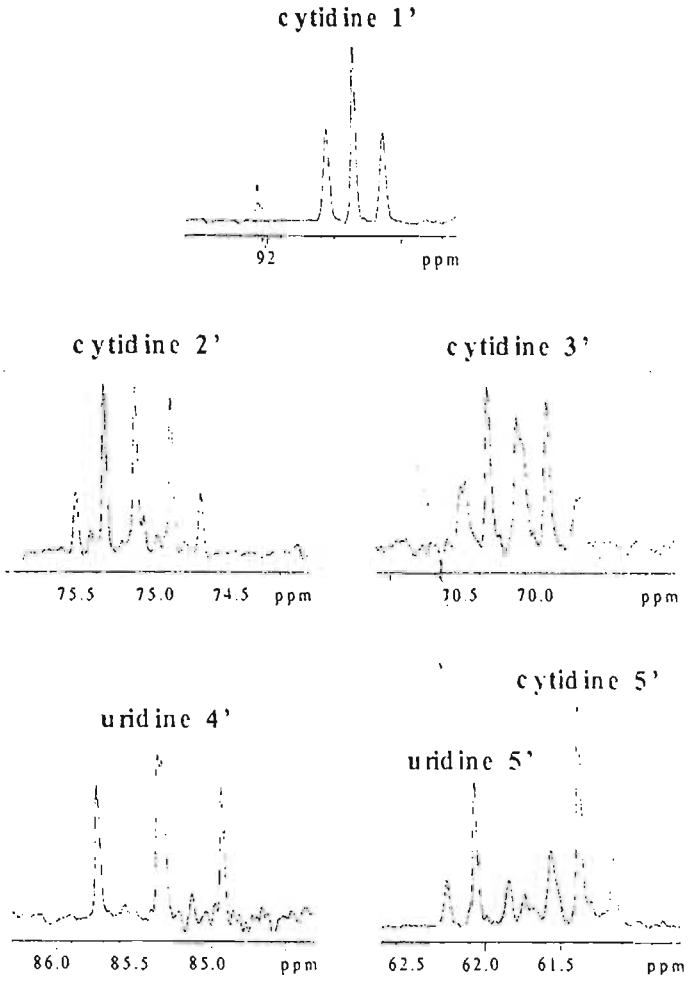

FIG. 1. ^{13}C multiplets for different carbons of ribosyl moieties of cytidine and uridine as indicated, extracted from the 2D HSQC NMR spectrum of the biomass hydrolysate from the wild-type strain JM101. These nucleosides presumably stem from hydrolyzed RNA. Assignments were unequivocally confirmed by comparison with ^{1}H and ^{13}C chemical shift values measured from the pure standards at identical pH in D_2O. The signals from C-2' and C-3' of cytidine were not included in the analysis because they suffered from overlap and low signal-to-noise ratios.

was used, is of key importance for the determination of the activities of the PP and the Entner–Doudoroff pathways. The [1-^{13}C]alanine isotopomer results from the breakdown of [1-^{13}C]glucose via the Entner–Doudoroff pathway. The [3-^{13}C]alanine isotopomer results from [1-^{13}C]glucose metabolized via the EM pathway. Moreover, the abundance of this isotopomer strongly reflects the activity of the oxidative PP pathway since operation of this pathway causes a loss of the ^{13}C label originating from C-1 of glucose. Therefore, the isotopomer composition of alanine in the hydrolysate was further investigated using one-dimensional ^{1}H spin echo difference spectroscopy as described in de Graaf *et al.* (2000). The measurements took advantage of the fact that the methyl proton resonance of alanine was well resolved in the hydrolysate. Using a total spin echo time of 7.6 ms and alternate nonselective inversion of ^{13}C, the total ^{13}C enrichment of alanine C-3 was determined from the difference signal. Using a total echo time of 192 ms and selective inversion of the 173–180 ppm spectral band in the ^{13}C dimension, the four alanine isotopomers containing a ^{13}C in position 1 were quantitated by deconvolution analysis of the signals in the difference spectrum.

Modeling of the *E. coli* metabolism and isotopomer distributions in all metabolites as well as determination of the metabolic flux distribution by nonlinear least-squares parameter fitting was performed using the ^{13}C-Flux software package (Wiechert *et al.*, 1999; Möllney *et al.*, 1999; Petersen *et al.*, 2000). A flux balance analysis was integrated in the flux analysis, and the inputs and outputs of the metabolic network, as determined from independent measurements of substrate uptake and product excretion rates, were input in the analysis. The precursor fluxes for biomass synthesis as derived from biomass composition data for *E. coli* were also input to the flux analysis program. As demonstrated in the study of Petersen *et al.* (2000), the resulting data set was greatly overdetermined, i.e., a large redundancy in the ^{13}C labeling data was present. Each ^{13}C flux analysis, as usual, was performed only once for cost reasons. Multiple calculations were performed starting from different starting flux distributions and the best solution that was reproducibly attained was assumed to represent the true flux distribution. While in some cases local minima were found, these were characterized by significantly worse residuals and therefore rejected. A statistical error analysis of the resulting fluxes was included in the calculations.

A standard model of *E. coli* metabolism was used. It included the reactions of glycolysis, the pentose phosphate pathway, the Entner–Doudoroff pathway, the citric acid cycle, and the glyoxylate cycle. As anaplerotic reactions, PEP carboxylase and malic enzyme were included. PEP carboxykinase was included as a gluconeogenic reaction. The following enzyme reactions were programmed as being reversible: transketolase, transaldolase, phosphoglucose isomerase, triosephosphate isomerase, the sequence of glycolytic reactions leading from glyceraldehyde 3-phosphate to PEP, and fumarase.

RESULTS AND DISCUSSION

Growth Rate and Glucose Transport Measurements

In order to provide an initial physiological characterization of the strains used in this study, we determined growth rate and glucose transport capacities for the wild-type

TABLE 2

Growth Rate μ and Initial Rate of [^{14}C]Glucose Uptake τ in Different *Escherichia coli* Strains

Strain	Genotype	μ^a	τ^b
JM101	Wild type	0.71	20.0
PB11	PTS$^-$Glc$^-$	0.10	1.7
PB12	PTS$^-$Glc$^+$	0.42	10.3
PB13	PTS$^-$Glc$^+$	0.49	11.7

[a] In h^{-1}, obtained on M9 medium supplemented with 2 g/L glucose.
[b] In nmol [^{14}C]Glc · min^{-1} · mg $protein^{-1}$.

JM101, the PTS$^-$Glc$^-$ strain PB11, and the PTS$^-$Glc$^+$ strains PB12 and PB13; the results are presented in Table 2. Strain JM101 had a specific growth rate (μ) of 0.71 h^{-1}; the effect of inactivation of PTS on growth rate can be clearly seen in the PTS$^-$Glc$^-$ strain PB11, the μ of which was only 0.10 h^{-1}. PB11-derivative PTS$^-$Glc$^+$ strains PB12 and PB13 had μ of 0.42 and 0.49 h^{-1}, respectively. Initial rates of [^{14}C]glucose uptake for these strains are also shown in Table 2; these results show that inactivation of PTS in strain PB11 caused a reduction in glucose transport capacity to 8.5% of that measured for the PTS$^+$ JM101 strain (20 nmol [^{14}C]glucose · min^{-1} · mg $protein^{-1}$). The PTS$^-$Glc$^+$ strains PB12 and PB13 partially recovered their glucose transport capacity; it corresponded to 42 and 47%, respectively, of that measured for JM101.

Glucokinase Measurements

The results of the Glk-specific activity measurements in JM101, PB12, and PB13 strains and their *glk*$^-$ derivatives are shown in Table 3. Strains PB12 and PB13 showed an increase of 122 and 138% of Glk-specific activity, respectively, compared to the wild-type strain. The disruption of the *glk* gene in PB12 and PB13 severely restrained the capacity of these strains for utilizing glucose as a carbon source (Table 3). It is important to notice, however, that the derivative strains with the interrupted *glk* gene, NF29 and NF30, still had a residual activity for glucokinase of 32 and 22 units, respectively; these results can be explained by the presence of other phosphorylating enzymes with low affinity for glucose.

In this sense, an earlier report on *glk* mutations by Curtis and Epstein (1975) clearly shows that a *ptsI–glk* double mutant (named by the authors *gpt-2 glk* mutant strain ZSC103) shows a 43% residual activity (2 μmol · min^{-1} g $protein^{-1}$) on glucose phosphorylation compared with the wild-type strains. In our case, the *glk*$^-$ strains show a residual glucose phosphorylating activity of 22 to 32% compared to the wild-type strain. In the same report, Curtis and Epstein also showed that an additional mutation on the

TABLE 3

Glk-Specific Activities and Phenotype of *glk* Mutant Strains

Strain	Genotype	Glk[a]	Phenotype[b]
JM101	Wild type	57	R
SM1	JM101 *glk*$^-$	27	R
PB12	PTS$^-$	127	R
NF29	PB12 *glk*$^-$	32	W
PB13	PTS$^-$	136	R
NF30	PB13 *glk*$^-$	22	W

Note. Results represent the averages of at least three different experiments.
[a] Specific activities reported as nmol substrate consumed · min^{-1} · mg $protein^{-1}$.
[b] Observed on MacConkey glucose plates. Red coloring of colonies was interpreted as the bacterial capacity to use glucose as carbon source. White coloring of colonies was interpreted as substantially reduced capacity to use glucose as carbon source. R, red colonies; W, white colonies.

mannose phosphotransferase structural gene (*gpt-2 mpt-1 glk* mutant strain ZSC112) decreased the residual glucose phosphorylating activity to almost 50% (1.1 μmol · min^{-1} g $protein^{-1}$), compared with the *gpt-2 glk* mutant strain ZSC103. These results indicate that there are other enzymes in *E. coli* with glucose phosphorylating capacities, in this case, the mannose phosphotransferase component of the mannose–PTS system. In the same report, Curtis and Epstein also found a glucokinase-dependent glucose phosphorylating activity value close to 0 (less than 1% of wild-type strain, meaning essentially absence of Glk protein), for both the ZSC103 and the ZSC112 strains.

The PCR amplification products (data not shown), and the important decrease of glucokinase activity in the NF29 and NF30 strains, clearly indicate that the chromosomal *glk* gene was interrupted in these derivative strains. From these data, we can conclude that glucokinase is the major glucose-phosphorylating enzyme in strains PB12 and PB13.

Measurement of the Pgi-, Zwf-, and Gnd-Specific Activities on PTS$^+$ and PTS$^-$ Glc$^+$ Strains

As part of the characterization of the PB12 and PB13 strains, we measured the specific activities of certain key enzymes of the central carbon metabolism. As can be seen in Table 4, important differences were observed for the specific activities of the Pgi, Zwf, and Gnd enzymes, compared to the wild-type strain JM101. Values for the Pgi-specific activities in strains PB12 and PB13 were respectively 3.9 and 3.3 times higher than those of JM101. Higher specific activities were also detected for Zwf; however, in this case the specific activity was 1.5 and 1.9 times higher for PB12 and PB13, respectively. On the other hand, the Gnd-specific activity of these two mutant strains was 50% lower than the value

Metabolic Engineering 4, 124–137 (2002)
doi:10.1006/mben.2001.0209

TABLE 4

Pgi-, Zwf-, and Gnd-Specific Activities[a] of Various *E. coli* Strains

Strain	Genotype	Pgi	%	Zwf	%	Gnd	%	Pgi/Zwf
JM101	Wild type	1448	100	180	100	255	100	8.0
PB11	PTS$^-$Glc$^-$	132	9	136	76	114	45	1.0
PB12	PTS$^-$Glc$^+$	5699	394	267	148	130	51	21.3
PB13	PTS$^-$Glc$^+$	4737	327	314	174	123	48	15.1

[a] Reported as nmol substrate consumed · min^{-1} · mg protein.

determined for the wild-type JM101 strain. These data could suggest significant differences in the carbon flux distribution over the glycolytic pathway and the oxidative branch of the pentose phosphate pathway in the wild-type *E. coli* and the PTS$^-$Glc$^+$ mutant strains.

^{13}C Labeling and NMR Spectroscopy Analysis

Isotopic labeling with a mixture of [1-^{13}C]glucose and [U-$^{13}C_6$]glucose was utilized for determining metabolic flux differences between the wild type and the PTS$^-$Glc$^+$ mutants. We performed 2D [^{13}C, ^{1}H] HSQC NMR spectroscopic analysis of the acidic hydrolysates from bacterial cultures of the wild-type and mutant strains. From the spectra, we integrated the ^{13}C multiplets reflecting differently labeled isotopomer species. The values for all the integrated signals are presented in the Appendix. These data were input to the flux analysis program yielding the carbon flux values of the central carbon metabolism in mmol · h^{-1} · g biomass^{-1} for the wild-type JM101 strain and the PB11, PB12, and PB13 mutants. Representative statistical relative error estimates for the oxidative pentose phosphate pathway flux as well as for the C4-decarboxylating PEP carboxykinase and malic enzyme fluxes were 10%. In none of the strains was a significant (i.e., more than 10% of the glucose uptake rate) flux over the Entner–Doudoroff pathway or the glyoxylate shunt detected. As a result of this analysis, we found significant differences in the carbon fluxes between these strains in the EM pathway, the PP pathways, and at the TCA cycle (Fig. 2), as will be discussed in the next paragraphs.

Embden–Meyerhof pathway. As suggested by the Pgi-specific activity measurements (see Table 4), the PB12 and PB13 strains apparently have a higher glycolytic flux than the wild-type strain; this hypothesis was confirmed by NMR spectroscopy. The wild-type JM101 strain directed 76.6% of total carbon flux through the first step of the EM pathway (from G6P to F6P, see Fig. 2a). Compared to JM101, the PTS$^-$Glc$^-$ strain PB11 showed a much lower flux through the first step of the EM pathway (40.3%). The differences between JM101 and the PTS$^-$Glu$^-$PB11 strains are the result of the absence of the PTS system, the low glucose uptake, and the low growth rate of PB11. In the PB12 and PB13 PTS$^-$Glc$^+$ mutant strains, one of the important differences with the wild-type strain is located in the first step of the EM pathway; values for carbon flux on this part of the glycolytic pathway are 93.1 and 89.2 molar percentage, respectively, for PB12 and PB13 strains (Figs. 2c and 2d). There are no important differences between strains JM101, PB12, and PB13 in the remaining steps of the EM pathway down until the synthesis of PEP.

The hypothesis at the start of the study on carbon metabolism in *E. coli*, confirmed by Báez and co-workers (2001), was that the absence of the PTS system, i.e., the major PEP-utilizing system, as well as the usage of a different system to internalize and phosphorylate glucose, would lead to an increase in the amount of PEP that could be used in the biosynthesis of aromatic compounds. Although when studying the PB12 and PB13 strains we found no changes in the PEP carbon flux into the synthesis of aromatic compounds between the wild-type and the mutant strains (Fig. 2), this was an expected result since the common aromatic pathway displays strong regulation at the level of the DAHP synthase isoenzymes. Other, less regulated metabolic reactions using PEP as substrate, like those catalyzed by the pyruvate kinases A and F (PykAF) (Ponce *et al.*, 1995), showed increased fluxes in the same strains (Fig. 2).

PEP is utilized for the synthesis of pyruvate via the PTS system and the PykAF enzymes; pyruvate is the precursor of ACoA, which in turn is utilized for the synthesis of citrate by the citrate synthase enzyme. PEP is also used for providing oxaloacetate by way of the Ppc enzyme and pyruvate can be carboxylated to yield malate. Certainly, two of the

TABLE 5

Carbon Fluxes[a] Obtained from the ^{13}C NMR Flux Analysis (Molar percentage)

	Reaction[b]							
Strain	1	2	3	4	5	6	7	8
JM101	76.6	22.3	40.7	44.1	7.7	0.0	38.1	55.4
PB12	93.1	5.3	128.3	40.3	0.0	3.7	28.5	36.0
PB13	89.2	9.6	141.3	50.7	0.0	9.8	34.8	53.1

[a] All flux values are given as percentage of glucose utilization rate in that strain expressed in mmol Glc · h^{-1} · g biomass^{-1}.

[b] Reactions: (1) G6P → F6P, EM pathway carbon flux; (2) G6P → 6PG, PP pathway carbon flux; (3) PEP → PYR, PykAF carbon flux; (4) ACoA + OAA → CIT, GltA carbon flux; (5) OAA → PEP + CO_2, Pck carbon flux; (6) OAA → PYR + CO_2, Mez carbon flux; (7) MAL → OAA, Mdh carbon flux; (8) acetic acid production.

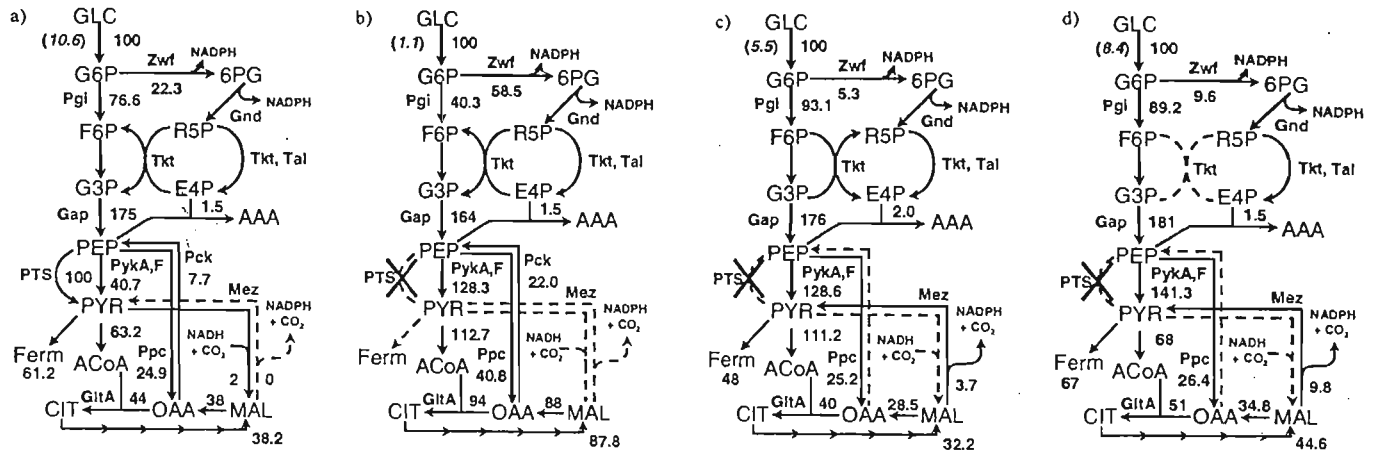

FIG. 2. Relevant metabolic routes and carbon fluxes determined by the flux analysis in *E. coli* JM101 (a) and derivative strains PB11 PTS$^-$Glc$^-$ (b) and the two PTS$^-$Glc$^+$ strains PB12 (c) and PB13 (d). Values in italic represent the glucose uptake in mmol Glc·h^{-1}·g biomass^{-1}. Other values are molar percentages of glucose uptake of specific nodes. Arrows show the main direction of the carbon flux. Dashed lines means zero or near-zero values for the corresponding fluxes.

important differences between the wild-type JM101 strain, which utilizes the PTS system for glucose uptake, and the PTS$^-$ strains are that in the mutant strains the carbon flux through the PykAF enzymes (as shown in Fig. 2) is highly increased and that pyruvate is differently utilized for the synthesis of ACoA and malate (see below). Interestingly, approximately the same fraction of PEP originally used by the PTS system in the wild-type *E. coli* is consumed by the pyruvate kinases A and F in strains PB11, PB12, and PB13. The carbon flux through the PykAF enzymes increased from 40.7 in the wild-type strain to 128.3, 128.6, and 141.3%, respectively, in the three mutants. The increase is close to the 100% of molar carbon usage by the PTS system in the wild-type strain (Table 5, Figs. 2b, 2c, and 2d). The high flux through the PykAF enzymes in the mutant strains PB12 and PB13 is in agreement with an increase in PEP availability when the glucose transporter changes from PTS to a PEP-independent transporter like GalP.

The analysis of acetic acid production (Table 5 and Fig. 2) shows that while JM101 and PB13 strains synthesized almost the same amount of acetic acid, 55 and 56% molar percentage, respectively, PB12 directed a lower flux (36%) to the synthesis of this molecule. These results are in agreement with previous observations on acetic acid production synthesized in these strains (Sigüenza *et al.*, 1999). Other fermentation products in *E. coli* are mostly ethanol and formic acid. The total carbon flux until fermentation products, including acetic acid production, accounts for 61.2% in the wild-type JM101 strain, 48% in the PB12 strain, and 67% in the PB13 strain (Figs. 2a, 2c, and 2d). Mathematical modeling for the PB11 strain did not suggest any fermentation products nor were they detected by ^{1}H NMR spectroscopy.

Pentose phosphate pathway. At the level of the PP pathway, there are three important differences detected between the studied strains. JM101 directed 22% of total carbon flux through the Zwf enzyme when growing aerobically on glucose as carbon source, consistent with previously reported values of around 20 to 30% obtained using biochemical (Neidhardt *et al.*, 1990) or NMR analysis (Szyperski, 1998). The PTS$^-$Glc$^-$ PB11 strain presented a higher flux through the oxidative branch of the PP pathway of 58.5%, while the PTS$^-$Glc$^+$ strains PB12 and PB13 had a strongly diminished carbon flux through the PP pathway of 5.3 and 9.6%, respectively. This reduction corroborates the tendency observed in the analysis of Pgi- and Zwf-specific activities (Table 4). A carbon flux reduction over the oxidative branch of the PP pathway may have consequences for the bacterial physiology and metabolism (see below), since some metabolites, like NADPH and ribose 5-phosphate, are produced mainly by this pathway, when the bacteria are growing on glucose as carbon source (Fraenkel, 1996).

The NMR results and the mathematical model showed that the main ribose-producing metabolism is different between strains PB12 and PB13. As can be seen in Fig. 3, histidine, which is derived from ribose 5-phosphate, shows clearly different patterns of its carbon C-3 in the 2D [^{13}C, ^{1}H] HSQC NMR spectrum. In PB12, the nonoxidative branch of the PP pathway is utilizing intermediates of the EM pathway to synthesize R5P and E4P, using the Tkt, Rpi, and Rpe enzymes. In PB13 the carbon flux through the nonoxidative branch of the PP pathway, which is normally utilized to produce E4P and R5P, is close to zero. In PB13, E4P and R5P are produced, upon oxidative-branch usage, as the products of Gnd, Rpi, Rpe, Tkt, and Tal reactions (Fraenkel 1996) (Table 6, Fig. 2d).

Metabolic Engineering 4, 124–137 (2002)
doi:10.1006/mben.2001.0209

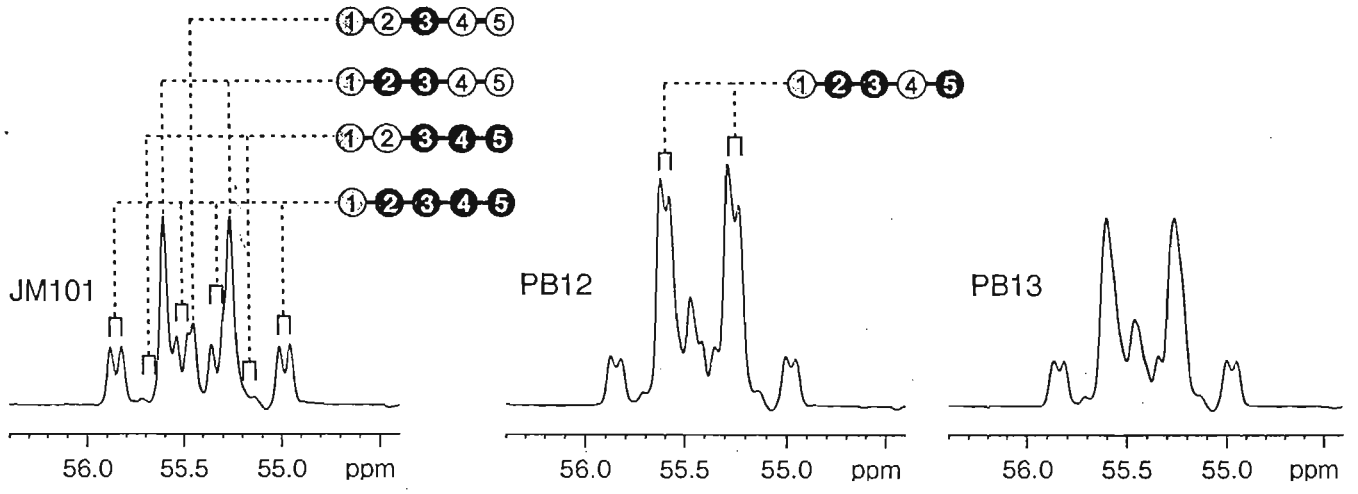

FIG. 3. ^{13}C multiplets from C-3 of histidine reflecting different isotopomeric compositions of this amino acid in the wild-type JM101 and the PTS$^-$Glc$^+$, PB12 and PB3 strains. Filled circles represent ^{13}C, open circles represent ^{12}C, gray circles represent uncertainty about the label state of the indicated carbon. The signals were extracted from 2D HSQC NMR spectra taken from biomass hydrolysates. The multiplets for JM101 and PB13 show a strong presence of intact C5 fragments of the precursor ribose 5-phosphate, which can only be produced by the oxidative branch of the pentose phosphate pathway. For the PB12 strain, the multiplet structure indicates a significantly increased content of isotopomers in which the ^{13}C-3–^{13}C-4 and/or ^{13}C-4–^{13}C-5 bond has been cleaved. This kind of labeling suggests an increase in the carbon flux through the nonoxidative branch of the PP pathway. See Fig. 2.

Tricarboxylic acid cycle. Oxaloacetate and acetyl-CoA are substrates of the citrate-synthase enzyme (GltA), an enzyme that incorporates carbon skeletons into the TCA cycle (Cronan and LaPorte, 1996). Carbon flux through the GltA and the Ppc enzymes represents the principal route for carbon feeding of the TCA cycle. Carbon depletion of this cycle is generated mostly from the activity of Pck and Mez enzymes as well as from the carbon withdrawal by biosynthetic processes (Neidhardt *et al.*, 1990). The flux analysis showed only small differences in the carbon flux through the GltA enzyme between the wild-type JM101 (44%) and the PB12 (40%) and the PB13 (51%) mutant strains (Fig. 2, Table 5). In contrast, the carbon fluxes producing oxaloacetate, especially from PEP and malate, varied.

In the PB11 PTS$^-$Glc$^-$ strain, there is a great interchange between PEP and oxaloacetate. The carbon flux through the Ppc enzyme is 40.8%, while the backflow through the Pck enzyme is 22%. The TCA carbon flux (through the GltA enzyme) is 94% of the total glucose consumed (Fig. 2b). All these data suggest a high TCA activity in the PB11 strain, with a consequent high energy production per mole of glucose; nevertheless, it is important to remember that PB11 is a very special strain that grows very slowly in glucose.

TCA replenishing by Ppc activity has similar values in the JM101, PB12, and PB13 strains. In JM101, there is carbon flux interchange between PEP and OAA mediated by the Ppc and Pck enzymes (Fig. 2a); the flux from PEP to OAA by Ppc was 24.9%, while 7.7% flowed back via Pck. However, the carbon flux through Pck is absent in the PB12 and PB13 mutant strains, showing a net increase in TCA feeding from PEP carboxylation. On the other hand, the oxaloacetate synthesized from the malate dehydrogenase enzyme decreased from 38% carbon flux in the JM101 strain, to 28.5 and 34.8% carbon flux in PB12 and PB13, respectively (Fig. 2). Therefore, in the JM101 wild-type strain, carbon flux through the Ppc is apparently replenishing the carbon skeletons withdrawn from the TCA cycle by biosynthetic reactions and by the Pck gluconeogenic enzyme, while in the mutant strains, Ppc replenishes malate that is utilized by the malic enzymes to produce NADPH and pyruvate. Changes in carbon fluxes involving oxaloacetate were clearly reflected in the extracted profile of the

TABLE 6

Carbon Fluxes in the Pentose Phosphate Pathway[a]

	Strain		
Reaction[b]	JM101	PB12	PB13
ppp1	22	5	10
ppp1a	21	5	9
ppp2	6	1	2
ppp3	6	1	2
ppp4	3	−3	0

[a] All flux values are given as percentage of glucose utilization rate in that strain expressed in mmol Glc·h^{-1}·g biomass^{-1}. Negative value indicates backward reaction.

[b] Reactions: ppp1, G6P → 6PG; ppp1a, 6PG → P5P + CO_2; ppp2, P5P + P5P → S7P + G3P; ppp3, S7P + G3P → F6P + E4P; ppp4, P5P + E4P → F6P + G3P.

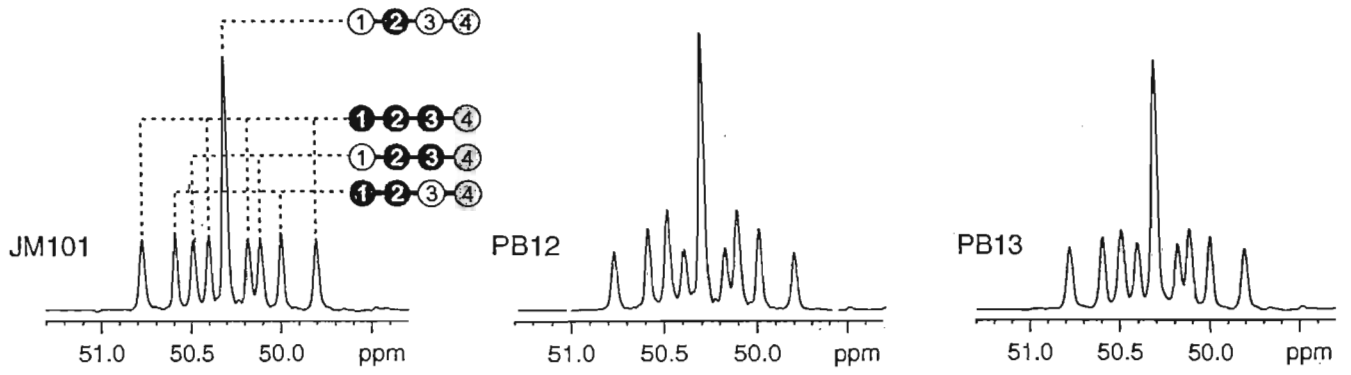

FIG. 4. ^{13}C multiplets for C-2 of aspartic acid in the wild-type JM101 and the PTS$^-$Glc$^+$, PB12 and PB13, derivative strains. The significantly increased contribution of [1,2-$^{13}C_2$] and [2,3-$^{13}C_2$] aspartate moieties for PB12 reflect altered carbon fluxes at the oxaloacetate node. See Fig. 3.

signal for C-2 of aspartic acid, which derives directly by transamination from oxaloacetate (Fig. 4).

The NADP-dependent malic enzyme (Mez) oxidizes malate to produce pyruvate, CO_2, and NADPH. Mez is an important producer of reducing power in *E. coli,* but the PP pathway is the major supplier of reducing power when bacteria are growing on glucose as carbon source (Csonka and Fraenkel, 1977; Szyperski, 1995; Fiaux *et al.,* 1999). Mutant strains on *sfcA* and *b2463* genes coding for the NAD- and NADP-dependent malic enzymes have been recently developed. Using these strains, it has been determined that the lack of oxidative decarboxylation of malate has no effect in wild-type *E. coli* when growing on glucose as carbon source (van der Rest *et al.,* 2000). As determined from the ^{13}C-labeling experiments and mathematical modeling, the carbon fluxes through the malic enzyme were almost negligible in the wild-type strain. In contrast, in the PB12 and PB13 mutant strains the carbon flux was 3.7 and 9.8%, respectively (Fig. 2). Sauer and co-workers (1999) have found, by a similar approach, less than 5% of ^{13}C labeling from malate on pyruvate molecules, suggesting the existence of a small carbon flux through the malic enzymes in the wild-type JM101 strain. In the same report, they also found an increase to approximately 20% in the same kind of ^{13}C labeling on pyruvate molecules when analyzing a JM101 *pykAF* mutant (PB25 strain, unable to produce pyruvate from PEP by pyruvate kinases; Ponce *et al.,* 1995). As seen in the work reported by Sauer and in our results, two different strains that have different modifications in PEP utilization showed an increased carbon flux through the malic enzymes.

As reviewed by Stols and Donnely (1997) and van der Rest *et al.* (2000), the main function of the malic enzymes is to synthesize pyruvate and reducing power from malate; however, NAD-dependent malic enzyme in wild-type *E. coli* can act in the reverse direction, by carboxylating pyruvate, to synthesize malate, using NADH as cofactor (Fig. 2). We have found that the wild-type JM101 strain has a 2% molar carbon flux through these enzymes in the direction of pyruvate carboxylation (Fig. 2a); however, this flux was absent in the PB12 and PB13 mutant strains (Figs. 2c and 2d). It is possible that the behavior of the Ppc, Pck, and Mez enzymes may reflect a concerted mechanism that the bacterium utilizes for regulating carbon fluxes under certain physiological conditions. In the case of the JM101 strain, reducing power, as NADPH, is supplied mostly by the oxidative branch of the PP pathway, and the PEP–PYR balancing is mediated by the Ppc and Pck enzymes. In the PTS$^-$Glc$^+$ mutant strains, due to the reduced carbon flux through the oxidative branch of the PP pathway, the NADP-dependent malic enzyme synthesizes NADPH using malate, an intermediate of the TCA cycle. In the PB12 and PB13 mutant strains, the PEP–PYR balance is in the direction of PEP catabolism, and because of the lack of PTS system, apparently there is no need for PEP synthesis by the Pck enzyme. Another possible reason for the absence of carbon flux through Pck in the PTS$^-$Glc$^+$ mutants is the drain of carbon skeletons from the TCA cycle due to the malic enzymes activities; in this way, the cell may respond to PEP availability and/or TCA carbon depletion in *E. coli,* regulating the carbon flux through the Pck enzyme.

Further Predictions of Specific Effects on Certain Mutants

The results from the NMR measurements and mathematical modeling allowed the prediction of certain specific effects of further genetic manipulations incorporated into the PB12 and PB13 strains.

Case I: The pgi *gene.* The calculations based on the ^{13}C labeling results showed that PB12 and PB13 strains had a diminished carbon flux through the oxidative branch of the pentose phosphate pathway. These strains presented a 3- to 4-fold increase in the Pgi-specific activity with respect to the wild-type strain (Table 4). At the same time, these strains also showed, as already mentioned, an increase of the Zwf-specific activity, the enzyme that commits carbon flux through the oxidative branch of the pentose phosphate

Metabolic Engineering 4, 124–137 (2002)
doi:10.1006/mben.2001.0209

pathway (Fig. 2). The calculated Pgi/Zwf quotient (Table 4) is in accordance with the tendency observed by NMR measurements showing a greater glycolytic flux and a decrease in carbon flux through the oxidative branch of the PP pathway. Under these conditions Pgi and Zwf are competing for the common substrate glucose 6-phosphate and the increase in both Pgi and Zwf activities might be part of the PTS$^-$ strain adaptation to efficiently use glucose as a carbon source and to retain the capacity to direct enough carbon flux through the oxidative branch of the PP pathway for physiological needs, i.e., NADPH, ribose 5-phosphate, and erythrose 4-phosphate (see Case II: The *gnd* gene). To determine if the increase of the Zwf enzyme-specific activity may help, under certain physiological conditions in *E. coli,* to direct a higher carbon flux through the oxidative branch of the PP pathway, we decided to interrupt the *pgi* gene in the wild-type and the PB12 and PB13 strains. It has been reported that *pgi* mutants can only grow utilizing the carbon flux that is directed through the Zwf enzyme (Fraenkel, 1996). In the wild-type *E. coli* cells the growth rate dropped from 0.7 to 0.1 h^{-1} when the *pgi* gene was interrupted (86% less than the parental JM101 strain). In the PTS$^-$Glc$^+$ background, the growth rate dropped from 0.42 to 0.29 h^{-1} in SM31 *pgi*$^-$ strain, only 31% less than the parental PB12 strain, and from 0.49 to 0.35 h^{-1} in SM32, 29% less than the parental PB13 strain (see Table 6). The Zwf-specific activity for the strains SM14, SM31, and SM32 in neither case is higher than in the parental strains (data not shown), demonstrating that there is no adaptation to use glucose by means of a carbon flux adaptation through the PP-oxidative branch. Using these data and those presented in Table 5, it is possible to conclude that a higher Zwf-specific activity, perhaps together with a synergic effect of the mutational events that lead to the glucose utilization on the PTS$^-$Glc$^-$ strain, allows the PTS$^-$Glc$^+$ *E. coli* strains to direct more carbon through the PP pathway and, therefore, sustain relatively high growth rates in the absence of Pgi.

Case II: The gnd *gene.* Pentose phosphate metabolism is different between the PB12 and the PB13 strains. According to the NMR data, in PB12 the nonoxidative branch of the pentose phosphate pathway is the principal supplier of both R5P and E4P (Table 6, Figs. 2c and 3). However, in strain PB13, R5P is synthesized using the Gnd enzyme and part of the oxidative branch of the PP pathway, while most of the E4P is produced by transaldolase using the P5P synthesized by Gnd (Figs. 2d and 3). Because of these calculated differences, the interruption of the *gnd* gene may have different effects on these strains. A PB13 *gnd*$^-$ strain would be unable to produce R5P and E4P, needed for aromatic amino acid and vitamin biosynthesis. This situation will be different in PB12, in which the same modification should not have major effects on the growth rate in minimal medium. Therefore, the *gnd* gene was interrupted in strains JM101, PB12, and PB13. The *gnd*$^-$ derivative strains were studied using cultures grown on glucose as the sole carbon source. As can be seen in Table 7, strains SM8 (PB12 *gnd*$^-$) and PB12 had almost the same μ (0.39 and 0.42 h^{-1}, respectively). In contrast, strain SM9 (PB13 *gnd*$^-$) grew very slowly on glucose at 0.02 h^{-1}, while PB13 had a μ of 0.49 h^{-1}. These observations were thus fully in accordance with the predictions. The effect of the same *gnd*$^-$ modification in the wild-type strain was a reduction of μ from 0.71 to 0.56 h^{-1}; this effect was due to the accumulation of toxic levels of 6-phosphogluconate. It is possible that the carbon flux through Zwf is not enough to produce accumulation of 6PG to toxic levels in strain PB12.

CONCLUSIONS

We have measured, using biochemical and NMR spectroscopy techniques, the carbon fluxes in different *E. coli* strains modified in glucose transport. PTS$^-$Glc$^+$ strains PB12 and PB13 utilize GalP to internalize glucose and, as we have shown in this study, Glk to phosphorylate it once inside the cell. However, the glucose-transporting capacity developed in these mutant strains reached only half of the original transport capacity provided by the PTS system in the wild-type strain. This reduced capacity could partly explain the measured increases of the Pgi- and Zwf-specific activities in the PTS$^-$Glc$^+$ strains. These higher activities could also be the result of uncoupling glucose transport–phosphorylation and glucose catabolism. *E. coli,* like other biological systems, might have a metabolite channeling mechanism involved in glucose catabolism. As reviewed by several authors, channeling is present in some metabolic pathways and it has some clear advantages for certain

TABLE 7

Growth Rates (μ) of *pgi* and *gnd* Mutants of *E. coli*

Strain	Genotype	μ^a	%
JM101	Wild type	0.71	100
SM14	JM101 *pgi*$^-$	0.10	14
SM6	JM101 *gnd*$^-$	0.57	80
PB12	PTS$^-$Glc$^+$	0.42	100
SM31	PB12 *pgi*$^-$	0.29	69
SM8	PB12 *gnd*$^-$	0.39	93
PB13	PTS$^-$Glc$^+$	0.49	100
SM32	PB13 *pgi*$^-$	0.35	71
SM9	PB13 *gnd*$^-$	0.02	4

[a] In h^{-1}, obtained on M9 medium supplemented with 2 g/L glucose.

metabolic features (Mendes *et al.* 1996; Vértessy *et al.* 1997; Edwards, 1998; Spivey and Ovádi, 1999). The GalP–Glk proteins replacing the PTS system in the PTS$^-$Glc$^+$ mutants may not channel glucose 6-phosphate to the glycolytic enzymes in the cell; perhaps as part of the selection process to use glucose (Flores, 1995), the PTS$^-$Glc$^+$ cells apparently have raised the levels of Pgi and Zwf enzymes to achieve high glucose 6-phosphate catabolic rates.

The glucose transport capacity of the *E. coli* PTS$^-$ strain PB11 is 10 times lower than that of the wild-type JM101 strain. ^{13}C labeling and NMR techniques allowed us to determine metabolic fluxes in PB11, showing that this strain directed a higher carbon flux in the PP pathway and showed a higher conversion of glucose to CO_2 through the TCA cycle compared to the wild-type strain. The low glucose transport capacity in the PB11 strain may leave the bacteria with a low concentration of metabolic intermediates and the observed carbon flux distribution may reflect the metabolic routes with high substrate affinity or those best organized by substrate channeling. In the case of the high carbon flux through the PP-oxidative branch in the PTS$^-$ PB11 strain (58% of carbon usage compared to 22% in the wild-type JM101 strain), a simpler explanation could be that in PB11, the glucose utilization is low and limited before G6P; the reaction catalyzed by Zwf is irreversible with a relatively low K_m, thus leading to more carbon usage when competing with Pgi for their common substrate G6P.

The Pgi and Zwf enzymes compete for glucose 6-phosphate as a substrate. While Zwf commits the carbon flux through the oxidative branch of the pentose phosphate pathway, Pgi channels carbon into the glycolytic pathway. The biochemical data obtained from specific enzyme activity measurements allowed us to propose that the central carbon metabolism in the PTS$^-$Glc$^+$ strains has changed compared to the wild-type strain JM101. The data showed an increase in both the Pgi- and the Zwf-specific activities for the PTS$^-$Glc$^+$ strains; however, the Pgi/Zwf quotient, which was 8 for the wild-type strain, increased to 21 and 15 in PB12 and PB13, respectively. This result suggests that in these mutant strains, there should be an increase in carbon flux through the EM pathway and consequently a decrease in carbon flux through the PP pathway. Nevertheless, the extent of the modification of carbon fluxes around the glucose 6-phospate node cannot be evaluated utilizing only the Pgi- and the Zwf-specific activity analysis.

We therefore applied ^{13}C labeling, NMR, and mathematical modeling allowing us to determine that the carbon flux through the oxidative branch of the pentose phosphate pathway was decreased from 22% in JM101 to 5% in PB12 and 10% in PB13, even while the Zwf-specific activity was 48 and 74% higher, respectively, in these mutant strains.

The flux analysis also showed that Gnd is the main ribose-producing enzyme in PB13. The interruption of the gene that codes for this enzyme in PB13 makes this strain incapable of growing on glucose as the carbon source; however, the same modification in PB12 and JM101 caused no major changes in the growth rate. These results were also inferred from the NMR data and mathematical modeling, which predicted that in PB12, ribose 5-phosphate synthesis is shared by Gnd and the nonoxidative branch of the PP (i.e., Tkt).

Another interesting result obtained from the NMR measurements and mathematical modeling is that the carbon flux through the malic enzymes was essentially absent in the wild-type strain, while carbon flux through this enzyme was 4 and 10% in the two PTS$^-$Glc$^+$ mutant strains. These effects could be seen as a compensatory mechanism in these mutant strains for the impaired synthesis of NADPH due to the reduced carbon flux through the oxidative branch of the pentose phosphate pathway.

It is important to notice that in these two mutants a second compensatory mechanism was found to operate at the level of the TCA cycle. Due to the increase of the carbon flux through the malic enzymes, the TCA cycle is to some extent depleted of oxaloacetate. The way the cell apparently responds to this situation is by increasing the net synthesis of oxaloacetate from PEP by down-regulating carbon depletion of the TCA cycle by the Pck enzyme. These metabolic differences present in the mutant PTS$^-$Glc$^+$ strains could well reflect the normal capacities of the cell to react to and compensate for changes in metabolism imposed by different physiological conditions that are fixed in these mutants. Finally, the characterization of these strains as performed in this study will likely allow a better design for the construction of more robust strains for overproduction purposes.

APPENDIX

Multiplet Composition (cf. Szyperski, 1995) for Selected Carbons, Extracted from 2D NMR Spectra

Abbreviations used: S, singlet; da, doublet with the larger scalar coupling; db, doublet with the smaller scalar coupling; dd, doublet of doublets or triplet; ddd, doublet of doublets of doublets.

(a) Strain JM101

C atom	s	da	db	dd	ddd
Cytidine-1′	0.408	0.592			
Histidine-5	0.455	0.545			
Histidine-3	0.075	0.032	0.427	0.467	
Histidine-2	0.055	0.068	0.026	0.851	

Metabolic Engineering 4, 124–137 (2002)
doi:10.1006/mben.2001.0209

Uridine-4′	0.102	0.898			
Uridine-5′	0.536	0.464			
Glycerol-1,3	0.552	0.448			
Glycerol-2	0.048	0.123		0.829	
Glycine-2	0.123	0.877			
Serine-2	0.056	0.183	0.072	0.689	
Serine-3	0.688	0.312			
Phenylalanine-2	0.051	0.031	0.057	0.861	
Phenylalanine-3	0.520	0.410		0.069	
Alanine-2	0.037	0.024	0.086	0.853	
Alanine-3	0.651	0.349			
Leucine-2	0.517	0.291	0.123	0.069	
Leucine-3	0.393	0.507		0.100	
Isoleucine-2	0.383	0.415	0.101	0.101	
Valine-2	0.097	0.682	0.040	0.181	
Valine-3	0.035	0.508		0.329	0.128
Aspartate-2	0.293	0.175	0.185	0.347	
Aspartate-3	0.403	0.201	0.227	0.169	
Threonine-4	0.436	0.564			
Glutamate-2	0.370	0.212	0.204	0.213	
Glutamate-3	0.222	0.499		0.278	
Glutamate-4	0.453	0.250	0.194	0.103	
Proline-2	0.379	0.211	0.230	0.180	
Proline-5	0.052	0.948			
Tyrosine-δ	0.486	0.432		0.082	
Tyrosine-ε	0.123	0.291		0.586	

(b) Strain PB11

C atom	s	da	db	dd	ddd
Cytidine-1′	0.448	0.552			
Histidine-5	0.521	0.479			
Histidine-3	0.250	0.056	0.328	0.367	
Histidine-2	0.104	0.174	0.002	0.721	
Uridine-4′	0.342	0.658			
Uridine-5′	0.393	0.607			
Glycerol-1,3	0.457	0.543			
Glycerol-2	0.065	0.238		0.696	
Glycine-2	0.340	0.660			
Serine-2	0.175	0.280	0.157	0.388	
Serine-3	0.651	0.349			
Phenylalanine-2	0.122	0.046	0.152	0.681	
Phenylalanine-3	0.418	0.477		0.105	
Alanine-2	0.089	0.063	0.200	0.649	
Alanine-3	0.515	0.485			
Leucine-2	0.428	0.376	0.099	0.097	
Leucine-3	0.544	0.392		0.064	
Isoleucine-2	0.413	0.360	0.111	0.117	
Valine-2	0.226	0.535	0.082	0.156	
Valine-3	0.084	0.574		0.217	0.125
Aspartate-2	0.328	0.263	0.200	0.209	
Aspartate-3	0.333	0.263	0.213	0.191	
Threonine-4	0.458	0.542			
Glutamate-2	0.331	0.258	0.219	0.192	
Glutamate-3	0.383	0.467		0.150	
Glutamate-4	0.356	0.359	0.147	0.138	
Proline-2	0.336	0.264	0.212	0.188	
Proline-5	0.137	0.863			
Tyrosine-δ	0.363	0.494		0.143	
Tyrosine-ε	0.234	0.336		0.430	

(c) Strain PB12

C atom	s	da	db	dd	ddd
Cytidine-1′	0.753	0.247			
Histidine-5	0.824	0.176			
Histidine-3	0.102	0.034	0.595	0.269	
Histidine-2	0.045	0.074	0.010	0.870	
Uridine-4′	0.115	0.885			
Uridine-5′	0.631	0.369			
Glycerol-1,3	0.535	0.465			
Glycerol-2	0.017	0.095		0.888	
Glycine-2	0.135	0.865			
Serine-2	0.048	0.176	0.072	0.704	
Serine-3	0.685	0.315			
Phenylalanine-2	0.050	0.026	0.062	0.862	
Phenylalanine-3	0.510	0.412		0.077	
Alanine-2	0.043	0.029	0.088	0.840	
Alanine-3	0.656	0.344			
Leucine-2	0.524	0.276	0.133	0.068	
Leucine-3	0.330	0.535		0.135	
Isoleucine-2	0.432	0.349	0.121	0.099	
Valine-2	0.097	0.681	0.035	0.187	
Valine-3	0.045	0.430		0.350	0.174
Aspartate-2	0.298	0.181	0.242	0.279	
Aspartate-3	0.341	0.188	0.253	0.219	
Threonine-4	0.368	0.632			
Glutamate-2	0.348	0.188	0.238	0.227	
Glutamate-3	0.209	0.497		0.294	
Glutamate-4	0.380	0.207	0.262	0.151	
Proline-2	0.341	0.192	0.242	0.225	
Proline-5	0.068	0.932			
Tyrosine-δ	0.462	0.435		0.103	
Tyrosine-ε	0.113	0.284		0.603	

(d) Strain PB13

C atom	s	da	db	dd	ddd
Cytidine-1′	0.672	0.328			
Histidine-5	0.754	0.264			

Histidine-3	0.095	0.036	0.538	0.321	
Histidine-2	0.041	0.077	0.005	0.877	
Uridine-4′	0.124	0.876			
Uridine-5′	0.575	0.425			
Glycerol-1,3	0.540	0.460			
Glycerol-2	0.030	0.098		0.872	
Glycine-2	0.130	0.870			
Serine-2	0.044	0.108	0.066	0.782	
Serine-3	0.659	0.341			
Phenylalanine-2	0.049	0.021	0.061	0.870	
Phenylalanine-3	0.511	0.416		0.073	
Alanine-2	0.051	0.030	0.093	0.826	
Alanine-3	0.645	0.355			
Leucine-2	0.512	0.278	0.141	0.069	
Leucine-3	0.368	0.523		0.109	
Isoleucine-2	0.405	0.382	0.107	0.106	
Valine-2	0.108	0.672	0.038	0.182	
Valine-3	0.041	0.446		0.355	0.158
Aspartate-2	0.298	0.173	0.211	0.318	
Aspartate-3	0.379	0.193	0.233	0.194	
Threonine-4	0.390	0.610			
Glutamate-2	0.366	0.192	0.226	0.216	
Glutamate-3	0.213	0.496		0.291	
Glutamate-4	0.425	0.232	0.225	0.118	
Proline-2	0.377	0.197	0.223	0.203	
Proline-5	0.077	0.923			
Tyrosine-δ	0.452	0.444		0.104	
Tyrosine-ε	0.109	0.285		0.606	

ACKNOWLEDGMENTS

We thank Mercedes Enzaldo (Instituto de Biotecnología–UNAM, México) and Christina Mack (Forschungszentrum, Institut für Biotechnologie 1, Germany) for technical support. S. Flores was financially supported by fellowships from CONACyT, UNAM, and Fundación Telmex. This work was partially supported by CONACyT Grant NC-230 and by PROBIOMED–CONACyT Contract P-506.

REFERENCES

Báez, J. L., Bolívar, F., and Gosset, G. (2001). Determination of 3-deoxy-D-arabino-heptulosonate 7-phosphate productivity and yield from glucose in *Escherichia coli* devoid of the glucose phosphotransferase transport system. *Biotechnol. Bioeng.* 73, 530–535.

Bolívar, F., Rodríguez, R. L., Greene, P. J., Betlach, M. C., Heynecker, H. L., Boyer, H. W., Crosa, J. H., and Falkow, S. (1977). Construction and characterization of new cloning vehicles. II. A multipurpose cloning system. *Gene* 2, 95–113.

Cronan, J. E., and LaPorte, D. (1996). Tricarboxylic acid cycle and glyoxylate bypass. *In* "*Escherichia coli* and *Salmonella:* Cellular and Molecular Biology" (F. C. Neidhardt, Ed.), 2nd ed., Vol. 1, pp. 206–216, Am. Soc. Microbiol., Washington, DC.

Csonka, L. N., and Fraenkel, D. G. (1977). Pathways of NADPH formation in *Escherichia coli*. *J. Biol. Chem.* 252, 3382–3391.

Curtis, J. S., and Epstein, W. (1975). Phosphorylation of d-glucose in *Escherichia coli* mutants defective in glucose phosphotransferase, mannose phosphotransferase, and glucokinase. *J. Bacteriol.* 122, 1189–1199.

Edwards, M. R. (1998). From a soup or a seed? Pyritic metabolic complexes in the origin of life. *Trends Ecol. Evol.* 13, 178–181.

de Graaf, A. A., Mahle, M., Möllney, M., Wiechert, W., Stahmann, P., and Sahm, H. (2000). Determination of full ^{13}C isotopomer distributions for metabolic flux analysis using heteronuclear spin echo difference NMR spectroscopy. *J. Biotechnol.* 77, 25–35.

Fiaux, J., Andersson, C. I. J., Holmberg, N., Bülow, L., Kallio, P. T., Szyperski, T., Bailey J. E., and Würtrich, K. (1999). ^{13}C NMR flux ratio analysis of *Escherichia coli* central carbon metabolism in microaerobic bioprocesses. *J. Am. Chem. Soc.* 121, 1407–1408.

Flores, N. (1995). "Construcción y Caracterización de Cepas de *Escherichia coli* Mutantes en el Sistema de Transporte de Carbohidratos PTS," Univ. Nacional Autónoma de México, Cuernavaca. [M.D. thesis]

Flores, N., Xiao, J., Berry, A., Bolivar, F., and Valle, F. (1996). Pathway engineering for the production of aromatic compounds in *Escherichia coli*. *Nat. Biotechnol.* 14, 620–623.

Fraenkel, D. G. (1996). Central metabolism. *In* "*Escherichia coli* and *Salmonella:* Cellular and Molecular Biology" (F. C. Neidhardt, Ed.), 2nd ed., Vol. 1, pp. 189–198, Am. Soc. Microbiol., Washington, DC.

Gosset, G., Yong-Xiao, J., and Berry, A. (1996). A direct comparison of approaches for increasing carbon flow to aromatic biosynthesis in *Escherichia coli*. *J. Ind. Microbiol.* 17, 47–52.

Lessie, T. G., and Vander Wyk, J. C. (1972). Multiple forms of *Pseudomonas multivorans* glucose-6-phosphate and 6-phosphogluconate dehydrogenases: Differences in size, pyridine nucleotide specificity, and susceptibility to inhibition by adenosine 5′-triphosphate. *J. Bacteriol.* 110, 1107–1117.

Maitra, P. K., and Lobo, Z. (1971). A kinetic study of glycolytic enzyme synthesis in yeast. *J. Biol. Chem.* 246, 475–488.

McDonald, T. P., Walmsley, A. R., and Henderson, P. J. F. (1997). Asparagine 394 in putative helix 11 of the galactose-H^+ symport protein (GalP) from *Escherichia coli* is associated with the internal binding site for cytochalasin B and sugar. *J. Biol. Chem.* 272, 15189–15199.

Mendes, P., Kell, D. B., and Westerhoff, H. V. (1996). Why and when channelling can decrease pool size at constant net flux in a simple dynamic channel. *Biochim. Biophys. Acta* 1289, 175–186.

Möllney, M., Wiechert, W., Kownatzki, D., and de Graaf, A. A. (1999). Bidirectional reaction steps in metabolic networks. Part IV. Optimal design of isotopomer labeling experiments. *Biotechnol. Bioeng.* 66, 86–103.

Nasoff, M. S., and Wolf, R. E., Jr. (1980). Molecular cloning, correlation of genetic and restriction maps, and determination of the direction of transcription of *gnd* of *Escherichia coli*. *J. Bacteriol.* 143, 731–741.

Neidhardt, F. C., Ingraham, J. L., and Schcachter, M. (1990). Biosynthesis and fueling. *In* "Physiology of the Bacterial Cell. A Molecular Approach," pp. 133–173, Sinauer, Sunderland, MA.

Palmeros, B. (2001). "Diseño y Construcción de Sistemas Genéticos para la Regulación Concertada de Genes Cromosomales en *Escherichia coli*," Univ. Nacional Autónoma de México, Cuernavaca. [Ph.D. thesis]

Patnaik, R., Spitzer, R. G., and Liao, J. C. (1995). Pathway engineering for production of aromatics in *Escherichia coli:* Confirmation of stoichiometric analysis by independent modulation of AroG, Tkt, and Pps activities. *Biotechnol. Bioeng.* 46, 361–370.

Petersen, S., de Graaf, A. A., Eggeling, L., Möllney, M., Wiechert, W., and Sahm, H. (2000). *In vivo* quantification of parallel and bidirectional

Metabolic Engineering 4, 124–137 (2002)
doi:10.1006/mben.2001.0209

fluxes in the anaplerosis of *Corynebacterium glutamicum*. *J. Biol. Chem.* 275, 35932–35949.

Ponce, E., Flores, N., Martínez, A., Valle, F., and Bolívar, F. (1995). Cloning of two pyruvate kinase isoenzymes structural genes from *Escherichia coli:* The relative role of these enzymes in pyruvate biosynthesis. *J. Bacteriol.* 177, 5719–5722.

Postma, P. W., Lengeler, J. W., and Jacobson, G. R. (1996). Phosphoenolpyruvate:carbohydrate phosphotransferase system. *In* "*Escherichia coli* and *Salmonella:* Cellular and Molecular Biology" (F. C. Neidhardt, Ed.), 2nd ed., Vol. 1, pp. 1149–1174, Am. Soc. Microbiol., Washington, DC.

Sauer, U., Lasko, R. W., Fiaux, J., Hochuli, M., Glaser, R., Szyperski, T., Wüthrich, K., and Bailey, J. E. (1999). Metabolic flux ratio analysis of genetic and environmental modulations of *Escherichia coli* central carbon metabolism. *J. Bacteriol.* 181, 6679–6688.

Schuster, S., Dandekar, T., and Fell, D. A. (1999). Detection of elementary flux nodes in biochemical networks: A promising tool for pathway analysis and metabolic engineering. *Trends Biotechnol.* 17, 53–60.

Sigüenza, R., Flores, N., Hernández, G., Martínez, A., Bolívar, F., and Valle, F. (1999). Kinetic characterization in batch continuous culture of *Escherichia coli* mutants affected in phosphoenolpyruvate metabolism: Differences in acetic acid production. *World J. Microbiol. Biotechnol.* 15, 587–592.

Spivey, H. O., and Ovádi, J. (1999). Substrate channeling. *Methods* 19, 306–321.

Stols, L., and Donnelly, M. I. (1997). Production of succinic acid through overexpression of NAD^+-dependent malic enzyme in an *Escherichia coli* mutant. *Appl. Environ. Microbiol.* 63, 2695–2701.

Szyperski, T. (1995). Biosynthetically directed fractional ^{13}C-labeling of proteinogenic amino acids—An efficient analytical tool to investigate intermediary metabolism. *Eur. J. Biochem.* 232, 433–448.

Szyperski, T. (1998). ^{13}C-NMR, MS and metabolic flux balancing in biotechnology research. *Q. Rev. Biophys.* 1, 41–106.

Valle, F., Muñoz, E., Ponce, E., Flores, N., and Bolívar, F. (1996). Basic and applied aspects of metabolic diversity: The phosphoenolpyruvate node. *J. Ind. Microbiol.* 17, 458–462.

Van der Rest, M. E., Frank, C., and Molenaar, D. (2000). Functions of the membrane-associated and cytoplasmic malate dehydrogenases in the citric acid cycle of *Escherichia coli*. *J. Bacteriol.* 182, 6892–6899.

Varma, A., Boesch, B. W., and Palsson, B. O. (1993). Biochemical production capabilities of *Escherichia coli*. *Biotechnol. Bioeng.* 42, 59–73.

Vértessy, G. B., Orosz, F., Kovács, J., and Ovádi, J. (1997). Alternative binding of two sequential glycolytic enzymes to microtubules: Molecular studies in phosphofructokinase/aldolase/microtubule system. *J. Biol. Chem.* 272, 25542–25546.

Wiechert, W., Möllney, M., Isermann, N., Wurzel, M., and de Graaf, A. A. (1999). Bidirectional reaction steps in metabolic networks. Part III. Explicit solution and analysis of isotopomer labelling systems. *Biotechnol. Bioeng.* 66, 69–85.

Printed by Tiger Publishing Systems, Tempelhof 41, B-8000 Brugge, Belgium

JOURNAL OF BACTERIOLOGY, Oct. 1995, p. 5719–5722
0021-9193/95/$04.00+0

Vol. 177, No. 19

Cloning of the Two Pyruvate Kinase Isoenzyme Structural Genes from *Escherichia coli*: the Relative Roles of These Enzymes in Pyruvate Biosynthesis

ELIZABETH PONCE, NOEMÍ FLORES, ALFREDO MARTINEZ, FERNANDO VALLE, AND FRANCISCO BOLÍVAR*

Departamento de Microbiología Molecular, Instituto de Biotecnología, Universidad Nacional Autónoma de México (UNAM), Cuernavaca, Morelos 62271, Mexico

Received 12 May 1995/Accepted 20 July 1995

We report the cloning of the *pykA* and *pykF* genes from *Escherichia coli*, which code for the two pyruvate kinase isoenzymes (ATP:pyruvate 2-*O*-phosphotransferases; EC 2.7.1.40) in this microorganism. These genes were insertionally inactivated with antibiotic resistance markers and utilized to interrupt one or both *pyk* genes in the *E. coli* chromosome. With these constructions, we were able to study the role of these isoenzymes in pyruvate biosynthesis.

Pyruvate is a key intermediate in catabolic and biosynthetic reactions, and this is the reason why there are several metabolic routes that can deliver this compound (Fig. 1). *Escherichia coli*, when growing on glucose as the only carbon source, synthesizes most of its pyruvate through the coupled mechanism of glucose transport by the phosphotransferase transport system (PTS or PT system) (5). During this process, the phosphate group from phosphoenolpyruvate (PEP) is transferred to glucose, generating pyruvate and glucose-6-phosphate (9, 10). Pyruvate can also be synthesized from gluconate through the Entner-Doudoroff pathway (3). Another mechanism to synthesize pyruvate is through the action of pyruvate kinase (ATP:pyruvate 2-*O*-phosphotransferase; EC 2.7.1.40), which catalyzes the conversion of PEP and ADP into pyruvate and ATP, at the final stage of the glycolytic pathway. In *E. coli*, there are two pyruvate kinase isoenzymes, PykF and PykA, encoded by the *pykF* and *pykA* genes, respectively.

Garrido-Pertierra and Cooper have reported that in *E. coli*, under aerobic conditions and in the absence of pyruvate kinase activities, a functioning PT system can provide enough pyruvate to sustain wild-type normal growth rates. In the same report, it was mentioned that the absence of PykA did not seem to affect growth on any of many carbon sources; therefore, in that study, the role of PykA was not clearly defined (4).

We report here the cloning of both *pykA* and *pykF* structural genes from *E. coli* and the construction and analysis of strain derivatives in which the chromosomal copy of one or both genes was interrupted by antibiotic resistance markers. We present data on cell growth effects of these mutations, in the wild-type background and in strains that lack the PT system but are capable of glucose transport by using the galactose permease (GalP) (2). Results obtained strongly suggest that, at least under conditions where glucose is the only carbon source, both pyruvate kinase isoenzymes have an active role in pyruvate biosynthesis, but it appears that the PykF isoenzyme contributes to a greater extent. As expected, a double *pykA pykF* mutant is capable of growing on glucose and on gluconate but incapable of growing on ribose as the only carbon source, and the triple *pts pykA pykF* mutant is capable of growing on gluconate but incapable of growing on glucose or ribose.

Cloning and sequencing of the *E. coli pykA* and *pykF* structural genes. Using PCR standard techniques and primers specific for both of the two pyruvate kinase genes, we cloned these two structural genes into plasmids. The nucleotide sequences of both genes were obtained and were found to be almost identical to the deposited sequences (GenBank release 86.0) (data not shown).

Generation of *pykA* and *pykF* insertional inactivation mutants. *E. coli* mutants altered in one or both *pyk* genes were isolated after insertional mutagenesis of the *pykA* or *pykF* gene. This was performed by using antibiotic resistance cassettes (Table 1). These insertional mutations were separately integrated into the chromosome of *E. coli* ATCC 47002 (F⁻ *recB21 recC22 sbc-15 leu-6 ara-14 his-4* λ⁻) (8) and subsequently transduced into strain JM101 [*supE thi* Δ(*lac-proAB*) (F' *traD36 proAB lacI*^{q}ZΔM15)] or PB12 [same as JM101 but Δ(*ptsH-I-crr*)::*kan*; Glc$^+$]. Chromosomal gene interruptions were confirmed, in all cases, by Southern hybridization (data not shown).

Effect of *pyk* and *pts* mutations on cell growth on glucose as the only carbon source. To study the relative roles of the two *pyk* genes and their products in cell metabolism, one or both genes were interrupted in the bacterial chormosome. Also, because the PT system is the major source of pyruvate in *E. coli* (5), we isolated a mutant capable of glucose transportation through the GalP permease (2), in a background strain that carries a deletion of the PT system (a deletion mutant lacking *ptsH*, *ptsI*, and *crr* genes) (6). Using this *pts* Glc$^+$ mutant PB12, we separately incorporated each or both of the *pyk* mutations in this background. When these strains were grown in a 6-liter fermentor with M9 medium supplemented with glucose and Casamino Acids (11), no differences in growth patterns were observed for any of them; all grew as well as the parental strain JM101 (data not shown). However, if the M9 medium used did not contain Casamino Acids, interesting differences were observed. In this type of medium, all cultures of mutants and parental strains reached the same final optical density (data not shown). However, strains carrying *pyk* or *pts* mutations presented different growth rates, reported here as the generation time (t_D) obtained during the exponential growth phase

* Corresponding author. Mailing address: Departamento de Microbiología Molecular, Instituto de Biotecnología, Universidad Nacional Autónoma de México (UNAM), Apdo. Postal 510-3, Cuernavaca, Morelos 62271, México. Phone and fax: (52) (73) 17-23-99. Electronic mail address: valle@pbr322.ceingebi.unam.mx.

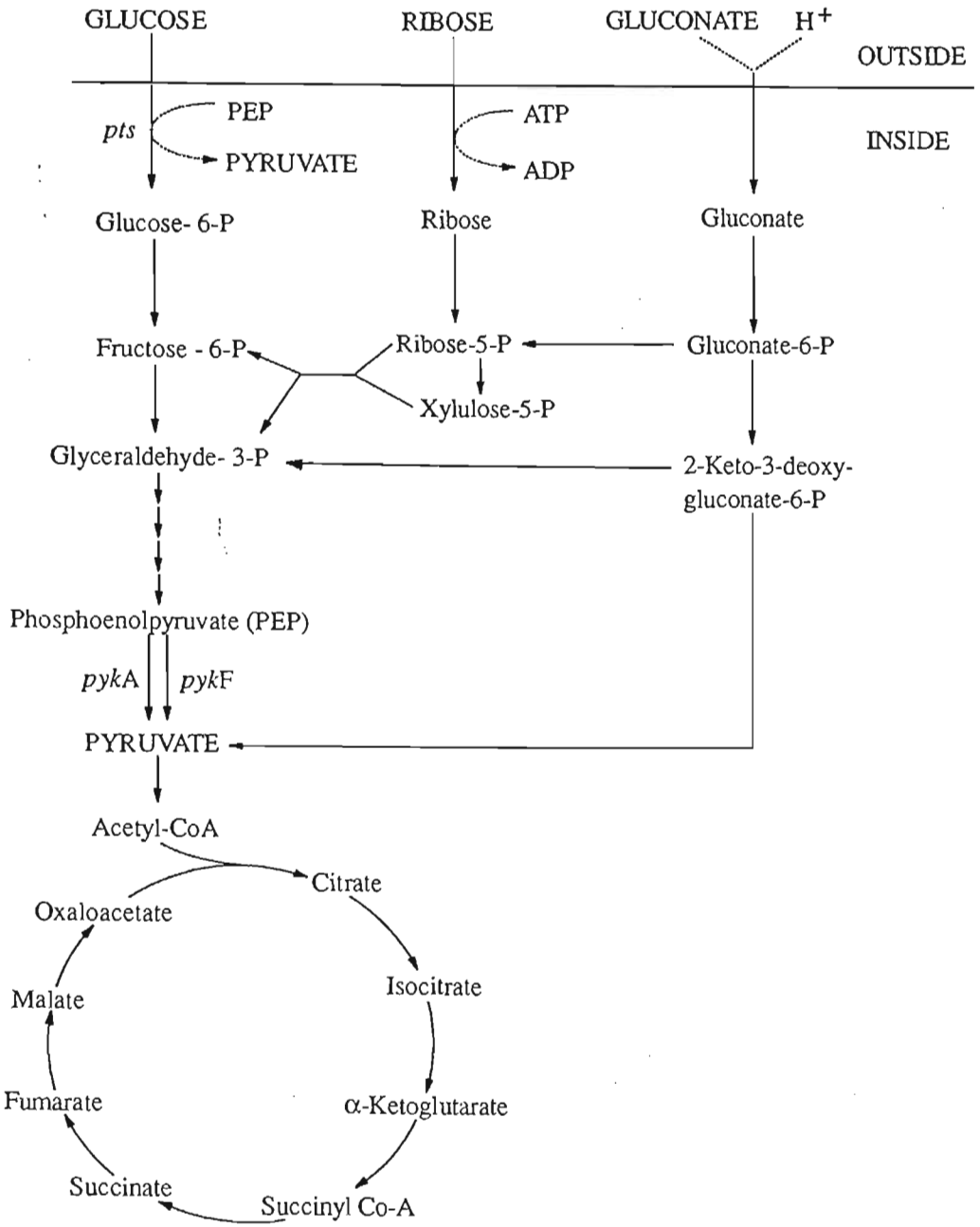

FIG. 1. Metabolic routes in *E. coli* that allow the synthesis of pyruvate from different carbon sources. CoA, coenzyme A; Glucose-6-P, glucose 6-phosphate.

(Table 1). Strains carrying the single *pykA* or *pykF* mutations, in a wild-type (Pts^+) background, showed a slight increase in their t_D in comparison with the parental strain. The strain carrying the double *pykA pykF* mutation showed a t_D 40% higher than that observed for JM101 (Table 1). The wild-type strain and the single *pyk* mutants needed 7 and 8 h, respectively, to reach maximum cell density (data not shown). PB12 (*pts* Glc^+) showed a t_D of 106.4 min (80% higher than the t_D obtained for the wild-type strain and 40% higher than that for the strain carrying the *pykA pykF* double mutation). The t_D obtained for the *pts pykA* mutant (98.5 min) was similar to the t_D of the strain carrying only the *pts* deletion, and this double mutant also took the same time to reach stationary phase. However, the introduction of the *pykF* mutation into the *pts* (Glc^+) background had the strongest effect in slowing cell growth. This strain showed a t_D of 141 min (an increase of almost 140% over the t_D shown by the wild-type strain). Finally, as expected, the triple *pts pykA pykF* mutant was incapable of growing on glucose as the only carbon source (Table 1).

Measurements of the two pyruvate kinase specific activities in the *pyk* and *pts* mutants on glucose as the only carbon source. The specific activities of both pyruvate isoenzymes were measured for the wild type and the *pyk* and *pts* mutants in the same set of experiments as those described above, by the method reported by Malcovati and Valentini (7). The results presented in Table 1 show that under these conditions, in the wild-type strain the specific activity of the PykF enzyme was

TABLE 1. t_Ds, pyruvate kinase specific activities, and comparative growth on different carbon sources for the wild type and strains carrying the *pyk* and *pts* mutations

Strain (description)	t_D (min)[a]	Sp act (IU/mg of protein)[a]		Comparative growth on carbon source[b]:		
		PykF	PykA	Glucose	Ribose	Gluconate
JM101 (wild type)	58.8 ± 2.10	0.42 ± 0.03	0.026 ± 0.002	+++++	+++++	+++++
PB22 (same as JM101 but *pykA*::*cat*[c])	69.3 ± 3.95	0.50 ± 0.04	ND	++++	++++	++++
PB24 (same as JM101 but *pykF*::*cat*)	69.4 ± 1.72	ND	0.029 ± 0.003	++++	+++	+++
PB25 (same as JM101 but *pykA*::*kan*[d] *pykF*::*cat*)	82.2 ± 0.60	ND	ND	+++	−	++
PB12[e] [same as JM101 but Δ(*ptsH-I-crr*)::*kan*; Glc$^+$]	106.4 ± 2.79	0.25 ± 0.02	0.037 ± 0.003	+++	++	++++
PB26 (same as PB12 but *pykA*::*cat*)	98.5 ± 1.62	0.25 ± 0.03	ND	+++	++	+++
PB27 (same as PB12 but *pykF*::*cat*)	141.0 ± 0.06	ND	0.042 ± 0.004	++	+	++
PB28 (same as PB12 but *pykA*::*cat pykF*::*gen*[f])		ND	ND	−	−	+

[a] Data are presented as the average of two to four independent measurements. Cultures were grown aerobically in a 6-liter fermentor in M9 medium supplemented with glucose as the only carbon source. ND, not detected.

[b] The growth response was observed after 48 h of cultivation at 37°C on minimal medium plates supplemented with either glucose (10 mM), ribose (15 mM), or gluconate (10 mM) as the only carbon source.

[c] The chloramphenicol resistance gene was obtained, as a *Sma*I fragment, from plasmid PCAT19 (1).

[d] The kanamycin resistance gene was obtained, as a *Bam*HI fragment, from plasmid pNK862 (13).

[e] An article giving a description and analysis of this strain is in preparation (2).

[f] The gentamycin resistance gene was obtained, as a *Sma*I fragment, from plasmid pGMΩ1 (12).

more than 15 times higher than that of the PykA isoenzyme. When one of the two *pyk* genes was interrupted, the enzymatic level of the remaining pyruvate kinase was slightly increased. Interestingly, strains with the *pts* background showed differences in both pyruvate kinase specific activities in comparison with those in the parental and single *pyk* backgrounds. In the *pts* background, the PykF specific activity decreased from 0.42 IU/mg of protein (in the parental strain) to 0.25 IU/mg of protein. On the other hand, the PykA specific activity in the *pts* background increased slightly over the level in the wild-type strain (Table 1).

The results presented thus far demonstrate that under the growth conditions tested, with glucose as the only carbon source, mutations in one or both *pyk* genes did affect cell growth kinetics in strains with a functional PT system. These effects were most obvious in the *pykF pykA* double mutant.

These results are in agreement with the proposition that *E. coli* in fact needs both pyruvate kinases to reach maximal growth rates (Table 1). However, cultures of the *pyk* mutants finally reached the same final optical density as did those of the parental strain JM101 (data not shown). One explanation for these results could be that the PT system and the two pyruvate kinase enzymes are coordinated in order to maintain a very low level of PEP, an allosteric regulator of several glycolytic enzymes and therefore a key intermediate in the biosynthesis of pyruvate and glucose 6-phosphate.

A deletion of the PT system, on the other hand, caused a strong increase in the generation time in comparison with that of the parental strain. Interestingly, the PykF specific activity decreased 40% in the *pts* background compared with the activity in the wild-type strain, while in the same background the PykA specific activity increased approximately by the same percentage. Nevertheless, in the *pts* mutant, under these conditions, the PykF specific activity was still eight times superior to that of PykA.

In addition, it was observed that both pyruvate kinase isoenzymes maintained the same specific activities throughout the exponential and stationary phases in each particular strain (data not shown). These results suggest that both Pyk enzymes are important throughout the life cycle of the organism and not only in a particular phase.

Effects of *pyk* and *pts* mutations on cell growth on other carbon sources. When ribose, a non-PT system sugar, was used as the only carbon source (Table 1), single *pykA* or *pykF* mutants were capable of growing on this sugar. However, the strain carrying the double *pykA pykF* mutation was unable to grow on ribose but capable of growing on gluconate, which is catabolized through the Entner-Doudoroff pathway to yield pyruvate (3). The double *pykA pykF* mutant did not grow on ribose because it lacks the ability to produce pyruvate. However, if the *E. coli* strain carries only one of the *pyk* mutations, the strain is capable of growing on ribose because pyruvate is synthesized via the remaining pyruvate kinase (Fig. 1). Finally, it is important to notice that a *pykA* strain grew better than a *pykF* strain with ribose as the only carbon source (Table 1).

Taken together, these results suggest that both pyruvate kinase isoenzymes have active roles in pyruvate biosynthesis, but it appears that the PykF enzyme contributes to a greater extent. Since pyruvate is a key intermediate in cell metabolism, it is important for the bacterial cell to have several alternatives to allow its synthesis. These different mechanisms are probably differentially regulated in order to have adequate responses to environmental changes.

We thank Paul Gaytán and Eugenio López for oligonucleotide synthesis and Alan Berry for a critical review of the manuscript.

This work was supported by grants 2031-N9302 from Consejo Nacional de Ciencia y Tecnología, México, PNUD/MEX/93/019 from Programa de las Naciones Unidas para el Desarrollo, and Genencor International.

REFERENCES

1. **Clairborne, W. F.** 1992. An improved chloramphenicol resistance gene cassette for site-directed marker replacement mutagenesis. BioTechniques 12: 223–225.
2. **Flores, N., et al.** Unpublished data.
3. **Fraenkel, D. G.** 1987. Glycolysis, pentose phosphate pathway, and Entner-Doudoroff pathway, p. 142–149. *In* F. C. Neidhardt, J. L. Ingraham, B. Magasanik, M. Schaechter, and H. E. Umbarger (ed.), *Escherichia coli* and *Salmonella typhimurium*: cellular and molecular biology. American Society for Microbiology, Washington, D.C.
4. **Garrido-Pertierra, A., and R. A. Cooper.** 1977. Pyruvate formation during the catabolism of simple hexose sugars by *Escherichia coli*: studies with pyruvate kinase-negative mutants. J. Bacteriol. 129:1208–1214.
5. **Holms, W. H.** 1986. The central metabolic pathway of *Escherichia coli*: relationship between flux and control at a branch point, efficiency of conversion to biomass, and excretion of acetate, p. 69–105. *In* B. L. Horecker and E. R. Stadtman (ed.), Current topics in cell regulation. Academic Press, Inc., New York.
6. **Lévy, S., G.-Q. Zeng, and A. Danchin.** 1990. Cyclic AMP synthesis in *Esch-*

erichia coli strains bearing known deletions of the *pts* phosphotransferase operon. Gene **86**:27–33.
7. Malcovati, M., and G. Valentini. 1982. AMP- and fructose 1,6-bisphosphate-activated pyruvate kinases from *Escherichia coli*. Methods Enzymol. **90**:170–179.
8. Oden, K. L., L. C. DeVeaux, C. R. T. Vibat, J. E. Cronan, Jr., and R. B. Gennis. 1990. Genomic replacement in *Escherichia coli* K-12 using covalently closed circular plasmid DNA. Gene **96**:29–36.
9. Postma, P. W., J. W. Lengeler, and G. R. Jacobson. 1993. Phosphoenolpyruvate: carbohydrate phosphotransferase system of bacteria. Microbiol. Rev. **57**:543–594.
10. Saier, M. H., Jr., and A. M. Chin. 1990. Energetics of bacterial phosphotransferase system in sugar transport and the regulation of carbon metabolism, p. 273–299. *In* T. A. Krulwich (ed.), The bacteria: a treatise on structure and function, vol. XII. Bacterial energetics. Academic Press, Inc., New York.
11. Sambrook, J., E. F. Fritsch, and T. Maniatis. 1989. Molecular cloning: a laboratory manual, 2nd ed. Cold Spring Harbor Laboratory Press, Cold Spring Harbor, N.Y.
12. Schweizer, H. P. 1993. Small broad-host-range gentamycin resistance gene cassettes for site-specific insertion and deletion mutagenesis. BioTechniques **15**:831–833.
13. Way, J. C., M. A. Davies, D. Morisato, D. E. Roberts, and N. Kleckner. 1984. New Tn10 derivatives for transposon mutagenesis and for construction of *lacZ* operon fusions by transposition. Gene **32**:369–379.

Journal of Industrial Microbiology (1996) 17, 458–462

Basic and applied aspects of metabolic diversity: the phosphoenolpyruvate node

F Valle, E Muñoz, E Ponce, N Flores and F Bolivar

Instituto de Biotecnología, Universidad Nacional Autónoma de México, Apdo, Postal 510-3, Cuernavaca, Morelos 62250, México

The phosphoenolpyruvate (PEP) node represents a metabolic crossroad where carbon is distributed into several metabolic pathways. This node is specially important for the industrial production of several metabolites. Depending on the organism and its habitat, the enzymes that utilize PEP are regulated by different effectors, and each branch of the node is important in PEP consumption. In this review we will focus our attention on the metabolic diversity of this node.

Keywords: central metabolism; glycolysis; bacterial metabolism; metabolic engineering

Introduction

Life processes depend on the different functions that proteins, nucleic acids and carbohydrates are capable of providing. Despite their complexity, these macromolecules are constructed by joining together a variety of simpler units. These units, or building blocks, are obtained through diverse cellular catabolic and biosynthetic routes. However, regardless which metabolic routes an organism uses, all cells synthesize the following twelve precursor metabolites: glucose-6-phosphate, fructose-6-phosphate, ribose-5-phosphate, erythrose-4-phosphate, triose-phosphate, 3-phosphoglycerate, phosphoenolpyruvate, pyruvate, acetyl CoA, α-ketoglutarate, succinyl CoA and oxaloacetate.

During balanced growth, each cell-type has evolved control mechanisms to guarantee that its major components remain relatively proportional to one another. These mechanisms should operate to assure the proper distribution of precursors to all biosynthetic routes. Furthermore, these control mechanisms need to be flexible enough to assure that under non-balanced growth conditions, an adequate distribution of metabolites is maintained. One way to fulfill both requirements has been through the activation and/or inhibition of key enzymes by allosteric effectors. These effectors can be products of energy metabolism such as AMP, ATP or NADH. Other intermediary metabolites like pyruvate (PYR), phosphoenolpyruvate (PEP), acetyl-CoA and aspartate control specific points of some of the metabolic routes involved.

For these reasons, it is important to understand how different microorganisms regulate fluxes through their primary metabolic routes. It is well known that, depending on the microorganism and its habitat, metabolic flux patterns can be different. For the applied sciences, knowledge about cellular metabolic fluxes and regulation of end-product formation is especially important at the present time. The diversity of microorganisms offers an enormous source of enzymes with different properties that may be used to improve commercial products or production processes. Furthermore, enzymes may be modified or new genes can be recruited to construct new metabolic pathways.

In this paper we will review some aspects of the enzymes that utilize PEP as substrate. PEP is a key intermediate for the biosynthesis of several important compounds. This strategic node has been studied extensively in *Corynebacterium glutamicum* [12,14,32] and in *Escherichia coli* [27,28]. From the enormous amount of information that exists about central metabolism, we have selected those references that make our points clear. This is not an exhaustive review, but one which hopefully encourages more research into bacterial metabolism, and more interest in taking advantage of the immense supply of enzymes and metabolic strategies that Nature can provide.

Two questions will be addressed: how diverse are the enzymes that participate in the PEP node?; and how can we benefit from this diversity? We will focus our discussion basically on bacteria, but, in a few instances, we will also use such examples as plant systems. Among the bacteria we will initially focus our discussion on *E. coli* metabolism, considering that no other microbe has been studied in such detail, where more than 80% of the cell's metabolic routes are known, and more than 60% of its genome sequenced. From there, discussion will be expanded to some other systems.

The phosphoenolpyruvate node

Glucose can be used by the cell to provide all the carbon skeletons needed to synthesize the twelve precursor metabolites mentioned, which are formed through the concerted action of the glycolytic, pentose phosphate and tricarboxylic acid (TCA) pathways [20]. Several biomolecules are derived from PEP (Figure 1), and it is one of the most important nodes for carbon distribution in all living cells. In *E. coli*, PEP is utilized basically by the reactions summarized in Figure 2. The phosphotransferase transport system (PTS) is the major PEP consumer and PYR producer, while

Correspondence: Dr F Valle, Instituto de Biotecnología, Universidad Nacional Autónoma de México, Apdo, Postal 510-3, Cuernavaca, Morelos 62250, México
Received 5 March 1996; accepted 20 June 1996

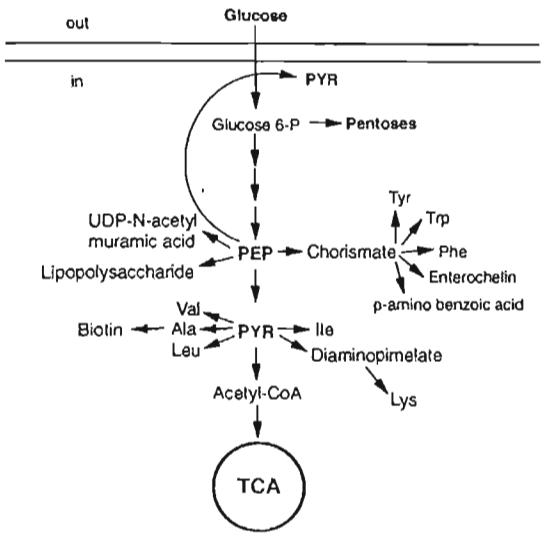

Figure 1 Major metabolic pathways in *Escherichia coli* that, directly or indirectly, utilize phosphoenolpyruvate.

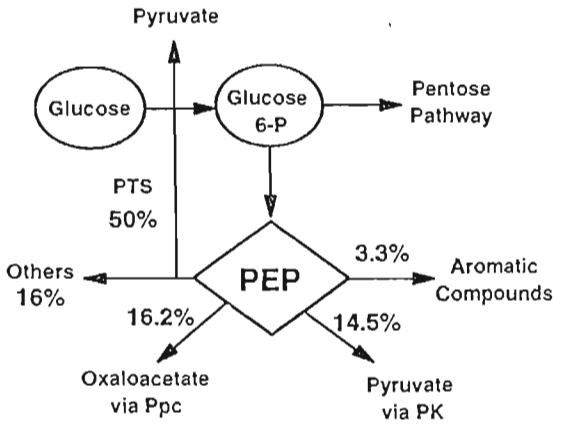

Figure 2 Distribution of phosphoenolpyruvate (PEP) in *Escherichia coli*. The percentages were calculated from data reported by Holms [11].

the phosphoenolpyruvate carboxylase (Ppc) and pyruvate kinase (PK) enzymes consume 16.2% and 14.5% of PEP, respectively. Only 3.3% of the PEP is diverted to aromatic compound synthesis [11].

The fact that an important portion of the studies on metabolism has been done in yeast, or in *E. coli*, could lead to the conclusion that central metabolism is based on the glycolytic or Embden–Meyerhof–Parnas (EMP) pathway. However, there are two alternative routes for glucose utilization: the hexose monophosphate shunt (HMS) and the Entner–Doudoroff (ED) pathways [20]. The HMS pathway oxidizes glucose to CO_2 and glyceraldehyde-3-phosphate, which in turn, can be directed into the TCA cycle via pyruvate by the EMP enzymes, providing NADPH and precursors for nucleotide and aromatic compounds biosynthesis. In bacteria like *E. coli*, this metabolic route consumes around 30% of the glucose-6-phosphate [11]. In certain microorganisms like *Thiobacillus novellus* and *Brucella abortus*, which lack the key enzymes of the EMP or ED pathways, the HMS route has a central role in glucose assimilation [20]. Likewise, it was recently demonstrated that in *Corynebacterium glutamicum*, the HMS pathway also has a major role, even though this microorganism has a functional EMP pathway [18].

Another route for glucose assimilation is the ED pathway which is widely distributed among bacteria. As in the HMS, the first intermediate in the ED pathway is 6-phosphogluconate. Two additional enzymes metabolize 6-phosphogluconate into pyruvate and glyceraldehyde-3-phosphate. In many *Pseudomonas* species and in *Zymomonas*, the Entner–Doudoroff pathway is the main glucose assimilatory route [15,35]. In microorganisms that utilize the HMS or ED metabolic routes to assimilate glucose, the importance of the PEP node and the allosteric regulation of the enzymes involved, will be different than in cells using the EMP pathway.

The phosphotransferase transport system

When *E. coli* is grown in minimal media with glucose as the only carbon source, the carbohydrate is transported inside the cell by the PTS. Concomitantly to its transport, glucose is phosphorylated to glucose-6-phosphate, the first intermediate of the glycolytic pathway (Figure 1). The PTS is also involved in transport and phosphorylation of a large number of carbohydrates, in signal transduction during chemotaxis toward certain carbohydrates, and in the global regulation of many metabolic pathways [30].

PTS is an extremely efficient uptake system; for example, if a transportable sugar is present in the medium at a concentration as low as 0.1 μM, PTS has the theoretical potential to accumulate the sugar against the concentration gradient up to 100 mM [26]. Such transport systems are essential for microorganisms living in media where carbohydrates are scarce. On the other hand, microorganisms that live in sugar-rich environments do not necessarily have PTS. For example, *Zymomonas mobilis* has a constitutive low-affinity high velocity facilitated diffusion system [5]; glucose is phosphorylated by glucokinase and metabolized through the ED pathway. Studies of the different properties of enzymes involved in glucose metabolism in *Zymomonas* have shown that they are operating at their near-maximal capacity, with no substantial allosteric control of the key enzymes [36].

The fact that PTS consumes at least 50% of the PEP made from glucose represents an important problem from the industrial point of view, since it decreases the availability of this intermediate for other reactions, such as aromatic compound synthesis. For example, it has been calculated that for tryptophan (Trp) synthesis, the achievable yield from glucose in a strain with an operating PTS (ie 1 mole of PEP per mole of glucose assimilated) is 20%. On the contrary, if PEP-consuming PTS was not involved and both PEP moles were available for Trp synthesis, the yield could be increased up to 41.8% [9]. This example clearly shows the importance of increasing the intracellular PEP availability for the synthesis of commercially important molecules. For example, it was demonstrated recently that an *E. coli* mutant devoid of the PTS, but capable of glucose transport by a non-PEP consuming mechanism, was able to redirect 50% more of its PEP into the aromatic aminoacid pathway [7]. These results demonstrate that it is possible

to exploit the metabolic diversity of the cell in order to construct mutants with new metabolic capabilities.

An alternative approach to the same problem was performed by exploiting the metabolic diversity among two different bacteria. In this system, the successful transfer and expression of the glucose permease and glucokinase structural genes from *Z. mobilis* in *E. coli pts* mutants, provided a new functional pathway for glucose uptake and phosphorylation. In the same report, it was suggested that the permease and glucokinase genes from *Z. mobilis*, could provide an alternative or supplemental route for glucose entry into glycolysis in other microorganisms [31].

Phosphoenolpyruvate carboxylase

Phosphoenolpyruvate carboxylase (Ppc) catalyzes CO_2-fixation on PEP yielding oxaloacetate. In most bacteria, green algae and in many plants, the major physiological role of this enzyme is to replenish the TCA cycle [3,14,25]. According to their properties, the Ppc enzymes have been classified in three types by Utter and Kolenbrander [34]: class 1 comprises those enzymes which are subject to both activation and inhibition, class 2 includes those proteins subject only to inhibition, and class 3 those enzymes that are subject neither to activation nor inhibition. For class 3, however, there are preliminary studies suggesting that in some cases reduced NADH is an activator of the enzyme [23].

The Ppc from *E. coli*, *S. thyphimurium*, *P. fluorescens* and several other organisms included in class 1, are activated by acetyl-CoA and inhibited by aspartate. Activation of the class 1 enzyme by ADP has also been reported in *P. citronellonis* and in *A. vinelandii*. However, ADP does not seem to affect Ppc from *E. coli* [24]. Nevertheless, the *E. coli* enzyme is allosterically regulated by multiple effectors such as fructose 1,6-diphosphate, GTP, certain long-chain-fatty acids and malate [4]. There are also reports describing that, among several other guanine nucleotides such as, GTP, GDP, GMP and ppGpp, the former is the most potent activator of the *E. coli* Ppc [33].

In contrast, the Ppc from *Z. mobilis* seems to be different and is not affected by acetyl Co-A. The enzyme is, however, inhibited competitively by intermediates of the TCA cycle, especially citrate, α-ketoglutarate and aspartate [4].

As in many mesophilic bacteria, the Ppc enzyme from *T. aquaticus* requires Mg^{2+}, and in the absence of acetyl Co-A, the enzyme is inactive. However, fructose-1,6-diphosphate, which activates several of the Ppc enzymes in mesophilic microbes, has no effect on Ppc action in *T. aquaticus* [3].

A NADH-activated form of Ppc has been reported in a *Pseudomonas* strain grown on methylamine. This enzyme is not activated by acetyl Co-A, ADP, GDP, or a wide variety of other metabolites [23].

It is generally assumed that in several bacterial species, the Ppc has an anaplerotic role, replenishing the tricarboxylic acid cycle (TCA) by supplying oxaloacetate directly from PEP. However, in the Chlorobiaceae, a group of photosynthetic bacteria, known also as the green sulfur bacteria, Ppc has a key role, participating actively in CO_2 fixation. These bacteria use a unique reductive TCA cycle that converts CO_2 into acetyl CoA, as shown in Figure 3. This pathway is unique in the sense that it is a tricarboxylic acid cycle that runs in the reverse direction. However, even though several of the TCA cycle reactions are reversible, three enzymes must be changed in order to drive the cycle in the reverse, or reductive direction [10]. Furthermore, the reductive TCA cycle has been proposed to be the ancestor of all carbon fixation pathways [36], and the evolutionary precursor of the oxidative TCA cycle [17,37].

The analysis of Ppc from plants also offers a rich source of diversity. One of the major characteristics of plants is their ability to fix atmospheric CO_2; the CO_2 fixation can be accomplished in two ways:

(1) In the Calvin Cycle or reductive pentose phosphate cycle, ribulose-1-5, biphosphate reacts with CO_2 to produce two molecules of glyceraldehyde-3-phosphate (PGA) in a reaction catalyzed by ribulose biphosphate carboxylase (RuDPCase). Because the initial carbon dioxide fixation product is a three-carbon compound (PGA), plants with this fixation pattern are often referred to as C_3 plants. The Calvin cycle occurs in many monocotyledons and dicotyledons, including such plants as wheat, rice, sugar beet, spinach, soybeans and tobacco [14].
(2) Another pattern of carbon dioxide assimilation features the production of a four-carbon compound as the CO_2-fixation product. Plants with this pathway are known as C_4 plants. In this type of plants, CO_2 reacts with PEP in the presence of Ppc to form oxaloacetate, where Ppc plays the key role of CO_2 assimilation, as does RuBPC in C_3 plants.

It is evident that the allosteric regulation of the Ppc from Chlorobiaceae and C_4 plants, should be different from the ones in microbes where its role is merely anaplerotic. Based on these data, and from the applied research point of view, it is possible to speculate that the use of a Ppc enzyme from C_4 plants or Chlorobiaceae sources, could be an interesting approach to direct more carbon into oxaloacetate for the overproduction of aspartate, lysine, threonine, methionine and isoleucine.

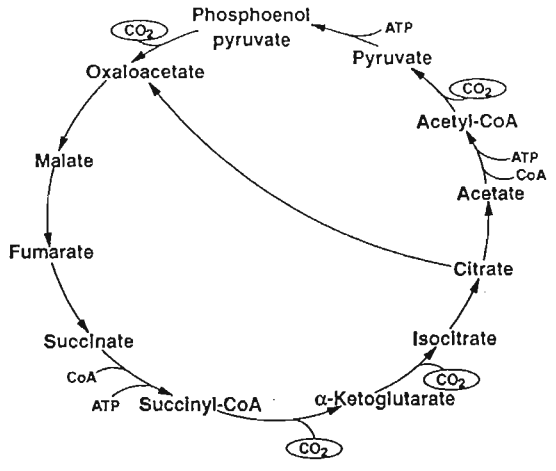

Figure 3 The reductive tricarboxylic acid cycle of the Chlorobiaceae. Adapted from [10 and 20].

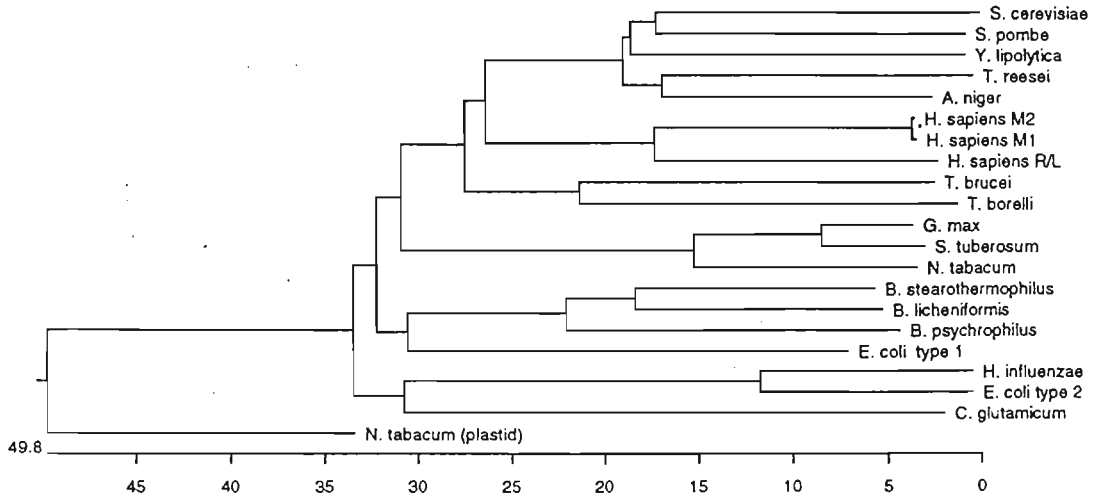

Figure 4 Phylogenetic tree of twenty one pyruvate kinases from different sources. The length of each pair of branches represents the distance between sequence pairs. The scale beneath the tree measures the distance between sequences. The tree was constructed using the Lasergene software (DNASTAR Inc, Madison, WI, USA).

Pyruvate kinases

Pyruvate kinases (PKs) catalyze the conversion of PEP into pyruvate coupled to the synthesis of one molecule of ATP, as shown in Figure 1. This reaction is the last step of the glycolytic pathway and it is irreversible under physiological conditions. Together with phosphofructokinase (PFK), PK plays a major role in glycolysis regulation [8]. No other enzyme of central metabolism has received so much attention as the PK. More than 30 PK structural genes, from different sources, have been cloned and sequenced. In many cases, the enzymes have been purified and some biochemical and kinetic parameters have been determined. One of the reasons for the interest in PK is that a deficiency in this enzyme may be the most common cause of hereditary nonspherocytic hemolytic anemia in humans [1]. Besides this anthropocentric reason, the PK enzymes provide an attractive model to understand some aspects of allosteric regulation, as well as the modulation of glycolysis.

Most bacterial species have one PK. However, *E. coli* and *S. typhimurium* have two PKs, classified as types 1 and 2 based on their allosteric regulation. In PK type 1, allosteric regulation is achieved by binding fructose-1,6-biphosphate (FBP), resulting in increased enzyme activity. Without FBP or in the presence of ATP the enzymatic activity is lower. The allosteric regulators of type 2 PK are AMP and ribose-5-phosphate. The relative roles of these two enzymes have been studied in *E. coli* [29].

The crystal structure of the PK type 1 from *E. coli* has been determined in the absence of PEP, providing the tridimensional structure of an enzyme with a low level of activity. Another well known PK is the mammalian muscle M1 enzyme [13,21]. Interestingly, this enzyme has no allosteric regulation and its crystallization provides the structure of a PK on its active conformation. The comparison of both structures shows that in most parts, they are very similar. However, for the transition from the inactive to the active form, a complicated set of domain and subunit motions need to be induced by the allosteric regulators [19].

Along these lines, there have been some efforts to change the allosteric regulation of the PK from *B. stearothermophilus*. For this purpose, amino acid sequence comparisons between allosteric and non-allosteric PKs from various sources, in conjunction with homology modelling of *B. stearothermophilus* PK on mammalian muscle crystal structures, have been used as criteria to predict regions implicated in allosteric regulation [16,22].

These two examples clearly show the advantage of comparing the structural and biochemical diversity among enzymes from different sources, to understand allosteric regulation or predict the type of changes that need to be introduced to create enzymes more suitable for certain applications.

Finally, we point out that progress on DNA sequencing methodologies, provides an enormous amount of new sequences constantly. In this sense, the abundance of amino acid sequences reported can complicate the identification of potentially interesting enzymes. For example, it is common to see reports of the sequence of a new PK enzyme. Normally, this sequence is compared with the data banks and a similarity percentage is calculated. This could lead to the notion that this new PK is just 'another one'. However, with the same data, it is possible to construct a phylogenetic tree, which in turn, could provide another type of information [6]. In Figure 4 we present a phylogenetic tree constructed from the alignment of 21 known PK sequences. As can be seen, the PK from *C. glutamicum* is more related to the type 2 PKs than to the type 1 enzymes of *E. coli*. Interestingly, it was previously assumed that the former PK was more closely related to the type 1 PKs [12]. This information could be useful if some property of a particular PK needs to be changed. In this case, in order to facilitate the identification of targets for mutagenesis, it could be more advantageous to compare the amino acid sequences of the closest relatives.

It is also evident from Figure 4 that the PK from the *N. tabacum* plastid is more closely related to the prokaryotic enzymes than to the one located in its own cytosol. In this sense, it would be interesting to study the biochemical

properties of the PKs from plastids, because they have been under different selection pressures and especially because, in this organelle, PK participates in a glycolytic pathway that supplies substrates and cofactors for fatty acid biosynthesis [2].

Conclusion

We have reviewed several aspects of the different enzymes that utilize PEP as a substrate. Depending on the organism, these enzymes are regulated by different effectors in several metabolic pathways. The PEP node represents a strategic metabolic crossroad where carbon skeletons are distributed and directed into various metabolic pathways for the biosynthesis of many important compounds. Each cell has evolved sophisticated mechanisms to assure the proper distribution of the precursors to all biosynthetic routes and for the applied sciences the possibility of modifying these control mechanisms, could yield important rewards.

In order to reduce the cost of industrial biosynthetic production of several important compounds, such as the aromatic amino acids, it is desirable to increase the flux of certain carbon skeletons into and through the aromatic compound pathway. This has been accomplished by using cells carrying specific mutations and amplified genes that direct more PEP into this pathway [7]. These results clearly indicate that it is possible to exploit metabolic diversity to design and construct organisms with novel properties.

References

1 Barociani L and E Beutler. 1993. Analysis of pyruvate kinase-deficiency mutations that produce nonspherocytic hemolytic anemia. Proc Natl Acad Sci USA 90: 4324–4327.
2 Blakeley S, S Gottlob-McHugh, J Wan, L Crews, B Miki, K Ko and DT Dennis. 1995. Molecular characterization of plastid pyruvate kinase from castor and tobacco. Plant Mol Biol 27: 79–89.
3 Bridger GP and TK Sundaram. 1976. Occurrence of phosphoenolpyruvate carboxylase in the extremely thermophilic bacterium *Thermus aquaticus*. J Bacteriol 125: 1211–1213.
4 Bringer-Meyer S and H Sahm. 1989. Junctions of catabolic and anabolic pathways in *Zymomonas mobilis*: phosphoenolpyruvate carboxylase and malic enzyme. Appl Microbiol Biotechnol 31: 529–536.
5 DiMarco AA and AH Romano. 1985. D-Glucose transport system of *Zymomonas mobilis*. Appl Environ Microbiol 49: 151–157.
6 Doolittle RF. 1986. Of URFS and ORFS. A Primer on How to Analyze Derived Aminoacid Sequences. pp 40–47, University Science Books, California.
7 Flores N, J Xiao, A Berry, F Bolivar and F Valle. 1996. Pathway engineering for the production of aromatic compounds in *Escherichia coli*. Nature Biotechnol 14: 620–623.
8 Fraenkel DG. 1992. Genetics and intermediary metabolism. Annu Rev Genet 26: 159–177.
9 Frost J and J Lievense. 1994. Prospects for biocatalytic synthesis of aromatics in the 21st century. New J Chem 18: 341–348.
10 Gottschalk G. 1986. Bacterial Metabolism. Springer-Verlag, New York.
11 Holms W. 1986. The central metabolic pathways of *Escherichia coli*: relationships between flux and control at a branch point; efficiency of conversion to biomass, and excretion of acetate. In: Current Topics in Cellular Regulation (Horecker BL and ER Stadtman, eds) , pp 69–105, Academic Press, NY.
12 Jetten MSM, GA Pitoc, MT Follettie and AJ Sinskey. 1994. Regulation of phospho(enol)-pyruvate- and oxaloacetate-converting enzymes in *Corynebacterium glutamicum*. Appl Microbiol Biotechnol 41: 47–52.
13 Larsen TM, LT Laughlin, HM Holden, I Rayment and GH Reed. 1994. Structure of rabbit muscle pyruvate kinase complexed with Mn^{2+}, K^+, and pyruvate. Biochemistry 33: 6301–6309.
14 Lepiniec L, J Vidal, R Chollet, P Gadal and C Crétin. 1994. Phosphoenolpyruvate carboxylase: structure, regulation and evolution. Plant Science 99: 111–124.
15 Lessie TG. 1984. Alternative pathways of carbohydrate utilization in pseudomonads. Ann Rev Microbiol 38: 359–387.
16 Lovell SC, AH Mullick, D Walker, A Rawas and H Muirhead. 1995. Structural and mutagenesis studies on the cooperativity of pyruvate kinase. Protein Engineering 8: 62.
17 Maden EBH. 1995. No soup for starters?; autotrophy and the origins of metabolism. Trends Biochem Sci 20: 337–341.
18 Marx A, AA de Graaf, W Wiechert, L Eggeling and H Sahm. 1996. Determination of fluxes in the central metabolism of *Corynebacterium glutamicum* by nuclear magnetic resonance spectroscopy combined with metabolite balancing. Biotechnol Bioeng 49: 111–129.
19 Mattevi A, G Valentini, M Rizzi, ML Speranza, M Bolognesi and A Coda. 1995. Crystal structure of *Escherichia coli* pyruvate kinase type I: molecular basis of the allosteric transition. Structure 3: 729–741.
20 Moat AG and JW Foster. 1988. Microbial Physiology. John Wiley & Sons, New York.
21 Muirhead H, DA Clayden, D Barford, CG Lorimer, LA Fothergill-Gilmore, E Schiltz and W Schmitt. 1986. The structure of cat muscle pyruvate kinase. EMBO J 5: 475–481.
22 Mullick AH, SC Lovell, D Walker and H Muirhead. 1995. Engineering the allosteric regulation of pyruvate kinase. Protein Engineering 8: 62.
23 Newaz SS and LB Hersh. 1975. Reduced nicotinamide adenine dinucleotide-activated phosphoenolpyruvate carboxylase in *Pseudomonas* MA: potential regulation between carbon assimilation and energy production. J Bacteriol 124: 825–833.
24 O'Brien RW, DT Chuang, BL Taylor and MF Utter. 1977. Novel enzymic machinery for the metabolism of oxaloacetate, phosphoenolpyruvate, and pyruvate in *Pseudomonas citronellolis*. J Biol Chem 252: 1257–1263.
25 O'Leary MH. 1982. Phosphoenolpyruvate carboxylase: an enzymologist's view. Ann Rev Plant Physiol 33: 297–315.
26 Parr TR and MH Saier. 1992. The bacterial phosphotransferase system as a potential vehicle for entry of novel antibiotics. Res Microbiol 143: 443–447.
27 Patnaik R and JC Liao. 1994. Engineering of *Escherichia coli* central metabolism for aromatic metabolite production with near theoretical yield. Appl Environ Microbiol 60: 3903–3908.
28 Patnaik R, R Spitzer and JC Liao. 1995. Pathway engineering for production of aromatics in *Escherichia coli*: confirmation of stoichiometric analysis by independent modulation of AroG, TktA, and Pps activities. Biotechnol Bioeng 46: 361–370.
29 Ponce E, N Flores, A Martínez, F Valle and F Bolívar. 1995. Cloning of the two pyruvate kinase isoenzyme structural genes from *Escherichia coli*: the relative roles of these enzymes in pyruvate biosynthesis. J Bacteriol 177: 5719–5722.
30 Postma PW, JW Lengeler and JR Jacobson. 1993. Phosphoenolpyruvate carbohydrate phosphotransferase systems of bacteria. Microbiol Rev 57: 543–594.
31 Snoep J, N Arfman, L Yomano, R Fliege, T Conway and L Ingram. 1994. Reconstitution of glucose uptake and phosphorylation in a Glucose-negative mutant of *Escherichia coli* by using *Zymomonas mobilis* genes encoding the glucose facilitator protein and glucokinase. J Bacteriol 176: 2133–2135.
32 Stephanopoulos G and JJ Vallino. 1991. Network rigidity and metabolic engineering in metabolite overproduction. Science 252: 1675–1681.
33 Taguchi M, K Izui and H Katsuki. 1977. Activation of *Escherichia coli* phosphoenolpyruvate carboxylase by guanosine-5'-diphosphate-3'-diphosphate. FEBS Lett 77: 270–272.
34 Utter MF and HM Kolenbrander. 1972. Formation of oxaloacetate by CO_2 fixation of phosphoenolpyruvate In: The Enzymes, vol VI (Boyer PD, ed), pp 117–168, Academic Press, New York.
35 Viikari L. 1988. Carbohydrate metabolism in *Zymomonas*. CRC Crit Rev Biotech 7: 237–261.
36 Viikari L and M Korhola. 1986. Fructose metabolism in *Zymomonas mobilis*. Appl Microbiol Biotechnol 24: 471–496.
37 Wächtershäuser G. 1990. Evolution of the first metabolic cycles. Proc Natl Acad Sci USA 87: 200–204.

World Journal of Microbiology & Biotechnology 15: 587–592, 1999.

Kinetic characterization in batch and continuous culture of *Escherichia coli* mutants affected in phosphoenolpyruvate metabolism: differences in acetic acid production

R. Sigüenza[1], N. Flores[1], G. Hernández[1], A. Martínez[1], F. Bolivar[1] and F. Valle[2,*]
[1]*Departamento de Microbiología Molecular, Instituto de Biotecnología, Universidad Nacional Autónoma de México, AP 510-3, Cuernavaca, Morelos 62271, México*
[2]*Genencor International Inc., 925 Page Mill Road, Palo Alto, CA 94304-1013, USA*
**Author for correspondence: Fax: 650 845-6509, E-mail: fvalle@genencor.com*

Received 4 January 1999; accepted 6 May 1999

Keywords: Acetic acid production, carbon metabolism, continuous culture, *Escherichia coli*, metabolic engineering

Summary

The growth kinetics of an *Escherichia coli* wild type strain and two derivative mutants were examined in batch cultures and in glucose-limited chemostats. One mutant (PB12) had an inactive phosphotranferase transport system and the other (PB25) had interrupted *pykA* and *pykF* genes that code for the two pyruvate kinase isoenzymes. In both batch and continuous culture, important differences in acetic acid accumulation and other metabolic activities were found. Compared to the wild type strain, we observed a reduction in acetic acid accumulation of 25 and 80% in PB25 and PB12 strains respectively, in batch culture. Continuous culture experiments revealed that compared to the other two strains, PB25 accumulated less acetic acid as a function of dilution rate. In continuous cultures, oxidoreductase metabolic activities were substantially affected in the two mutant strains. These changes in turn were reflected in different levels of biomass and CO_2 production, and in oxygen consumption.

Introduction

Acetic acid production by *Escherichia coli* strains has been a serious drawback for the commercial production of recombinant proteins and chemicals (Han *et al.* 1991; Sun *et al.* 1993; Gschaedler *et al.* 1994). As an uncoupler of the energetic process, acetic acid has toxic affects on cell growth. In addition, it has a negative impact on the yield of products (Koh *et al.* 1992; Lischke *et al.* 1993). Several authors have discussed the acetic acid accumulation as a carbon overflow mechanism. Apparently, under certain growth conditions the TCA cycle is not capable of completely managing the pyruvate fluxes derived from pyruvate kinase (PK) activities and the phosphotransferase system (PTS). This is particularly true at high growth rates (Majewski & Domach 1990; Han *et al.* 1991).

PTS is the most important mechanism for glucose internalization in *Escherichia coli* and in many other *Enterobacteriaceae* (Bouvet & Grimont 1987). This mechanism couples glucose transport to its phosphorylation, by transferring the high-energy phosphoryl bond from phosphoenolpyruvate (PEP) to the sugar molecule (see Figure 1). The phosphotransferase system is extremely efficient and in theory, it could concentrate glucose up to 10^6-fold against a concentration gradient (Parr & Saier 1992). The glycolytic pathway produces two moles of PEP per mole of glucose assimilated, and because the PTS uses one of them, only one molecule of PEP is left for the rest of the reactions that require PEP directly. Two important reactions of the central metabolism consume PEP. One is catalysed by phosphoenolpyruvate carboxylase (Ppc), which converts PEP into oxaloacetate (see Figure 1). In the other reaction, pyruvate kinase (PK) converts PEP into pyruvate. In the case of *Escherichia coli* there are two PK isoenzymes, PKA and PKF.

As it stands, the present design of central metabolism in gram negative bacteria complicates the overproduction of compounds that require PEP for their synthesis, and this is why PTS and PK isoenzymes and their respective structural genes are important targets for metabolic engineering. Recently, our group has shown that the use of an alternative glucose transport system that does not consume PEP for glucose phosphorylation, and the absence of both PK enzymes, positively affect the formation of aromatic compounds in *Escherichia coli* (Berry 1996; Flores *et al.* 1996; Gosset *et al.* 1996). Furthermore, the reaction catalyzed by the PK isoenzymes has been suggested as an important target for metabolic engineering to diminish acetate formation (Goel *et al.* 1995).

In the present study we report the kinetic characterization of, and the production of acetic acid in, two

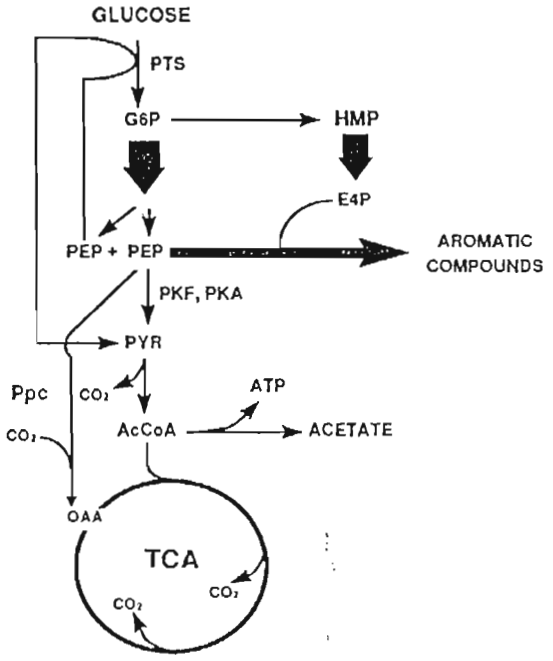

Figure 1. Scheme showing some of the metabolic pathways involved in glucose assimilation and in the formation of certain products in *Escherichia coli*. The heavy arrows indicate that multiple enzymatic reactions are involved. G6P: Glucose-6-phosphate; PEP: Phosphoenolpyruvate; HMP: monophosphate shunt; E4P: Erythrose-4-phosphate; PYR: Pyruvate; AcCoA: Acetyl-CoA; Ppc: Phosphoenolpyruvate carboxylase; TCA: Tricarboxylic acids cycle; PTS: Phosphotransferase transport system; PKA and PKF: the two pyruvate kinase isoenzymes present in *Escherichia coli*.

isogenic *Escherichia coli* mutant strains. One mutant transports glucose by a non-PTS mechanism, using ATP for glucose phosphorylation (Flores *et al.* 1996). In the other strain, the two PK isoenzymes have been eliminated. This leaves PTS as the only source of pyruvate (Ponce *et al.* 1995, 1998). We believe this characterization will contribute to a better understanding of the role of these enzymes in carbon metabolism and will also provide better tools for metabolic engineering in *Escherichia coli*.

Materials and Methods

Bacterial strains

The mutant strains used in this work were constructed in our laboratory and they are derivatives of *Escherichia coli* JM101 *sup*E *thi* Δ(*lac*⁻*pro*AB)(F′ *tra*D36 *pro*AB *lac*I^{q}ZΔM15). PB12 is a Δ(*pts*H-I-*crr*)::*kan* Glc$^+$ derivative (Flores *et al.* 1996) and PB25 is a *pyk*A::*kan* *pyk*F::*cam* derivative (Ponce *et al.* 1995).

Media and inoculum

M9 medium was utilized for batch and continuous culture experiments; inocula were prepared in Luria Broth (Sambrook *et al.* 1989). The starting cultures were prepared by inoculating 3 ml of LB from a frozen cell stock, kept in 10% glycerol at −70 °C, and incubating overnight in a G25 orbital incubator shaker (New Brunswick Inc. New Brunswick, NJ), at 37 °C and 300 rev/min. One ml of the overnight culture was centrifuged, washed with a 10 mM NaCl, transferred to a 500 ml flask with 50 ml of M9 medium, and incubated for 12 h at 37 °C and 300 rev/min. A portion of the culture was used to inoculate the fermentor to an initial optical density at 600 nm (OD_{600}) between 0.05 and 0.1.

Fermentations

The batch and continuous culture experiments were performed in a 2-l fermentor (LSL Biolafitte, Inc. Princeton, NJ) with 1.2 and 0.78 l of operation volume respectively. The data from these experiments were reported as representative runs and were always compared for accuracy with at least one replicated trial. Continuous culture experiments were initiated from batch cultures growth to late exponential phase. In the different dilution rates tested, the steady state was achieved after at least six residence times. Constant signals of q_{O_2}, q_{CO_2}, dissolved oxygen, and OD_{600} were used to measure stability of the cultures. Once a steady state was obtained in each one of the cultures, five samples were taken in 3 to 4 h intervals each one to determine residual glucose, biomass, glycogen and organic acids concentrations (see below). All cultivations were done at 37 °C (±0.003%); pH 7 (±0.007%); with an aeration of 1 VVM; pH was controlled with the automatic addition of a 1 M NH_4OH. Off-gas analysis for oxygen and carbon dioxide were performed on-line by a MGA-1200 mass spectrometer (Perkin-Elmar, Pomona, Calif.).

Analytical methods

During batch experiments, the biomass was calculated from OD measurements, using a calibration curve (1 OD_{600} unit = 0.36 g/l). In continuous culture experiments, the dry weight was determined by centrifuging 10 ml aliquots for 10 min in an Eppendorf centrifuge (Brinkmann, Inc., Westbury, NY). The pellets were suspended in 10 mM NaCl and centrifuged again. All the samples were dried for 24 h, in a vacuum oven at 90 °C. Residual glucose in the media was determined using a multiple enzymatic analyzer Ektachem DT60 II (Kodak, Rochester, NY). Glycogen was determined as reported by Förberg *et al.* (1988). Organic acids were quantified by HPLC (Waters, Millipore Corp. Milford, MA) using an Aminex HPX-87H 300 × 7.8 mm column (Bio-Rad, Hercules, CA) at 60 °C, H_2SO_4 5 mM as eluant, with a flow rate of 0.5 ml/min.

Results

Batch culture experiments

We used batch cultures to compare several growth parameters of the JM101 strain and its two derivatives PB12 and PB25 wherein the PEP metabolism had been affected by specific mutations. These three strains exhibit different growth rates (Figure 2). In addition, the PB25 culture reached a different final biomass concentration compared to the JM101 and PB12 cultures. Differences between the strains were also found in the level of glucose consumption. Interestingly, a substantial change in the rate and level of acetate accumulated by these strains was also observed. Furthermore, acetate consumption was also detected in JM101 and PB25 cultures, after almost all the glucose was exhausted and growth ceased. In contrast, in PB12 cultures, acetate was only detected at later time points and never accumulated to more than 0.05 g/l (see Figure 2). Other organic acids (lactate, pyruvate, and succinate), as well as the storage carbohydrate glycogen, were not detected in significant concentrations in the three strains examined (data not shown).

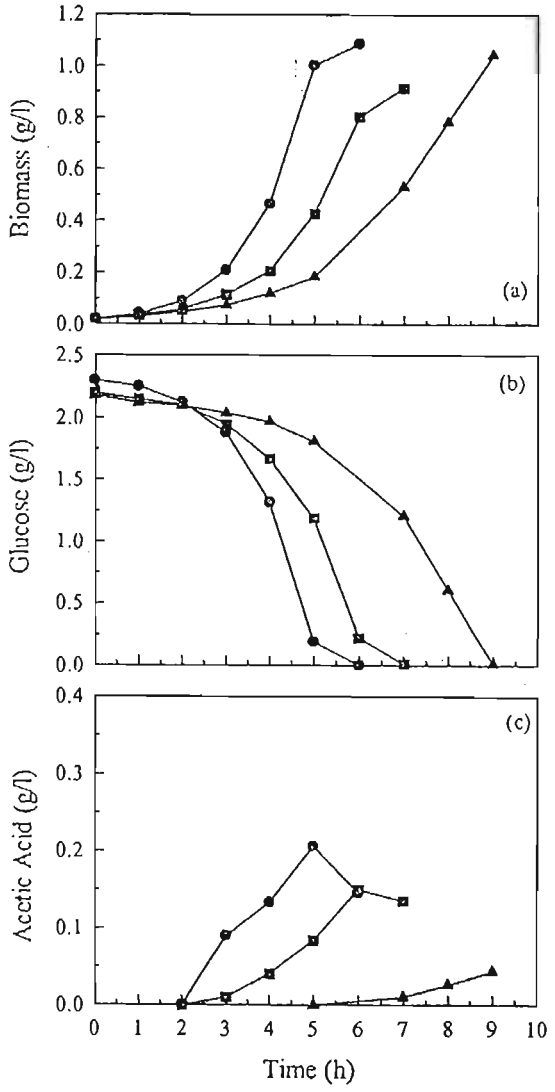

Figure 2. Cell growth (a), glucose consumption (b) and acetic acid accumulation (c) measurements for the three *Escherichia coli* strains tested in batch culture experiments, using M9 medium with glucose (2 g/l) as the only carbon source. Symbols: (●) JM101, (▲) PB12, (■) PB25. Data from one representative run, compared for accuracy with at least one duplicated experiment.

The data generated by these experiments were utilized to calculate specific rates and yields, which are presented in Table 1. The highest specific growth rate was obtained in the JM101 culture, whereas PB25 and PB12 cultures showed respectively, a 20 and 40% decreases in their growth rates as compared to the parental JM101. A higher biomass yield was observed in the PB12 culture, in accordance with the lowest acetate accumulation observed for this strain. Interestingly, when compared with JM101, the PB25 strain showed a lower biomass yield, despite having accumulated less acetate. These results suggest that in the PB25 strain, more substrate was diverted away from biomass to other metabolic routes. In this sense, we observed that total CO_2 production was higher in PB25 cultures than in the other two strains (data not shown). In agreement with these results, it has been previously determined (Ponce *et al.* 1998), that in the PB25 strain, the pentose pathway increases its participation in glucose catabolism.

Different values of specific glucose consumption rate and acetate production were observed in the tested strains. The highest specific glucose consumption rate was observed in JM101, while the lowest was found in the PB12 culture. The glucose consumption value for the PB25 strain was very similar to the one obtained for the JM101 strain. Regarding acetate production, the PB25 strain showed the highest specific production rate. It has been pointed out that in *Escherichia coli* cultures, acetate accumulation is a direct function of growth rate (Meyer *et al.* 1984; El-Mansi & Holms 1989). Although the PB12 strain showed a consistent behaviour in this respect, it was not the case for the PB25 strain which compared with the other strains, showed a higher production of acetate per unit of biomass (see Table 1).

Table 1. Results from batch culture experiments with the three *E. coli* strains examined[a].

Strain	μ_{max} (h^{-1})	$Y^b_{X/S}$ (g/g)	$Y^b_{HAc/X}$ (g/g)	q^c_S (g/g/h)	q^c_{HAc} (g/g/h)
JM101	0.78	0.47	0.14	1.67	0.112
PB12	0.47	0.54	0.064	0.87	0.03
PB25	0.62	0.4	0.197	1.54	0.121

[a] These calculations are derived from one representative run and compared for accuracy with at least one replication.
[b] Biomass yield on consumed glucose and acetic acid production by produced biomass, calculated from the exponential phase data.
[c] Specific rates of glucose consumption and acetic acid production, from the exponential phase data.

Based on these results and to obtain a deeper insight into the kinetic behaviour of these strains, we used glucose-limited continuous cultures to obtain steady states at different growth rates for each strain, and to measure the acetate production rates under these conditions.

Continuous culture experiments

Considering that the mutations incorporated into the PB12 and PB25 strains involved glucose transport, PEP metabolism and pyruvate supply, the first parameter that we wanted to study on these strains was the yield, that is, the amount of biomass produced per gram of glucose consumed. In the range of dilution rates tested, the JM101 strain showed a slight decrease in the yield as the growth rate increased. This behaviour was more pronounced in strain PB25, while in PB12, the yield increased as the dilution rate was also increased (see Figure 3a). As can be seen in Figure 3b, no acetate was produced at the 0.2 and 0.3 h^{-1} dilution rates by any of the cultures. However at a dilution rate of 0.35 h^{-1}, the production of acetate by the PB12 culture was 40% lower than in the JM101 culture. Interestingly, at this dilution rate, the PB25 culture did not produce acetate. All the cultures produced acetate at a dilution rate of 0.5 h^{-1}; however, at this growth rate and when compared with JM101, the PB12 and PB25 cultures produced 30% and 55% less acetate, respectively (see Figure 3b). The strains examined under these conditions did not show significant accumulation of other organic acids (lactate, pyruvate and succinate) or glycogen as a function of dilution rate (data not shown).

As expected, the specific glucose consumption rate increased with the dilution rate, although each culture exhibited a different slope (see Figure 4a). As shown in Figure 4b, the specific CO_2 production rate of the three strains showed a linearly increasing trend with dilution rate. At 0.2 h^{-1} and when compared to JM101, the PB12 culture showed a slightly higher specific CO_2 production rate but the corresponding value was significantly lower

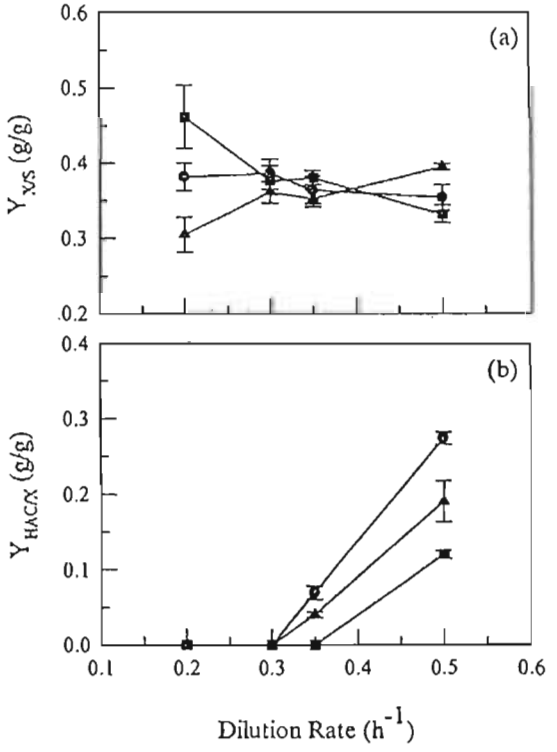

Figure 3. Determination of the yields of biomass (a) and acetic acid (b) in strains JM101 (●), PB12 (▲) and PB25 (■) in continuous cultures, at different dilution rates. $Y_{X/S}$, grams of biomass produced by grams of consumed glucose; $Y_{HAc/X}$, grams of acetic produced by grams of biomass. These data were computed from average values of five samples taken at steady state.

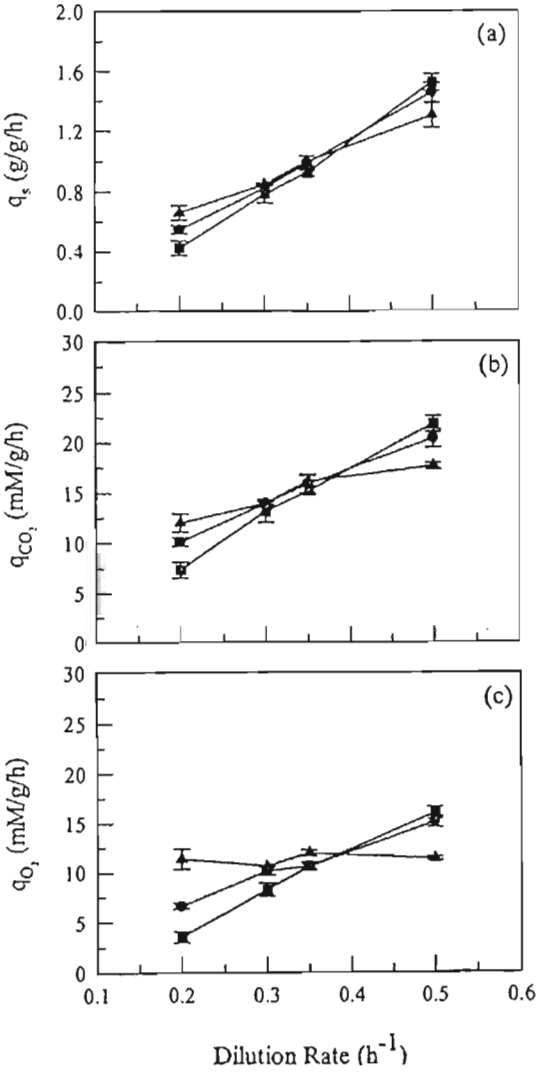

Figure 4. Specific rates showed by the three *Escherichia coli* strains tested in continuous culture experiments at different dilution rates: q_s, specific glucose consumption rate (a); q_{CO_2}, specific CO_2 production rate (b); q_{O_2}, specific oxygen consumption rate. Symbols: (●) JM101, (▲) PB12 and (■) PB25. These data were computed from average values of five samples taken at steady state.

than that for JM101 at 0.5 h^{-1}. In the PB25 culture and when compared to JM101, the specific CO_2 production rate was slightly lower at 0.2 h^{-1}, whereas at 0.5 h^{-1}, it was nearly the same as in JM101 (see Figure 4b). Regarding the specific oxygen uptake rate, in both JM101 and PB25 cultures, as expected, a linear increase with growth rate was observed. Interestingly, the PB12 culture showed a relatively constant specific oxygen consumption rate. The differences observed on specific rates of CO_2 production and oxygen consumption for all the strains, clearly indicates different oxidative-reductive metabolic activities.

Discussion

The *Escherichia coli* mutant strains PB12 and PB25 were constructed in an attempt to modify the carbon flux distribution at the PEP node. In the PB12 strain, glucose is transported and phosphorylated by the action of the galactose permease and glucokinase, respectively (Flores *et al.* 1996). This new metabolic strategy implies that in this strain, no PEP is consumed directly for glucose phosphorylation, and that the formation of pyruvate is not necessarily coupled to glucose transport. In addition, due to the multiple regulatory roles that PTS plays in different processes, important changes in cell physiology can be envisaged on this strain. Furthermore, it has been reported by our group that a strain with a similar phenotype to PB12 was able to produce more aromatic compounds, suggesting an increase in the metabolic availability of PEP (Flores *et al.* 1996, Gosset *et al.* 1996). On the other hand, the PK reaction is the last step of the glycolytic pathway and is an important source of pyruvate (Ponce *et al.* 1995, 1998). Our group has also elucidated that an *Escherichia coli* strain devoid of PK activity, carrying a PTS deletion, increases the availability of PEP to produce aromatic compounds (Gosset *et al.* 1996).

The data obtained from batch and continuous cultures of PB12 and PB25 strains show important differences in the carbon flux distributions when compared to the parental JM101 strain. In the two mutants, acetate production was substantially lower. This result may be associated with a decreasing carbon flux into pyruvate. In general, it is accepted that in *Escherichia coli* aerobic cultures, acetate is produced after a certain growth rate (i.e., carbon flux through central metabolism) is achieved, when the TCA cycle is saturated and it is unable to manage the flux that glycolysis delivers (Majewski & Domach 1990). Under these circumstances, the excess of carbon flux is directed towards the formation of acetate. As shown in Figure 1, this strategy also provides an extra source of ATP. In this scenario, the PEP node plays an important role acting as a distribution point of carbon to produce building blocks for growth or for the synthesis of organic acids (see Figure 1). On the other hand, the metabolic activities of the central pathways are modulated to satisfy the carbon and energy requirements for growth. These activities are reflected in biomass and CO_2 production, as well as in oxygen consumption. At dilution rates below the onset of acetate production, an oxidative metabolism predominates and the substrate is transformed only into biomass and CO_2, whereas at dilution rates above the onset both oxidative and fermentative metabolisms occur, with the consequent production of biomass, CO_2 and acetate (Meyer *et al.* 1984). Interestingly, different metabolic trends were observed in continuous cultures with the three tested strains. At 0.2 h^{-1}, PB12 when compared to the other strains, showed a much higher metabolic activity, which was indicated by higher values of CO_2 production and oxygen consumption. On the contrary, at 0.5 h^{-1}, the PB12 culture showed a lower metabolic activity (i.e., lower rates for CO_2 production and oxygen consumption rate); however, despite these changes, a higher biomass yield was observed at this dilution rate. This was perhaps due to a more efficient utilization of the carbon from glucose as reflected by the lower CO_2 production. The fact that in PB25 cultures, acetate was still produced at 0.5 h^{-1}, could indicate that the pyruvate supplied by PTS, was enough to overflow the TCA cycle. Furthermore, the fact that the onset of acetate production in JM101 and PB12 strains was the same (0.35 h^{-1}) (see Figure 3b), suggests that this strain has been able to regain enough flux to pyruvate and overflow the TCA cycle. In this sense, we have not identified all the mutations that occurred in PB12. However, we do know that in this strain, the glucokinase enzyme (Glk) is overproduced and glucose is transported through the galactose permease (GalP) (Flores *et al.* 1996; unpublished results). Under this new scenario, glucose flux through GalP and Glk depends on the pull exerted by the glycolytic enzymes. It is evident from the results reported in this paper that none of the mutations present in the PB12 strain affected the onset of acetate formation.

Finally, we believe that the characterization of these mutants, which have been already utilized for the overproduction of aromatic compounds (Flores *et al.* 1996; Gosset *et al.* 1996), will contribute in the design of better strategies for the production of other important molecules in *Escherichia coli*.

Acknowledgements

We would like to thank Dr Rodolfo Quintero and Dr Guillermo Gosset for a critical review of the manuscript, and Mercedes Enzaldo for technical support. This investigation was supported by grants 25375-N from Consejo Nacional de Ciencia y Tecnología, México, IN206696 from DGAPA-UNAM, México, and Genencor International. Our thanks are also due to Consejo Nacional de Ciencia y Tecnología, for providing an scholarship to one of us (R.S).

References

Berry, A. 1996 Improving production of aromatic compounds in *Escherichia coli* by metabolic engineering. *Trends in Biotechnology* 14, 250–256.

Bouvet, O.M. & Grimont, P.A. 1987 Diversity of the phosphoenolpyruvate/glucose phosphotransferase system in the Enterobacteriaceae. *Annales de l'Institut Pasteur/Microbiology* 138, 3–13.

El-Mansi, E.M. & Holms, W.H. 1989 Control of carbon flux to acetate excretion during growth of *Escherichia coli* in batch and continuous culture. *Journal of General Microbiology* 135, 2875–2883.

Flores, N., Xiao, J., Berry, A., Bolivar, F. & Valle, F. 1996 Pathway engineering for the production of aromatic compounds in *Escherichia coli*. *Nature Biotechnology* 14, 620–623.

Förberg, C., Eliaeson, T. & Häggström, L. 1988 Correlation of theoretical and experimental yields of phenylalanine from non-growing cells of a *rec Escherichia coli* strain. *Journal of Biotechnology* 7, 319–332.

Goel, A., Lee, J., Domach, M.M. & Attai, M.M. 1995 Suppressed acid formation by cofeeding of glucose and citrate in *Bacillus* cultures: Emergence of pyruvate kinase as a potential metabolic engineering site. *Biotechnology Progress* 11, 380–385.

Gosset, G., Yong-Xiao, J. & Berry, A. 1996 A direct comparison of approaches for increasing carbon flow to aromatic biosynthesis in *Escherichia coli*. *Journal of Industrial Microbiology* 17, 47–52.

Gschaedler, A., Le, N.T. & Boudrant, J. 1994 Glucose and acetate influences on the behavior of the recombinant strain *Escherichia coli* HB 101 (GAPDH). *Journal of Industrial Microbiology* 13, 225–232.

Han, K.H., Lim, C. & Hong, J. 1991 Acetic acid formation in *Escherichia coli*. *Biotechnology and Bioengineering* 39, 663–671.

Koh, B.T., Nakashimada, U., Pfeiffer, M. & Yap, M.G.S. 1992 Comparison of acetate inhibition on growth of host and recombinant *E. coli* K12 strains. *Biotechnology Letters* 14, 1115–1118.

Lischke, H.H.L., Brandes, L., Wu, X. & Schügerl, K. 1993 Influence of acetate on the growth of recombinant *Escherichia coli* JM103 and product formation. *Bioprocess Engineering* 9, 155–157.

Majewski, R.A. & Domach, M.M. 1990 Simple constrained-optimization view of acetate overflow in *E. coli*. *Biotechnology and Bioengineering* 35, 732–738.

Meyer, H.P., Leist, C. & Fiechter, A. 1984 Acetate formation in continuous culture of *Escherichia coli* K12 D1 on defined and complex media. *Journal of Biotechnology* 1, 355–358.

Parr, T.R. & Saier, M.H. 1992 The bacterial phosphotransferase system as a potential vehicle for the entry of novel antibiotics. *Research in Microbiology* 143, 443–447.

Ponce, E., Flores, N., Martinez, A., Valle, F. & Bolivar, F. 1995 Cloning of the two pyruvate kinase isoenzyme structural genes from *Escherichia coli*: The relative roles of these enzymes in pyruvate biosynthesis. *Journal of Bacteriology* 177, 5719–5722.

Ponce, E., Martinez, A., Bolivar, F. & Valle, F. 1998 Stimulation of glucose catabolism through the pentoses pathway by the absence of the two pyruvate kinase isoenzymes in *Escherichia coli*. *Biotechnology and Bioengineering* 58, 292–295.

Sambrook, J., Fritsch, E.F. & Maniatis, T. 1989 Molecular cloning. A laboratory manual. 2nd edn, Cold Spring Harbor Laboratory Press. ISBN 0-87969309-6.

Sun, W.J., Lee, C., George, H.A., Powell, A.L., Dahlgren, M.E., Greasham, R. & Park, C.H. 1993 Acetate inhibition on growth of recombinant *E. coli* and expression of fusion protein TGF-PE40. *Biotechnology Letters* 15, 809–814.